PROTECTION COORDINATION IN TRANSMISSION AND DISTRIBUTION SYSTEMS

Ph.D. THESIS

by

MAHAMAD NABAB ALAM

DEPARTMENT OF ELECTRICAL ENGINEERING
INDIAN INSTITUTE OF TECHNOLOGY ROORKEE
ROORKEE – 247667 (INDIA)
DECEMBER, 2017

PROTECTION COORDINATION IN TRANSMISSION AND DISTRIBUTION SYSTEMS

A THESIS

Submitted in partial fulfilment of the requirements for the award of the degree

of

DOCTOR OF PHILOSOPHY

in

ELECTRICAL ENGINEERING

by

MAHAMAD NABAB ALAM

DEPARTMENT OF ELECTRICAL ENGINEERING
INDIAN INSTITUTE OF TECHNOLOGY ROORKEE
ROORKEE – 247667 (INDIA)
DECEMBER, 2017

INDIAN INSTITUTE OF TECHNOLOGY ROORKEE
ROORKEE

CANDIDATE'S DECLARATION

I hereby certify that the work which is being presented in the thesis entitled **"PROTECTION COORDINATION IN TRANAMISSION AND DISTRIBUTION SYSTEMS"** in partial fulfilment of the requirements for the award of the Degree of Doctor of Philosophy and submitted in the **Department of Electrical Engineering** of the **Indian Institute of Technology Roorkee, Roorkee** is an authentic record of my own work carried out during a period from January, 2013 to December, 2017 under the supervision of **Dr. Biswarup Das**, Professor, Department of Electrical Engineering, Indian Institute of Technology Roorkee, Roorkee.

The matter presented in this thesis has not been submitted by me for the award of any other degree of this or any other Institution.

(MAHAMAD NABAB ALAM)

This is to certify that the above statement made by the candidate is correct to the best of my knowledge.

(Biswarup Das)
Supervisor

Dated:

Abstract

Proper protection coordination is one of the inherent requirements to run a distribution system with highest reliability. It is known that most of the faults of power system occur in distribution system. Therefore, if the protection schemes are not coordinated properly then many consumers have to suffer unnecessary outages. For reliable operation of the distribution system, its primary protection scheme must react to a fault as quickly as possible to isolate the faulty parts from the healthy parts, but if primary protection fails only then its backup protection scheme should operate. This condition is the most desired feature of any protection system as primary protection removes only faulted part whereas the operation of the backup protection isolates a larger portion of the system.

Commonly, directional overcurrent relays (DOCRs) are used for issuing the trip signal for circuit breakers (CBs) to isolate the faulted section in distribution or sub-transmission networks. In ring or multiple source power distribution networks, DOCRs are necessary. The operation of DOCRs depends on its two parameters, namely time multiplier setting (TMS) and plug setting (PS). The time gap between operations of primary protection and its corresponding backup protection, known as coordination time interval (CTI), can be achieved by optimum settings of TMS and PS of all the DOCRs used and thus a proper protection coordination can be obtained. In general, optimum settings of the relays are obtained by solving protection coordination problem as an optimization problem where the objective is to minimize the sum of the operating times of all the relays in their primary mode of operation while maintaining coordination constraints among all relays.

In radial distribution systems, the feeders are protected by reclosers and fuses. Fuses are placed at feeders which are at more remote position from substation. Whenever a transient fault occurs in any feeder, the corresponding fuse does not melt because the recloser's fast operation allows the transient fault to self-clear. But, whenever a permanent fault occurs, the concerned fuse must melt just before the last delay trip of the recloser in order to prevent the loads between the recloser and the fuse from being interrupted. Therefore, there must be a proper coordination between the operation of recloser and fuses. Moreover, the increasing penetration of distributed generation (DG) in distribution systems has added more complexity to the protection coordination problems

(as presence of DG changes the magnitudes and directions of the short circuit currents in the distribution system). Thus, an appropriately coordinated protection scheme (in absence of DG) may not be able to perform its coordination function correctly, in the presence of DGs.

The protection coordination problem of DOCRs is formulated as either linear programming (LP), nonlinear programming (NLP) or mixed-integer nonlinear programming (MINLP) problems and various optimization techniques are applied to solve these problems. In LP formulation, the PS of the relays are assumed to be known and the sum of operating times of the relays are expressed as a linear function of the TMS of the relays. When both PS and TMS are to be determined simultaneously, the coordination problem becomes an NLP problem. Further, when it is necessary to find discrete optimum values of PSs then this problem is termed as an MINLP one. Normally, electromechanical/static relays need discrete values whereas numerical/digital relays need continuous values of variables. Both analytical as well as meta-heuristic optimization algorithms have been used for solving this problem. As this problem is very complex, meta-heuristic algorithms have been preferred as they are independent of the nature of problem formulation and the types of variables. Now, because of the availability of several meta-heuristic optimization methods for coordination of DOCRs, it is a natural curiosity to find the most effective meta-heuristic optimization method for practical implementation. Further, in the medium and large interconnected distribution systems, it is necessary to minimize the operating times of primary and the corresponding backup relays without any mis-coordination in reasonable time. To achieve these requirements, it is necessary to develop a new formulation which also minimizes the operating times of backup relays along with the operating times of primary relays without any constraint violation. Also, protection coordination of DOCRs needs to be obtained which should be robust enough to protect the systems under various system operating conditions such as (N-1) contingency.

Initially, a comparative study of different meta-heuristic optimization approaches, which had been proposed in the literature for DOCRs, is presented. Towards this goal, five most effective meta-heuristic optimization approaches such as genetic algorithm (GA), particle swarm optimization (PSO), differential evolution (DE), harmony search (HS) and seeker optimization algorithm (SOA) have been considered. The performances of these optimization methods have been investigated on several power system networks of different sizes. The comparative performances of these methods have been studied by executing each method 100 times with the same initial conditions and based on the obtained results, the best meta-heuristic optimization method for solving the coordination problem of DOCRs is identified.

Subsequently, for minimizing the operating times of primary and backup relays simultaneously, a new objective function (NOF) has been developed. In the proposed formulation, different types of relays (electromechanical, static and numerical) with different characteristic curves (IDMT, VI and EI) have been considered. As a result this problem becomes a MINLP one because of discrete nature of PS values of electromechanical and static relays. Further, to solve this MINLP problem, two interior point method (IPM) based algorithms have been developed. Both these algorithms are two phase optimization techniques and are named as IPM-BBM and IPM-IPM, respectively. In the first phase of both the methodologies, IPM is used to obtain continuous values of TMSs and PSs of DOCRs. In the second phase of IPM-BBM technique, branch and bound method (BBM) and in the second phase of IPM-IPM technique, IPM is used to obtain final settings (continuous TMS values and discrete PS values) of DOCRs. The effectiveness of the proposed solution methods and the developed objective function has been investigated on three power system networks of different sizes. The suitability of the proposed method for coordination of DOCRs in meshed networks has been established by comparing its performance with that obtained by GA, DE and two hybrid algorithms (IPM with GA and DE) for the developed objective function. Also, the superiority of the developed objective function has been established by comparing the protection coordination results obtained by using NOF with those obtained by the other objective functions reported in the literature.

Further, a contingency constrained robust protection coordination scheme of DOCRs is discussed. The robust protection coordination scheme provides single settings of DOCRs which will be valid for the credible (N-1) topologies created after outage of any element. For selecting the feasible contingencies, a composite security index (CSI) has been used. The robust protection coordination scheme has been posed as an optimization problem and solved using an IPM based algorithm. The feasibility of the proposed formulation and solution algorithm has been demonstrated on three power system networks of different sizes.

For the protection of radial distribution networks, an optimum recloser-fuse coordination scheme is proposed in the presence of DGs. The proposed approach formulates optimum recloser-fuse coordination problem as an optimization problem and applies IPM based algorithm to solve this optimization problem for obtaining the optimum recloser and fuse settings. The proposed scheme gives a single set of settings of the reclosers and fuses which is robust enough to coordinate the operations of the reclosers and fuses properly with and without the presence of single/multiple DGs in the system. The proposed approach has been tested on two radial distribution systems for three different scenarios: i) no DG in the system, ii) a single DG in the system and iii) multiple DGs in the system. The test results prove the robustness and effectiveness of the presented scheme.

Finally, an optimum recloser-fuse coordination in reconfigurable radial distribution systems in the presence of DGs is proposed. In the proposed scheme, the problem of recloser-fuse coordination in reconfigurable radial distribution networks has been formulated as an optimization problem. The formulated recloser-fuse coordination problem has been solved using IPM based algorithm. In order to obtain all possible reconfigurable radial networks, a new graph theory based approach has been developed. The proposed approach has been applied to obtain optimum recloser-fuse settings for two radial distribution systems in the presence of DG. Further, to test the effectiveness of the proposed approach, cases of mis-coordination have been analyzed in all feasible configurations of the radial systems in the presence of DGs at single and multiple locations. The test results prove the effectiveness of the presented scheme.

Acknowledgements

In the name of Allah, the infinitely Good, the All Merciful

All praise is due to Allah, Lord of the Universe.

I take this opportunity to express my sincere gratitude toward my guide: Prof. Biswarup Das, Head of the Department of Electrical Engineering, Indian Institute of Technology Roorkee. I have been very fortunate to receive his continued academic advice, constant encouragement, endless patience, and priceless guidance and support throughout this work. He has been training me the skill and art to identify attractive and important research problems and to propose effective solutions to them.

I would like to especially thank Dr. Vinay Pant, Department of Electrical Engineering, who has been my second guide throughout the Ph.D. course. I would like to thank Prof. Narayan Prasad Padhy, Dean, Academic Affairs, Indian Institute of Technology Roorkee and Prof. Manoj Mishra, Department of Computer Science and Engineering for their constant suggestions and advices. Further, I would like to thank Prof. R. Prasad, Chairman DRC, Prof. Pramod Agrawal, former Dean, Academic Affairs and Prof. S. P. Srivastava, former Head of the Department of Electrical Engineering for their continued support. In addition, I would like to thank Prof. G. N. Pillai, Prof. G. K. Singh, Dr. Premalata Jena and Dr. Ganesh Kumbhar for their valuable suggestions. Also, officers in the department office, Mr. Mohan Singh and Rishabh Verma in particular, have been continuously helping me in all possible steps. Also, the technician at the Power System Simulation Laboratory, Mr. Ravindar and his colleagues, deserve my highest appreciation.

I have been blessed with many friends during this course, including: Pushkar Triphati, Akhilesh Mathur, Javed Dhillon, Rajkumar Viral, Haresh Shabhadia, Hari Krishna Muda, Afroz Alam, Kanhaiya Kumar, Firdaus Nazir, Arun Balodi, Shuklal Sisodiya, Yogesh Makwana, Kunal Bhat, Sandeep Kaur, Soumetri Jena and many more. I am very fortunate to be blessed with a very especial friend Novalio Daratha from Indonesia. He was my senior and graduate his Ph.D. course last year. He has been a constant source of guidance and support throughout his stay at this Institute and I have learned many things from him. In additions, I have been blessed with many friends from the Institute including: Shahid Alam, Inaam Qazi, Farhaad Illahi Bux, Seraj Ahmad, Arshad Arzoo and many more. All have been a great source of happiness throughout my stay at the Institute.

My Ph.D. is dedicated to my father (late) Md. Samsul Ansari. He was recalled by the Almighty on 28 April 2015 when I have been in the middle of this course. He has been the real source of love, help, inspiration, guidance and everything to me. He always tried his best to fulfill all my dreams. He has been a great father and I am proud of his being one of the sons. In fact, he has been and will always remain everything to me. It is nothing but his dedication towards my studies which let me continue to complete this course.

Further, I especially thank all of my family members, including my mother, grandmother, brothers, sisters and kids. Their patience and support are priceless. I especially would like to thank my elder brother M Aslam Ansari for making me, feel free to get the best possible education since my childhood. I am at this stage because of him.

Finally, I would like to thank the Ministry of Human Resource Development, Government of India, for providing fellowship throughout this course and Indian Institute of Technology Roorkee for giving me the opportunity to start my research career as a Ph.D. student.

Mahamad Nabab Alam

Roorkee, December 2017

Contents

List of Tables

List of Figures

List of Abbreviations

AMPL A Mathematical Programming Language.

BBM Branch and Bound Method.

BFSM Backward Forward Sweep Method.

BVSI Bus Voltage Security Index.

BW Band Width.

CB Circuit Breaker.

CF Crossover Factor.

CNC (N-1) Contingency Network Configuration.

CNC-OLTC (N-1) Contingency Network Configuration in the presence of On-Load Tap Changer.

CR Crossover Rate.

CSI Composite Security Index.

CT Current Transfermer.

CTI Coordination Time Interval.

CTR Current Transfermer Ratio.

DE Differential Evolution.

DG Distributed Generation.

DOCR Directional Overcurrent Relay.

EG External Grid.

EIN Extremely Inverse.

Eqn. Equation.

Eqns. Equations.

ESS Electric Sub-Station.

GA Genetic Algorithm.

GAMS General Algebraic Modeling System.

HM Harmony Memory.

HMCR Harmony Memory Consideration Rate.

HS Harmony Search.

i.e. that is to say.

IBDG Inverter Based Distributed Generator.

IDMT Inverse Definite Minimum Time.

IEC International Electrotechnical Commission.

IEEE Institute of Electrical and Electronics Engineering.

ILP Integer Linear Programming.

IPM Interior Point Method.

kVA kilo Volt Ampere.

kW kilo Watt.

LP Linear Programming.

LPFSI Line Power Flow Security Index.

MATLAB MATLAB (**Mat**rix **Lab**oratory) is a multi-paradigm numerical computing environment developed by MathWorks.

MBPS Minimum Break Point Set.

MCT Minimum Coordination Time.

MF Mutation Factor.

MFCTI Minimum Fuse Coordination Time Interval.

MILP Mixed-Integer Linear Programming.

MINLP Mixed-Integer Non Linear Programming.

MRCTI Minimum Recloser Coordination Time Interval.

MVA Mega Volt Ampere.

MW Mega Watt.

NLP Non-Linear Programming.

NNC Normal Network Configuration.

NOF New Objective Function.

NOFC New Objective Function under Contingency.

NRLF Newton-Raphson Load Flow.

OCR Overcurrnt Relay.

OF Objective Function.

OFC Objective Function under Contingency.

OFV Objective Function Value.

OLF Over Load Factor.

OLTC On-Load Tap Changer.

PAR Pitch Adjustment Rate.

PCS Pickup Current Setting.

PS Plug-Setting.

PSO Particle Swarm Optimization.

pu per unit.

SACTI Sum of the Actual Coordination Time Interval.

SOA Seeker Optimization Algorithm.

SOTB Sum of Operating times of all Backup Relays.

SOTPBR Sum of the Operating Times of the Primary and Backup Relays.

SOTR Sum of Operating Times of all the Relays.

SW Switch.

TCC Time Current Characteristic.

TDS Time Dial Setting.

TMS Time Multiplier Setting.

VIN Very Inverse Relay.

List of Symbols

i Individuals of population $i \in \{1, 2, ..., N\}$.

j Components of an individual $j \in \{1, 2, ..., D\}$.

k Iteration counter ($k \in \{1, 2, ..., Maxite\}$).

μ_{max} Maximum value of membership degree.

μ_{min} Minimum value of membership degree.

bc $bc \in \{bc_1, bc_2, bc_3\}$ is an index of best seeker of first, second and third $1/3^{rd}$ of population.

BW Bandwidth for harmony search.

BW_{max} Maximum value of bandwidth.

BW_{min} Minimum value of bandwidth.

b Index of the best individual in population.

CF Crossover factor.

CR Crossover rate.

c Index of the worst individual in population.

c_1 & c_2 Acceleration factor.

F Mutation factor for differential evolution.

$HMCR$ Harmony memory consideration rate.

$Maxite$ Maximum number of iterations.

MF Mutation factor for genetic algorithm.

PAR Pitch adjustment rate of harmony.

PAR_{max} Maximum value of pitch adjustment rate.

PAR_{min} Minimum value of pitch adjustment rate.

w Inertia factor.

w_{max} Maximum value of inertia factor.

w_{min} Minimum value of inertia factor.

A_{inc} Bus incidence matrix.

$I_{fbackup}$ Maximum value of fault current passing through backup relay.

I_{fmax} Maximum value of fault current.

I_{fmin} Minimum value of fault current.

$I_{fprimary}$ Maximum value of fault current passing through primary relay.

I_{Lmax} Maximum value of load current.

t_{ob} Operating time of backup relay.

t_{opF} Operating time of fuse.

t_{opR} Operating time of recloser.

t_{op} Operating time of primary relay.

Y_{bus} Bus admittance matrix.

Z_{bus} Bus impedance matrix.

$abs(\cdot)$ Return an absolute value of an input complex number.

$f(\cdot)$ Objective function to be evaluated.

$randi(N)$ Return a uniformly generated random integer such that $randi(N) \in \{1, 2, ..., N\}$.

rand Uniformly generated random number in the range [0, 1].

$RAND(\mu_i^k, 1)$ Uniformly generate random number in the range $[\mu_i^k, 1]$.

$rand_j$ Uniformly generated random numbers in [0, 1] for j^{th} component of an individual.

$sign(\cdot)$ Signum function on each variable of the input vector.

$\alpha_{i,j}^k$ j^{th} component of step size of i^{th} seeker at iteration k.

δ_j^k Step length of j^{th} component of a seeker at iteration k.

μ_i^k Membership degree of i^{th} seeker at iteration k.

$d_{i,j,alt1}$ j^{th} component of global altruistic direction of i^{th} seeker.

$d_{i,j,alt2}$ j^{th} component of local altruistic direction of i^{th} seeker.

$d_{i,j,ego}$ j^{th} component of egotistic direction of i^{th} seeker.

$d_{i,j,pro}$ j^{th} component of proactiveness direction of i^{th} seeker.

F_i^k Value of objective function for i^{th} individual of population at iteration k.

$Gbest_j^k$ j^{th} component of the best individual of population upto iteration k.

$Lbest_j^k$ j^{th} component of local best seeker of population at iteration k.

NHV_j j^{th} component of new harmony vector.

$Pbest_{i,j}^k$ Personal best j^{th} component of i^{th} individual of population upto iteration k.

TF_i Value of objective function for trial solution i at iteration k.

$TX_{i,j}$ j^{th} component of i^{th} individual of trial solution.

$U_{i,j}$ j^{th} component of i^{th} individual of trial solution obtained after crossover operation.

$V_{i,j}^k$ Velocity of j^{th} component of i^{th} individual of population at iteration k.

$Xbest_{bc,j}^k$ j^{th} component of the best seeker of a subpopulation $bc \in \{bc_1, bc_2, bc_3\}$ at iteration k.

$X_{i,j}^k$ j^{th} component of i^{th} individual of population at iteration k.

$X_{max,j}$ Maximum value of j^{th} component of an individual of population.

$X_{min,j}$ Minimum value of j^{th} component of an individual of population.

Gbest^k The global best individual of population upto iteration k.

Lbest^k The local best seeker of population at iteration k.

Pbest$_i^k$ Personal best of i^{th} individual of population upto iteration k.

V Initial velocity of N individuals each having D components.

X Population of N individuals each having D components (variables).

$\mathbf{X}_i^k$ i^{th} individual of population **X** at iteration k i.e., $\mathbf{X}_i^k = [X_{i,1}^k, X_{i,2}^k, ..., X_{i,D}^k]$.

$\alpha_{i,j}^k$ j^{th} component of step size of i^{th} seeker at iteration k.

$d_{i,j,alt1}$ j^{th} component of global altruistic direction of i^{th} seeker.

$d_{i,j,alt2}$ j^{th} component of local altruistic direction of i^{th} seeker.

$d_{i,j,ego}$ j^{th} component of egotistic direction of i^{th} seeker.

$d_{i,j,pro}$ j^{th} component of proactiveness direction of i^{th} seeker.

Chapter 1

Introduction

Abstract

In this chapter, detailed introduction of the thesis is presented. Proper coordination is one of the most inherent requirements to run any distribution system with highest reliability. An economic and effective protection scheme for meshed or multi-sourced power systems requires directional overcurrent relays (DOCRs). In radial distribution systems, the feeders are protected by means of reclosers and fuses.

1.1 Overview

A properly coordinated protection scheme is one of the inherent requirements to operate a power system with highest reliability. A good protection scheme removes only the smallest possible portion of the system whenever a fault occurs, so as to maintain supply to the rest of the healthy system unaffected by the fault. Each equipment of a power system is protected with two lines of defence, which are known as primary protection and backup protection. For reliable operation of the system, primary protection must react to a fault as quickly as possible to isolate the faulty parts from the healthy parts, but if primary protection fails to operate, the backup protection should operate. This condition is the most desired feature of any protection scheme as primary protection removes only faulted part whereas, whenever backup protection operates, a larger portion of the system has to suffer from outage unnecessarily. For ensuring that only the faulted portion of the network is disconnected thereby reducing the possibility of unwanted power outage, proper co-ordination among the protective devices is necessary [1–6].

For designing an economic protection system, directional overcurrent relays (DOCRs) are used for primary protection of meshed or multi-sourced sub-transmission and distribution systems as well as for secondary protection of transmission systems [7–10]. A proper coordination among DOCRs is necessary to reduce the possibility of unwanted outages and thus improve the system reliability by ensuring that only a faulted portion of the network is disconnected from the healthy system. Essentially, through coordination, the proper time multiplier setting (TMS) and plug setting (PS) of the relays are determined such that any fault is cleared by the corresponding primary relay as soon as possible. Further, both these settings of any relay should also be properly coordinated with the relays protecting the adjacent equipments which, in turn, makes the co-ordination problem quite complex [11, 12]. In addition, the complexity of the problem is dependent on the type of the DOCRs (electromechanical, static or numerical/digital). In numerical relays, both TMS and PS can take continuous values whereas in other relays (electromechanical and static) TMS can take continuous values and PS can take only discrete values. This further increases the complexity of the problem. Moreover, these relays may follow different characteristic curves such as inverse definite minimum time (IDMT), very inverse (VIN) or extremely inverse (EIN) making the selection of TMS and PS very difficult. It is to be noted that the directions of the DOCRs are always fixed and are considered to be towards the line being protected.

In radial distribution systems, the feeders are protected by means of reclosers and fuses. Fuses are placed at laterals which are at a more remote position from the substation. Whenever a temporary fault occurs in any feeder, the corresponding fuse does not melt because the fast operation of recloser allows the temporary fault to self-clear. But, whenever a permanent fault occurs, the concerned fuse must melt just before the final trip operation of the recloser in order to prevent the loads between the recloser and the fuse from being interrupted. So, a recloser must have at least two operating times and characteristic curves. The proper operating times of recloser are obtained by fixing the proper values of its time dial settings (TDSs). The required operating times of fuses are obtained by selecting the fuses with suitable values of fuse constants.

Through coordination of recloser-fuse, the proper values of TDSs for the recloser and the proper values of fuse constants are obtained. Poor coordination causes momentary voltage interruption and voltage sag which ultimately determine the overall power quality of the system. Therefore, there must be a proper coordination between the recloser and fuses [13–15]. Moreover, integration of distributed generators (DGs) makes the protection coordination more complex. Now, in radial distribution systems, the flow of currents is unidirectional whereas in the presence of DGs into the system, the flow of currents no longer remains unidirectional. Further, integration of DGs at multiple locations can completely alter the flow of currents in the feeder sections during the fault. As a result, there are always chances of miscoordination in the operation of recloser and fuses in the presence of DGs [16, 17].

Any protective device is required to satisfy four basic functional characteristics which are as follows:

- reliability
- selectivity
- speed
- sensitivity

The reliability of a protective device implies that the device should operate when it is required otherwise it should remain idle. The selectivity of a protective device is its ability to isolate the faulty part of the system from the healthy part of the system. Selectivity is achieved in two ways: (a) unit system of protection (section selectivity is achieved on the basis of comparison of electrical quantities at each end of the protected section) and (b) non-unit system of protection (selectivity is obtained on the basis of measurement of electrical quantities at one end of the protected section by the measuring relays and, in some cases, on the exchange of logic signals between the ends). A protective device should neither be too slow (which may result in damage to the equipment), nor it should be too fast (which may result in undesirable operation during transient conditions). A protective device should be sufficiently sensitive so that it can operate reliably to detect smallest values of fault current or system abnormalities and operate correctly at its pre-set settings. It is normally expressed in terms of minimum volt-amperes required for the operation of the relay [18].

1.2 Literature review

To achieve the most effective protection scheme with DOCRs in medium and large interconnected system, the protection coordination problem should be formulated such that the operating times of primary as well as the backup relays are minimized. Further, an appropriate solution procedure should also be developed such that the formulated protection coordination problem is solved in a reasonably short time without any constraint violation. Moreover, in radial distribution system, to achieve the most effective protection scheme with recloser and fuses, the protection coordination should follow the proper operating sequences of recloser and fuses. Next two subsections discuss the prior works available in the literature for addressing the above mentioned issues.

1.2.1 Coordination of directional overcurrent relays coordination

The most important objective in the selection of the settings of relay is to obtain the minimum possible operating times while maintaining coordination among all relays. In the last few decades, several methods have been proposed to achieve the above objective. Commonly, these methods are classified as 1) topological approach and 2) optimization approach.

Topology based approach includes application of linear graph theory and loop breaking approach in multiple loop networks [19–25]. In [20], a study of minimum break point set (MBPS) for all primary and backup relay pairs has been conducted for all simple loops in both directions considering linear graph theory. In [22], a study of optimum break point set (OBPS) for relay pairs has been conducted using integer linear programming. In [24], a graphical procedure has been discussed for selecting the settings of relays whereas in [25] an effort has been made to reduce miscoordination by identifying MBPS by applying expert system.

On the other hand, the optimization based approach formulates the protection coordination problem as i) linear/nonlinear programming (LP/NLP) and ii) Mixed-Integer linear/nonlinear programming (MILP/MINLP) problem which in turn, are solved using suitable optimization approaches. The operating time of a relay depends on two adjustable variables which are TMS and PS as discussed above. It is to be noted that the operating time of a relay is linearly dependent on TMS whereas nonlinearly dependent on PS. As PS is dependent on the maximum load current and minimum fault current so sometimes PS values are fixed to make the optimization problem simple. As a result, the operating time of the relay in such situation only depends on the value of TMS. Therefore, the optimum coordination problem of DOCRs in such cases can be formulated as an LP problem [26], whereas when PS is also considered as a variable then the coordination problem can be formulated as an NLP problem. Now, depending on the type of variables (continuous or discrete) these problems are termed as MILP or MINLP problem [27]. If TMS is considered as a discrete variable in LP problem then it is termed as MILP problem whereas if TMS or PS is considered as a discrete variable in NLP problem then it is termed as MINLP problem. The nature of TMS or PS (discrete or continuous) depends on the type of the relay. Normally, electromechanical/static relays need discrete values whereas numerical/digital relays need continuous values of variables.

In [28, 29], Simplex and Dual-Simplex methods have been adopted to solve relay coordination problems formulated as LP problems. Sequential quadratic programming based algorithms have been used in [30–33] for solving coordination problem of DOCRs formulated as an NLP problem. In [34], the relay coordination problem has been formulated as an MINLP problem which is solved using General Algebraic Modeling System (GAMS) software. Apart from classical optimization techniques, various metaheuristic optimization techniques have also emerged as promising tools for finding the optimal settings of the DOCRs [35–52], in which the problem was formulated as an NLP/MINLP problem. The application of these algorithms has been demonstrated on several small to medium sized systems in all these works. However, it is well known that, these evolutionary algorithms too suffer from getting trapped into local minima and as a result, these algorithms need to be run repeatedly by varying the parameters before selecting the statistically most important result. Consequently, some significant amount of time is required before the final settings of the relays are obtained by the heuristic optimization based approaches.

Moreover, in medium and large interconnected networks it is very difficult to satisfy all the DOCR coordination constraints as observed in [53–55]. Consequently, the protection coordination problems have been reformulated as unconstrained optimization problem by using penalty function approach for handling constraint violations. Such formulations have been solved using genetic algorithm [53, 54] and MBPS [55]. However, several violations of coordination constraints have been observed in these works.

In all the above works, a fixed topology of the network has been assumed. In practice, the system may be operated in different topologies due to outages of the transmission lines, transformers, and generating units. Under such situations the changes in the network topology may lead to miscoordination of DOCRs [56–58]. In [57], the coordination problem considering multiple network topologies has been formulated as an MILP problem and solved using a hybrid method based on LP and genetic algorithm (GA). However, the involvement of GA increases the computational time. In [58], interval linear programming (ILP) has been used to solve the coordination problem considering multiple network topologies where the problem has been formulated as an LP problem. However, as the actual coordination problem of DOCRs is an NLP/MINLP one, both the above methods involve a significant level of approximations.

1.2.2 Recloser-fuse coordination

Proper protection coordination is one of the inherent requirements to operate a distribution system with the highest reliability. Since most of the faults in a power system occur in the distribution system, a sizeable number of consumers will have to suffer unnecessary outages if the protection schemes are not coordinated properly.

Recloser-fuse coordination in radial distribution networks has been widely studied in the literature without considering the presence of any DG [59–63]. In such radial distribution systems, proper coordination can be guaranteed without any miscoordination as the flow of currents remain unidirectional even during the fault. However, the recloser-fuse coordination in the presence of DGs is not a simple task to achieve without any miscoordination. Several studies have been reported in the literature to address the coordination problem of recloser and fuses in the presence of DGs.

In [64], an adaptive protection coordination scheme for recloser and fuses has been studied for radial distribution systems in the presence of high penetration of DGs. In this scheme, the whole network in divided into few zones separated by the remotely controlled circuit breaker. In [65], an adaptive relaying strategy for recloser-fuse coordination by changing recloser settings has been proposed. The adaptive scheme modifies both time delay and instantaneous overcurrent (51 and 50) elements of the recloser dynamically as and when the location and output power of the DG change. However, in these studies, remotely controlled and communication enabled breakers and reclosers are required. In [66], a method to obtain maximum DG injection without affecting recloser-fuse coordination in radial distribution system has been developed. In [67], two complementary solutions have been presented which aim to maintain the recloser-fuse coordination by a) changing DG location and injection level and b) changing fuse and recloser characteristic curves. This approach provides improved coordination by reducing the number of cases of recloser-fuse miscoordination. In [68], a new control strategy for preventing recloser-fuse miscoordination in distribution systems with inverter based DG (IBDG) has been proposed. It is to be noted that to obtain recloser and fuses coordination in all these studies, initially, time dial settings (TDS) for recloser fast and slow modes of operations have been selected and subsequently, with the help of recloser time-current characteristics of the recloser, the characteristics of the fuses have been obtained. Further, in all these studies, it is not possible to achieve absolute coordination with a fixed characteristics of recloser and fuses under various operating conditions of DGs. [69]

In modern radial distribution systems, reconfiguration of the network is an effective method for reducing losses, mitigating operational constraint violations, and improving system performance. By changing the status of tie and sectionalizing switches, a radial configuration can be attained to satisfy the operational requirements [70]. However, the change in network topology adversely affects recloser-fuse coordination and may compromise the system. In [71], feeder reconfiguration considering protective device (recloser and fuses) coordination has been discussed. In order to ensure that the protective devices remain properly coordinated during feeder reconfiguration, the locations of the fuses in the distribution system under study are determined by using a heuristic algorithm. A set of switchable regions within which switch operations are allowed for feeder reconfiguration has been identified. Once the locations of the switches and the switchable regions are determined, the feeders can be reconfigured in real-time distribution system operation with all protective devices properly coordinated by changing the open/closed states of the switches in the switchable regions. However, this study is limited to small or medium size reconfigurable distribution systems. In [72], similar studies have been performed to obtain reconfiguration of radial distribution systems without affecting recloser-fuse coordination. In this study, GA has been used to obtain the new configuration of the system (for achieving minimum active power loss and voltage deviation) while maintaining proper coordination among the protective devices. The proposed method has been validated on IEEE 33-bus, 69-bus and 119-bus distribution test systems. In both the above two studies, main focus was to obtain optimum configuration of the system without affecting recloser-fuse coordination adversely. Also, the impact of DG penetrations has not been considered in these works.

In [73], a new protection scheme involving recloser and fuses has been discussed by utilizing modern available technologies such as smart hardware sensors, redundant communication infrastructure, standard communication protocols and flexible multi-functional software algorithms. The proposed approach has also considered change in network topologies including varying DG penetration. However, because of the presence of several hardware and software elements, this scheme is complex and costly.

1.3 Motivation

Optimization based approach has shown great potential to solve protection coordination problem of DOCRs using various optimization algorithms. Both analytical as well as meta-heuristic optimization algorithms have been used for solving this problem. The actual protection coordination problem of DOCRs is an MINLP one, so meta-heuristic algorithms have been preferred as they are independent of the types of variables. Now, because of the availability of several meta-heuristic optimization methods for co-ordination of DOCRs, it is a natural curiosity to find the most effective meta-heuristic optimization method for practical implementation. However, in the literature, no such comprehensive comparative study is available. Further, in medium and large distribution systems, it is necessary to compute the settings of the DOCRs efficiently in order to minimize the operating times of primary and the corresponding backup relays without any miscoordination. To achieve these requirements, it is necessary to developed a new and effective formulation which also minimizes the operating times of backup relays along with the operating times of primary relays without any constraints violation. Also, protection coordination of DOCRs needs to be obtained which should be robust enough to protect the systems under various system operating conditions such as (N-1) contingency.

In radial distribution system, recloser-fuse coordination studies have been performed mostly using trial and error procedures. However, in the modern network, it is very difficult ot obtain an effective coordination with such procedures when integration of DGs is considered. Further, modern radial distribution systems are equipped to change the configuration to achieve the minimum loss and better voltage profile from time to time. So, it is necessary to obtain a robust settings which can protect the entire systems under such conditions. Recloser-fuse coordination can be formulated as an optimization problem subject to the satisfaction of all required conditions and be solved using a suitable algorithm.

1.4 Contribution of the author

Following the discussion in the above subsection, the studies carried out in this thesis for the coordination of DOCRs are as follows:

- A comparative assessment of meta-heuristic methods for finding out the most effective one.

- Formulation of DOCR coordination problem as an optimization problem to minimize the operating times of primary and backup relays simultaneously without any constraint violation for large interconnected systems.
- Development of a new analytical optimization algorithm to solve the formulated problem effectively and efficiently.
- Calculation of robust settings of DOCRs which can ensure proper coordination under feasible (N-1) contingencies.

Similarly, the following studies are conducted for the coordination of recloser and fuses for radial distribution system:

- Formulation of the recloser-fuse coordination problem as an optimization problem.
- Calculation of settings for recloser-fuse coordination in radial distribution systems in the presence of DGs.
- Calculation of settings for recloser-fuse coordination for reconfigurable radial distribution systems in the presence of DGs.

1.5 Thesis organization

Apart from this chapter, there are six more chapters in this thesis. In Chapter 2, a comparative study of various meta-heuristic optimization algorithms has been carried out. In this chapter, five popular meta-heuristic algorithms have been used to solve the coordination problem of DOCRs on six different systems. On the basis of the comparative study, one of the algorithms has been found to be the best in solving protection coordination problem of DOCRs. In Chapter 3, initially, the existing problem formulations available in the literature have been studied and subsequently, a new problem formulation is proposed to minimize the operating time of primary and backup relays simultaneously while satisfying coordination requirements. Also, two distinct two-phase analytical optimization algorithms have been developed for solving the formulated problem. The effectiveness of the proposed formulation and the algorithms have been validated by solving the protection coordination problem of three power system networks of various sizes. In Chapter 4, robust protection coordination of DOCRs is discussed which has the ability to coordinate properly under allowable (N-1) contingencies. The proposed approach has been validated on three interconnected test systems of medium and large size. Chapters 5 and 6 discuss the optimum recloser-fuse coordination problem. In Chapter 5, recloser-fuse coordination problem of radial distribution system is formulated as an optimization problem and subsequently is solved using the developed analytical algorithm. The proposed approach has been validated by solving recloser-fuse coordination problem on two radial distribution systems of various sizes in the presence of DGs. In Chapter 6, the developed formulation and algorithm of Chapter 5 have been extended to solve the recloser-fuse coordination problem of reconfigurable radial distribution systems in the presence of DGs. The proposed approach has been validated on two reconfigurable radial distribution systems in the presence of DGs. Finally, the conclusions of the thesis are presented in Chapter 7

In this thesis all simulation studies have been carried out in MATLAB 12a [74] and AMPL environment [75].

In the next chapter, review of protection coordination using metaheuristic optimization techniques is discussed.

Chapter 2

Comparison of Metaheuristic Algorithms for Protection Coordination of Directional Overcurrent Relays

Abstract

In this chapter, a comparative study of different meta-heuristic optimization approaches, which had been proposed in the literature for directional overcurrent relay coordination (DOCRs), is presented. Towards this goal, five most effective meta-heuristic optimization approaches such as genetic algorithm (GA), particle swarm optimization (PSO), differential evolution (DE), harmony search (HS) and seeker optimization algorithm (SOA) have been considered. The performances of these optimization methods have been investigated on several power system networks of different sizes. The comparative performances of these methods have been studied by executing each method 100 times with the same initial conditions and based on the obtained results, the best meta-heuristic optimization method for solving the coordination problem of directional overcurrent relays is identified.

2.1 Introduction

RECENTLY, meta-heuristic optimization approaches have shown great potential to solve protection coordination problems of directional overcurrent relays (DOCRs) [52]. Application of various meta-heuristic optimization approaches such as particle swarm optimization (PSO) [39, 76–78], genetic algorithm (GA) [31, 53, 79–82], differential evolution (DE) [83–87], harmony search (HS) [36], seeker optimization algorithm (SOA) [40] etc. have been proposed in the literature for solving the protection co-ordination problem. The applications of these algorithms have been demonstrated on several small to medium sized systems in all these works. Although these approaches are somewhat time consuming but they provide quite high quality solutions.

Now, because of the availability of several meta-heuristic optimization methods for co-ordination of DOCRs, it is a natural curiosity to find the most effective meta-heuristic optimization method for practical implementation. However, in the literature, no such comprehensive comparative study is available. Motivated by this fact, in this chapter, a comparative study is carried out for finding out the most effective method.

2.2 Problem formulation of protection coordination

The protection coordination problem can be formulated as an optimization problem where the objective is to minimize the sum of the operating times of all DOCRs for the near-end three phase fault current [28, 88]. Therefore, the objective function (OF) is expressed as,

$$\min \sum_{l=1}^{n} t_{op,l} \tag{2.1}$$

In eqn. (2.1), n is the number of relays in the system and $t_{op,l}$ is the operating time of the relay R_l. The operating times of the relays are obtained from their characteristic curves which are defined by IEC/IEEE [60] as,

$$t_{op} = \frac{\lambda \times \mathit{TMS}}{(I_F/\mathit{PS})^{\eta} - 1} + L \tag{2.2}$$

In eqn. (2.2) λ, η and L are the characteristic constants of the relays while I_F is the fault current through the relay operating coil. For standard inverse definite minimum time (IDMT) relays $\lambda = 0.14$, $\eta = 0.02$, and $L = 0$ [60]. On the other hand, for very inverse (VI) relays $\lambda = 13.5$, $\eta = 1$, and $L = 0$ and for extremely inverse (EI) relays $\lambda = 80$, $\eta = 2$, and $L = 0$ [60, 89].

The objective function defined above is subjected to the following sets of constraints [28, 29]:

1) *Limitations on TMS, PS and t_{op} of Relays*: The limits on *TMS*, *PS* and t_{op} of relays are expressed as,

$$\mathit{TMS}_{l,min} \leq \mathit{TMS}_l \leq \mathit{TMS}_{l,max} \tag{2.3}$$

$$\mathit{PS}_{l,min} \leq \mathit{PS}_l \leq \mathit{PS}_{l,max} \tag{2.4}$$

$$t_{l,min} \leq t_{op,l} \leq t_{l,max} \tag{2.5}$$

In eqn. (2.3), $\mathit{TMS}_{l,min}$ and $\mathit{TMS}_{l,max}$, in eqn. (2.4), $\mathit{PS}_{l,min}$ and $\mathit{PS}_{l,max}$ and in eqn. (2.5) $t_{l,min}$ and $t_{l,max}$ are the minimum and maximum limits of TMS, PS and operating time (t_{op}) of relay R_l, respectively. Now, from eqns. (2.2)-(2.5), it may appear that if eqns. (2.3) and (2.4) are satisfied, then eqn. (2.5) is redundant. However, this is not so, as the operating time of the relay depends not only on TMS and PS but also on the fault current (I_F) according to eqn. (2.2).

Even if TMS and PS are in the correct range, the operating time of the relay may not be in the correct range. For example, let us suppose that TMS and PS of a relay is 0.6 and 2.0, respectively, which are well within their respective ranges (these ranges are given in Section 2.4). Now, let us suppose that a fault occurs near the relay and causes 1600 A current to flow to the fault point. If current transformer (CT) ratio is 500:1, then 3.2 A current will flow through the secondary of the transformer and hence through the relay. Now, operating time of the relay (according to eqn. (2.2) for IDMT type) in this situation will be 8.8942 seconds $(0.14 \times 0.6/((3.2/2)^{0.02} - 1))$ which is very large and not in the range of [0.1, 4.0] seconds (as mentioned in Section 2.4).

2) $Protection\ Coordination\ Criteria$: If primary relay R_l has a backup relay R_m for a fault at any point k, then the corresponding coordination constraint can be expressed as

$$t_{ob,m} - t_{op,l} \geq \textit{CTI} \tag{2.6}$$

In eqn. (2.6), $t_{op,l}$ and $t_{ob,m}$ are the operating time of primary relay R_l and its backup relay R_m, respectively, for the same fault and *CTI* is the coordination time interval required for proper operation of primary/backup relays.

2.3 Metaheuristic optimization algorithms to solve protection coordination problems

Five highly efficient metaheuristic algorithms suitable for solving the protection coordination problems are investigated in this chapter. These five algorithms are GA, PSO, DE, HS and SOA. All these methods start from an initial solution to attain the optimum point in the search space. The size of the population is considered as N and the dimension of each element of the population is considered as D, where D represents the total number of variables. Thus, the initial solution is denoted as $\mathbf{X} = [\mathbf{X}_1,\mathbf{X}_2,...,\mathbf{X}_N]^T$, where $'T'$ denotes the transpose operator. Each individual $\mathbf{X}_i$ $(i = 1, 2, ..., N)$ is given as $\mathbf{X}_i = [X_{i,1}, X_{i,2}, ..., X_{i,D}]$. A protection scheme with n DOCRs will have $2 \times n$ number of variables (i.e., $D = 2n$). The first n variables represent TMS values whereas the next n variables represent PS values of the relays in the system. The detailed algorithms of various methods are described below for completeness. In all these algorithms, the index i varies from 1 to N whereas the index j varies from 1 to D. Further, in all these algorithms, the superscript 'k' denotes the iteration number.

2.3.1 Genetic Algorithm

Genetic algorithm (GA) is a nature inspired meta-heuristic optimization approach suitable to solve any optimization problem irrespective of the type of objective function. The algorithm starts with a randomly generated solution called chromosomes and endeavors to reach the optimum point by reproduction, crossover and mutation operations. The crossover factor (CF) is expressed as the probability of pairs of chromosomes to produce offsprings (crossover) whereas mutation factor (MF) represents the probability of changing the status of a randomly selected binary bit of a chromosome from 0 to 1 and vice versa (mutation). The different steps of GA are as follows [31]:

1. Set parameter *CF* and *MF* of GA
2. Initialize population of chromosomes i.e., the solution $\mathbf{X}$
3. Set iteration $k = 1$
4. Calculate fitness of chromosomes $F_i^k = f(\mathbf{X}_i^k), \forall i$ and find the index of the best chromosome $b \in \{1, 2, ..., N\}$
5. Perform selection of chromosomes, crossover of parents and mutation of offsprings to form a new set of chromosomes $\mathbf{X}_i^{k+1}, \forall i$
6. Evaluate fitness $F_i^{k+1} = f(\mathbf{X}_i^{k+1}), \forall i$ and identify the best chromosome $b1$
7. If $F_{b1}^{k+1} < F_b^k$ then $b = b1$
8. If $k < \textit{Maxite}$ then $k = k + 1$ and goto step 5 else goto step 9
9. Print optimum solution as $\mathbf{X}_b^k$

2.3.2 Particle Swarm Optimization

Particle swarm optimization (PSO) is inspired by social and cooperative behavior displayed by various species to fill their needs in the search space. The algorithm is guided by personal experience (Pbest), overall experience (Gbest) and the present movement of the particles to decide their next positions in the search space. Further, the experiences are accelerated by two factors c_1 and c_2, and two random numbers generated between [0, 1] whereas the present movement is multiplied by an inertia factor w varying between $[w_{min}, w_{max}]$. The initial velocity of the population is denoted as $\mathbf{V}$ = $[\mathbf{V}_1, \mathbf{V}_2, ..., \mathbf{V}_N]^T$, where $'T'$ denotes the transpose operator. Thus, the velocity of each particle $\mathbf{X}_i$ $(i = 1, 2, ..., N)$ is given as $\mathbf{V}_i$=$[V_{i,1}, V_{i,2}, ..., V_{i,D}]$. The different steps of PSO are as follows [90]:

1. Set parameter w_{min}, w_{max}, c_1 and c_2 of PSO

2. Initialize population of particles having positions $\mathbf{X}$ and velocities $\mathbf{V}$

3. Set iteration $k = 1$

4. Calculate fitness of particles $F_i^k = f(\mathbf{X}_i^k), \forall i$ and find the index of the best particle b

5. Select $\mathbf{Pbest}_i^k = \mathbf{X}_i^k, \forall i$ and $\mathbf{Gbest}^k = \mathbf{X}_b^k$

6. $w = w_{max} - k \times (w_{max} - w_{min})/$*Maxite*

7. Update velocity and position of particles

   $V_{i,j}^{k+1} = w \times V_{i,j}^k + c_1 \times rand \times (Pbest_{i,j}^k - X_{i,j}^k) + c_2 \times rand \times (Gbest_j^k - X_{i,j}^k);\ \forall j$ and $\forall i$

   $X_{i,j}^{k+1} = X_{i,j}^k + V_{i,j}^{k+1};\ \forall j$ and $\forall i$

8. Evaluate fitness $F_i^{k+1} = f(\mathbf{X}_i^{k+1}), \forall i$ and find the index of the best particle $b1$

9. Update Pbest of population $\forall i$

   If $F_i^{k+1} < F_i^k$ then $\mathbf{Pbest}_i^{k+1} = \mathbf{X}_i^{k+1}$ else $\mathbf{Pbest}_i^{k+1} = \mathbf{Pbest}_i^k$

10. Update Gbest of population

    If $F_{b1}^{k+1} < F_b^k$ then $\mathbf{Gbest}^{k+1} = \mathbf{Pbest}_{b1}^{k+1}$ and set $b = b1$ else $\mathbf{Gbest}^{k+1} = \mathbf{Gbest}^k$

11. If $k <$ *Maxite* then $k = k + 1$ and goto step 6 else goto step 12

12. Print optimum solution as $\mathbf{Gbest}^k$

2.3.3 Differential Evolution

Differential evolution (DE) is a parallel direct search method guided by crossover, mutation and selection operations on a population. For each element of the population a mutant element is generated by adding the difference between two mutually independent elements multiplied by a mutation factor F. Subsequently, crossover is performed to make trial elements of the same size as the population with a crossover rate (CR). After that, selection is performed to pickup better trial elements. The different steps of DE used in this study are as follows [91]:

1. Set parameter F and *CR* of DE
2. Initialize population of elements $\mathbf{X}$
3. Set iteration $k = 1$
4. Calculate fitness of elements $F_i^k = f(\mathbf{X}_i^k), \forall i$ and find the index of the best particle b
5. Perform mutation with three mutually different random indices $a_1, a_2, a_3 \in \{1, 2, ..., N\}$ to generate trial solution

   $TX_{i,j} = X_{a_1,j}^k + F \times (X_{a_2,j}^k - X_{a_3,j}^k)\ ;\ \forall j$ and $\forall i$
6. Perform crossover on trial solution with the help of the *CR* and a randomly generated index $randb$ where $randb = randi(D) \in \{1, 2, ..., D\}$

$$U_{i,j} = \begin{cases} TX_{i,j} & if\ rand \leq CR\ or\ j = randb \\ X_{i,j}^k & if\ rand > CR\ and\ j \neq randb \end{cases}$$

7. Evaluate trial fitness $TF_i = f(U_{i,1}, U_{i,2}, ..., U_{i,D}), \forall i$
8. Perform selection of trial solution $\forall i$

$$X_{i,j}^{k+1} = \begin{cases} U_{i,j}\ \forall j\ if\ TF_i < F_i^k \\ X_{i,j}^k\ \forall j\ if\ TF_i \geq F_i^k \end{cases}$$

9. Evaluate fitness $F_i^{k+1} = f(\mathbf{X}_i^{k+1}), \forall i$ and find the index of the best element b

10. If $k < \mathit{Maxite}$ then $k = k + 1$ and goto step 5 else goto step 11

11. Print optimum solution as $\mathbf{X}_b^k$

2.3.4 Harmony Search

Harmony search (HS) algorithm is inspired by the creative process of music composition where music players improvise the pitches of their instruments to obtain better harmony. The algorithm is guided by harmony memory consideration rate (HMCR), pitch adjustment rate (PAR) and bandwidth (BW) to obtain improved harmony memory (HM) i.e., solution vectors after each iteration. The different steps of HS are as follows [92]:

1. Set parameter BW_{min}, BW_{max}, PAR_{min}, PAR_{max} and HMCR of HS

2. Initialize population of harmonies $\mathbf{X}$

3. Calculate fitness of harmony $F_i^k = f(\mathbf{X}_i^k), \forall i$ and find the index of the best harmony b and the index of the worst harmony c

4. Set iteration $k = 1$

5. $\mathit{PAR} = \mathit{PAR}_{min} + k \times (\mathit{PAR}_{max} - \mathit{PAR}_{min})/\mathit{Maxite}$

6. $\mathit{BW} = \mathit{BW}_{max} - k \times (\mathit{BW}_{max} - \mathit{BW}_{min})/\mathit{Maxite}$

7. Generate a new harmony with randomly generated numbers $r_1 \in [0, 1]$ and $r_j \in [0, 1], \forall j$

$$\mathit{NHV}_j = \begin{cases} X_{randi(N),j} + rand \times \mathit{BW},\ if\ r_1 < \mathit{HMCR} \text{ and } r_j < \mathit{PAR} \\ X_{randi(N),j},\ \ if\ r_1 < \mathit{HMCR} \text{ and } r_j > \mathit{PAR} \\ X_{min,j} + rand \times (X_{max,j} - X_{min,j}),\ \ otherwise \end{cases}$$

8. Evaluate trial fitness $\mathit{TF} = f(\mathit{NHV}_1, \mathit{NHV}_2, ..., \mathit{NHV}_D)$

9. If $\mathit{TF} < F_b^k$ then $X_{b,j}^k = \mathit{NHV}_j, \forall j$ elseif $\mathit{TF} < F_c^k$ then $X_{c,j}^k = \mathit{NHV}_j, \forall j$ and find the index of the worst harmony c else goto step 7

10. If $k < \mathit{Maxite}$ then $k = k + 1$ and goto step 5 else goto step 11

11. Print optimum solution as $\mathbf{X}_b^k$

2.3.5 Seeker Optimization Algorithm

The seeker optimization algorithm (SOA) is a computational search algorithm inspired by the behaviour of human memory consideration, experience gained, uncertainty reasoning, and social learning. A simple fuzzy rule is used to evaluate seekers step length. The different steps of SOA are as follows [93]:

1. Set parameter w_{min}, w_{max}, μ_{min} and μ_{min} of SOA

2. Initialize the solution i.e., population of seekers $\mathbf{X}$

3. Set iteration $k = 1$

4. Calculate fitness of seeker $F_i^k = f(\mathbf{X}_i^k), \forall i$ and find the index of the best seeker b and the indices of locally best seekers bc_1, bc_2 and bc_3 among first, second and third 1/3rd of population, respectively.

5. Select $\mathbf{Pbest}_i^k = \mathbf{X}_i^k, \forall i$, $\mathbf{Gbest}^k = \mathbf{X}_b^k$, $\mathbf{Lbest}^k = \mathbf{X}_b^k$ and $\mathbf{Xbest_{bc}^k} = \mathbf{X}_{bc}^k, \forall bc$ where $bc \in \{bc_1, bc_2, bc_3\}$

6. Calculate search direction $\forall j$ and $\forall i$

   $d_{i,j,ego} = sign(Pbest_{i,j}^k - X_{i,j}^k)$

   $d_{i,j,alt1} = sign(Gbest_j^k - X_{i,j}^k)$

   $d_{i,j,alt2} = sign(Lbest_j^k - X_{i,j}^k)$

   $d_{i,j,pro} = sign(X_{i,j}^{k_1} - X_{i,j}^{k_2})$

   where $k_1, k_2 \in \{k, k-1, k-2\}$ such that $f(X_i^{k_1}) < f(X_i^{k_2})$

   $sd_{i,j} = \{d_{i,j,ego}, d_{i,j,alt1}, d_{i,j,alt2}, d_{i,j,pro}\}$

$$d_{i,j}^{k+1} = \begin{cases} 0, \; if \; rand_j < (no. \; of \; zeros \; in \; sd_{i,j})/4 \\ +1, \; elseif \; rand_j < (no. \; of \; zeros + no. \; of \; ones \; in \; sd_{i,j})/4 \\ -1, \; else \end{cases}$$

7. Calculate step size $\forall j$ and $\forall i$

   $w = w_{max} - k \times (w_{max} - w_{min})/\textit{Maxite}$

   $\mu_i^{k+1} = \mu_{max} - (s - I_i^{k+1}) \times (\mu_{max} - \mu_{min}), \forall i$

   $\delta_j^{k+1} = w \times abs(Xbest_{bc\_1,j}^{k+1} - X_{bc\_2,j}^{k+1}), \forall j$

   $\alpha_{i,j}^{k+1} = \delta_j^{k+1} \sqrt{-\log(\textit{RAND}(\mu_i, 1))}$; $\forall j$ and $\forall i$

   where $s = \{1, 2, ..., N\}$, I_i= index of sorted fitness function, bc_1 and bc_2 are two mutually different indices of locally best seekers $bc \in \{bc_1, bc_2, bc_3\}$ and $\textit{RAND}(\mu_i, 1)$ generates random number uniformly in $[\mu_i, 1]$

8. Update seeker position

   $X_{i,j}^{k+1} = X_{i,j}^{k} + \alpha_{i,j}^{k+1} \times d_{i,j}^{k+1}$; $\forall j$ and $\forall i$

9. Evaluate fitness $F_i^{k+1} = f(\mathbf{X}_i^{k+1}), \forall i$ and find the index of the best seeker $b1$ and the indices of locally best seekers bc_1, bc_2, and bc_3 of the first, second and third 1/3rd of the newly generated solution $\mathbf{X}^{k+1}$

10. Update Pbest, Gbest, Lbest and Xbest

    If $F_i^{k+1} < F_i^k$ then $\mathbf{Pbest}_i^{k+1} = \mathbf{X}_i^{k+1}, \forall i$ else $\mathbf{Pbest}_i^{k+1} = \mathbf{Pbest}_i^k, \forall i$

    If $F_{b1}^{k+1} < F_b^k$ then $\mathbf{Gbest}^{k+1} = \mathbf{Pbest}_{b1}^{k+1}$ and $b = b1$ else $\mathbf{Gbest}^{k+1} = \mathbf{Gbest}^k$

    $\mathbf{Lbest}^{k+1} = \mathbf{Pbest}_{b1}^{k+1}$

    $\mathbf{Xbest}_{bc}^{k+1} = \mathbf{Pbest}_{bc}^{k+1}$

11. If $k < \textit{Maxite}$ then $k = k + 1$ and goto step 6 else goto step 12

12. Print optimum solution as $\mathbf{Gbest}^k$

In this work, for evaluating the reproducibility of results obtained by different methods, each method has been executed 100 times. Subsequently, with these results obtained from 100 runs, various statistical parameters such as mean, standard deviation etc. have been calculated for the purpose of overall comparison. Figure 2.1 shows the comprehensive flowchart for the overall procedure adopted in this work.

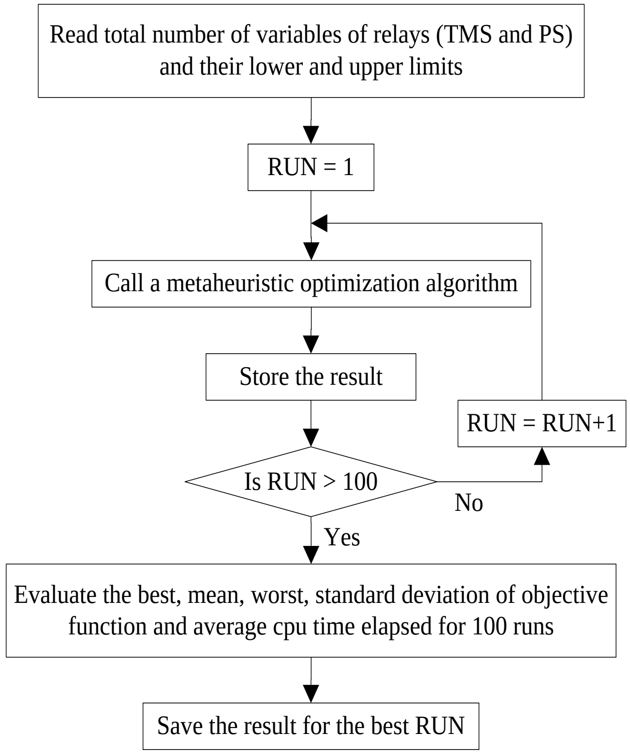

Figure 2.1: Flowchart of the basic procedure.

The following parameters have been considered for executing various methods. The population size of all the methods has been taken as 60 except DE and HS for which it is taken as 30 and 10, respectively, which gives better result. The crossover factor (*CF*) and the mutation factor (*MF*) for GA have been considered as 0.8 and 0.01, respectively, [31]. For PSO, the two acceleration coefficients (c_1 and c_2) and the minimum and maximum value of inertial factor (w_{min} and w_{max}) have been taken as 2.025, 2.025 and 0.4, 0.9, respectively, [90]. For DE, the crossover rate (*CR*) and the mutation factor (F) have been considered as 0.4 and 0.5, respectively, [91]. For HS, the harmony memory consideration rate (*HMCR*) and minimum and maximum values of bandwidth (BW_{min} and BW_{max}) and pitch adjustment rate (PAR_{min} and PAR_{max}) are considered as 0.9 and 0.0001, 1.0 and 0.4, 0.7, respectively, [92]. Finally, for SOA, the minimum and maximum values of inertia factor (w_{min} and w_{max}) and membership degree (μ_{min} and μ_{max}) have been considered as 0.1, 0.9 and 0.0111, 0.95, respectively, [93].

For further reference, all these above values of the parameters are termed as ”standard values”. Initially, the performances of all the algorithms have been investigated with these standard values. However, for further investigations of the performances of the algorithms, these parameters have been varied from their ”standard values” as follows: a) the values of *CF*, *MF*, *CR*, *F* and *HMCR* have been varied randomly by $\pm 20\%$ (vis-a-vis their standard values), b) the values of interval factor (for PSO and SOA), bandwidth and pitch adjustment rate (for HS) have been chosen randomly within their respective specified limits (instead of following the equations given in Section 2.3.2, 2.3.4 and 2.3.5) and c) following the recommendation of [93], the values of (μ_{min} and μ_{max}) are kept unchanged. For further reference these modified values are termed as ”perturbed values”.

2.4 Results and discussion

The algorithms described in Section 2.3 have been applied to solve the protection coordination problem of six power distribution systems of different sizes. In all these systems, numerical relays with standard IDMT characteristics have been considered. However, in the third test system, two cases have been considered. In the first case IDMT characteristics of all the relays have been assumed whereas the second case considers other characteristic curves of the relays in addition to IDMT characteristics. The minimum and the maximum limits on TMS have been considered as 0.1 and 1.1, respectively, whereas the minimum and the maximum limits on PS are taken as: $PS_{min} = max\{0.5, min\{1.25 \times I_{Lmax}, 1/3 \times I_{Fmin}\}$; and $PS_{max} = min\{2.5, 2/3 \times I_{Fmin}\}$, where I_{Lmax} and I_{Fmin} are the maximum load current and minimum fault current, respectively, [31, 40]. Further, the minimum CTI considered for all the six system is 0.2 seconds [31]. Also, the minimum and the maximum limits on t_{op} has been considered as 0.1 and 4.0 seconds, respectively. All these meta-heuristic optimization techniques have been implemented in MATLAB environment [74]. To investigate the performances of the algorithms comprehensively, all the algorithms have been executed using two sets of parameter values: ”standard values” and ”perturbed values” (as described in the previous section). In the following subsections, the results obtained on these six systems are presented in detail.

2.4.1 System I: 9-bus test system

Figure 2.2 shows the single line diagram of the 9-bus single source ring main distribution system. This system is fed at bus 1. The detailed information about the system is available in [31]. In this system, there are 12 lines (L1,L2,..., L12) and 24 relays (R1,R2,...,R24) having 32 combinations of primary-backup relationship among them. Table 2.1 shows these 32 combinations of primary-backup relationship among all the 24 relays. The fault currents passing through the primary and

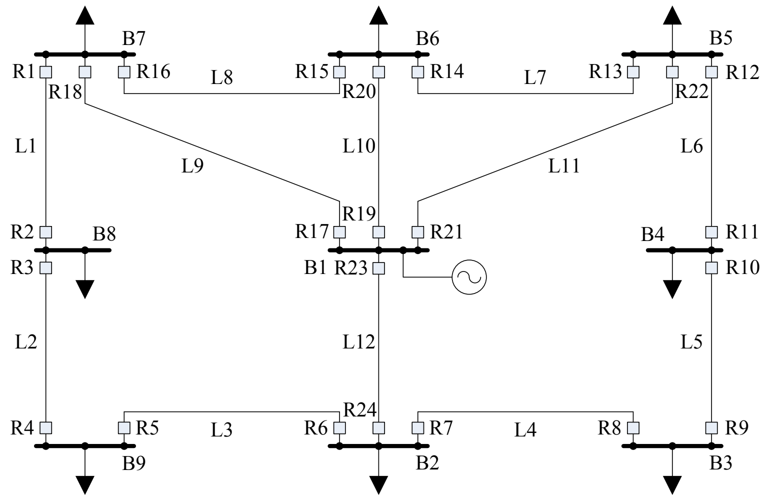

Figure 2.2: Single-line diagram of the 9-bus system.

the corresponding backup relays for various near-end three phase faults and the maximum as well as minimum fault current through the relays are given in [31] and hence are not repeated here. The current transformer (CT) ratio required for each relay is also given in [31].

Table 2.1: Primary/backup relay pairs of the 9-bus system

Fault Zone	Primary Relay	Backup Relay	Fault Zone	Primary Relay	Backup Relay
L1	1	15, 17	L7	13	11, 21
	2	4		14	16, 19
L2	3	1	L8	15	13, 19
	4	6		16	2, 17
L3	5	3	L9	17	–
	6	8, 23		18	2, 15
L4	7	5, 23	L10	19	–
	8	10		20	13, 16
L5	9	7	L11	21	–
	10	12		22	11, 14
L6	11	9	L12	23	–
	12	14, 21		24	5, 8

The optimum settings i.e., TMS and PS of the relays obtained by different methods using standard parameter values are given in Table 2.2 whereas the coordination time interval (*CTI*) between the time of operations of the primary relay (t_{op}) and that of the corresponding backup relays (t_{ob}) are plotted in Figure 2.3. It is to be noted that the best results (for the minimum value of objective function) obtained after 100 runs of each method corresponding to the standard parameter values are given in Table 2.2 and Figure 2.3. The last row in Table 2.2 gives the values of the sum of the operating times of all the relays i.e., objective function value (OFV) corresponding to the set of TMSs and PSs obtained by each method. Table 2.3 shows the summary of the results obtained after 100 runs by different methods with standard parameter values whereas Table 2.4 shows the corresponding values obtained with the perturbed parameter values. These tables summarise the best, mean and the worst values of the objective function along with its standard deviation and the average elapsed time (sec) for executing each algorithm.

Table 2.2: Optimum settings of relays for the 9-bus system obtained with standard parameter values

Relays	GA		PSO		DE		HS		SOA	
	TMS	PS	TMS	PS	TMS	PS	TMS	PS	TMS	PS
1	0.4395	0.5	0.2806	1.2478	0.1241	2.5	0.1447	2.1741	0.2662	1.2732
2	0.3086	0.5001	0.1636	1.8196	0.1	2.0899	0.1	2.294	0.2076	1.52
3	0.317	1.3484	0.3878	0.5	0.137	2.5	0.1684	1.8739	0.2928	1.1975
4	0.2194	1.5477	0.2015	2.4998	0.1089	2.5	0.1138	2.4472	0.3192	0.6701
5	0.4358	0.5111	0.2126	1.8823	0.1237	2.5	0.1309	2.4175	0.2879	1.0785
6	0.2289	1.6634	0.4266	0.5	0.1277	2.5	0.1384	2.2897	0.3677	0.6311
7	0.4339	0.5	0.2045	2.5	0.1277	2.5	0.1388	2.3249	0.3006	0.9637
8	0.2093	1.7504	0.193	2.5	0.1237	2.5	0.13	2.4176	0.2905	1.1393
9	0.3897	0.5	0.3401	0.5	0.1089	2.5	0.1212	2.2509	0.2476	1.1994
10	0.374	0.5	0.4048	0.5	0.137	2.5	0.1598	2.0335	0.248	1.7451
11	0.3491	0.5	0.2246	1.0882	0.1	2.0899	0.1	2.3288	0.2578	0.8454
12	0.2015	1.909	0.4084	0.5	0.1241	2.5	0.1393	2.259	0.3665	0.6461
13	0.2756	1.1158	0.3046	0.5537	0.1	2.2969	0.1021	2.3465	0.2581	0.9784
14	0.1965	1.607	0.1661	2.4561	0.109	2.5	0.1141	2.4932	0.3117	0.886
15	0.3812	0.6744	0.1832	2.0707	0.109	2.5	0.1165	2.4666	0.2921	0.8993
16	0.3034	0.5002	0.3109	0.5	0.1	2.2969	0.1183	1.936	0.3633	0.5004
17	0.298	0.8949	0.1555	1.9859	0.1	2.1606	0.1	2.3568	0.256	0.9197
18	0.1	0.5193	0.1	0.5041	0.1	0.5	0.1002	0.6198	0.1038	0.5003
19	0.1686	1.6592	0.2265	0.75	0.1	1.6462	0.1292	1.2409	0.2589	0.7629
20	0.1	0.5	0.1001	0.5031	0.1	0.5	0.1001	0.7395	0.1002	0.5041
21	0.2587	0.7805	0.1286	2.5	0.1	2.1606	0.1	2.4717	0.2758	0.8902
22	0.1	0.5	0.1001	0.504	0.1	0.5	0.1002	0.7203	0.101	0.5008
23	0.2607	0.9776	0.2967	0.7501	0.1	1.9435	0.1334	1.4234	0.1757	1.5724
24	0.1	0.5001	0.1	0.5041	0.1	0.5	0.1002	0.5572	0.1014	0.5017
OFV	14.5426		13.9472		**8.6822**		9.2339		14.2338	

Table 2.3: Summary of results obtained after 100 independent runs for the 9-bus system with standard parameter values

Methods	Objective function value			Standard deviation	Average elapsed time (sec)
	Best	Mean	Worst		
GA	14.5426	15.6592	16.8083	0.4110	360.70
PSO	13.7150	20.6491	31.0790	3.6823	22.22
DE	**8.6822**	**8.7162**	**9.4859**	**0.1233**	**7.29**
HS	9.2339	9.6180	10.1411	0.2152	122.15
SOA	14.2338	16.5710	19.9820	1.2133	30.20

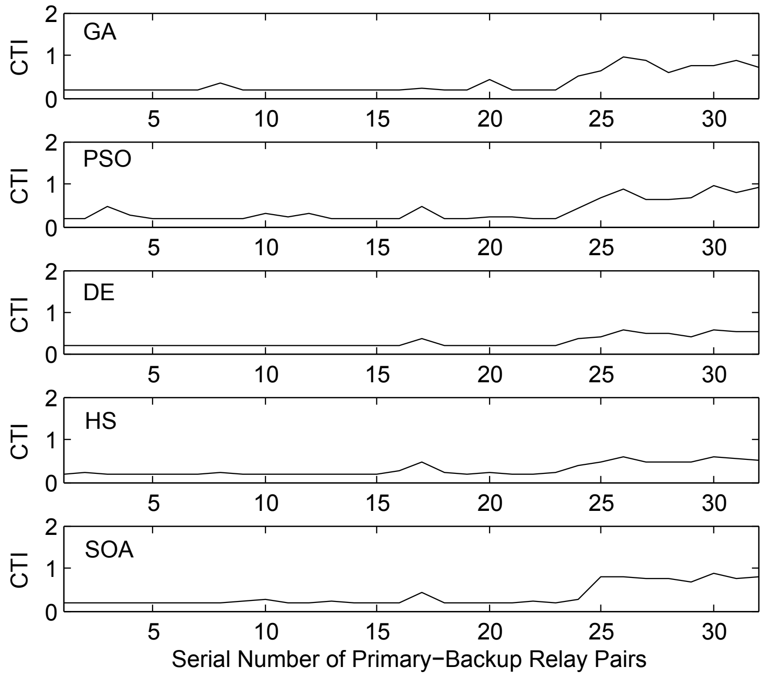

Figure 2.3: CTI otained by various methods for the 9-bus system obtained with standard parameter values.

Table 2.4: Summary of results obtained after 100 independent runs for the 9-bus system with perturbed parameter values

Methods	Objective function value			Standard deviation	Average elapsed time (sec)
	Best	Mean	Worst		
GA	14.5888	15.888	18.0465	0.6271	314.44
PSO	13.6084	22.7949	31.8319	4.8349	**3.97**
DE	**8.6822**	**8.7060**	**9.5716**	**0.1212**	15.06
HS	9.2098	9.2205	9.4667	0.0368	155.56
SOA	14.2501	16.3973	21.6199	1.1969	33.74

From Table 2.3 it is observed that among all these five methods, the DE method gives the least value of the objective function (8.6822 seconds) and the standard deviation (0.1233). As the standard deviation is quite low for DE as compared to the other methods, it can be inferred that DE gives the most predictable results when it is executed repeatedly as compared to the other four methods. Further, the results obtained by DE are of high quality as the mean and the worst values of the objective function are close to the best value. Also, from Figure 2.3, it is observed that among these five methods, the DE gives the lowest values of CTI.

Again, from Table 2.4 it is observed that DE gives the best result (the least value of the objective function) among all these five methods. It is also observed from Tables 2.3 and 2.4 that with DE, the best value of the objective function remains the same with standard parameter values as well as with perturbed parameter values. Therefore, the best value (of the objective function) obtained by DE can be considered to be immune to variation in the parameter values. However, for the other four methods, the best values (and also the other values) of the objective functions change with variation in the parameter values. Also, DE is reasonably time efficient (fastest with standard parameters and second fastest with perturbed parameters) as compared to the other algorithms.

2.4.2 System II: 15-bus test system

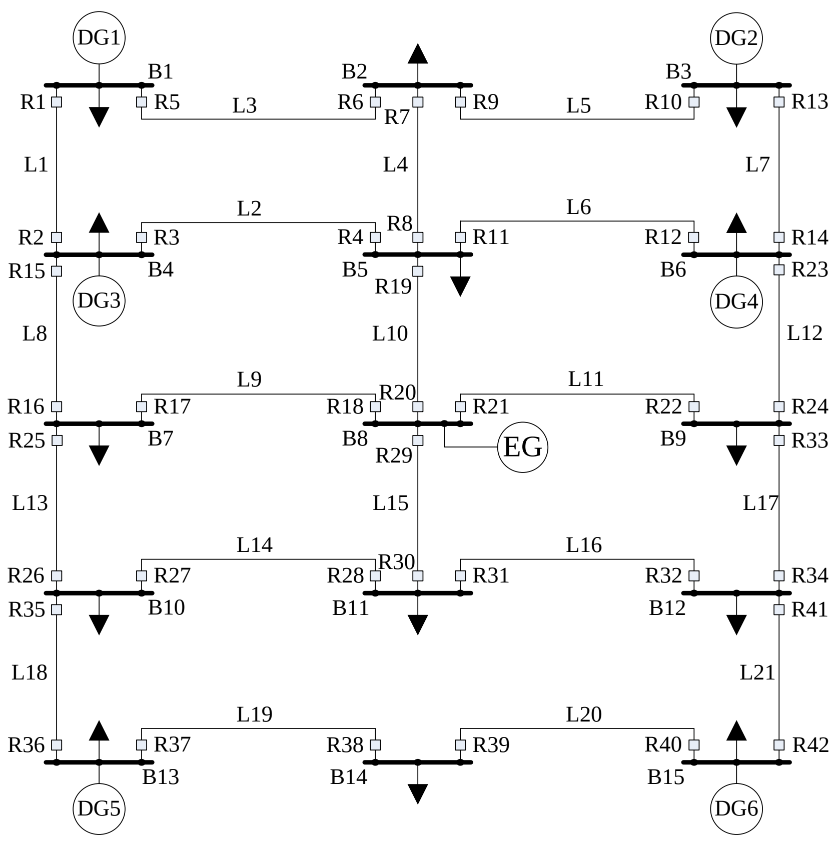

Figure 2.4: Single-line diagram of the 15-bus system.

Figure 2.4 shows single line diagram of the 15-bus network fed by an external grid (EG) at bus 8 and six distributed generators (DGs) connected at buses 1, 3, 4, 6, 13 and 15. The detailed information about the system is available in [40]. In this system, there are 21 lines (L1,L2,...,L21) and 42 relays (R1,R2,...,R42) having 82 combinations of primary-backup relationship among them. Table 2.5 shows these 82 combinations of primary-backup relationship among all the 42 relays. The fault currents passing through the primary and the corresponding backup relays for various near-end three phase faults and the maximum as well as minimum fault current through the relays are given in [40] and hence are not repeated here. The CT ratio required for each relay is also given in [40].

Table 2.5: Primary/backup relay pairs of the 15-bus system

Fault Zone	Primary Relay	Backup Relay	Fault Zone	Primary Relay	Backup Relay
L1	1	6	L12	23	11, 13
	2	4, 16		24	21, 34
L2	3	1, 16	L13	25	15, 18
	4	7, 12, 20		26	28, 36
L3	5	2	L14	27	25, 36
	6	8, 10		28	29, 32
L4	7	5, 10	L15	29	17, 19, 22
	8	3, 12, 20		30	27, 32
L5	9	5, 8	L16	31	27, 29
	10	14		32	33, 42
L6	11	3, 7, 20	L17	33	21, 23
	12	13, 24		34	31, 42
L7	13	9	L18	35	25, 28
	14	11, 24		36	38
L8	15	1, 4	L19	37	35
	16	18, 26		38	40
L9	17	15, 26	L20	39	37
	18	19, 22, 30		40	41
L10	19	3, 7, 12	L21	41	31, 33
	20	17, 22, 30		42	39
L11	21	17, 19, 30	–	–	–
	22	23, 34		–	–

The optimum settings of the relays obtained by different methods obtained with standard parameter values are given in Table 2.6 whereas the *CTI* between the time of operations of the primary relay (t_{op}) and that of the corresponding backup relays (t_{ob}) are plotted in Figure 2.5. Again, in this case, the best results obtained after 100 runs of each method corresponding to the standard parameter values are given in Table 2.6 and Figure 2.5. Table 2.7 shows the summary of the results obtained after 100 runs by the different methods with standard parameter values whereas Table 2.8 shows the corresponding values obtained with the perturbed parameter values. As in previous case, these summaries include the best, mean and the worst values of the objective function along with its standard deviation and the average elapsed time (sec) for executing each algorithm.

From Table 2.7 it is again observed that for this system also the DE based technique is the best

Table 2.6: Optimum settings of relays for the 15-bus system obtained with standard parameter values

Relays	GA		PSO		DE		HS		SOA	
	TMS	PS	TMS	PS	TMS	PS	TMS	PS	TMS	PS
1	0.2217	0.5001	0.1	2.5	0.1	1.2464	0.1	1.5933	0.1555	1.2031
2	0.2199	0.5001	0.1001	1.4853	0.1	0.9762	0.1001	1.2598	0.2241	0.6255
3	0.2134	0.9256	0.2134	2.436	0.1	2.0644	0.1001	2.299	0.289	0.5859
4	0.2169	0.5372	0.1541	1.3103	0.1	1.2439	0.1001	1.4479	0.1642	1.0809
5	0.2956	0.5	0.1636	2.5	0.1	2.1758	0.1114	1.9875	0.3541	0.5
6	0.1814	1.2591	0.2949	0.5	0.1	2.1084	0.1057	2.09	0.2449	0.6088
7	0.2777	0.5001	0.3441	0.7587	0.1	2.0689	0.1112	1.9172	0.2026	1.3521
8	0.1503	1.3329	0.3677	1.2353	0.1	1.5847	0.1001	1.7086	0.2693	0.5414
9	0.2361	0.7428	0.3529	0.6833	0.1	2.1181	0.1001	2.3959	0.3097	0.5182
10	0.2701	0.5001	0.1581	2.0514	0.1	1.7132	0.1001	2.3148	0.1793	1.1962
11	0.2358	0.5	0.1	2.5	0.1	1.2818	0.1	1.5747	0.1772	0.6782
12	0.1692	0.9745	0.4058	0.5	0.1	1.4139	0.1125	1.259	0.268	0.5052
13	0.2566	0.5109	0.4223	0.5	0.1	2.1779	0.1001	2.3661	0.241	0.9259
14	0.1435	1.1425	0.1	2.5	0.1	1.1156	0.114	1.0666	0.1642	0.7968
15	0.2047	0.5004	0.2635	0.5001	0.1	1.0275	0.1001	1.2831	0.1974	0.583
16	0.2355	0.5017	0.3067	0.5	0.1	1.4475	0.1	1.7563	0.2421	0.6353
17	0.2459	0.5194	0.3741	0.5239	0.1	1.5796	0.1001	1.7009	0.2359	0.6312
18	0.1775	0.6713	0.1284	1.4146	0.1	1.0498	0.1002	1.3617	0.1698	0.7761
19	0.2276	0.7222	0.2671	1.2694	0.1	1.809	0.1133	1.5598	0.2842	0.6357
20	0.2037	0.6488	0.1445	2.2975	0.1	1.3105	0.1001	1.5965	0.2564	0.5014
21	0.245	0.5002	0.1	2.3325	0.1	1.1437	0.1028	1.2364	0.2022	0.8159
22	0.2556	0.5029	0.391	0.5216	0.1	1.6929	0.1001	2.2202	0.214	1.1688
23	0.2422	0.5042	0.1243	2.5	0.1	1.1259	0.1	1.6651	0.1224	1.5117
24	0.2221	0.5001	0.1409	2.2981	0.1	1.4548	0.1043	1.4555	0.2704	0.5298
25	0.19	1.2263	0.1867	2.5	0.1	2.0088	0.1086	1.9376	0.1819	1.5846
26	0.1858	1.0327	0.1378	2.4997	0.1	1.7277	0.1001	2.2356	0.2921	0.5003
27	0.2698	0.5009	0.3496	1.2764	0.1	2.0028	0.1	2.3822	0.2058	1.197
28	0.2826	0.5035	1.0999	0.5	0.1043	2.5	0.1069	2.4603	0.3516	0.5066
29	0.2476	0.5285	0.26	2.5	0.1	1.5738	0.1001	1.8345	0.2023	1.0813
30	0.1931	0.9965	0.2592	0.5	0.1	1.7436	0.1	1.9207	0.259	0.5573
31	0.2118	0.9393	0.3694	1.8484	0.1	1.8766	0.1001	2.4235	0.2158	1.1079
32	0.2553	0.5001	0.4379	1.4562	0.1	1.6002	0.1001	1.8187	0.1352	1.9317
33	0.3207	0.5001	0.3022	2.3931	0.1	2.4993	0.1397	1.635	0.3247	0.6672
34	0.2809	0.6255	0.4165	0.5	0.1066	2.5	0.1222	2.1549	0.3283	0.5265
35	0.1449	1.8638	0.3862	0.5	0.1	2.0723	0.1009	2.1173	0.3162	0.5019
36	0.193	1.0986	0.1763	2.3456	0.1	1.8503	0.1004	1.974	0.1966	1.1711
37	0.2321	0.9507	0.423	0.5	0.1023	2.5	0.108	2.428	0.3008	0.5912
38	0.1644	1.9288	0.1634	2.5	0.1042	2.5	0.1198	2.0702	0.2967	0.5405
39	0.2657	0.5221	0.2078	2.5	0.1014	2.5	0.115	2.1461	0.2776	0.5006
40	0.2318	0.9407	0.2483	0.9811	0.1031	2.5	0.1361	1.7633	0.2201	1.2674
41	0.3092	0.5001	0.2052	1.4688	0.1035	2.5	0.1164	2.3633	0.3534	0.5323
42	0.1571	1.3041	0.2322	2.4999	0.1	1.578	0.1	1.7788	0.1491	1.5585
OFV	18.9033		26.8093		**11.7591**		12.6225		20.4068	

among the five meta-heuristic methods in terms of the values of the objective function (11.7591 seconds) and standard deviation (0.0004). Therefore, for this system also, out of the five methods, DE gives the best and most predictable results. Moreover, it is to be noted that the best objective function value obtained for this system so far reported in the literature is 12.2325 seconds as reported in [40], which is higher than the value of the objective function obtained by DE. Further,

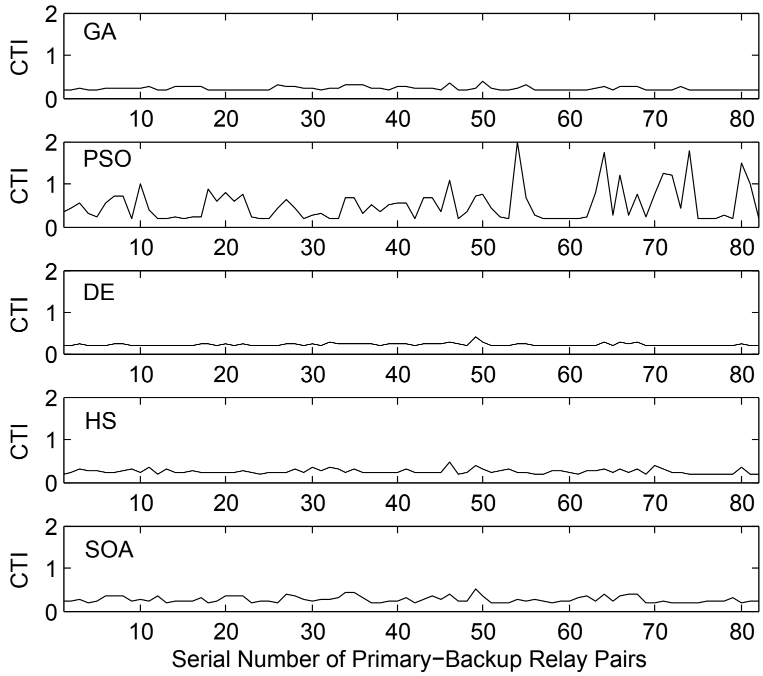

Figure 2.5: CTI otained by various methods for the 15-bus system obtained with standard parameter values.

Table 2.7: Summary of results obtained after 100 independent runs for the 15-bus system with standard parameter values

Methods	Objective function value			Standard	Average elapsed
	Best	Mean	Worst	deviation	time (sec)
GA	18.9033	19.9538	21.2223	0.6395	694.35
PSO	26.8093	35.0252	44.8147	5.3496	**20.95**
DE	**11.7591**	**11.7594**	**11.7615**	**0.0004**	167.46
HS	12.6225	12.9014	13.2637	0.1983	291.76
SOA	20.4068	24.9451	32.5519	1.8947	72.59

Table 2.8: Summary of results obtained after 100 independent runs for the 15-bus system with perturbed parameter values

Methods	Objective function value			Standard	Average elapsed
	Best	Mean	Worst	deviation	time (sec)
GA	24.6598	31.9816	41.3916	4.5996	421.42
PSO	28.1412	46.9385	66.9602	9.1491	**9.71**
DE	**11.7591**	**11.7610**	**11.8045**	**0.0073**	98.39
HS	12.4895	12.5288	13.0173	0.0901	311.20
SOA	20.1276	23.6208	31.4109	2.3619	80.98

from Figure 2.5, it is observed that among these five methods, DE gives the lowest values of CTI.

Again, from Table 2.8 it is observed that DE gives the best result (the least value of the objective function) among all these five methods. It is also observed from Tables 2.7 and 2.8 that with DE, the best value of the objective function remains the same with standard parameter values as well as with the perturbed parameter values, thereby again establishing the fact that the best value obtained by DE is immune to the variation of the parameter values. However, again for the other four methods, the best values (and also the other values) of the objective functions change with variation in the parameter values. Also, DE is reasonably time efficient (third fastest) as compared to the other algorithms.

2.4.3 System III: 33 kV section of the IEEE 30-bus test system

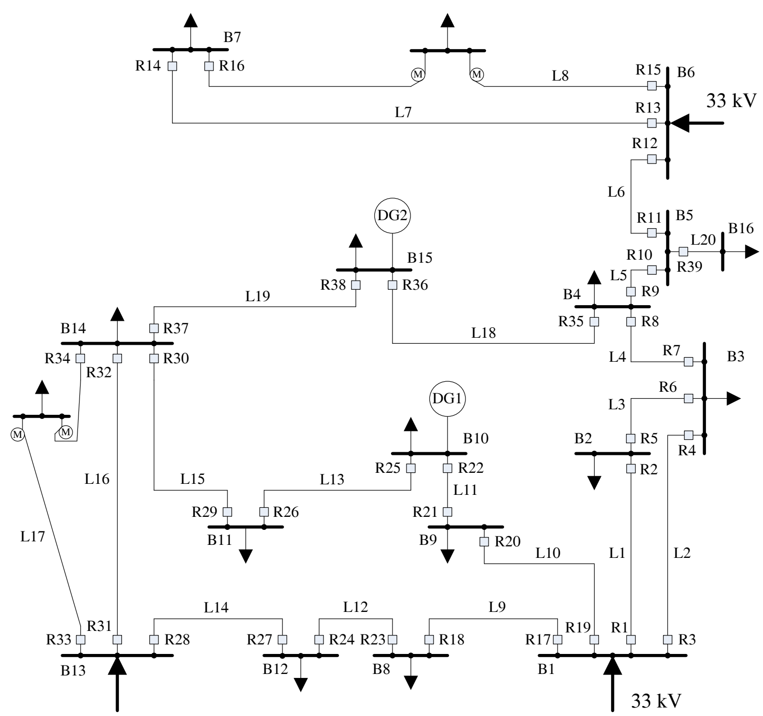

Figure 2.6: Single-line diagram of 33 kV section of the IEEE 30-bus system.

Figure 2.6 shows the 33 kV section of the IEEE 30-bus system. The system is fed through three 50 MVA, 132/33 kV transformers connected at buses 1, 6, and 13. In addition to the above three supply points, two DGs connected at bus no. 10 and 15 are also supplying the system. The detailed information about the system is available in [55, 94]. The system has 20 lines (L1,L2,...,L20) and is protected with 39 directional OCRs (R1,R2,...,R39) having 64 primary-backup combinations among them. Table 2.9 shows all the possible 64 combinations of the primary-backup relationships among the 39 relays. The fault currents passing through the primary and the backup relays for various near-end three phase faults are given in [55] and hence are not repeated here. The CT ratio for each relay is considered to be 500:1.

It is to be noted that for this system some of the primary-backup relationships have been ignored while solving the coordination problem. These primary-backup relationships are 1-4, 17-4, 19-4, 28-34, 30-33, 31-34, 32-33 and 37-33. The reason behind this is the fact that for these combinations, the fault current passing through the corresponding backup relays are small (less than two times of the maximum load current of the relay) causing larger operating time of the backup relays and therefore, the minimum CTI requirements are always maintained for these combinations.

For this test system two cases have been considered. In the first case, all the relays are assumed to have standard IDMT characteristics whereas in the second case different characteristics curves of the relays have been considered.

Table 2.9: Primary/backup relay pairs of the 30-bus system

Fault Zone	Primary Relay	Backup Relay	Fault Zone	Primary Relay	Backup Relay
L1	1	4, 18, 20	L11	21	19
	2	6		22	26
L2	3	2, 18, 20	L12	23	17
	4	5, 8		24	28
L3	5	1	L13	25	21
	6	3, 8		26	30
L4	7	3, 5	L14	27	23
	8	10, 36		28	32, 34
L5	9	7, 36	L15	29	25
	10	12		30	31, 33, 38
L6	11	9	L16	31	27, 34
	12	–		32	29, 33, 38
L7	13	11	L17	33	27, 32
	14	15		34	29, 31, 38
L8	15	11	L18	35	7, 10
	16	13		36	37
L9	17	2, 4, 20	L19	37	29, 31, 33
	18	24		38	35
L10	19	2, 4, 18	L20	39	9, 12
	20	22		–	–

2.4.3.1 Case A: Relays with standard IDMT characteristics

For this case, the optimum settings of the relays obtained (corresponding to the best run out of 100 independent runs) by the various methods corresponding to the standard parameter values are given in Table 2.10 whereas the *CTI* between the time of operations of the primary relay (t_{op}) and that of the corresponding backup relays (t_{ob}) are plotted in Figure 2.7. Table 2.11 shows the summary of the results obtained after 100 runs by the different methods with standard parameter values whereas Table 2.12 shows the corresponding values obtained with the perturbed parameter values. As in the previous cases, these tables show the best, mean and the worst values of the objective function along with its standard deviation and the average elapsed time (sec) for executing each algorithm.

Table 2.10: Optimum settings of relays for the 30-bus system obtained with IDMT characteristics and standard parameter values

Relays	GA		PSO		DE		HS		SOA	
	TMS	PS	TMS	PS	TMS	PS	TMS	PS	TMS	PS
1	0.348	0.5416	0.4339	0.7311	0.1	1.9683	0.1001	2.2823	0.2456	1.419
2	0.1001	0.5001	0.1	0.7793	0.1	0.5	0.1001	0.5006	0.1006	0.51
3	0.3798	1.1261	0.4759	1.5442	0.1709	2.5	0.2008	2.0845	0.4053	1.2032
4	0.3554	0.7318	0.2506	2.2529	0.137	2.5	0.1534	2.1177	0.3748	1.6489
5	0.3299	1.1605	0.6753	0.5	0.1372	2.5	0.1568	2.2603	0.4308	0.7438
6	0.4352	0.5002	0.771	0.5	0.1455	2.5	0.1618	2.1949	0.4538	0.964
7	0.1809	0.941	0.2404	0.6273	0.1	2.163	0.1093	1.9959	0.1838	0.9266
8	0.4889	0.5	0.3494	2.4872	0.1514	2.5	0.1678	2.3441	0.4547	0.894
9	0.1936	0.5473	0.1219	2.4353	0.1	2.154	0.1001	2.1813	0.1816	0.6927
10	0.5572	0.5001	0.4973	1.6339	0.1825	2.5	0.2191	1.9803	0.6056	0.5109
11	0.1215	0.5388	0.1	2.4992	0.1	0.7809	0.104	0.73	0.1156	0.6022
12	0.1	0.5581	0.1001	1.7099	0.1	0.5	0.1001	0.5614	0.1	0.795
13	0.1001	0.5801	0.1001	0.8006	0.1	0.5544	0.1052	0.5235	0.1289	0.5031
14	0.1001	0.5025	0.1003	0.5	0.1	0.5	0.1001	0.5003	0.1008	0.5007
15	0.3973	0.6834	0.5204	0.5002	0.1654	2.5	0.1832	2.361	0.4841	1.0237
16	0.4765	0.7692	0.9705	0.5	0.181	2.5	0.2513	1.5888	0.7017	0.5098
17	0.3487	1.2317	0.696	0.5	0.1571	2.5	0.1935	2.0471	0.4025	1.4966
18	0.4408	0.6306	0.3678	2.451	0.1387	2.5	0.168	2.089	0.3972	1.1425
19	0.476	0.7478	0.4302	2.291	0.1901	2.5	0.2282	2.0034	0.5379	1.2087
20	0.5129	0.7213	0.5525	1.4055	0.1924	2.5	0.226	2.128	0.4411	1.4649
21	0.2186	1.9997	0.2516	2.1498	0.135	2.5	0.1631	2.0815	0.5264	0.6436
22	0.3895	1.1956	0.7658	0.8065	0.1729	2.5	0.2064	2.189	0.4336	1.4988
23	0.3605	1.1951	0.6002	1.0292	0.1602	2.5	0.1889	2.1125	0.507	1.2602
24	0.6013	0.5393	0.6159	1.0636	0.209	2.5	0.2606	1.89	0.4521	1.4362
25	0.2874	1.5387	0.5342	0.5	0.151	2.5	0.1656	2.414	0.5957	0.5518
26	0.4992	0.5	0.6434	0.8444	0.1425	2.5	0.173	2.1852	0.2889	2.0495
27	0.4259	0.5	0.2614	2.5	0.1267	2.5	0.1574	1.9668	0.4197	1.0216
28	0.3122	1.8681	0.315	2.5	0.173	2.5	0.1903	2.4121	0.5891	0.5366
29	0.3118	1.494	0.2962	2.5	0.1578	2.5	0.1867	2.1393	0.4805	0.8305
30	0.2663	1.7012	0.2875	2.4979	0.1239	2.5	0.1395	2.4161	0.3784	0.8871
31	0.1001	0.5001	0.1004	0.5	0.1	0.5	0.1	0.6023	0.1161	0.5024
32	0.1	0.5024	0.1	0.5001	0.1	0.5	0.1	0.7242	0.1075	0.5009
33	0.4798	0.5001	0.7428	0.5	0.1553	2.5	0.1783	2.2162	0.3787	1.3351
34	0.4032	0.6577	0.4862	1.2949	0.1389	2.5	0.1659	2.0189	0.4874	0.6885
35	0.2961	1.2358	0.5306	0.7374	0.1264	2.5	0.1417	2.3048	0.5641	0.5061
36	0.3305	1.6162	0.6806	0.5001	0.18	2.5	0.1983	2.3581	0.5417	0.7404
37	0.2389	1.1937	0.2153	2.0325	0.1	2.2539	0.1	2.4106	0.5053	0.5226
38	0.1	0.5062	0.1001	0.5	0.1	0.5	0.1001	0.6104	0.1074	0.5069
39	0.5123	0.5001	0.8827	0.717	0.1657	2.5	0.1898	2.2205	0.4268	0.9769
OFV	28.0195		39.1836		**17.8122**		19.2133		33.7734	

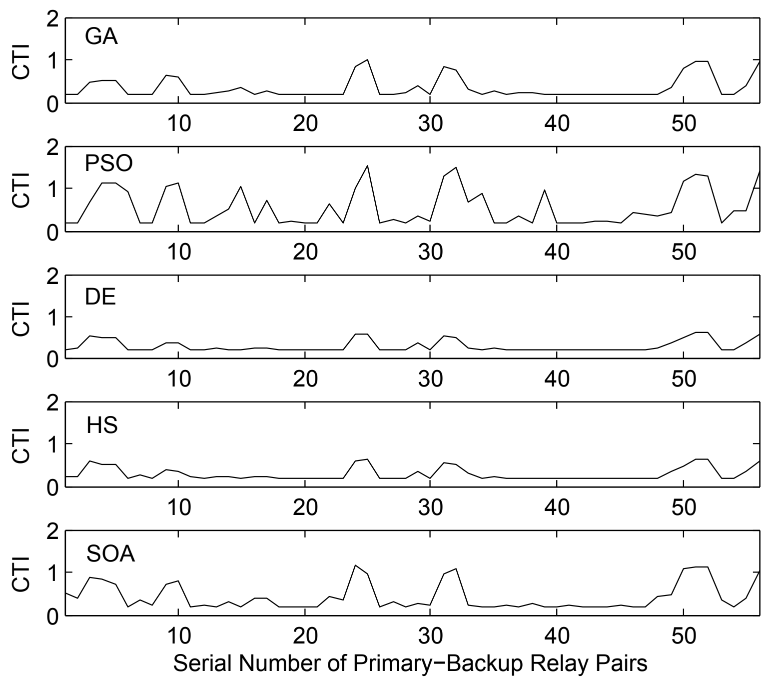

Figure 2.7: CTI otained by various methods for the 30-bus system considering IDMT characteristic curves of relays and standard parameter values.

Table 2.11: Summary of results obtained after 100 independent runs for the 30-bus system with standard parameter values and IDMT characteristics

Methods	Objective function value			Standard deviation	Average elapsed time (sec)
	Best	Mean	Worst		
GA	28.0195	29.2239	30.3700	0.6717	655.66
PSO	39.1836	46.0857	58.5692	6.1688	**13.37**
DE	**17.8122**	**18.4427**	21.4340	0.7226	123.22
HS	19.2133	19.7119	**20.2305**	**0.3626**	341.41
SOA	33.7734	35.8641	40.7814	2.0771	60.37

Table 2.12: Summary of results obtained after 100 independent runs for the 30-bus system with perturbed parameter values and IDMT characteristics

Methods	Objective function value			Standard deviation	Average elapsed time (sec)
	Best	Mean	Worst		
GA	33.2164	38.3621	45.4163	2.8409	396.45
PSO	34.7322	52.0418	76.1520	10.1870	**7.92**
DE	**17.8122**	**18.0856**	21.4402	0.6362	73.76
HS	19.0463	19.5602	**20.5018**	**0.2779**	313.10
SOA	31.3752	35.4262	60.1147	3.8634	68.85

From Table 2.11, again it is observed that among all these five methods, the DE gives the least value of the objective function (17.8122 seconds). Further, the standard deviation (0.7226) is also quite low, establishing the high predictability of the results obtained in different runs of DE. Further, the results obtained by the DE are of high quality as the mean and the worst values of the objective function is close to that of the best value. From Figure 2.7, it is again observed that among these five methods, DE gives the lowest values of CTI.

Again, from Table 2.12 it is observed that DE gives the best result (the least value of the objective function) among all these five methods. It is also observed from Tables 2.11 and 2.12 that with DE, the best value of the objective function remains the same with standard parameter values as well as with the perturbed parameter values, thereby again establishing the fact that the best value obtained by DE is immune to the variation of the parameter values. However, again for the other four methods, the best values (and also the other values) of the objective functions change with variation in the parameter values. Also, DE is reasonably time efficient (third fastest in this case) as compared to the other algorithms.

2.4.3.2 Case B: Relays with different characteristics

In this case relays with different characteristic curves have been considered. For this case, the relays which are connected to the external supply buses are considered to have very inverse (VI) characteristics, the relays which are connected to the DG buses are considered to have extremely inverse (EI) characteristics and the rest are considered to be of standard IDMT type relays. Table 2.13 shows the details of various relays along with the coefficients of their characteristic curves [60].

For this case, the optimum settings of the relays obtained (corresponding to the best run out of 100 independent runs) by the various methods corresponding to the standard parameter values are given in Table 2.14 whereas the *CTI* between the time of operations of the primary relay (t_{op}) and that of the corresponding backup relays (t_{ob}) are plotted in Figure 2.8. Table 2.15 shows the summary of the results obtained after 100 runs by the different methods with standard parameter values whereas Table 2.16 shows the corresponding values obtained with the perturbed parameter values. As in the previous cases, these tables show the best, mean and the worst values of the objective function along with its standard deviation and the average elapsed time (sec) for executing each algorithm.

From Table 2.15, again it is observed that among all these five methods, the DE gives the

Table 2.13: Types of relays and their characteristics coefficients for the 30-bus system

Relays types	Various relays	Characteristic coefficients		
		λ	η	L
EI	22, 25, 36, 37	80	2	0
VI	1, 3, 12, 13, 15, 17, 19, 28, 31, 33	13.5	1	0
IDMT	2-11, 14, 16, 18, 20, 21, 23, 24, 26-30, 32, 34, 35, 38, 39	0.14	0.02	0

Table 2.14: Optimum settings of relays obtained for the 30-bus system considering different characteristics curves and standard parameter values

Relays	GA		PSO		DE		HS		SOA	
	TMS	PS	TMS	PS	TMS	PS	TMS	PS	TMS	PS
1	0.647	1.4683	0.2793	2.4998	0.1694	2.3635	0.18	2.348	0.5029	1.5987
2	0.1824	0.5008	0.186	0.5	0.1	1.2324	0.1	1.4679	0.2059	0.5063
3	0.3398	1.2115	0.1001	2.497	0.7994	0.7886	0.972	0.7154	0.4044	1.1081
4	0.1006	0.5016	0.1098	0.5001	0.1	0.5	0.1001	0.6203	0.1041	0.5176
5	0.4587	0.5064	0.6303	0.5215	0.1581	2.5	0.1707	2.4009	0.3336	1.03
6	0.2236	0.9054	0.2761	0.5	0.1171	2.4999	0.1605	1.45	0.2345	0.9836
7	0.3806	0.5132	0.4464	0.5028	0.1227	2.5	0.1461	2.0543	0.3544	0.5
8	0.2104	1.445	0.1767	2.0551	0.1306	2.5	0.1396	2.4224	0.2742	0.922
9	0.1477	0.8937	0.2112	0.5	0.1	1.7143	0.1001	1.9709	0.1453	1.2266
10	0.3811	0.5365	0.25	2.0413	0.1374	2.5	0.1661	1.9697	0.3785	0.5018
11	0.1355	0.5276	0.1	1.8406	0.1	1.1477	0.1368	0.5098	0.1755	0.5
12	0.5993	1.9032	1.0998	2.5	0.417	1.9251	1.0044	1.3181	0.53	1.9725
13	0.2001	1.3997	0.1001	2.4887	0.758	0.7184	0.2195	1.3337	0.4676	0.9143
14	0.1001	0.5005	0.1	0.5	0.1	0.5	0.1001	1.0169	0.1047	0.5001
15	0.5759	0.8173	1.0345	0.6088	0.39	0.9903	0.3849	1.0011	0.2319	1.2838
16	0.1	0.5043	0.1	0.5	0.1	0.5001	0.1001	0.5831	0.1299	0.5021
17	0.4405	1.7051	0.7189	1.2503	0.1655	2.4998	0.256	2.0345	0.4782	1.6091
18	0.2514	0.5041	0.282	0.5	0.1	2.4118	0.1081	2.2048	0.2291	0.6349
19	0.1929	1.83	0.9854	0.8031	0.1	2.3236	0.5019	1.104	0.4061	1.3043
20	0.2166	0.5048	0.2281	0.6114	0.1	1.9251	0.1025	1.8833	0.2068	0.5503
21	0.2637	0.5005	0.1369	2.5	0.1191	2.4994	0.1479	1.7292	0.2771	0.5264
22	0.4443	2.0787	1.0999	1.3749	0.2546	2.4995	0.7544	1.4803	0.6251	1.7435
23	0.2203	0.5626	0.1	2.4877	0.1	2.1324	0.1003	2.1811	0.1984	0.6357
24	0.2663	0.74	0.1913	1.7264	0.1124	2.4999	0.1166	2.4503	0.2584	0.7423
25	0.3915	1.9055	0.5152	1.6743	0.4745	1.5596	0.3654	1.8084	0.6648	1.5422
26	0.2757	0.7377	0.2643	0.9374	0.1391	2.5	0.1654	1.8923	0.2522	0.9963
27	0.1759	0.5397	0.1011	2.2132	0.1	1.5244	0.1097	1.3109	0.1117	1.5258
28	0.7854	0.9435	0.8668	0.8643	0.1	2.1752	0.6654	0.9027	0.4642	1.1711
29	0.2145	0.6507	0.2398	0.5015	0.1	2.0647	0.1	2.3372	0.2658	0.5
30	0.2286	1.2619	0.4149	0.5	0.1277	2.5	0.136	2.3901	0.2304	1.2368
31	0.6503	1.1948	0.3959	1.692	0.1274	2.3779	0.1568	2.1845	0.5575	1.2866
32	0.171	0.5108	0.1	2.4999	0.1	1.1364	0.1	1.2598	0.1818	0.5
33	0.6897	0.7988	0.6425	0.8308	0.5672	0.8782	0.1871	1.5258	0.2935	1.2248
34	0.1001	0.5258	0.1	0.5112	0.1	0.5	0.1	0.7002	0.1001	0.5074
35	0.2758	1.0407	0.4552	0.5	0.1325	2.5	0.1451	2.2941	0.2338	1.4744
36	0.54	1.4168	0.1365	2.5	0.1176	2.4999	0.9769	0.9235	0.6707	1.21
37	0.5759	0.9354	0.1	2.4948	0.1001	1.9243	0.5773	0.862	0.3389	1.1365
38	0.1966	2.1341	0.4588	0.5087	0.1447	2.5	0.1556	2.3332	0.29	0.984
39	0.1001	0.5038	0.1	0.5001	0.1	0.5	0.1	0.7078	0.109	0.5
OFV	14.5616		17.127		**11.2444**		11.883		14.7367	

least value of the objective function (11.2444 seconds). Further, the standard deviation (0.0134) is also quite low, establishing the high predictability of the results obtained in different runs of DE.

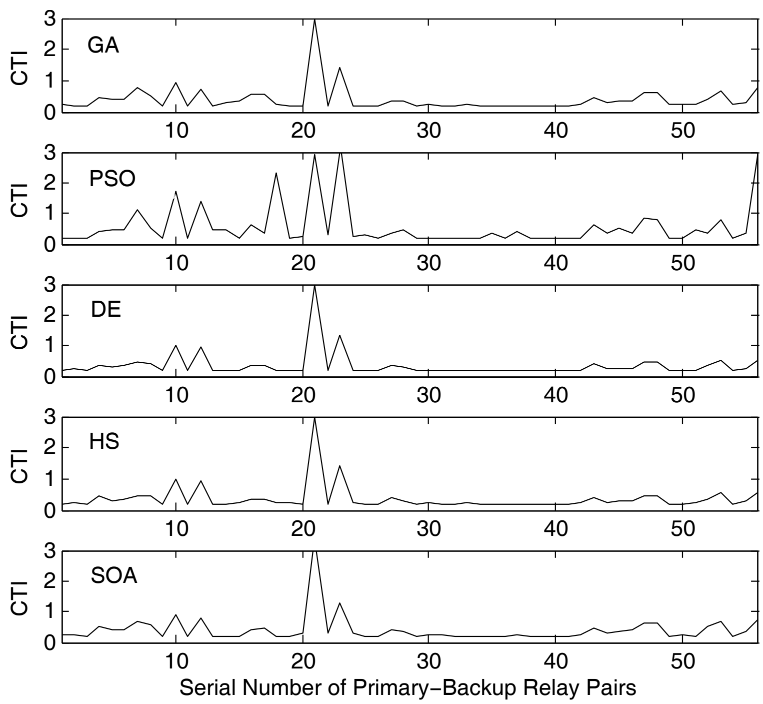

Figure 2.8: CTI otained by various methods for the 30-bus system considering different characteristics curves of the relays and standard parameter values.

Table 2.15: Summary of results obtained after 100 independent runs for the 30-bus system with different characteristics curves and standard parameter values

Methods	Objective function value			Standard deviation	Average elapsed time (sec)
	Best	Mean	Worst		
GA	14.5616	15.4757	16.5568	0.4148	394.74
PSO	17.1270	23.1064	33.2713	3.6491	**101.77**
DE	**11.2444**	**11.2778**	**11.3076**	**0.0134**	716.32
HS	11.8830	12.1572	12.5398	0.1467	624.96
SOA	14.7367	16.1104	18.6680	0.7146	124.54

Table 2.16: Summary of results obtained after 100 independent runs for the 30-bus system with different characteristics curves and perturbed parameter values

Methods	Objective function value			Standard deviation	Average elapsed time (sec)
	Best	Mean	Worst		
GA	14.5503	16.8485	21.9571	1.4913	261.7567
PSO	14.4910	23.8191	36.8190	4.8560	**125.1248**
DE	**11.2499**	**11.3053**	**11.6960**	**0.0709**	751.7813
HS	11.8067	12.1687	12.6070	0.1620	650.1724
SOA	14.1985	15.6728	18.3079	0.8336	181.7318

Further, the results obtained by the DE are of high quality as the mean and the worst values of the objective function is close to that of the best value. From Figure 2.8, it is again observed that among these five methods, DE gives the lowest values of CTI.

In this case of IEEE 30-bus system, it is observed that the sum of the operating times of all the relays is very low (11.2444 seconds) as compared to case A (17.8122 seconds, Table 2.11) in which all the relays are considered to be of IDMT characteristics. This is because of the fact that VI and EI types of relays operate much faster than the corresponding IDMT types of relays. Further, it is observed that the average execution time of various algorithms are higher than that in the previous case. The reason behind this lies in the increased complexity of the modelling because of different relay curves.

Again, from Table 2.16 it is observed that DE gives the best result (the least value of the objective function) among all these five methods. Also, from Tables 2.15 and 2.16 it is observed that with DE, the best value of the objective function obtained with the standard parameter values and the perturbed parameter values are very close to each other. Thus, the best value obtained by DE is virtually immune to the variation of the parameter values for all practical purposes. However, again for the other four methods, the best values (and also the other values) of the objective functions change with variation in the parameter values. In this particular case, although DE has produced the best solution like previous cases but has taken relatively longer time as compared to the other algorithms.

For the next three test systems, maximum load currents and fault currents are not readily available in the literature. For these three system, various currents have been calculated using the following procedures. The maximum load current (I_{Lmax}) has been calculated using Newton-Raphson load flow (NRLF) analysis. The fault current calculations have been carried out using bus impedance matrix (Z_{bus}) approach [95]. Three-phase-to-ground solid faults and line-to-line faults with a fault impedance of 0.1 p.u. [31] have been considered for calculating the maximum fault current (I_{fmax}) and the minimum fault current (I_{fmin}) passing through each relay, respectively. In this study, the faults have been applied at the middle of each line.

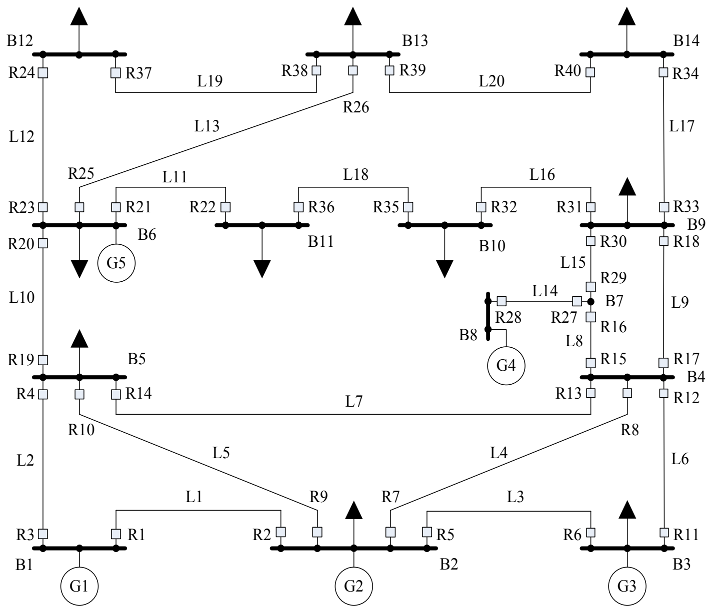

Figure 2.9: IEEE 14-bus system.

2.4.4 System IV: IEEE 14-bus test system

Figure 2.9 shows the IEEE 14-bus system supplied by five generating sources connected at buses 1, 2, 3, 6 and 8. More information about the system is available in [94]. In this system, there are 40 IDMT DOCRs (numerical/digital type) having 93 combinations of primary-backup relationship among them. Table A.1 of the appendix shows the maximum load current, minimum fault current and maximum fault current passing through all the relays. Table A.2 gives the CTRs of the various relays used in the system whereas, Table A.3 shows the 93 combinations of primary-backup relationship among all the 40 relays with the corresponding fault currents.

It is to be noted that some of the primary-backup relay combinations have not been considered during the optimization process as the current passing through the backup relays are less than the corresponding maximum load currents. There are 23 such combinations, which are: 1, 5, 8-11, 13, 14, 18, 20-22, 26, 30, 32, 35, 37, 40, 45, 47, 50, 54 and 61 (as given in Table A.3). The coordination constraints corresponding to these primary-backup combinations have been ignored as the MCT would be maintained for these combinations. Thus, only 70 primary-backup combinations have been considered during optimization process.

The optimum settings i.e., TMS and PS of the relays obtained by different methods using standard parameter values are given in Table 2.17 whereas the *CTI* between the time of operations of the primary relay (t_{op}) and that of the corresponding backup relays (t_{ob}) are plotted in Figure 2.10. It is to be noted that the best results (for the minimum value of objective function) obtained after 100 runs of each method corresponding to the standard parameter values are given in Table 2.17 and Figure 2.10. The last row in Table 2.17 gives the values of the sum of the operating times of all the relays i.e., objective function value (OFV) corresponding to the set of TMSs and PSs obtained by each method. Table 2.18 shows the summary of the results obtained after 100 runs by the different methods with standard parameter values whereas Table 2.19 shows the corresponding values obtained with the perturbed parameter values. These tables summarize the best, mean and the worst values of the objective function along with its standard deviation and the average elapsed time (sec) for executing each algorithm.

Table 2.17: Optimum settings of relays for the IEEE 14-bus system obtained with standard parameter values

Relays	GA		PSO		DE		HS		SOA	
	TMS	PS	TMS	PS	TMS	PS	TMS	PS	TMS	PS
1	0.1002	0.7505	0.1	0.75	0.1	0.75	0.1	0.8496	0.1043	0.7503
2	0.1001	0.5098	0.1001	0.6048	0.1	0.5	0.1002	0.5892	0.1004	0.5091
3	0.1	1.3455	0.1013	1.25	0.1	1.25	0.1	1.2724	0.102	1.2826
4	0.1	0.5002	0.1	0.5	0.1	0.5	0.1001	0.5416	0.1019	0.5149
5	0.1	1.4685	0.1	1.25	0.1	1.25	0.1	1.3114	0.1046	1.2724
6	0.1288	0.5035	0.1	0.8587	0.1	0.8184	0.1167	0.6431	0.1238	0.5483
7	0.1361	1.0618	0.1	1.0916	0.1	1	0.1017	1.0276	0.1324	1
8	0.1318	0.5503	0.1008	0.7116	0.1	0.6953	0.1001	0.7799	0.1453	0.5014
9	0.138	1.0231	0.1112	1.246	0.1	1.4397	0.1001	1.5159	0.1264	1.3105
10	0.1193	0.7269	0.1453	0.5005	0.1	0.618	0.1001	0.6734	0.1122	0.6705
11	0.2837	0.5032	0.1204	1.9999	0.1083	2	0.1362	1.4326	0.2501	0.5163
12	0.1257	1.2727	0.1	1.4348	0.1	1.2889	0.1059	1.2554	0.1025	1.3467
13	0.2379	0.5201	0.1	1.8988	0.1	1.4978	0.1	1.7317	0.1213	1.4801
14	0.1063	1.1009	0.1001	1	0.1	1	0.1001	1.1305	0.1289	1.0004
15	0.1816	1.05	0.105	2	0.1	1.3052	0.1002	1.6148	0.1732	1.1279
16	0.1007	0.5305	0.1	0.5	0.1	0.5	0.1	0.5597	0.1043	0.5001
17	0.2312	1.0008	0.232	1.3435	0.1	1.7099	0.1	1.868	0.2329	1.0138
18	0.1499	0.962	0.1	2	0.1	1.0293	0.1001	1.2288	0.2109	0.5051
19	0.1134	1.3636	0.104	2	0.1	1.25	0.1	1.3429	0.1249	1.384
20	0.1	0.5425	0.1	0.5015	0.1	0.5	0.1001	0.513	0.1016	0.5088
21	0.41	0.5008	0.4018	0.7591	0.1539	2	0.1798	1.6679	0.4252	0.5989
22	0.2677	1.0886	0.668	0.5007	0.1291	2	0.1389	1.9604	0.3865	0.5952
23	0.2748	0.9681	0.6793	0.7502	0.1056	2	0.1304	1.6112	0.2968	0.75
24	0.2918	0.6187	0.3394	0.5162	0.1	1.9172	0.1116	1.807	0.2816	0.829
25	0.2604	1.2751	0.2902	1.25	0.1277	2	0.1474	1.7628	0.3012	1.2519
26	0.3387	0.518	0.2092	2	0.1	1.7642	0.103	1.8026	0.2784	0.7944
27	0.1003	1.3168	0.1	1.25	0.1	1.25	0.1	1.4571	0.1123	1.2544
28	0.3289	0.9525	0.5626	0.5	0.1569	2	0.1906	1.5837	0.4714	0.5
29	0.1001	1.1366	0.1	1.9999	0.1	1	0.1001	1.157	0.1004	1.0014
30	0.2827	0.6618	0.2585	0.9608	0.1	1.905	0.1	1.9855	0.3118	0.5224
31	0.4214	0.5042	0.3847	1.7823	0.166	2	0.195	1.6211	0.4621	0.5047

Continued on next page

Table 2.17 – continued from previous page

Relays	GA		PSO		DE		HS		SOA	
	TMS	PS	TMS	PS	TMS	PS	TMS	PS	TMS	PS
32	0.2003	2.1823	0.3826	0.5	0.1354	2	0.2065	0.8136	0.4059	0.5244
33	0.2955	1.0908	0.2287	1.7588	0.1192	2	0.1325	1.7502	0.3476	0.8118
34	0.2446	1.5937	0.2816	2	0.1514	2	0.1639	1.9168	0.3297	1.044
35	0.2038	2.0998	0.614	0.6141	0.1478	2	0.1694	1.7019	0.3846	0.7192
36	0.3695	0.6666	0.4862	0.5	0.165	2	0.1797	1.859	0.4587	0.5203
37	0.3336	0.5146	0.3894	0.5002	0.1	1.8573	0.1173	1.6529	0.2765	0.774
38	0.2919	0.5797	0.2928	0.655	0.1	1.7752	0.1055	1.7716	0.2416	0.9221
39	0.3651	0.6226	0.2211	1.982	0.1368	2	0.1587	1.7156	0.3704	0.6379
40	0.2516	1.6182	0.3284	0.7019	0.1159	2	0.1201	1.9589	0.4262	0.5037
OFV	19.8211		22.6105		**13.2398**		14.0412		20.8203	

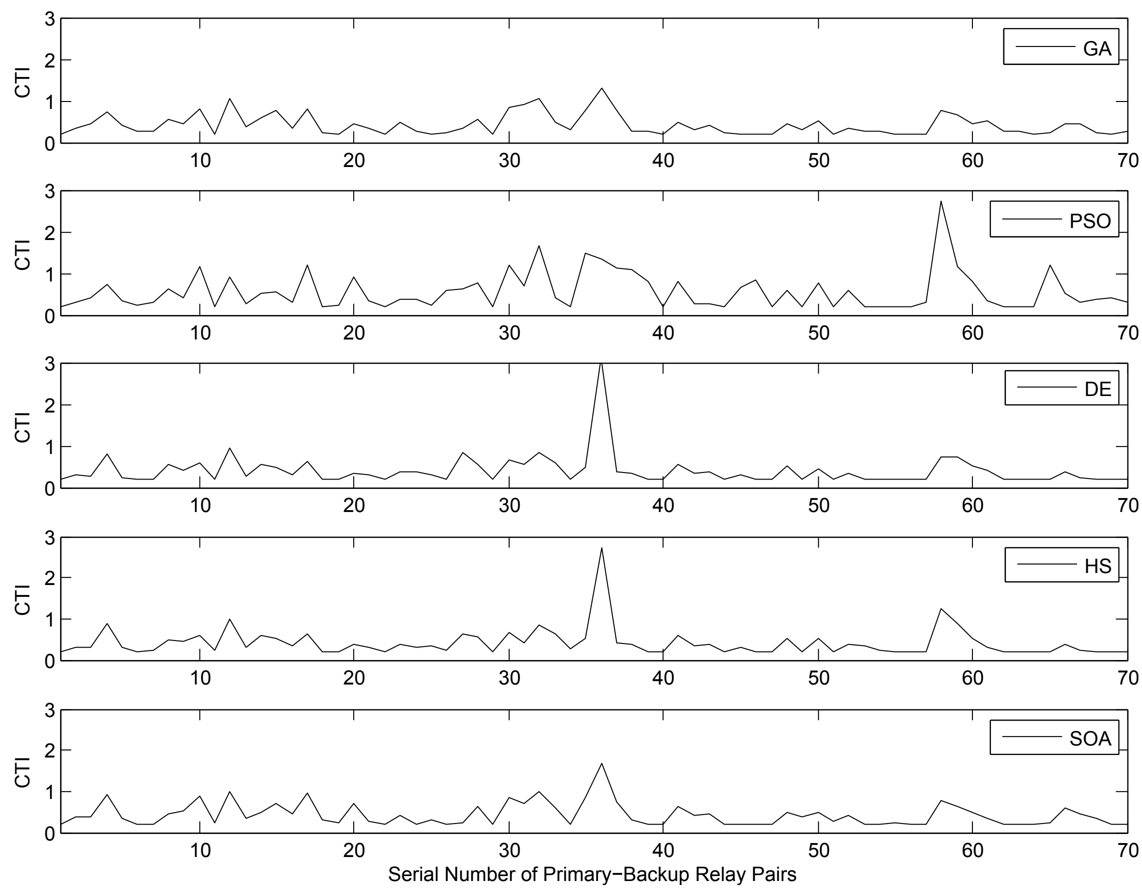

Figure 2.10: CTI obtained by various methods for the IEEE 14-bus system obtained with standard parameter values.

From Table 2.18 it is observed that among all these five methods, the DE gives the least value of the objective function (13.2398 seconds) and the standard deviation (0.0009). As the standard deviation is quite low for DE as compared to the other methods, it can be inferred that DE gives

Table 2.18: Summary of results obtained after 100 independent runs for the IEEE 14-bus system with standard parameter values

Methods	Objective function value			Standard deviation	Average elapsed time (sec)
	Best	Mean	Worst		
GA	19.8211	20.9276	22.1845	0.7915	96.1153
PSO	22.6105	28.4865	36.5781	5.3291	21.0991
DE	**13.2398**	**13.2401**	**13.2426**	**0.0009**	**18.9104**
HS	14.0412	14.2828	14.6179	0.2052	368.0828
SOA	20.8203	22.4179	24.2028	1.3141	53.4584

Table 2.19: Summary of results obtained after 100 independent runs for the IEEE 14-bus system with perturbed parameter values

Methods	Objective function value			Standard deviation	Average elapsed time (sec)
	Best	Mean	Worst		
GA	20.3602	22.9151	30.4782	3.2094	102.0449
PSO	19.2156	26.7031	34.962	5.4544	**24.9508**
DE	**13.2398**	**13.2399**	**13.2402**	**0.0001**	27.5279
HS	13.9514	23.1869	45.074	13.4726	420.1575
SOA	19.8291	20.668	21.7699	0.641	65.3597

the most predictable results when it is executed repeatedly as compared to the other four methods. Further, the results obtained by DE are of high quality as the mean and the worst values of the objective function are close to the best value. Also, from Figure 2.10, it is observed that among these five methods, the DE gives the lowest values of CTI.

Again, from Table 2.19 it is observed that DE gives the best result (the least value of the objective function) among all these five methods. It is also observed from Tables 2.18 and 2.19 that with DE, the best value of the objective function remains the same with standard parameter values as well as with perturbed parameter values. Therefore, the best value (of the objective function) obtained by DE can be considered to be immune to variation in the parameter values. However, for the other four methods, the best values (and also the other values) of the objective functions change with variation in the parameter values.

2.4.5 System V: IEEE 30-bus test system

Figure 2.11 shows the IEEE 30-bus system supplied by six generating sources connected at buses 1, 2, 5, 8, 9 and 13. More information about the system is available in [94]. In this system, there are 82 IDMT DOCRs (numerical/digital type) having 195 combinations of primary-backup relationship among them. Table A.4 shows the maximum load current, minimum fault current and maximum

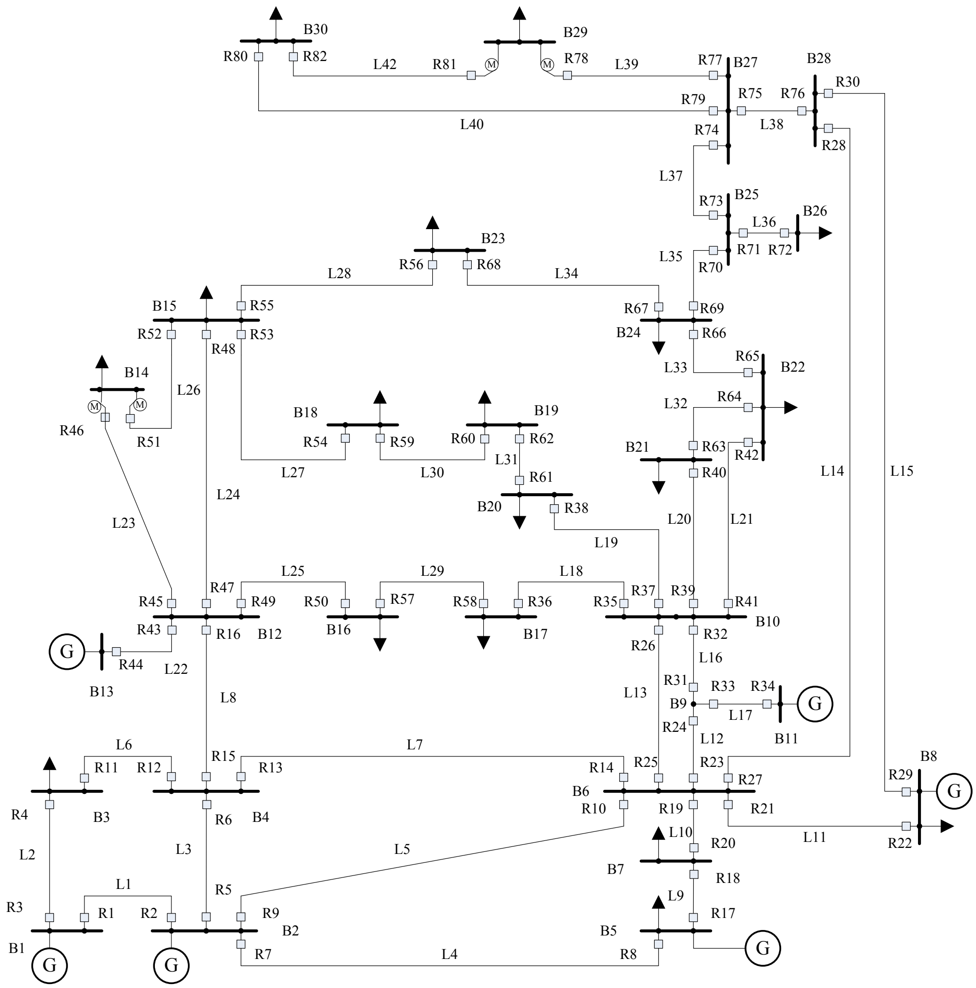

Figure 2.11: IEEE 30-bus system.

fault current passing through all the relays. Table A.5 gives the CTRs of the various relays used in the system whereas, Table A.6 shows the 195 combinations of primary-backup relationship among all the 82 relays with the corresponding fault currents.

It is to be noted that some of the primary-backup relay combinations have not been considered during the optimization process as the current passing through the backup relays are less than the corresponding maximum load currents. There are 36 such combinations, which are: 1, 5, 7-10, 12-15, 17-19, 23, 25, 33, 37, 39, 42, 53, 55, 61, 63, 66, 71-73, 76, 79, 84, 89-90, 114, 137, and 189 (as given in Table A.6). The coordination constraints corresponding to these primary-backup combinations have been ignored as the MCT would be maintained for these combinations. Thus, only 159 primary-backup combinations have been considered during optimization process.

The optimum settings i.e., TMS and PS of the relays obtained by different methods using standard parameter values are given in Table 2.20 whereas the *CTI* between the time of operations of the primary relay (t_{op}) and that of the corresponding backup relays (t_{ob}) are plotted in Figure 2.12. It is to be noted that the best results (for the minimum value of objective function) obtained after 100 runs of each method corresponding to the standard parameter values are given in Table 2.20 and Figure 2.12. The last row in Table 2.20 gives the values of the sum of the operating times of all the relays i.e., objective function value (OFV) corresponding to the set of TMSs and PSs obtained by each method. Table 2.21 shows the summary of the results obtained after 100 runs by the different methods with standard parameter values whereas Table 2.22 shows the corresponding values obtained with the perturbed parameter values. These tables summarise the best, mean and the worst values of the objective function along with its standard deviation and the average elapsed time (sec) for executing each algorithm.

Table 2.20: Optimum settings of relays for the IEEE 30-bus system obtained with standard parameter values

Relays	GA		PSO		DE		HS		SOA	
	TMS	PS	TMS	PS	TMS	PS	TMS	PS	TMS	PS
1	0.1395	1.0583	0.1	1.0011	0.1013	1.0338	0.1001	1.0379	0.1009	1.0011
2	0.2147	0.5995	0.1	0.5	0.1002	0.5034	0.1	0.5497	0.1051	0.5007
3	0.1812	2.2627	0.7061	1.25	0.1002	1.5305	0.1001	1.5921	0.1656	1.2974
4	0.2185	0.5473	0.1	1.9593	0.1001	0.5101	0.1	0.583	0.1064	0.5128
5	0.5327	1.4485	1.0899	1.251	0.1014	1.6669	0.1001	1.8712	0.2376	1.3048
6	0.1724	0.7609	0.1124	0.5	0.1006	0.5809	0.1053	0.5331	0.1759	0.7444
7	0.2801	1.0017	0.1233	1.4891	0.1003	1.0712	0.1017	1.1261	0.2364	1.0005
8	0.3136	0.5156	0.1408	0.5	0.1015	0.9915	0.1024	0.9948	0.1639	0.7442
9	0.381	1.0931	0.2201	1.2989	0.1017	1.073	0.1001	1.2944	0.1723	1.2487
10	0.3738	0.5118	0.2138	1.3105	0.106	0.6134	0.1002	0.9261	0.1372	0.5002
11	0.28	1.202	0.2613	0.75	0.1056	0.8794	0.1004	0.9948	0.1837	0.7896
12	0.6663	0.7037	0.4286	1.9948	0.1023	1.5111	0.1013	1.5416	0.4576	0.5096
13	0.4828	1.2798	0.2648	1.2508	0.1001	1.2544	0.1002	1.44	0.1882	1.2793
14	0.7139	0.8374	0.6194	0.8035	0.1305	1.9663	0.209	0.6614	0.3795	1.1167
15	0.2287	1.4478	0.2384	1.2521	0.1003	1.5403	0.1044	1.5886	0.3302	1.3481
16	0.2205	1.4398	0.4354	0.5001	0.1006	0.8142	0.1002	0.9569	0.1602	1.2829
17	0.5697	1.5211	0.3954	2	0.1752	1.9582	0.2477	1.0991	0.3179	1.6958
18	0.2332	1.2288	0.1	2	0.1014	1.4987	0.1	1.6656	0.185	1.0195
19	0.4403	1.2332	0.1093	2	0.1034	1.9772	0.1083	1.8891	0.1988	1.0327
20	0.8398	0.5651	0.4218	1.9399	0.1659	1.92	0.2229	1.1152	0.3733	1.3651
21	0.4643	0.7776	0.2168	0.8087	0.1003	1.2566	0.1	1.2968	0.2938	0.7508
22	0.4173	2.309	0.4277	1.6386	0.1531	1.9059	0.1631	1.8429	0.6391	0.5008
23	0.4384	1.245	0.1537	2	0.1002	1.7485	0.1001	1.8944	0.2904	1.0266
24	0.281	0.5173	0.1001	0.5485	0.1001	0.5016	0.1002	0.7385	0.1376	0.5404
25	0.5899	1.0295	0.3784	1.0011	0.1147	1.9907	0.1229	1.9247	0.7408	1.0128
26	0.7454	0.5537	0.1	1.8188	0.1009	1.1487	0.1004	1.5581	0.1685	1.2535
27	0.4582	0.6302	0.1723	2	0.1007	1.4158	0.1057	1.3161	0.1265	1.7794
28	0.3823	1.0037	0.2915	1.0307	0.101	1.1434	0.1002	1.2374	0.2129	0.9642
29	0.3692	0.9042	0.2578	0.7761	0.1005	1.1506	0.1002	1.2383	0.2257	0.5888

Continued on next page

Table 2.20 – continued from previous page

Relays	GA		PSO		DE		HS		SOA	
	TMS	PS	TMS	PS	TMS	PS	TMS	PS	TMS	PS
30	0.3416	0.7022	0.3095	0.6333	0.1001	1.0373	0.1	1.1974	0.1334	1.5307
31	0.1259	1.3837	0.1001	1.6592	0.1002	1.2546	0.1001	1.2604	0.2011	1.25
32	0.253	1.8434	0.2271	1.3296	0.1021	1.6081	0.1001	1.9259	0.4679	1.1545
33	0.1168	1.1932	0.1	1.801	0.1004	1.0198	0.1002	1.1026	0.1163	1.0002
34	0.4129	2.1525	1.1	0.5097	0.1771	1.9999	0.1916	1.913	0.4432	1.3313
35	0.4596	1.3519	0.3894	1.2762	0.1704	1.9787	0.2394	1.215	0.4053	1.0515
36	0.8678	0.6136	0.4851	1.9591	0.2168	1.9981	0.2597	1.7369	0.607	0.7653
37	0.5497	0.8873	0.4876	0.978	0.2211	1.9317	0.2482	1.7921	0.5715	0.9323
38	0.5388	1.2741	0.3961	1.9763	0.199	1.9859	0.2665	1.3292	0.5787	0.729
39	0.5782	1.0311	0.5768	1.003	0.1984	1.9841	0.2207	1.8185	0.534	1.0083
40	0.3303	2.464	0.6745	0.5003	0.1774	1.9683	0.1762	1.9656	0.5186	0.593
41	0.5085	0.762	0.3635	1.9918	0.1341	1.9856	0.1363	1.9193	0.3741	1.061
42	0.449	0.9761	0.4101	0.8191	0.1069	1.9889	0.1151	1.9379	0.2744	1.3459
43	0.1436	0.6289	0.1	0.5	0.1009	0.5016	0.1004	0.5685	0.1	0.5175
44	0.7734	0.708	0.7473	0.6996	0.2041	1.9929	0.2352	1.8179	0.6166	0.5685
45	0.4512	0.7215	0.2254	1.6223	0.1183	1.95	0.151	1.6518	0.4401	0.5738
46	0.2998	1.1439	0.1451	1.9602	0.1003	1.6636	0.1001	1.8231	0.3308	0.811
47	0.537	1.015	0.4676	1	0.1757	1.9608	0.212	1.7011	0.4687	1.0019
48	0.4501	0.9283	0.2661	1.5096	0.1054	1.9819	0.1453	1.5527	0.7228	0.5069
49	0.773	0.7779	0.7473	0.5	0.2011	1.994	0.2257	1.9345	0.4095	1.4295
50	0.52	0.9058	0.2952	2	0.1679	1.9808	0.2042	1.6901	0.4326	1.0005
51	0.5216	0.9035	0.2911	1.7294	0.1525	1.9953	0.1966	1.6294	0.4631	0.8595
52	0.6499	0.5233	0.2251	0.8248	0.1023	1.9663	0.1096	1.799	0.3549	0.6174
53	0.7743	0.8151	0.4183	1.9886	0.2443	1.9931	0.2744	1.9634	0.6198	0.9379
54	0.3908	1.5523	0.3657	1.8242	0.1623	1.9704	0.196	1.7212	0.4898	1.3936
55	0.387	2.2233	0.5695	1.1402	0.1838	1.9787	0.204	1.7262	0.4257	1.105
56	0.4925	1.6552	0.5015	0.8348	0.1975	1.9936	0.2268	1.8855	0.5622	1.0363
57	0.8019	0.9676	0.8135	0.5037	0.2355	1.9537	0.2687	1.8981	0.521	1.2671
58	0.5474	0.8221	0.4165	1.2755	0.1624	1.9808	0.1903	1.7604	0.478	0.7298
59	0.5258	1.687	0.4584	1.9714	0.2421	1.9807	0.3464	1.184	0.6483	0.6148
60	0.4096	1.7155	0.3549	1.7073	0.1796	1.997	0.2083	1.77	0.576	0.8223
61	0.7196	0.6707	0.6617	0.5	0.2184	1.9949	0.2506	1.9531	0.5824	0.7537
62	0.431	1.6691	0.4762	1.1247	0.2151	1.9786	0.2672	1.5011	0.5873	0.9668
63	0.55	1.295	0.5178	1.6651	0.1976	1.9995	0.223	1.8245	0.6026	0.5598
64	0.5423	0.6208	0.457	1.1928	0.18	1.9352	0.1824	1.8458	0.4517	0.8091
65	0.5437	1.1819	0.761	0.7502	0.1842	1.9862	0.2155	1.7825	0.4496	1.3066
66	0.6347	0.6407	0.5182	0.9354	0.2076	1.9594	0.2084	1.9272	0.6409	0.5585
67	0.651	0.5951	0.7614	0.6018	0.1737	1.9615	0.1718	1.977	0.4781	0.8445
68	0.401	1.9925	0.3329	2	0.2076	1.9326	0.2303	1.9848	0.4953	1.563
69	0.3774	2.3441	0.5371	0.9786	0.1309	1.9222	0.1474	1.581	0.2133	1.4881
70	0.4564	1.2559	0.3713	1.9998	0.1567	1.9846	0.1551	1.9796	0.3641	1.3178
71	0.1356	0.7728	0.1	1.9292	0.1001	0.5064	0.1001	0.5865	0.1196	1.1563
72	0.1648	0.5807	1.0168	0.5	0.101	0.5046	0.1001	0.509	0.1096	0.6063
73	0.7442	0.5644	0.7101	0.5261	0.107	1.9829	0.1106	1.9323	0.2895	0.5224
74	0.5429	1.5087	1.0996	1.9713	0.2255	1.9822	0.2265	1.9205	0.64	1.3011
75	0.5254	0.6447	0.7546	0.5	0.1006	1.1802	0.1	1.2969	0.2106	0.738
76	0.4209	1.3758	0.6954	1.2502	0.1118	1.997	0.1203	1.8517	0.2929	1.5998
77	0.2986	1.7202	0.127	1.2597	0.1032	1.6086	0.116	1.2945	0.1149	1.5207
78	0.1313	0.698	0.1	0.5	0.1018	0.513	0.1002	0.579	0.1016	0.5
79	0.1009	1.106	0.4154	1.0059	0.1004	1.0303	0.1	1.0028	0.1099	1.0178
80	0.1944	0.6438	0.126	0.5	0.1001	0.5053	0.1001	0.624	0.1021	0.6647
81	0.1261	1.2395	0.1	1.2685	0.1008	1.0175	0.1	1.0218	0.1038	1.1635
82	0.1183	0.5533	0.1079	0.5	0.1012	0.5345	0.1001	0.5294	0.1091	0.622
OFV	88.7040		83.0638		**34.4264**		36.8141		67.9980	

From Table 2.21 it is observed that among all these five methods, the DE gives the least value

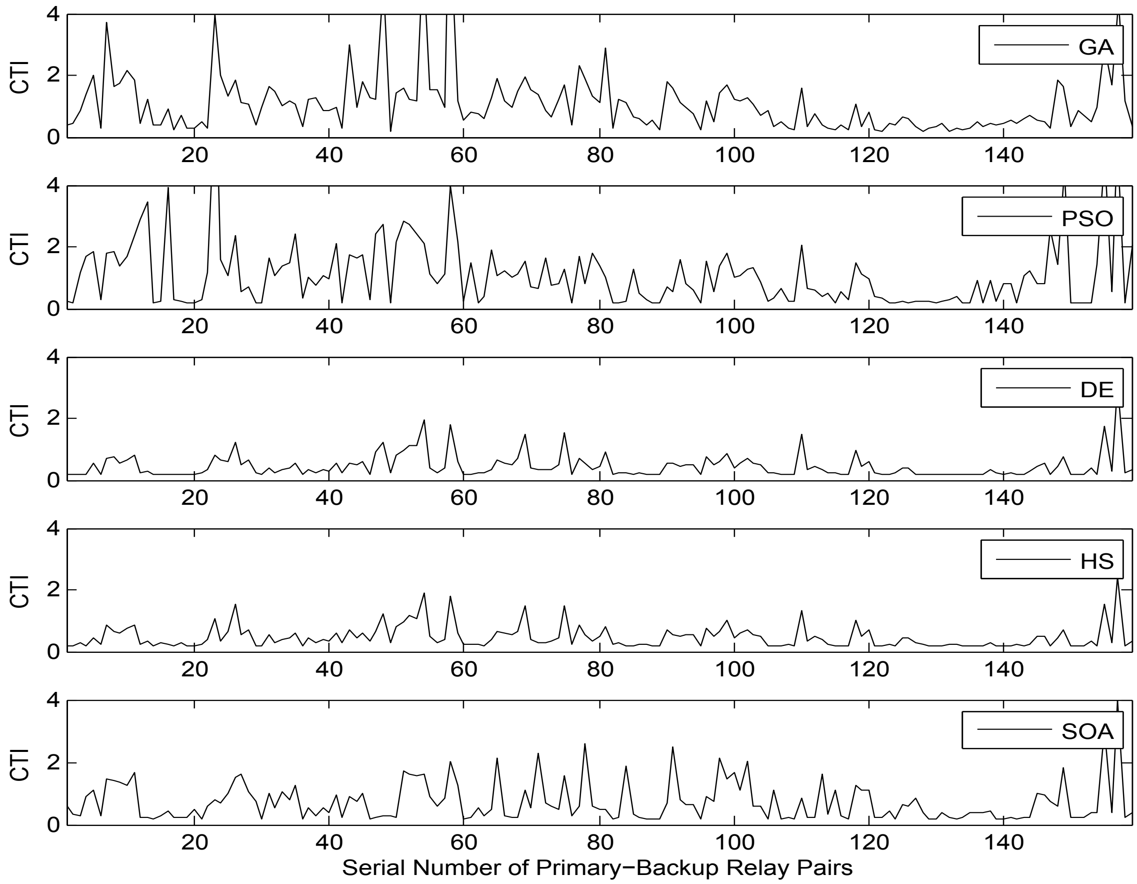

Figure 2.12: CTI otained by various methods for the IEEE 30-bus system obtained with standard parameter values.

Table 2.21: Summary of results obtained after 100 independent runs for the IEEE 30-bus system with standard parameter values

Methods	Objective function value			Standard deviation	Average elapsed time (sec)
	Best	Mean	Worst		
GA	88.7040	95.1436	101.2659	3.8934	193.7439
PSO	83.0638	2825.0616	15850.5737	5606.6798	**50.4117**
DE	**34.4264**	**34.5681**	**34.8389**	**0.1262**	210.0522
HS	36.8141	37.8501	38.8100	0.8138	1251.4073
SOA	67.9980	72.4438	80.6457	4.2576	146.4288

of the objective function (34.4264 seconds) and the standard deviation (0.1262). As the standard deviation is quite low for DE as compared to the other methods, it can be inferred that DE gives the most predictable results when it is executed repeatedly as compared to the other four methods. Further, the results obtained by DE are of high quality as the mean and the worst values of the objective function are close to the best value. Also, from Figure 2.12, it is observed that among

Table 2.22: Summary of results obtained after 100 independent runs for the IEEE 30-bus system with perturbed parameter values

Methods	Objective function value			Standard deviation	Average elapsed time (sec)
	Best	Mean	Worst		
GA	92.5227	97.7974	106.8746	4.8196	203.2241
PSO	77.7860	3541.8958	20274.9203	6820.0786	**55.2275**
DE	**33.5834**	**33.8376**	**34.0847**	**0.1588**	388.0306
HS	37.8966	7614.5027	17012.0565	6631.6364	386.7436
SOA	59.7455	65.9494	69.3523	2.8772	177.1454

these five methods, the DE gives the lowest values of CTI.

Again, from Table 2.22 it is observed that DE gives the best result (the least value of the objective function) among all these five methods. It is also observed from Tables 2.21 and 2.22 that with DE, the best value of the objective function remains the same with standard parameter values as well as with perturbed parameter values. Therefore, the best value (of the objective function) obtained by DE can be considered to be immune to variation in the parameter values. However, for the other four methods, the best values (and also the other values) of the objective functions change with variation in the parameter values.

2.4.6 System VI: IEEE 118-bus test system

Figure 2.13 shows the IEEE 118-bus system supplied by 54 generating sources connected at various buses. This system is having 186 lines. More information about the system is available in [94]. In this system, there are 372 IDMT DOCRs (numerical/digital type) having 1184 combinations of primary-backup relationship among them. Table A.7 shows the maximum load current, minimum fault current and maximum fault current passing through all the relays. Table A.8 gives the CTRs of the various relays used in the system whereas, Table A.9 shows the 1184 combinations of primary-backup relationship among all the 372 relays with the corresponding fault currents.

It is to be noted that some of the primary-backup relay combinations have not been considered during the optimization process as the current passing through the backup relays are less than the corresponding maximum load currents. There are 355 such combinations, which are (serial No.): 7, 17-18, 21, 33, 45, 51, 65, 67, 69, 100, 106-107, 111-112, 139,154, 159, 189, 209-213, 229, 233, 235, 239-240, 251, 260, 273, 310-311, 316, 318, 336-339, 341-343, 346, 348-360, 362-371, 383-385, 387-389, 405-406, 411-413, 416-420, 424, 430-431, 439-443, 445-447, 450-455, 458-489, 499-510, 514-516, 520-535, 547-549, 555, 569-570, 572-579, 587, 589-594, 608-609, 611-617,

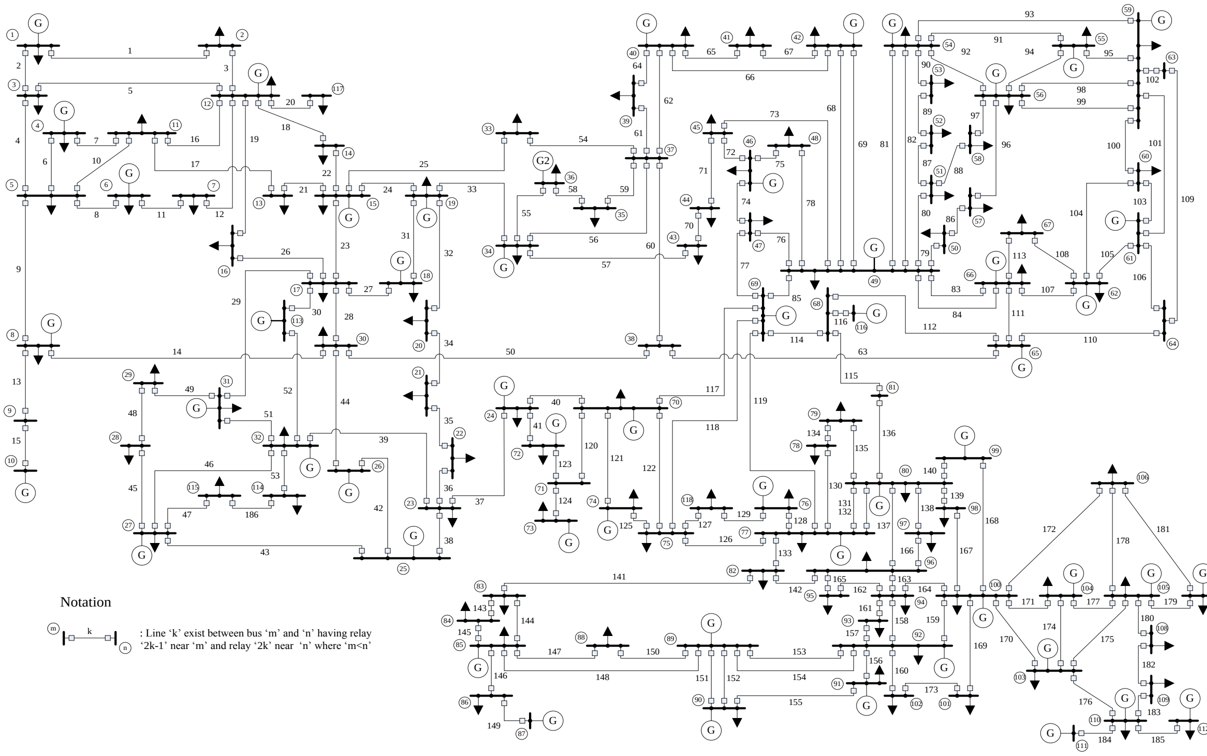

Figure 2.13: IEEE 118-bus system.

619-620, 622-634, 637-644, 664, 676-688, 708, 726-727, 729-730, 735-736, 738-739, 745, 747-749, 753, 762, 764, 767, 769-770, 784, 788-789, 791-792, 801, 803-804, 819, 821-822, 831-832, 834-835, 837-838, 846, 852-853, 855, 867-869, 872-873, 878-880, 882, 886-888, 890-892, 894-900, 916-917, 939, 941-944, 947-948, 951-952, 956-958, 963-964, 968, 970-971, 977, 979-982, 992-993, 998-999, 1001, 1005-1006, 1008-1009, 1011, 1015-1027, 1047, 1051, 1057, 1075-1078, 1080-1081, 1083, 1090, 1095-1096, 1103, 1108, 1112-1115, 1117-1127, 1129, 1134, 1142, 1160 and 1168 (as given in Table A.9). The coordination constraints corresponding to these primary-backup combinations have been ignored as the MCT would be maintained for these combinations. Thus, only 829 primary-backup combinations have been considered during optimization process.

For this test system two cases as considered in Section 2.4.3 have also been studied. In the first case, all the relays are assumed to have standard IDMT characteristics whereas in the second case different characteristics curves of the relays have been considered. As the standard parameters have always produced better results in all the above cases so in this particular system, results obtained corresponding to the standard parameters of the algorithms have been analysed only.

2.4.6.1 Case A: Relays with standard IDMT characteristics

In this case, all the relays are considered to follow standard IDMT characteristic curves [60]. The optimum settings i.e., TMS and PS of the relays obtained by different methods using standard parameter values are given in shown in Figure 2.14 whereas the *CTI* between the time of operations of the primary relay (t_{op}) and that of the corresponding backup relays (t_{ob}) are plotted in Figure 2.15. It is to be noted that the best results (for the minimum value of objective function) obtained after 100 runs of each method corresponding to the standard parameter values are given in Figures 2.14 and 2.15, respectively. Table 2.23 shows the summary of the results obtained after 100 runs by the different methods with standard parameter values.

Table 2.23: Summary of results obtained after 100 independent runs for the IEEE 118-bus system with standard IDMT characteristic curve standard parameter values

Methods	Objective function value			Standard deviation	Average elapsed time (sec)
	Best	Mean	Worst		
GA	470.5792	488.987	511.8876	11.4435	3502.0181
PSO	513.1012	713.648	935.049	141.1578	**472.6362**
DE	**307.9087**	331.8657	350.7796	15.1562	511.0281
HS	317.2963	**329.1893**	**341.6202**	**8.3652**	2337.2553
SOA	506.588	519.0389	531.9626	8.4885	813.3549

From Table 2.23 it is observed that among all these five methods, the DE gives the smallest value of the objective function (307.9087 seconds). However, the value of standard deviation obtained by HS is the least which is 8.3652 whereas that obtained by DE is 15.1562. As the standard deviation is also reasonably low for DE, it can be inferred that DE gives quite predictable results when it is executed repeatedly. Further, the results obtained by DE are of high quality as the mean and the worst values of the objective function are close to the best value. Also, from Figure 2.15, it is observed that among these five methods, the DE gives the lowest values of CTI.

2.4.6.2 Case B: Relays with different characteristics

In this case, relays with different characteristic curves have been considered as have been discussed in Section 2.4.3 (Case B). However, for simplicity, relays 1-200, 201-300 and 301-372 have been considered to follow standard IDMT, VI and EI characteristic curves, respectively, [60].

The optimum settings i.e., TMS and PS of the relays obtained by different methods using

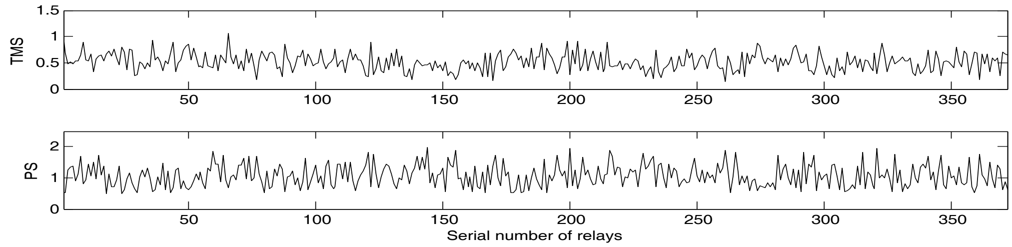

(a) Obtained using GA

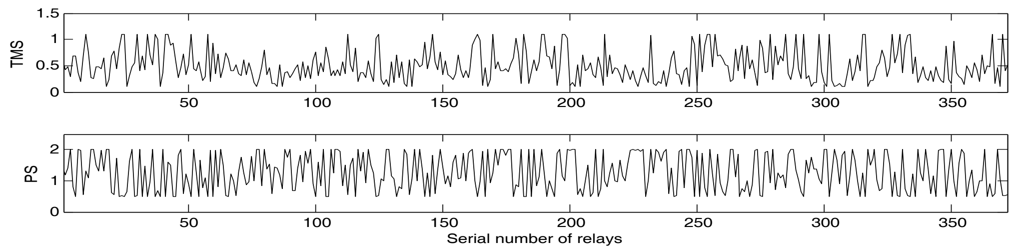

(b) Obtained using PSO

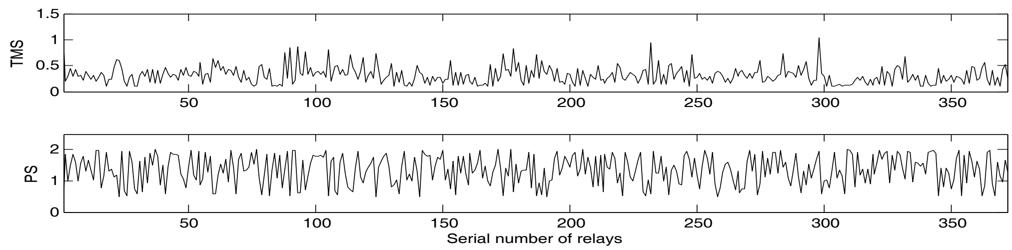

(c) Obtained using DE

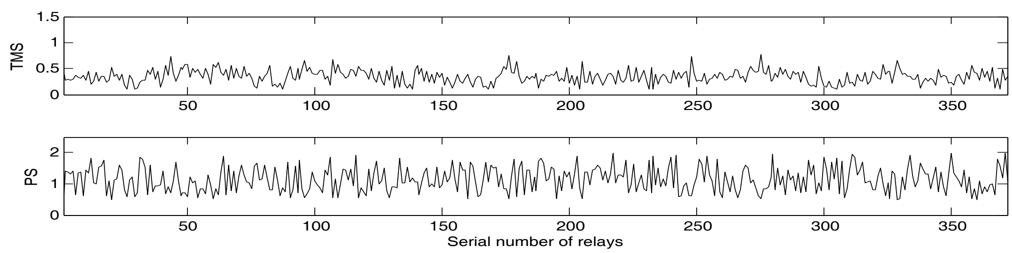

(d) Obtained using HS

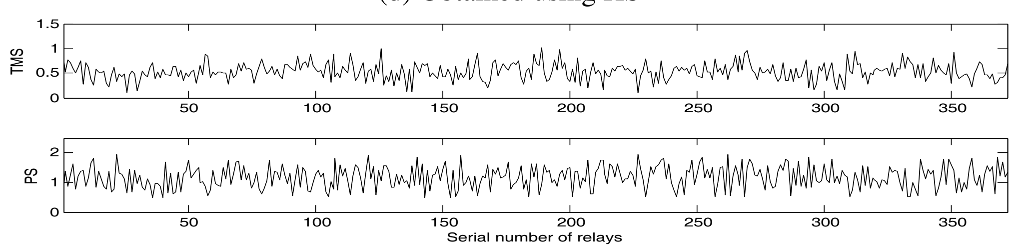

(e) Obtained using SOA

Figure 2.14: Optimum settings of DOCRs considering standard IDMT characteristic curves and standard parameters in the IEEE 118-bus system.

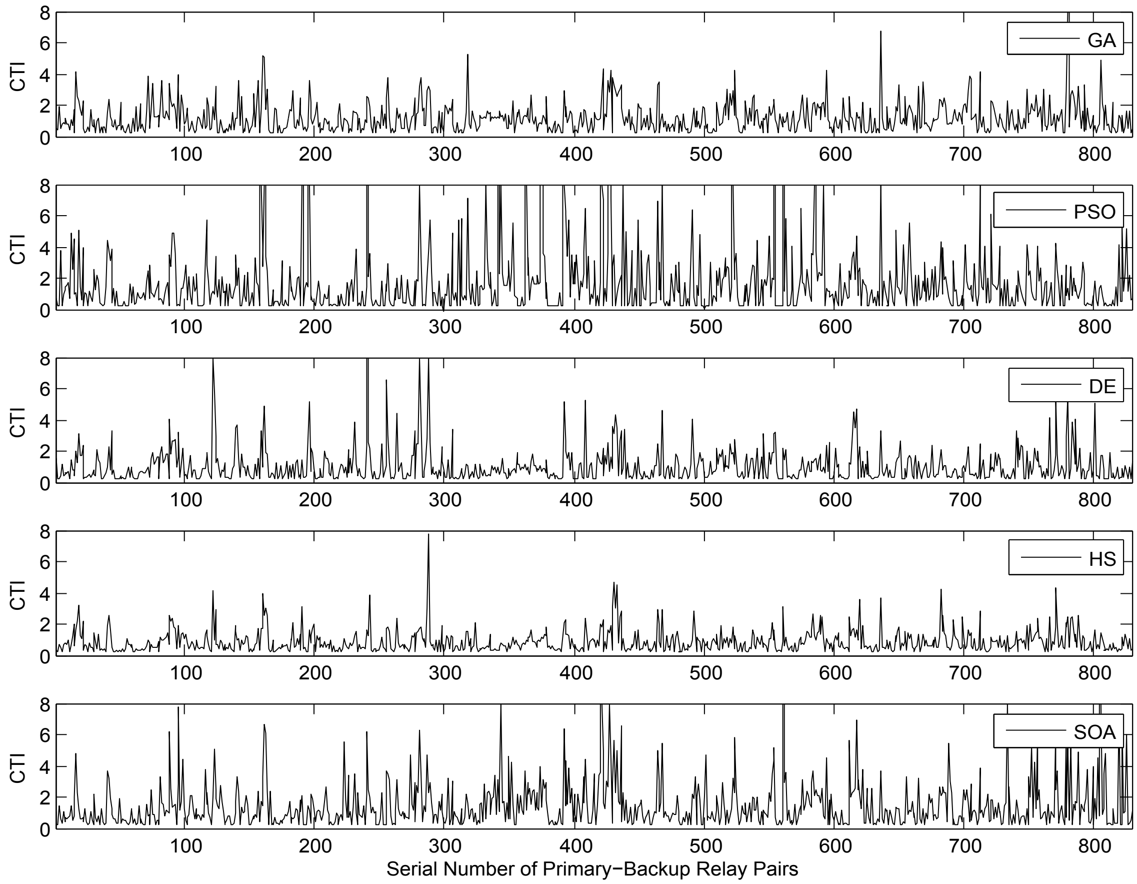

Figure 2.15: CTI obtained by various methods for the IEEE 118-bus system obtained with standard IDMT characteristic curves and standard parameter values.

standard parameter values are given in Figure 2.16 whereas the *CTI* between the time of operations of the primary relay (t_{op}) and that of the corresponding backup relays (t_{ob}) are plotted in Figure 2.17. It is to be noted that the best results (for the minimum value of objective function) obtained after 100 runs of each method corresponding to the standard parameter values are given in Figures 2.16 and 2.17. Table 2.24 shows the summary of the results obtained after 100 runs by the different methods with standard parameter values.

From Table 2.24 it is observed that among all these five methods, the DE gives the least value of the objective function (164.7287 seconds). However, the value of standard deviation obtained by GA is the least which is 4.4868 whereas that obtained by DE is 27.9267. As compared to the other methods DE gives the lowest values of the mean and the worst values of the objective function. Further, from Figure 2.17, it is observed that among these five methods, the DE gives the lowest

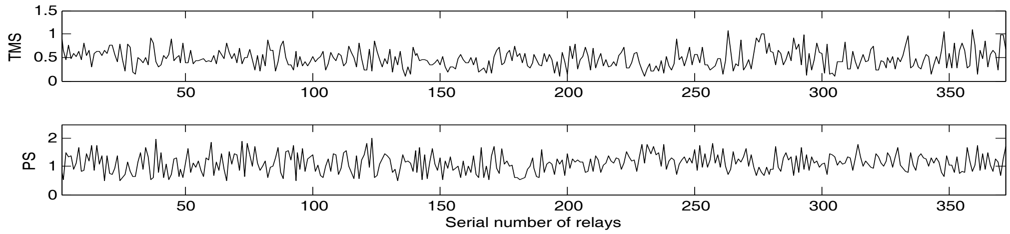

(a) Obtained using GA

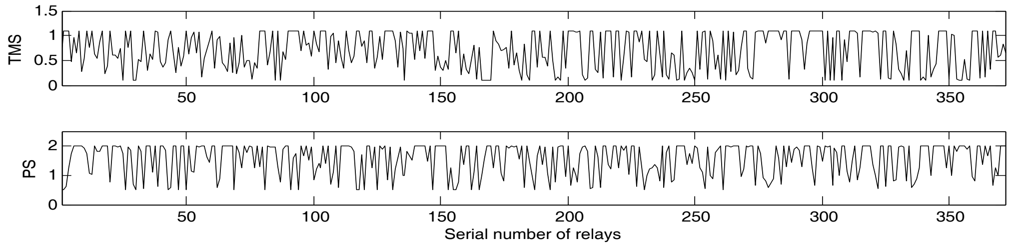

(b) Obtained using PSO

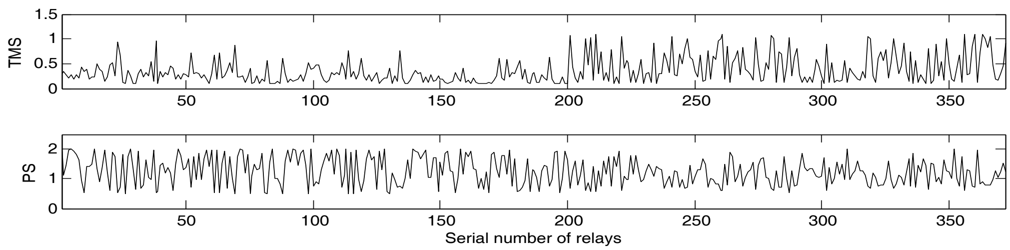

(c) Obtained using DE

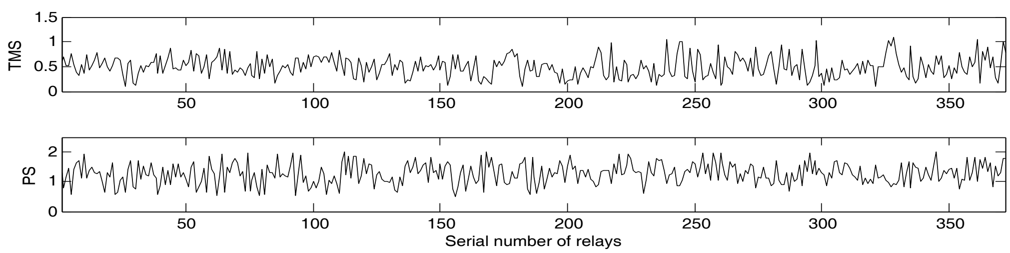

(d) Obtained using HS

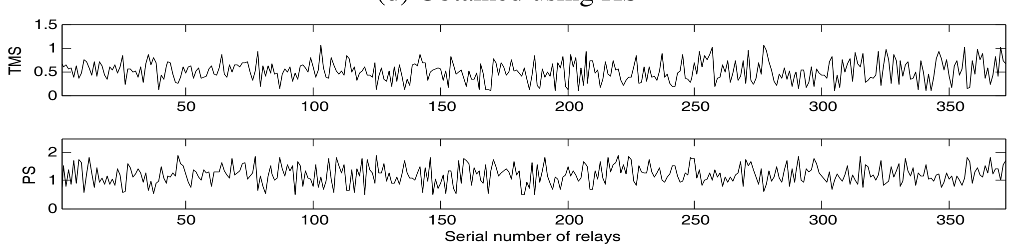

(e) Obtained using SOA

Figure 2.16: Optimum settings of DOCRs with mixed characteristic curves considering standard parameters in the IEEE 118-bus system.

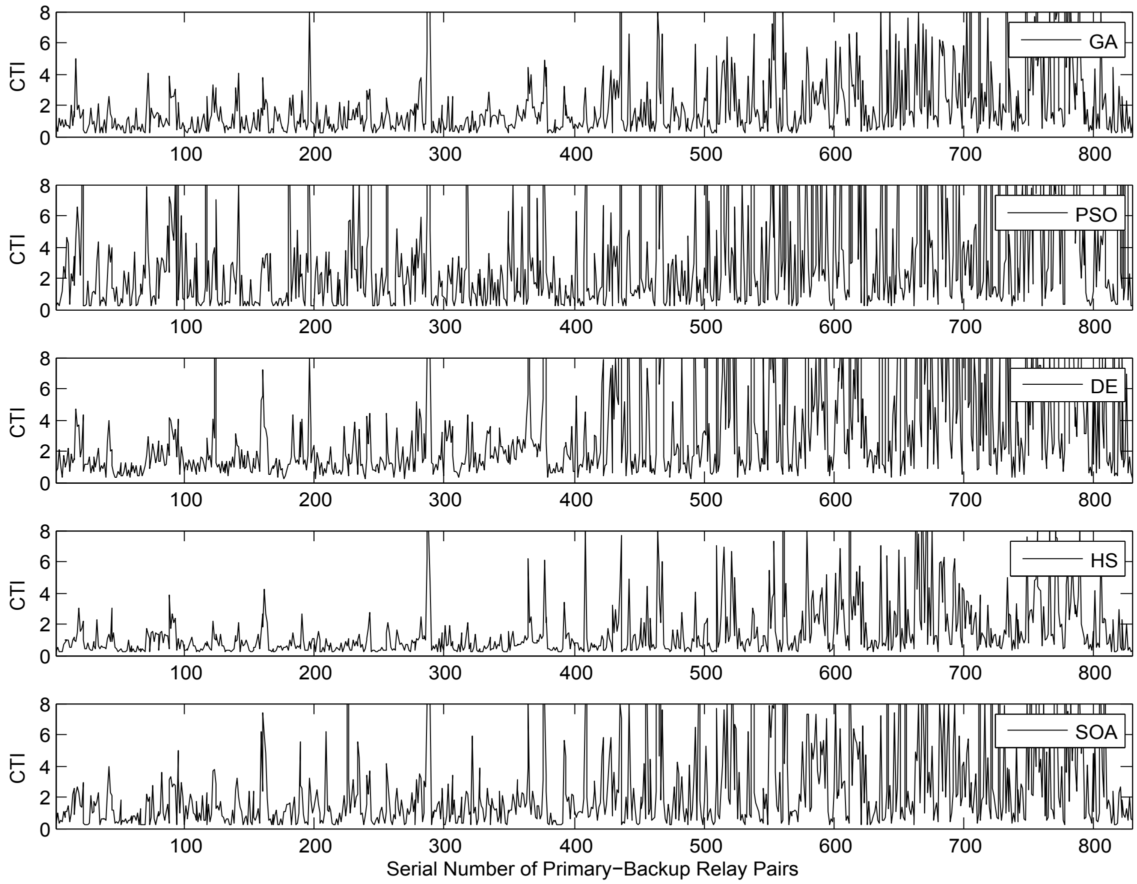

Figure 2.17: CTI obtained by various methods for the IEEE 118-bus system obtained with mixed characteristic curves and standard parameter values.

Table 2.24: Summary of results obtained after 100 independent runs for the IEEE 118-bus system with mixed characteristic curves and standard parameter values

Methods	Objective function value			Standard deviation	Average elapsed time (sec)
	Best	Mean	Worst		
GA	265.1947	274.7177	278.8986	**4.4868**	3862.3274
PSO	503.7209	723.7715	2057.5816	474.8644	**496.013**
DE	**164.7287**	**190.3008**	**266.2406**	27.9267	1563.598
HS	300.7774	451.522	1202.2637	299.0691	798.3414
SOA	301.0847	307.3838	314.4384	4.975	897.388

values of CTI.

2.5 Conclusion

In this chapter, the performances of five different metaheuristic algorithms, namely, GA, PSO, DE, HS and SOA have been investigated for solving the protection coordination problem of DOCRs.

Each algorithm has been executed 100 times with same initial condition as well as with standard and perturbed parameter values in six test systems of various sizes. Based on the studies carried out in this work, DE algorithm has been found to be the best one among the five algorithms studied in this chapter on following counts:

(i) The best value obtained by DE is always the lowest among the best values obtained by the five algorithms considered.

(ii) The best value obtained by DE is virtually immune to the variations of the parameters of DE.

(iii) Even with different characteristic curves of the relays, DE gives the lowest value of the objective function.

(iv) Because of low value of standard deviation, the values obtained by DE are quite predictable as compared to the other four methods.

(v) DE is relatively time efficient algorithm in solving DOCRs coordination problem.

As a result, DE can be considered to be the most suitable metaheuristic algorithm for the coordination of DOCRs among the five algorithms studied in this chapter.

In the next chapter, a new problem formulation for coordination of DOCRs and an analytical optimization approach for solving the coordination problem are discussed.

Chapter 3

Protection Coordination of Directional Overcurrent Relays Using Interior Point Method

Abstract

In this chapter, interior point method based protection coordination schemes are presented for coordinating directional overcurrent relays. Also, for minimizing the operating times of primary and backup relays simultaneously, a new objective function (NOF) is developed. The effectiveness of the proposed solution methods and the developed objective function has been investigated on three test systems (one small, one medium and one large). The suitability of the proposed method for coordination of directional overcurrent relays in meshed networks has been established by comparing its performance with that obtained by genetic algorithm, differential evolution and two hybrid algorithms for the developed objective function. Also, the superiority of the develop objective function has been established by comparing the protection coordination results obtained by using NOF with those obtained by the other objective functions reported in the literature.

3.1 Introduction

IN this chapter, a new formulation for DOCR coordination problem is proposed with an objective to minimize the operating times of both primary and backup relays for all possible primary-backup combinations. In the proposed formulation, different types of relays (electromechanical, static and numerical) with different characteristic curves (IDMT, VIN or EIN) are considered. As a result, both continuous and discrete variables are involved in the proposed formulation which makes it an MINLP problem. Further, to solve the protection coordination problem, two interior point [96] based algorithms are developed. Both these algorithms are two-phase optimization techniques and are named as IPM-IPM and IPM-BBM, respectively. In the first phase of both the methodologies, interior point method (IPM) is used to obtain continuous values of TMSs and PSs of DOCRs. In the second phase of IPM-BBM technique, branch and bound method (BBM) and in the second phase of IPM-IPM technique, IPM is used to obtain final settings (continuous TMS values and discrete PS values) of DOCRs.

The suitability of the newly proposed formulation and the solution procedures is demonstrated on IEEE 14, 30 and 118-bus systems. Further, the results obtained by the proposed methods have also been compared with those obtained by two metaheuristic and two hybrid optimization approaches. The metaheuristic approaches used in this chapter are: i) genetic algorithm (GA) and ii) differential evolution (DE). The two hybrid approaches are: a) IPM-GA and b) IPM-DE. Both these approaches are two phase optimization methods in which IPM is used in the first phase of both these methods. Subsequently, GA and DE are used in the second phase of IPM-GA and IPM-DE algorithms, respectively.

3.2 Problem formulation for overcurrent relay coordination

As discussed in the previous chapter, the objective of optimum protection coordination problem of DOCRs is to minimize the sum of operating times of all the relays corresponding to the maximum fault current [28, 31, 39], i.e.,

$$OF1 = \min \sum_{i=1}^{m} t_{op,i} \tag{3.1}$$

Subjected to:

$$t_{ob,j} - t_{op,i} \geq MCT \tag{3.2}$$

$$t_{i,min} \leq t_{op,i} \leq t_{i,max} \tag{3.3}$$

$$TMS_{i,min} \leq TMS_i \leq TMS_{i,max} \tag{3.4}$$

$$PS_{i,min} \leq PS_i \leq PS_{i,max} \tag{3.5}$$

In eqn. (3.1), $t_{op,i}$ is the operating time of the relay R_i and m is the total number of relays in the system. In eqn. (3.2), $t_{op,i}$ and $t_{op,j}$ are the operating time of primary relay R_i and its backup relay R_j, respectively, for the same fault and *MCT* is the minimum coordination time required. In eqn. (3.3), $t_{i,min}$ and $t_{i,max}$ are the minimum and maximum operating time of the relay R_i for the fault at any point in the zone of operation. In eqn. (3.4), $TMS_{i,min}$ and $TMS_{i,max}$ are the minimum and the maximum limits of TMS while in eqn. (3.5), $PS_{i,min}$ and $PS_{i,max}$ are the same quantities for PS corresponding to relay R_i. The operating time of relay R_i is obtained from its characteristic curve as defined in IEC/IEEE [60, 97],

$$t_{op,i} = \frac{\lambda \times TMS_i}{(I_{Fi}/PS_i)^{\eta} - 1} + L;\ \forall i \tag{3.6}$$

In eqn. (3.6), I_{Fi} is the fault current passing through relay R_i whereas, TMS_i and PS_i are the settings of relay R_i. In this equation, λ, η and L are the characteristic coefficients of DOCRs whose values for various relays are given in Table 3.1 [60, 98, 99].

Table 3.1: Characteristic curve coefficients of DOCRs

Characteristic curve of relay	λ	η	L
standard inverse definite minimum time (IDMT)	0.14	0.02	0
very inverse (VIN)	13.5	1	0
extremely inverse (EIN)	80.0	2	0

It is to be noted that the objective function defined in eqn. (3.1) minimizes the operating times of the primary relays only and there is no restriction on the operating times of the backup relays.

3.2.1 Other objective functions for coordination of DOCRs

To minimize the operating times of the backup relays along with those of the primary relays, several alternative objective functions have been proposed in the literature. In [53] a new objective function is formulated as,

$$OF2 = \min\left(\alpha_1 \sum_{i=1}^{m} (t_{op,i})^2 + \alpha_2 \sum_{j=1}^{n} (\Delta t_j - \beta(\Delta t_j - |\Delta t_j|))^2\right) \tag{3.7}$$

In eqn. (3.7), $\Delta t_j = t_{ob,j} - t_{op,i} - MCT$, α_1 and α_2 are nonnegative weight factors, β is a factor to penalize any miscoordination and n is number of combinations of primary-backup relays [100]. A simplified version of the objective function given in eqn. (3.7) is formulated in [54] as,

$$OF3 = \min\left(\alpha_1 \sum_{i=1}^{m} (t_{op,i})^2 + \alpha_2 \sum_{j=1}^{n} (\Delta t_j - |\Delta t_j|)^2\right) \tag{3.8}$$

In [55], another modified objective function is proposed considering priority of the constraint as,

$$OF4 = \min\left(\alpha_1 \sum_{i=1}^{m} (t_{op,i})^2 + \beta \sum_{j=1} BC_j\right) \tag{3.9}$$

In eqn. (3.9), BC_j is known as broken constraint and is defined as either zero or 1 depending on $\Delta t_j > \epsilon$ or $\Delta t_j < \epsilon$ for primary-backup combination j, respectively. The symbol ϵ represents a very small number of the order of 10^{-8}.

It is to be noted that in the objective functions of eqns. (3.7)-(3.9), the constraint given in eqn. (3.4) is incorporated indirectly with the help of penalty factors. As a result, the constraint of eqn. (3.4) is not considered separately while solving the relay coordination problem. However, in [53–55], it is observed that in some cases, the constraint violation can take place.

3.2.2 Proposed objective function for coordination of DOCRs

To ensure that the constraint of eqn. (3.4) is always satisfied while the operating times of the primary and backup relays are also minimized simultaneously, a new objective function (NOF) is formulated in this work as follows,

$$NOF = \min\left(\alpha_1 \sum_{i=1}^{m} (t_{op,i})^2 + \alpha_2 \sum_{j=1}^{n} (t_{ob,j} - MCT)^2\right) \tag{3.10}$$

The significance of the weighting factors α_1 and α_2 lies in providing a compromise between minimum operating times of primary and backup relays. If the first term is given full weightage (i.e., $\alpha_1 = 1$, $\alpha_2 = 0$) then the NOF tries to minimize the operating times of the primary relays without any restriction on the operating times of the backup relays. On the other hand, if the second term is given full weightage (i.e., $\alpha_1 = 0$, $\alpha_2 = 1$) then the NOF tries to minimize the operating times of the backup relays without any restriction on the operating times of the primary relays. It is to be noted that when the operating times of the backup relays are minimized, the effective coordination time intervals (CTIs) between the primary-backup relays are also minimized. Therefore, the proposed NOF also minimizes the CTIs along with the operating times of the primary and backup relays.

The proposed NOF is subjected to the same sets of constraints discussed earlier with some modifications as discussed below:

1) *Requirement of Protection Coordination Criteria*: The same as defined by eqn. (3.2).

2) *Limitations on Relay Operating Time*: The same as defined by eqn. (3.3).

3) *Limitations on TMS and PS of the Relays*: The same as defined by eqns. (3.4) and (3.5). However, the values of $PS_{i,min}$ and $PS_{i,max}$ are calculated as [60, 101],

$$PS_{i,min} = \max\left(0.5, \min\left(1.25 \times \frac{I_{Lmax,i}}{CTR_i}, \frac{I_{fmin,i}}{3\times CTR_i}\right)\right) \tag{3.11}$$

$$PS_{i,max} = \min\left(2, \frac{2\times I_{fmin,i}}{3\times CTR_i}\right) \tag{3.12}$$

In eqns. (3.11) and (3.12), CTR_i, $I_{fmin,i}$ and $I_{Lmax,i}$ are the current transformer ratio (CTR), minimum fault current and maximum load current corresponding to relay R_i, respectively. The first condition (eqn. (3.11)) ensures the blocking of mal-operation and the second condition (eqn. (3.12)) ensures the sensitivity of the relay. It is to be noted that the values of PSs are considered to be in the range of 0.5 to 2.0 (times the current transformer secondary rating) [53].

The following weighting factors are considered for the various objective functions as shown in Table 3.2 [53–55].

Table 3.2: Weighting factors for various objective functions

Weights	OF2	OF3	OF4	NOF
α_1	1	1	1	1
α_2	1	100	-	0.01
β	100	-	100	-

3.3 Details of the solution approach

The coordination problem of DOCRs formulated in the last section is a MINLP problem as the different types of relays (electromechanical, static or numerical) have been considered in this work. To solve this MINLP problem, two different two-phase solution approaches (hereafter, named as IPM-BBM and IPM-IPM) are proposed in this work. In Phase-I, the plug settings of the electromechanical and static relays are considered as continuous variables, thereby converting the MINLP problem to a NLP problem, which, in turn, is solved using IPM [102]. In Phase-II, the lower bounds of the PS parameters are restricted to the nearest lower discrete values of the corresponding results obtained in the first phase, whereas, the upper bounds of the same are restricted to the nearest higher discrete values. Subsequently, the coordination problem is solved as a MINLP problem using (a) BBM [103] (in IPM-BBM method) and (b) IPM [102] (in IPM-IPM method) to obtain the optimum settings of the relays, where the PS values of the relays are considered as discrete variables and the TMS values of the relays are considered as continuous variables. The detailed procedures for the proposed solution method are given below.

3.3.1 Fault analysis

For designing any protection scheme, initially the steady-state and fault analysis of the system under study need to be carried out. For obtaining the settings the DOCRs, the following quantities need to be known for each relay of the system under study.

1) Maximum load current (I_{Lmax})

2) Minimum fault current (I_{fmin})

3) Maximum fault current (I_{fmax})

4) Primary relay current ($I_{fprimary}$) and backup relay current ($I_{fbackup}$) for each primary-backup combination for the maximum fault current at the primary relay.

The Newton-Raphson load flow (NRLF) analysis has been carried out to calculate the maximum load current (I_{Lmax}) passing through the relays whereas bus impedance (Z_{bus}) matrix based fault analysis approach has been adopted to calculate the various fault currents passing through the relays in the system under study. For calculating the maximum fault current (I_{fmax}), three-phase-to-ground faults have been considered whereas for calculating the minimum fault current (I_{fmin}), line-to-line faults with a fault impedance of 0.1 p.u. [31, 104] have been considered. With the knowledge of the above mentioned currents, CTR for i^{th} relay (CTR_i) is calculated as [60],

$$CTR_i = \max\left(I_{Lmax,i}, \frac{I_{fmax,i}}{20}\right) \tag{3.13}$$

In eqn. (3.13), $I_{fmax,i}$ and $I_{Lmax,i}$ are the values of the I_{fmax} and I_{Lmax} for i^{th} relay, respectively. If $I_{fbackup}$ of a primary-backup relay combination satisfies the condition of eqn. (3.14), then such primary-backup relay combination is ignored because for such a combination the MCT requirement will always be satisfied.

$$I_{fbackup} < \max(2 \times I_{Lmax}, I_{fmin}) \tag{3.14}$$

3.3.2 Proposed optimization approach: Phase-I (IPM)

In Phase-I of the two-phase optimization approach, the following steps are adopted to obtain the intermediate solution;

1. Set lower and upper bounds on TMS as TMS_{min} and TMS_{max}.

2. Calculate CTR for all relays.

3. Set lower and upper bounds of PS using I_{Lmax}, I_{fmin}, and CTR with the help of eqns. (3.11) and (3.12).

4. Solve the NLP problem using IPM to obtain the values of TMS and PS of all the relays.

It is to be noted that the solutions of TMS and PS for all the relays obtained after Phase-I are all continuous values.

3.3.3 Proposed optimization approach: Phase-IIa (Second phase of IPM-BBM method)

In the second phase of IPM-BBM method, the final solution is obtained by employing BBM using the intermediate results calculated in Phase-I. The detailed procedures are as follows;

1. Upper and lower bounds on PS are modified as,

$$PS_{i,min} = floor(4 \times PS_{i,phase-I})/4 \tag{3.15}$$

$$PS_{i,max} = ceil(4 \times PS_{i,phase-I})/4 \tag{3.16}$$

   where $PS_{i,phase-I}$ is the value of PS of relay R_i obtained after Phase-I of the procedure whereas, functions $floor(x)$ and $ceil(x)$ return lower and upper integer values of x, respectively. It is to be noted that the multiplication and the division by 4 have been performed on PS of Phase-I in order to obtain lower and upper discrete limits of the same for Phase-II.

2. Initial TMS values are set to be equal to the results obtained in Phase-I.

3. Initial PS values are set to be equal to $PS_{i,min}$.

4. A new variable for handling the discrete values of PS is defined as [105] (for electromechanical and static relays only, as these relays consider PS as discrete quantities),

$$PS_i = PS_{i,min} + b_i \times ds_i \tag{3.17}$$

   where ds_i is the step size of PS and b_i is a binary variable having values {0,1} for relay R_i. It is to be noted that for numerical/digital relays, PS values are continuous and therefore in this phase, the final solution of these quantities will be calculated by BBM.

5. Apply BBM to solve the MINLP problem.

6. Print the final optimum settings of the relays.

3.3.4 Proposed optimization approach: Phase-IIb (Second phase of IPM-IPM method)

In the second phase of IPM-IPM method, IPM is again employed to calculate the final settings. This stage uses the intermediate results calculated in Phase-I. The detailed procedures are as follows;

1. Upper and lower bounds on PS are modified using eqns. (3.15) and (3.16).

2. Initial TMS values are set to be equal to the results obtained in Phase-I.

3. Initial PS values are set to be equal to $PS_{i,min}$.

4. Discrete values of PS are obtained with the help of one equality and two inequality constraints using two sets of continuous variables $u_i, v_i \in \{0, 1\}$ as [105] (for electromechanical and static relays only, as these relays consider PS as discrete quantities),

$$PS_i = PS_{i,min} + db_i \times ds_i \tag{3.18}$$

   Subjected to:

$$u_i \geq 0 \tag{3.19}$$

$$v_i \geq 0 \tag{3.20}$$

$$u_i \times v_i = 0 \tag{3.21}$$

   where u_i and v_i are two continuous variables and are defined as $u_i = db_i$ and $v_i = 1 - db_i$, respectively, while db_i being the required discrete variable for relay R_i. It is to be noted that for numerical/digital relays, PS values are continuous and therefore in this phase, the final solution of these quantities will be calculated by IPM.

5. Apply IPM with three additional constraints described in eqns. (3.19)-(3.21) to solve the MINLP problem.

6. Print the final optimum settings of the relays.

The solution obtained after Phase-II is optimum with continuous values of TMS and discrete values of PS of the relays. A flowchart with detailed information of the two-phase optimization approach is shown in Figure 3.1.

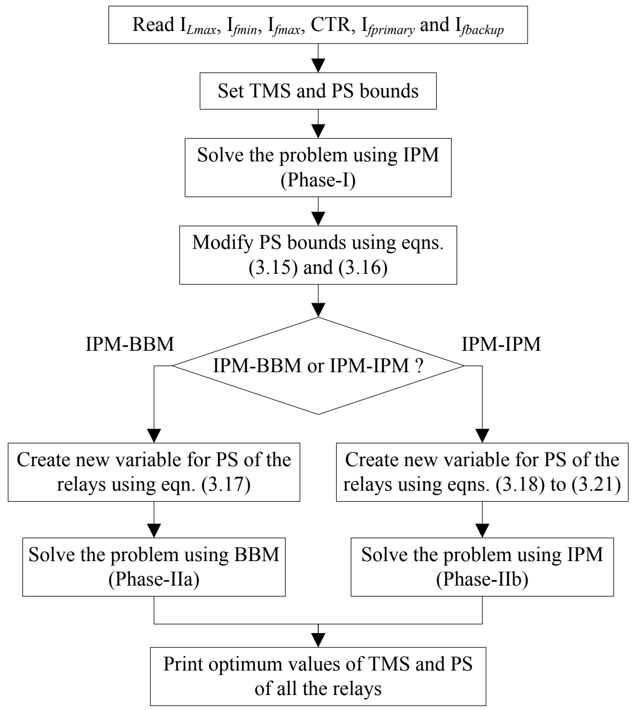

Figure 3.1: Comprehensive flowchart for the proposed optimization approach.

3.4 Results and discussion

The effectiveness of the proposed formulation along with that of both the two-phase solution techniques has been investigated on three test systems. The first test system is the IEEE 14-bus system having 5 generators and 20 lines [94]. To protect this system with DOCRs, a total of 40 ($= 20\times2$) DOCRs need to be installed and coordinated in this system. The second test system is the IEEE 30-bus system having 7 generators and 41 lines [94]. To protect this system, a total of 82 ($= 41\times2$) DOCRs need to be used and coordinated with each other. The third test system is a large power system network (IEEE 118-bus system) having 54 generators and 186 lines [94]. In this system, a total of 372 ($= 186\times2$) DOCRs need to be used and coordinated with each other. In this work, all simulation studies have been carried out in MATLAB 12a [74].

For comparison purpose, protection coordination problems of all these test systems have also been solved using two heuristic optimization approaches, namely GA and DE. Additionally, these problems have also been solved using two hybrid (two-phase) optimization approaches, namely, IPM-GA and IPM-DE. In the first phase of both the hybrid optimization approaches, IPM has been used to obtain the intermediate results (which are continuous in nature), whereas in the second phase GA and DE have been used to obtain the final (continuous and discrete) results. In these methods population size has been considered as 100. The crossover factor (CF) and the mutation factor (MF) for GA have been considered as 0.8 and 0.01, respectively, [31, 106], whereas the crossover rate (CR) and the mutation factor (F) for DE have been considered as 0.4 and 0.5, respectively [91, 106].

3.4.1 Case-I: IEEE 14-bus system

The detailed description of this system is given in Section 2.4.4. The optimal settings of the relays obtained corresponding to the proposed objective function (NOF) using metaheuristic methods (GA and DE), hybrid methods (IPM-GA and IPM-DE) and the proposed methods (IPM-BBM and IPM-IPM) are given in Table 3.3. It is to be noted that the results in Table 3.3 are the best results (corresponding to the minimum value of objective function) obtained after 100 runs of each method. From Table 3.3 it is observed that both the proposed methods (IPM-BBM and IPM-IPM) give lower values of the sum of operating times of all the relays (for the maximum fault current).

Further, Table 3.4 shows the statistical summary of the results obtained by all the six methods. For generating the results of Table 3.4, following procedure has been adopted. Initially, a set of 100 initial solutions have been generated randomly. Subsequently, with each initial solution, the proposed two-phase solution approaches (IPM-BBM and IPM-IPM) and two-phase hybrid solution approaches (IPM-GA and IPM-DE) have been followed to compute the relay settings. Also, with the same 100 initial solutions, GA and DE have been executed 100 times independently guided by uniformly generated different seeds of random numbers. Thus, both the proposed approaches (IPM-BBM and IPM-IPM), metaheuristic methods (GA and DE) and hybrid (IPM-GA and IPM-DE) optimization approaches have been executed 100 times. From Table 3.4 it is observed that the sum of operating times of the relays obtained by the proposed two-phase optimization methods (IPM-BBM and IPM-IPM) are less than those obtained by the metaheuristic methods (GA and DE) and hybrid optimization approaches (IPM-GA and IPM-DE). Further, the standard deviations for the two hybrid methods and the two proposed methods are quite low indicating that for each of these four methods, the results produced in each run are quite close to each other (i.e., the results are nearly reproducible) even when each run starts from different initial conditions. This is not the case for the two metaheuristic methods. However, among all the six methods, IPM-IPM is fastest

Table 3.3: Settings of the relays obtained for NOF using metaheuristic methods, hybrid methods and proposed methods for the IEEE 14-bus system

Relays	Metaheuristic methods				Hybrid methods				Proposed methods			
	GA		DE		IPM-GA		IPM-DE		IPM-BBM		IPM-IPM	
	TMS	PS	TMS	PS	TMS	PS	TMS	PS	TMS	PS	TMS	PS
1	0.1726	0.75	0.1001	0.75	0.1	0.75	0.1	1	0.1	0.75	0.1	0.5
2	0.2651	0.5	0.1001	0.5	0.1004	0.5	0.1001	0.75	0.1	0.5	0.1	0.5
3	0.1744	1.25	0.1001	1.5	0.1001	1.25	0.1001	1.5	0.1	1.5	0.1	1.25
4	0.3301	0.5	0.1001	2	0.1001	0.75	0.1001	0.75	0.1	0.75	0.1	0.5
5	0.2148	1.25	0.1001	2	0.1001	1.25	0.1001	1.5	0.1	1.25	0.1	1.25
6	0.2522	0.5	0.1051	0.75	0.1	1	0.1	1	0.105	0.75	0.1	1
7	0.2217	1	0.1001	1.25	0.1045	1	0.1001	1.25	0.1	1	0.1	1
8	0.4493	0.5	0.1111	0.75	0.1317	0.5	0.1012	0.75	0.1	0.75	0.1	0.75
9	0.2969	1	0.1267	1.5	0.1059	1.5	0.1192	1.25	0.1109	1.25	0.1	1.5
10	0.2647	0.5	0.1228	0.5	0.1001	0.75	0.1001	0.75	0.1153	0.5	0.1	0.75
11	0.6507	0.5	0.222	0.5	0.1225	1.75	0.1835	0.75	0.1083	2	0.1176	1.75
12	0.338	1.25	0.1001	2	0.1002	1.5	0.1	1.5	0.1	1.5	0.1	1.5
13	0.4198	0.5	0.1068	1.75	0.1073	1.5	0.1065	1.5	0.1	1.5	0.1	1.5
14	0.2116	1	0.1001	2	0.1	1.25	0.1	1.25	0.1	1	0.1	1
15	0.2354	1	0.1287	1	0.1012	1.5	0.1048	1.25	0.1	1.5	0.1	1.5
16	0.219	0.5	0.1	0.5	0.1	0.5	0.1001	0.75	0.1	0.5	0.1	0.5
17	0.1414	2	0.1001	1.75	0.1	1.75	0.1137	1.5	0.1	1.75	0.1	1.75
18	0.4079	0.5	0.1001	2	0.1071	1	0.1001	1.25	0.1063	1	0.1	1.25
19	0.2461	1.25	0.1001	2	0.1013	1.5	0.1001	1.5	0.1	1.25	0.1	1.25
20	0.2174	0.5	0.1	1.75	0.1001	0.5	0.1001	0.75	0.1	0.5	0.1	0.5
21	0.5382	0.5	0.1554	2	0.1698	1.75	0.1596	2	0.1558	2	0.155	2
22	0.3614	0.5	0.1323	2	0.1427	1.75	0.1295	2	0.1291	2	0.1291	2
23	0.225	2	0.1097	2	0.1182	1.75	0.108	2	0.1181	1.75	0.1079	2
24	0.3598	0.5	0.1106	1.75	0.123	1.5	0.1828	0.75	0.1214	1.5	0.1373	1.25
25	0.2526	1.25	0.1323	2	0.1302	2	0.1281	2	0.1277	2	0.1277	2
26	0.1901	2	0.1001	2	0.1062	2	0.1	2	0.1017	1.75	0.1	2
27	0.174	1.25	0.1001	2	0.1	1.5	0.1001	1.5	0.1	1.25	0.1	1
28	0.5898	0.5	0.1585	2	0.159	2	0.26	0.75	0.1569	2	0.1569	2
29	0.126	1	0.1001	1.75	0.1	1	0.1001	1	0.1	1	0.1	0.75
30	0.3309	0.5	0.1	2	0.1076	1.75	0.1003	2	0.1	2	0.1	2
31	0.4085	0.5	0.168	2	0.1692	2	0.1664	2	0.166	2	0.166	2
32	0.4235	0.5	0.1378	2	0.1383	2	0.2137	0.75	0.1475	1.75	0.1373	2
33	0.3101	0.75	0.1219	2	0.138	1.75	0.1219	2	0.1199	2	0.1218	2
34	0.4047	0.5	0.1829	1.5	0.1675	1.75	0.1518	2	0.1514	2	0.1514	2
35	0.2237	2	0.1502	2	0.1518	2	0.1482	2	0.1478	2	0.1478	2
36	0.5307	0.5	0.1671	2	0.1674	2	0.1733	2	0.1678	2	0.1666	2
37	0.4261	0.5	0.1091	1.75	0.1002	2	0.1001	2	0.1	2	0.1	2
38	0.1756	2	0.1	2	0.1075	1.75	0.1065	2	0.1	2	0.1	2
39	0.3365	0.75	0.1431	2	0.1407	2	0.1371	2	0.1368	2	0.1368	2
40	0.352	0.5	0.1199	2	0.1345	1.75	0.1198	2	0.1168	2	0.1198	2
$\sum_{i=1}^{40} t_{op,i}$	27.8972		14.8033		13.8917		14.1399		13.5101		**13.3623**	

along with the least value of the sum of operating times of all the relays. This makes the IPM-IPM approach superior to all the other approaches.

The time of operations of the primary relays and the corresponding backup relays along with the coordination time interval (CTI) between the combination are shown in Figure 3.2 for all primary-backup relay combinations obtained by the IPM-IPM optimization approach. As observed from this figure, the actual values of CTI are always more than the minimum CTI considered in this

Table 3.4: Comparative results obtained for NOF by using various methods after 100 independent runs for the IEEE 14-bus system

Methods	Sum of operating times of all relays			Standard deviation	Mean solution time (sec)
	Best	Mean	Worst		
GA	27.8972	56.8149	67.9266	11.3069	127.2859
DE	14.8033	15.2207	15.6963	0.2798	25.8915
IPM-GA	13.8917	14.3579	15.3133	0.5338	396.1411
IPM-DE	14.1399	14.1751	14.1872	0.0184	35.2562
IPM-BBM	13.5101	**13.5944**	**13.6333**	**0.0351**	108.2678
IPM-IPM	**13.3623**	13.6292	13.8239	0.1321	**3.3103**

work (0.2 sec).

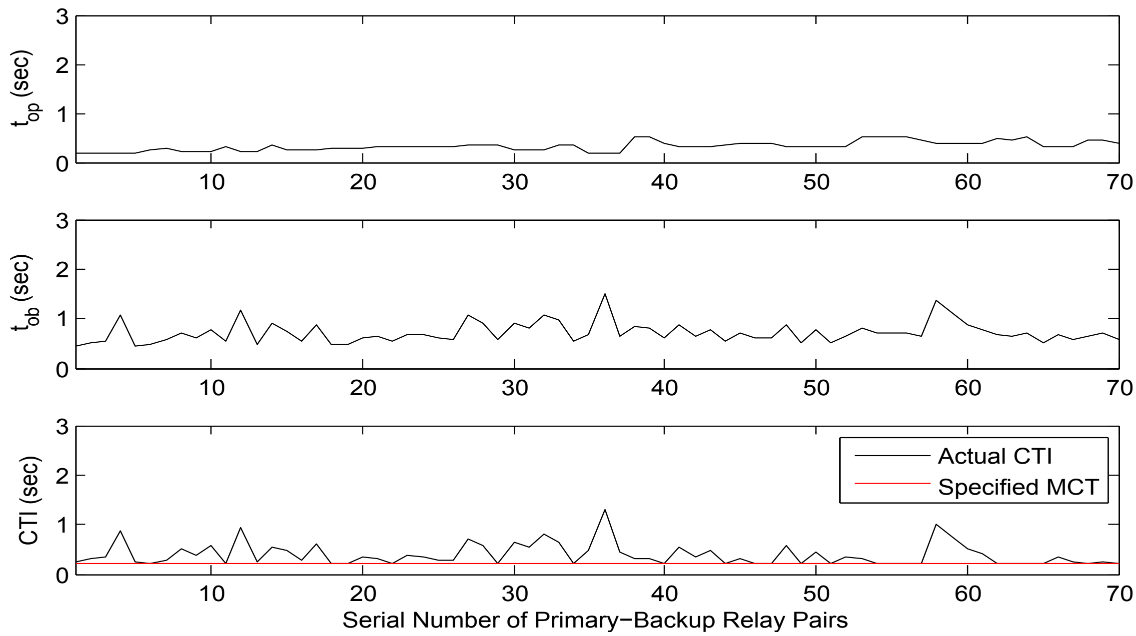

Figure 3.2: Operating times of primary relays, backup relays and CTI in the IEEE-14 bus system.

Now, to test the effectiveness of the proposed objective function NOF, the results obtained by IPM-IPM method corresponding to the different objective functions (OF1, OF2, OF3, OF4 and NOF) have also been compared. Table 3.5 gives the summary of the coordination results corresponding to the different objective functions (OF1, OF2, OF3, OF4 and NOF) in terms of sum of operating times of all the relays for the maximum fault current (SOTR), sum of operating times of all backup relays (SOTB), sum of the actual coordination time interval (SACTI) between the primary-backup combination and number of coordination constraint violations (violation of eqn. (3.4)).

Table 3.5: Comparative results obtained using IPM-IPM for various objective functions for the IEEE 14-bus system

Various Terms	OF1	OF2	OF3	OF4	NOF
SOTR	13.1676	15.2945	13.347	13.3491	13.3621
SOTB	50.7553	48.2785	51.7435	51.7501	49.8429
SACTI	28.484	20.9101	29.1298	29.1327	27.3943
Cases of Violation	0	0	0	0	0

From Table 3.5 it is observed that the objective function OF1 gives the least value of SOTR whereas the objective function OF2 gives the least value of SOTB and SACTI. Further, it can be observed that objective functions OF3 and OF4 are not suitable as they give higher values of SOTB and SACTI as compared to OF1, OF2 and NOF. However, higher value of SOTR corresponding to OF2 makes it inferior to OF1 and NOF. Moreover, as observed from Table 3.5, the value of SOTB and SACTI obtained by NOF are considerably reduced (1.80% and 3.82%, respectively) at the cost of small increment in SOTR (0.15%) as compared to those values corresponding to OF1. Further, the sum of the values of SOTR and SOTB corresponding to NOF is 2.53% lower as compared to sum of SOTB and SOTR corresponding to OF1. Therefore, the proposed objective function minimizes the total operating times of primary and backup relays while always satisfying the coordination constraints. This makes the proposed objective function NOF superior to the other objective functions considered in the literature.

In all the above studies, no relay on the generator feeders has been considered. However, to provide backup protection to the relays installed on the lines which are directly connected to the generator buses, it may be necessary to install DOCRs on each of the generator feeders. Figure 3.3 shows the IEEE 14-bus system equipped with DOCRs at each generator feeder. In this case, these DOCRs also need to be coordinated with the DOCRs installed on the lines connected to the generator buses. To consider this possibility, each of the generator feeder is now assumed to be equipped with a DOCR of IDMT characteristic. These relays are numbered as 41, 42, 43, 44 and 45 (corresponding to generator feeders 1, 2, 3, 4 and 5, respectively). As there are a total of 13 line ends connected to these five generator buses (as shown in Figure 3.3), a total of 13 additional primary backup relay pairs also need to be considered. These additional primary-backup relay pairs are as follows: 1-41, 3-41, 2-42, 5-42, 7-42, 9-42, 6-43, 11-43, 28-44, 20-45, 21-45, 23-45, and 25-45. Thus, after considering DOCRs on each of the generator feeders, total number of relays and total number of primary-backup pairs become 45 and 83, respectively. For co-ordination of these relays, maximum load currents and various fault currents have again been calculated using the same procedure as discussed in Section 3.3.1.

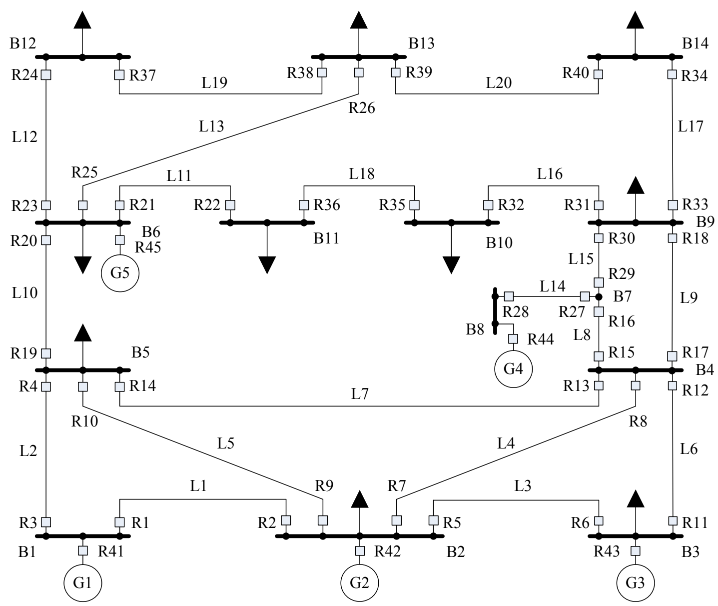

Figure 3.3: IEEE 14-bus system having a DOCR at each generator feeder.

Now, the results presented so far show that the combination of the proposed NOF and the proposed IPM-IPM method gives the best co-ordination result. Therefore, the co-ordination of the augmented protection system (comprising of 45 relays and 83 primary backup pairs) has been carried out for this combination (NOF and IPM-IPM) only. The new settings (TMS and PS) of all the 45 relays are shown in Table 3.6. Also, the operating times of all primary relays, backup relays and CTI corresponding to all 83 pairs are shown in Figure 3.4.

Comparison of the results of Table 3.3 (last two columns) and Table 3.6 shows that TMS values of 9 relays (relay no. 7-10, 12, 15, 18, 37 and 38) have increased and that of one only relay (relay no. 23) has decreased, while those of the remaining 30 relays remain unchanged. The maximum change observed in TMS values is 0.0278 for relay no. 8. Further, PS value of 12 relays (relay no. 3, 5-10, 12, 15, 18, 37 and 38) have decreased by 0.25, while the PS values of the other

Table 3.6: Settings of the relays obtained with NOF and IPM-IPM method for the IEEE 14-bus augmented system

Relays	TMS	PS	Relays	TMS	PS	Relays	TMS	PS
1	0.1	0.5	16	0.1	0.5	31	0.166	2
2	0.1	0.5	17	0.1	1.75	32	0.1373	2
3	0.1	1	18	0.1036	1	33	0.1218	2
4	0.1	0.5	19	0.1	1.25	34	0.1514	2
5	0.1	1	20	0.1	0.5	35	0.1478	2
6	0.105	0.75	21	0.155	2	36	0.1666	2
7	0.1199	0.75	22	0.1291	2	37	0.1057	1.75
8	0.1278	0.5	23	0.1075	2	38	0.1102	1.75
9	0.1109	1.25	24	0.1373	1.25	39	0.1368	2
10	0.1198	0.5	25	0.1277	2	40	0.1198	2
11	0.1176	1.75	26	0.1	2	41	0.1015	1.25
12	0.103	1.25	27	0.1	1	42	0.1017	1
13	0.1	1.5	28	0.1569	2	43	0.1256	2
14	0.1	1	29	0.1	0.75	44	0.1564	1.75
15	0.1044	1.25	30	0.1	2	45	0.1103	1.75

$\sum_{i=1}^{40} t_{op,i}$	13.3115 seconds
$\sum_{i=1}^{45} t_{op,i}$	15.5797 seconds

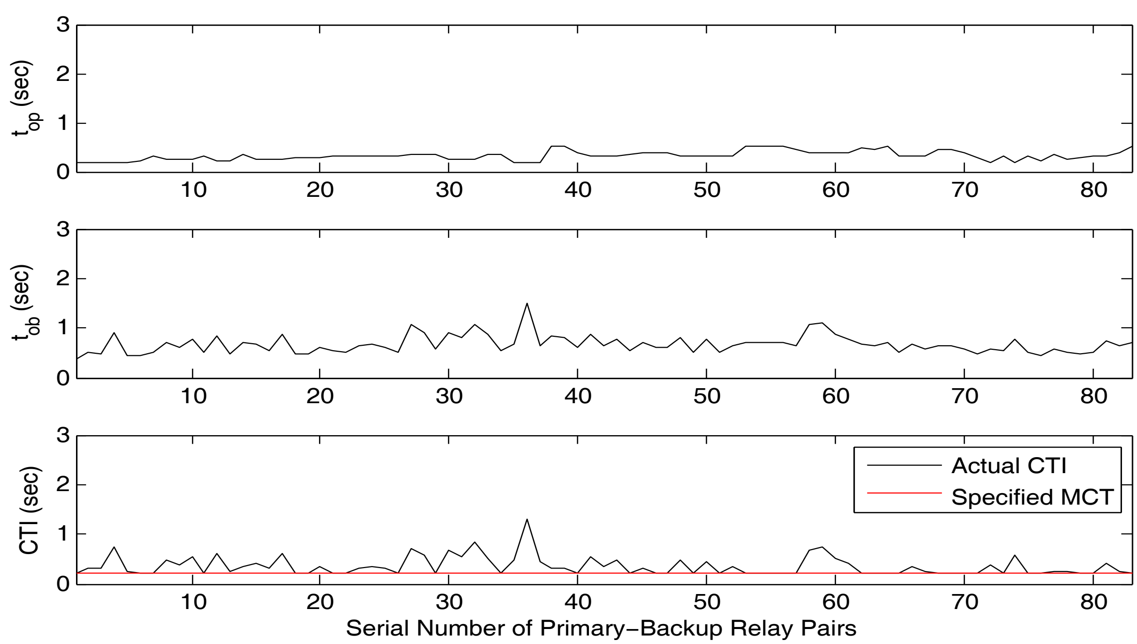

Figure 3.4: Operating times of primary relays, backup relays and CTI in the IEEE 14-bus augmented protection system.

relays remain the same. Thus, the operating times of only 13 relays have changed marginally. Comparison of Figures 3.2 and 3.4 shows that the presence of DOCRs on the generator feeders changes the operating times of the relays marginally.

3.4.2 Case-II: IEEE 30-bus system

The detailed description of this system is given in Section 2.4.5. The optimal settings of the relays obtained corresponding to the proposed objective function (NOF) using metaheuristic methods (GA and DE), hybrid methods (IPM-GA and IPM-DE) and the proposed methods (IPM-BBM and IPM-IPM) are given in Table 3.7. It is to be noted that the results in Table 3.7 are the best results (for the minimum value of objective function) obtained after 100 runs of each method. From, Table 3.7 it is observed that both the proposed methods (IPM-BBM and IPM-IPM) give lower values of the sum of operating times of all the relays (for the maximum fault current).

Table 3.7: Settings of the relays obtained for NOF using metaheuristic methods, hybrid methods and proposed methods for the IEEE 30-bus system

Relays	Metaheuristic methods				Hybrid methods				Proposed methods			
	GA		DE		IPM-GA		IPM-DE		IPM-BBM		IPM-IPM	
	TMS	PS	TMS	PS	TMS	PS	TMS	PS	TMS	PS	TMS	PS
1	0.1003	1.0016	0.1001	1	0.1018	1.0113	0.1083	1.108	0.1	1	0.1	1
2	0.109	0.6179	0.1001	0.5	0.1041	0.6661	0.1003	0.5453	0.1	0.5	0.1	0.5
3	0.1329	1.257	0.1001	1.4941	0.1387	1.2557	0.1118	1.4178	0.1	1.4948	0.1	1.4948
4	0.1933	0.5137	0.1001	0.5	0.1091	0.6066	0.1046	0.5149	0.1	0.5	0.1	0.5
5	0.1427	1.3123	0.1001	1.6786	0.1334	1.5149	0.1121	1.5108	0.1	1.6793	0.1	1.6793
6	0.1061	0.5857	0.1001	0.5679	0.1024	0.6266	0.1059	0.6564	0.1	0.5682	0.1	0.5682
7	0.1311	1.0502	0.1001	1.0472	0.1056	1.0552	0.1078	1.023	0.1	1.0473	0.1	1.0473
8	0.1165	0.8776	0.1001	1.0065	0.1012	1.109	0.1037	1.1401	0.1	1.0072	0.1	1.0072
9	0.1363	1.0348	0.1001	1.076	0.1047	1.0589	0.1046	1.0576	0.1	1.0761	0.1	1.0761
10	0.1916	0.5019	0.1001	0.658	0.1182	0.5482	0.1261	0.5063	0.1	0.6586	0.1	0.6586
11	0.1293	0.8386	0.1001	0.9371	0.1291	0.7547	0.109	0.8867	0.1	0.9374	0.1	0.9374
12	0.2256	0.5958	0.1001	1.5143	0.1049	1.5854	0.1016	1.562	0.1	1.5153	0.1	1.5153
13	0.1287	1.2511	0.1001	1.25	0.115	1.253	0.104	1.2602	0.1	1.25	0.1	1.25
14	0.202	1.7084	0.1281	1.9813	0.1394	1.8216	0.1378	1.7917	0.1274	2	0.1274	2
15	0.1262	1.5128	0.1001	1.4924	0.1176	1.342	0.124	1.2612	0.1	1.4914	0.1	1.4914
16	0.1228	0.9211	0.1001	0.8004	0.1044	0.9204	0.1004	0.8309	0.1	0.801	0.1	0.801
17	0.3481	0.716	0.1703	1.9972	0.1835	1.8299	0.1818	1.8675	0.17	2	0.17	2
18	0.1196	1.2415	0.1001	1.513	0.1002	1.6115	0.1055	1.5614	0.1	1.5144	0.1	1.5144
19	0.129	1.5064	0.102	1.9882	0.1102	1.8154	0.1149	1.8297	0.1015	2	0.1015	2
20	0.287	1.0272	0.1599	1.9914	0.1678	1.9297	0.1745	1.7594	0.1594	2	0.1594	2
21	0.1357	1.302	0.1001	1.2175	0.1371	1.1698	0.1071	1.202	0.1	1.2185	0.1	1.2185
22	0.2869	0.8911	0.1787	1.3901	0.1905	1.299	0.1919	1.2511	0.1781	1.3978	0.1781	1.3978
23	0.1652	1.2572	0.1001	1.6746	0.1115	1.6372	0.1147	1.5243	0.1	1.6733	0.1	1.6733
24	0.1014	0.5109	0.1001	0.5003	0.1073	0.6977	0.1322	0.5346	0.1	0.5	0.1	0.5
25	0.2335	1.0271	0.1099	1.9976	0.1303	1.759	0.1241	1.827	0.1095	2	0.1095	2
26	0.1346	1.0784	0.1001	1.1256	0.1078	1.1089	0.1159	1.0933	0.1	1.1257	0.1	1.1257
27	0.1085	1.5286	0.1001	1.3671	0.1068	1.2935	0.1053	1.3136	0.1	1.368	0.1	1.368
28	0.1566	0.9553	0.1001	1.1157	0.1168	1.0166	0.1117	1.0077	0.1	1.1155	0.1	1.1155
29	0.137	1.0048	0.1001	1.1247	0.1121	1.0524	0.1082	1.1601	0.1	1.1253	0.1	1.1253
30	0.1324	0.9868	0.1001	1.0405	0.1046	1.0639	0.1021	1.0528	0.1	1.0404	0.1	1.0404
31	0.1021	1.2516	0.1001	1.25	0.1007	1.2572	0.1035	1.3303	0.1	1.25	0.1	1.25
32	0.188	1.0229	0.1001	1.5499	0.1099	1.5136	0.1057	1.6369	0.1	1.5486	0.1	1.5486
33	0.1003	1.0048	0.1001	1	0.1001	1.0061	0.1003	1.0164	0.1	1	0.1	1
34	0.3947	0.5899	0.1729	1.9968	0.1962	1.7526	0.19	1.817	0.1724	2	0.1724	2
35	0.273	1.3047	0.1654	1.9816	0.1758	1.9206	0.1755	1.9665	0.1642	2	0.1642	2

Continued on next page

Table 3.7 – continued from previous page

Relays	Metaheuristic methods				Hybrid methods				Proposed methods			
	GA		DE		IPM-GA		IPM-DE		IPM-BBM		IPM-IPM	
	TMS	PS	TMS	PS	TMS	PS	TMS	PS	TMS	PS	TMS	PS
36	0.4046	0.7492	0.2098	1.9969	0.2314	1.7986	0.231	1.7701	0.2092	2	0.2092	2
37	0.368	1.058	0.2126	1.9989	0.2373	1.7941	0.2293	1.9167	0.2115	2	0.2115	2
38	0.3733	0.805	0.1933	1.9989	0.2158	1.7747	0.2149	1.771	0.1929	2	0.1929	2
39	0.3195	1.1179	0.1922	1.9946	0.2073	1.8891	0.1995	1.9915	0.1915	2	0.1915	2
40	0.324	0.7704	0.1988	1.5181	0.1998	1.7556	0.1865	1.7543	0.1702	2	0.1702	2
41	0.216	1.2577	0.1318	1.995	0.1549	1.7933	0.1323	1.9998	0.1288	2	0.1288	2
42	0.1839	1.3515	0.1099	1.8888	0.1192	1.8184	0.1228	1.7526	0.1095	1.8919	0.1095	1.8919
43	0.118	1.5179	0.1001	0.5014	0.101	0.6288	0.1044	0.5673	0.1	0.5	0.1	0.5
44	0.4016	0.883	0.1987	1.9953	0.2164	1.8681	0.2122	1.8983	0.1981	2	0.1981	2
45	0.2238	1.0555	0.1132	1.9977	0.131	1.7672	0.1244	1.9533	0.1129	2	0.1129	2
46	0.1348	1.5577	0.1001	1.6238	0.1158	1.5638	0.1125	1.5082	0.1	1.6229	0.1	1.6229
47	0.2881	1.2404	0.1684	1.9946	0.1877	1.8234	0.1764	1.9805	0.1678	2	0.1678	2
48	0.1975	1.3807	0.101	1.9962	0.1224	1.7512	0.1078	1.9709	0.1006	2	0.1006	2
49	0.4513	0.6212	0.1963	1.9987	0.2199	1.7839	0.2129	1.9005	0.1959	2	0.1959	2
50	0.2847	1.1871	0.1629	1.9928	0.1778	1.8814	0.1758	1.871	0.1622	2	0.1622	2
51	0.2301	1.5413	0.1488	1.9952	0.1628	1.8826	0.1732	1.7587	0.1483	2	0.1483	2
52	0.1522	1.3507	0.1001	1.9543	0.1085	1.9567	0.1106	1.8813	0.1	1.955	0.1	1.955
53	0.3603	1.3849	0.2385	1.9942	0.2587	1.8502	0.251	1.9875	0.2378	2	0.2378	2
54	0.3329	0.7748	0.158	2	0.1778	1.8008	0.1659	1.9404	0.1563	2	0.1563	2
55	0.3417	0.8425	0.1805	1.9896	0.2009	1.8124	0.1917	1.8804	0.1777	2	0.1777	2
56	0.3141	1.2719	0.1931	1.9915	0.2133	1.8219	0.2043	1.9531	0.1923	2	0.1923	2
57	0.5004	0.5151	0.2264	1.9987	0.2487	1.8113	0.2487	1.8143	0.2259	2	0.2259	2
58	0.3159	0.8581	0.1572	1.9972	0.1732	1.8373	0.1643	1.9825	0.1568	2	0.1568	2
59	0.3916	1.1102	0.235	1.9973	0.2608	1.7691	0.2535	1.9085	0.2345	2	0.2345	2
60	0.2847	1.3542	0.175	1.9906	0.1963	1.7763	0.1875	1.9045	0.1732	2	0.1732	2
61	0.4067	0.7995	0.2124	1.9967	0.2337	1.8095	0.2267	1.9493	0.2119	2	0.2119	2
62	0.3983	0.8041	0.2096	1.9982	0.2339	1.7762	0.2215	1.961	0.2082	2	0.2082	2
63	0.3101	1.1948	0.192	1.9904	0.2142	1.7663	0.2	1.9806	0.191	2	0.191	2
64	0.2552	1.4223	0.176	1.9858	0.1981	1.7638	0.1777	1.9648	0.1704	2	0.1704	2
65	0.2632	1.6161	0.18	1.9861	0.193	1.8983	0.1904	1.9587	0.1789	2	0.1789	2
66	0.254	1.8261	0.2042	1.99	0.2253	1.807	0.205	1.9943	0.1994	2	0.1994	2
67	0.3196	0.8146	0.1692	1.9931	0.1922	1.7597	0.1855	1.7649	0.1661	2	0.1661	2
68	0.3892	0.7933	0.1991	1.9958	0.2163	1.8695	0.2111	1.9482	0.1985	2	0.1985	2
69	0.2218	1.1136	0.1387	1.9911	0.1523	1.7793	0.1422	1.7708	0.127	2	0.127	2
70	0.2229	1.4301	0.1543	1.9809	0.1714	1.823	0.1563	1.9795	0.1507	2	0.1507	2
71	0.1003	0.5	0.1001	2	0.1	0.75	0.1095	0.75	0.1	0.5	0.1	0.5
72	0.1209	0.5	0.1001	0.5	0.1001	0.5	0.1027	0.75	0.1	0.5	0.1	0.5
73	0.2557	0.5	0.1223	2	0.1351	1.75	0.1104	2	0.1071	2	0.1071	2
74	0.3231	1.25	0.221	2	0.2305	2	0.2254	2	0.2177	2	0.2177	2
75	0.1991	0.5	0.1001	2	0.1178	1	0.1028	1.25	0.1	1.25	0.1	1.25
76	0.1976	1.25	0.1097	2	0.1522	1.5	0.15	1.5	0.1256	1.75	0.1256	1.75
77	0.1435	1.25	0.1056	2	0.1053	1.5	0.1023	1.75	0.1	1.75	0.1043	1.5
78	0.1383	0.5	0.1001	0.5	0.1067	0.5	0.1207	0.75	0.1	0.5	0.1	0.5
79	0.1305	1	0.1001	2	0.1068	1.25	0.1009	1.25	0.1	1	0.1	1
80	0.1252	0.5	0.1001	2	0.1053	0.75	0.1089	0.75	0.1	0.5	0.1	0.5
81	0.1362	1	0.1001	2	0.1015	1	0.1039	1.25	0.1	1	0.1	1
82	0.1017	0.5	0.1001	2	0.1004	0.5	0.1085	0.75	0.1	0.5	0.1	0.5
$\sum_{i=1}^{82} t_{op,i}$	45.0978		34.669		36.3598		35.8858		33.6625		**33.6528**	

Further, Table 3.8 shows the statistical summary of the results obtained by all the six methods. For generating the results of Table 3.8, following procedure has been adopted. Initially, a set of 100 initial solutions have been generated randomly. Subsequently, with each initial solution, the proposed two-phase solution approaches (IPM-BBM and IPM-IPM) and two-phase hybrid solution approaches (IPM-GA and IPM-DE) have been followed to compute the relay settings. Also, with the same 100 initial solutions, GA and DE have been executed 100 times independently guided by uniformly generated different seeds of random numbers. Thus, both the proposed approaches (IPM-BBM and IPM-IPM), metaheuristic approaches (GA and DE) and hybrid (IPM-GA and IPM-DE) optimization approaches have been executed 100 times. From Table 3.8 it is observed that the sum of operating times of the relays obtained by the proposed two-phase optimization methods (IPM-BBM and IPM-IPM) are less than those obtained by the metaheuristic methods (GA and DE) and hybrid optimization approaches (IPM-GA and IPM-DE). Further, the standard deviations for the two proposed methods are quite low indicating that for the both methods, the results produced in each run are quite close to each other (i.e., the results are nearly reproducible) even when each run starts from different initial conditions. This is not the case for the two metaheuristic methods and the two hybrid methods. However, among all the six methods, IPM-IPM is fastest along with the least value of the sum of operating times of all the relays. This makes the IPM-IPM approach superior to all the other approaches.

Table 3.8: Comparative results obtained for NOF by using various methods after 100 independent runs for the IEEE 30-bus system

Methods	Sum of operating times of all relays			Standard deviation	Mean solution time (sec)
	Best	Mean	Worst		
GA	45.0978	46.8762	48.1154	0.9237	1054.3125
DE	34.669	34.8339	35.0697	0.1438	1063.32
IPM-GA	36.3598	37.2739	38.4904	0.6355	1043.9306
IPM-DE	35.8858	37.4693	42.8917	2.0856	1240.6635
IPM-BBM	33.6625	**33.6898**	**33.7153**	**0.0141**	248.7264
IPM-IPM	**33.6528**	33.7392	33.7998	0.0572	**13.6314**

The time of operations of the primary relays and the corresponding backup relays along with the coordination time interval (CTI) between the combination are shown in Figure 3.5 for all primary-backup relay combinations obtained by the IPM-IPM optimization approach. As observed from this figure, the actual values of CTI are always more than the minimum CTI considered in this work (0.2 sec).

Now, to test the effectiveness of the proposed objective function NOF, the results obtained by IPM-IPM method corresponding to the different objective functions (OF1, OF2, OF3, OF4 and NOF) have also been compared. Table 3.9 gives the summary of the coordination results

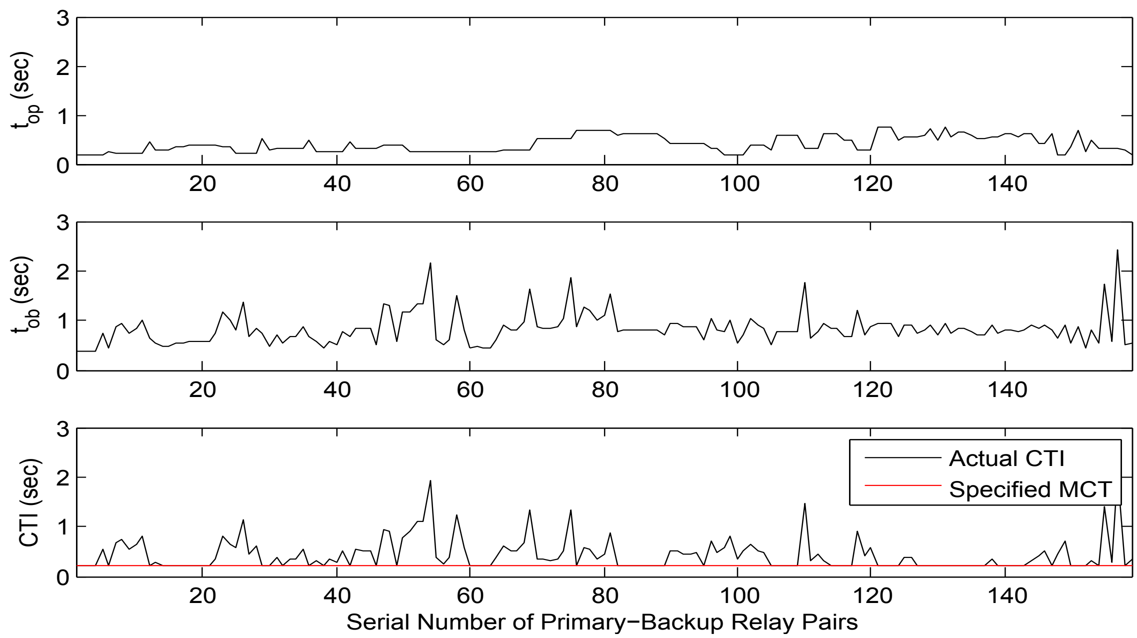

Figure 3.5: Operating times of primary relays, backup relays and CTI in the IEEE 30-bus system.

corresponding to the different objective functions (OF1, OF2, OF3, OF4 and NOF) in terms of SOTR, SOTB, SACTI and number of coordination constraint violations (violation of eqn. (3.4)).

Table 3.9: Comparative results obtained using IPM-IPM for various objective functions for the IEEE 30-bus system

Various Terms	OF1	OF2	OF3	OF4	NOF
SOTR	33.586	39.7784	33.586	33.5922	33.6528
SOTB	135.0722	129.1089	135.0722	135.0872	132.3868
SACTI	70.8254	48.855	70.8254	70.8273	68.0548
Cases of Violation	0	0	0	0	0

From Table 3.9 it is observed that the objective function OF1 gives the least value of SOTR whereas the objective function OF2 gives the least value of SOTB and SACTI. Further, it can be observed that OF4 gives the higher values of SOTR, SOTB and SACTI as compared to OF3 and the results of F3 is the same as those of OF1. However, higher value of SOTR corresponding to OF2 makes it inferior to OF1 and NOF. Moreover, as observed from Table 3.9, the value of SOTB and SACTI obtained by NOF are considerably reduced (1.99% and 3.91%, respectively) at the cost of small increment in SOTR (0.2%) as compared to those values corresponding to

OF1. Further, the sum of the values of SOTR and SOTB corresponding to NOF is 2.65% lower as compared to sum of SOTB and SOTR corresponding to OF1. Therefore, the proposed objective function minimizes the total operating times of primary and backup relays while always satisfying the coordination constraints. This makes the proposed objective function NOF superior to the other objective functions considered in the literature.

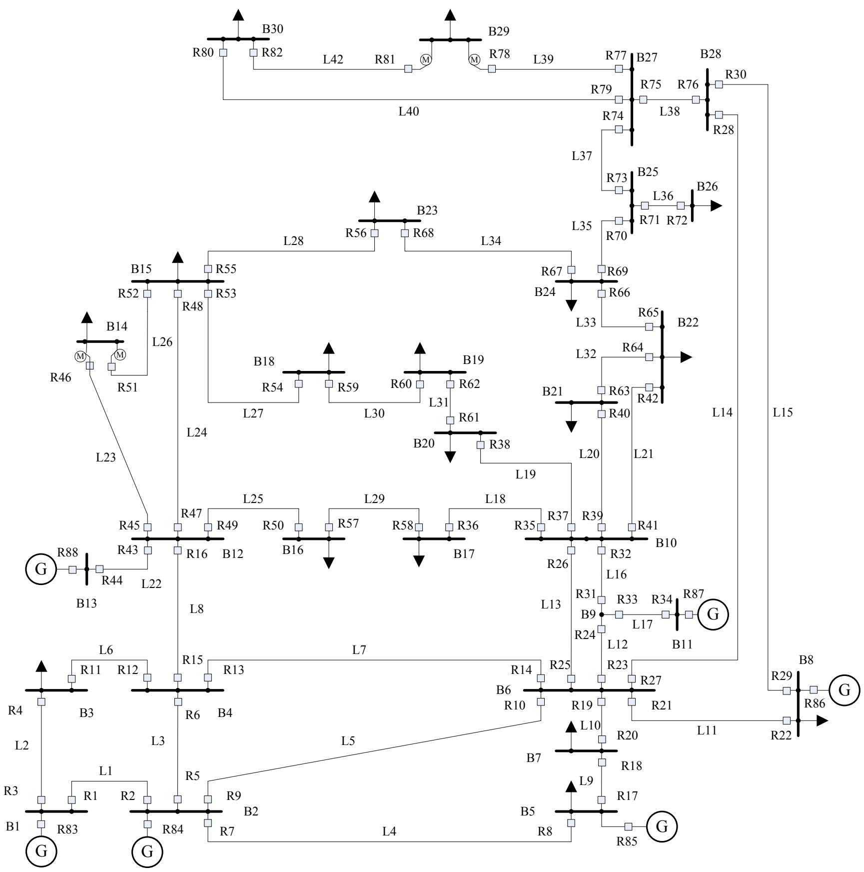

Figure 3.6: IEEE 30-bus system having a DOCR at each generator feeder.

In all the above studies, no relay on the generator feeders has been considered. However, to provide backup protection to the relays installed on the lines which are directly connected to the generator buses, it may be necessary to install DOCRs on each of the generator feeders. Figure 3.6 shows the IEEE 30-bus system equipped with DOCRs at each generator feeder. In that case, these DOCRs also need to be coordinated with the DOCRs installed on the lines connected to the generator buses. To consider this possibility, each of the generator feeder is now assumed to be equipped with a DOCR of IDMT characteristic. These relays are numbered as 83, 84, 85, 86, 87 and 88 (corresponding to generator feeders 1, 2, 5, 8, 11 and 13, respectively). As there are a total of 12 line ends connected to these six generator buses (as shown in Figure 3.6), a total of 12 additional primary backup relay pairs also need to be considered. These additional primary-backup relays pairs are as follows: 1-83, 3-83, 2-84, 5-84, 7-84, 9-84, 8-85, 17-85, 22-86, 29-86, 34-87 and 34-88. Thus, after considering DOCRs on each of the generator feeders, total number of relays and total number of primary-backup pairs become 88 and 171, respectively. For co-ordination of these relays, maximum load currents and various fault currents have again been calculated using the same procedure as discussed in Section 3.3.1.

Table 3.10: Settings of the relays obtained with NOF and IPM-IPM method for the IEEE 30-bus augmented system

Relays	TMS	PS	Relays	TMS	PS	Relays	TMS	PS	Relays	TMS	PS
1	0.1	1	23	0.1	1.6733	45	0.1129	1.9998	67	0.1661	2
2	0.1	0.5001	24	0.1	0.5002	46	0.1	1.6229	68	0.1985	2
3	0.1	1.4948	25	0.1096	1.9999	47	0.1678	2	69	0.127	1.9997
4	0.1	0.5	26	0.1	1.1258	48	0.1007	1.9999	70	0.1507	2
5	0.1	1.6792	27	0.1	1.3604	49	0.1959	1.9999	71	0.1	0.5
6	0.1	0.5682	28	0.1	1.1155	50	0.1622	1.9999	72	0.1	0.5
7	0.1	1.0473	29	0.1	1.1253	51	0.1483	1.9999	73	0.1071	2
8	0.1	1.0072	30	0.1	1.0218	52	0.1	1.955	74	0.2177	2
9	0.1	1.076	31	0.1	1.2501	53	0.2378	2	75	0.1	1.25
10	0.1	0.6586	32	0.1	1.5486	54	0.1563	2	76	0.1257	1.75
11	0.1	0.9374	33	0.1	1.0002	55	0.1777	2	77	0.1043	1.5
12	0.1	1.5153	34	0.1724	1.9999	56	0.1923	2	78	0.1	0.5
13	0.1	1.25	35	0.1642	1.9998	57	0.2259	1.9999	79	0.1	1
14	0.1274	1.9999	36	0.2092	1.9999	58	0.1568	1.9999	80	0.1	0.5
15	0.1	1.4914	37	0.2115	1.9999	59	0.2345	2	81	0.1	1
16	0.1	0.801	38	0.1929	2	60	0.1732	1.9999	82	0.1	0.5
17	0.17	1.9999	39	0.1915	2	61	0.2119	2	83	0.1818	0.5
18	0.1	1.5144	40	0.1702	1.9999	62	0.2082	1.9998	84	0.1022	1
19	0.1016	1.9996	41	0.1288	2	63	0.1911	2	85	0.3873	0.5
20	0.1594	1.9999	42	0.1095	1.8915	64	0.1704	2	86	0.1666	2
21	0.1	1.2186	43	0.1	0.5002	65	0.1789	2	87	0.313	1
22	0.1585	1.7491	44	0.1981	1.9999	66	0.1994	1.9999	88	0.319	1.25
$\sum_{i=1}^{82} t_{op,i}$			33.6315 seconds								
$\sum_{i=1}^{88} t_{op,i}$			37.5075 seconds								

Now, the results presented so far show that the combination of the proposed NOF and the proposed IPM-IPM method gives the best co-ordination result. Therefore, the co-ordination of the augmented protection system (comprising of 88 relays and 171 primary backup pairs) has been carried out for this combination (NOF and IPM-IPM) only. The new settings (TMS and PS) of all the 88 relays are given in Table 3.10. Also, the operating times of all primary relays, backup relays

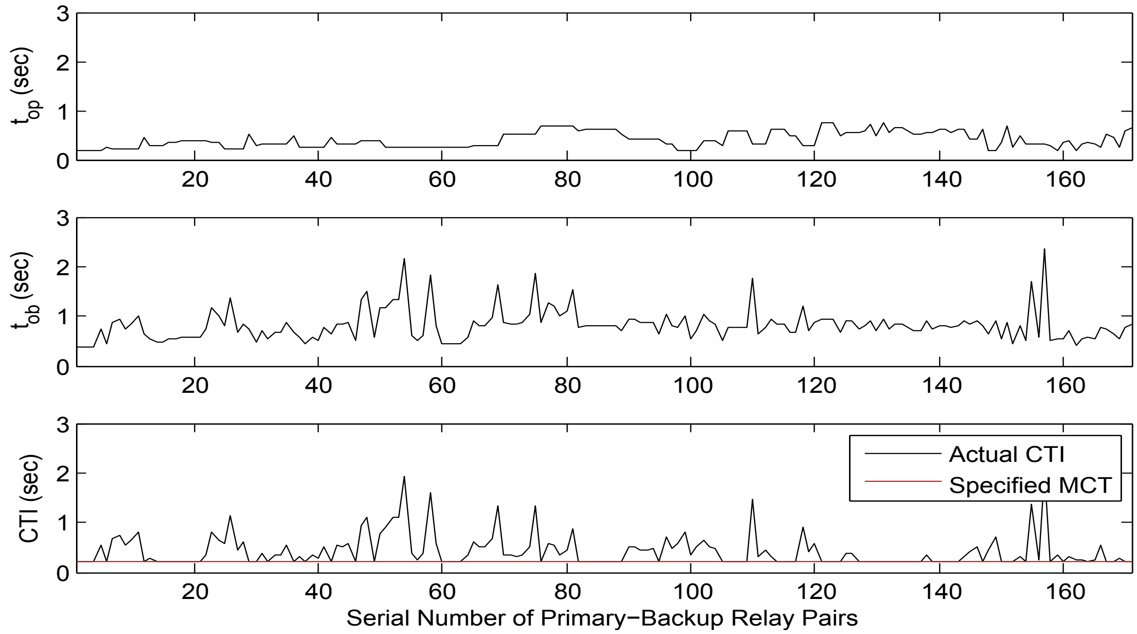

Figure 3.7: Operating times of primary relays, backup relays and CTI in the IEEE 30-bus augmented protection system.

and CTI corresponding to all 171 pairs are shown in Figure 3.7.

Comparison of the results of Table 3.7 (last two columns) and Table 3.10 shows that TMS values of 23 relays (out of the original 82 relays) have changed, while those of the remaining 59 relays remain unchanged. Out of the 23 changes in TMS values, values of TMS for 3 relays have increased while TMS values for 20 relays have reduced. Similarly, the PS values of 51 relays have increased, 18 relays have reduced and those of the remaining 13 relays remained same. Also, for 11 relays, both TMS and PS values did not change at all. From Tables 3.7 and 3.10, it can be observed that the maximum change in TMS and PS are 0.0196 and 0.3509, respectively. Comparison of Figures 3.5 and 3.7 shows that the presence of DOCRs on the generator feeders changes the operating times of the relays marginally.

3.4.3 Case-III: IEEE 118-bus system

The detailed description of this system is given in Section 2.4.6. For this system, different types of DOCRs with various characteristics have been considered. These are;

1) 1-200: IDMT (numerical/digital type)

2) 201-260: VIN (numerical/digital type)

3) 261-300: EIN (numerical/digital type)

4) 301-372: IDMT (electromechanical type)

The same minimum and maximum limits on TMS and PS of the relays as mentioned in Case-I have also been considered in this case. The TMSs have been considered to be continuous variables for all the relays whereas the PSs have been considered to be a) continuous for numerical relays and b) discrete for electromechanical relays. The possible discrete values are from 0.5 to 2.0 times of current transformer secondary rating in equal steps of 0.25. The MCT considered for this system is 0.2 seconds. In this case also, the minimum and the maximum limits on t_{op} has been considered as 0.1 and 4.0 seconds, respectively, [106].

As in the previous case, to test the effectiveness of the proposed optimization approach, the results obtained corresponding to NOF have been compared with that obtained by two metaheuristic optimization approaches (GA and DE) and two hybrid optimization approaches (IPM-GA and IPM-DE). Table 3.11 shows the summary of the results obtained by all these six methods. For obtaining the results of Table 3.11, the procedure described for case-I has also been followed here.

Table 3.11: Comparative results obtained using NOF by various methods after 100 independent runs for the IEEE 118-bus system

Methods	Sum of operating times of all the relays			Standard deviation	Mean solution time (sec)
	Best	Mean	Worst		
GA	491.1625	513.4992	530.0956	12.7324	**479.2117**
DE	254.7816	414.114	563.2866	146.8028	1223.7982
IPM-GA	124.4382	130.6693	150.5527	7.5844	6756.6623
IPM-DE	106.5501	113.6577	119.3666	4.9577	2813.3477
IPM-BBM	99.5477	**99.6600**	**99.7820**	**0.0954**	15195.1994
IPM-IPM	**99.0291**	99.6846	100.1619	0.2932	7663.3385

From Table 3.11 it is observed that the sum of operating times of the relays obtained by the proposed two-phase optimization methods (IPM-BBM and IPM-IPM) are appreciably less than those obtained by the metaheuristic methods (GA and DE) and are also less than those obtained by the hybrid optimization approaches (IPM-GA and IPM-DE). Also, the standard deviation of the results obtained by the proposed methods (IPM-BBM and IPM-IPM) are quite small indicating that the results obtained at different runs are quite close to each other (i.e., the results are nearly reproducible) even when different runs start from different initial conditions. This is not the case with metaheuristic methods and hybrid optimization approaches. From Table 3.11 it is also observed that IPM-IPM is relatively faster than IPM-BBM along with the least value of the sum of operating times of all the relays. This makes IPM-IPM optimization approach superior to all the other five approaches considered in this work.

Similarly, as in the previous case, to test the effectiveness of the proposed objective function NOF, the result obtained by IPM-IPM method corresponding to the different objective functions (OF1, OF2, OF3, OF4 and NOF) have also been compared. Table 3.12 gives the summary of coordination results obtained with different objective functions. From Table 3.12 it is observed that out of the five objective functions, only OF1 and NOF are able to satisfy all constraints. However, the values of SOTR, SOTB and SACTI obtained by NOF are less than the corresponding values obtained by OF1 by 1.22%, 6.91% and 9.81%, respectively. Further, the sum of the values of SOTR and SOTB corresponding to NOF is 6.07% lower as compared to the corresponding value obtained with OF1. Therefore, for this system also, the proposed objective function minimizes the operating times of primary and backup relays along with the coordination time interval while always satisfying the coordination constraints. This makes the proposed objective function NOF superior to the other objective functions considered in the literature for this system also.

Table 3.12: Comparative results obtained using IPM-IPM for various objective functions for the IEEE 118-bus system

Various Terms	OF1	OF2	OF3	OF4	NOF
SOTR	100.2499	92.7036	80.849	202.6345	99.0291
SOTB	580.2369	573.9753	526.9968	1194.356	540.1593
SACTI	379.2258	381.21	348.2403	784.5178	342.0130
Cases of Violation	0	329	513	157	0

The optimum values of TMS and PS of all the relays obtained by the IPM-IPM approach and corresponding to NOF are shown in Figure 3.8. Also, the time of operations of the primary relays and the corresponding backup relays along with the actual CTI between the combinations are shown in Figure 3.9 for all primary-backup relay combinations. It is to be noted that the results in Figures 3.8 and 3.9 are the best results (corresponding to the minimum value of objective function NOF) obtained by the IPM-IPM method. In this case also, the final values of CTI for all combinations are more than the minimum CTI considered (0.2 sec).

So far, in this system, no DOCR has been considered on any of the generator feeders. For

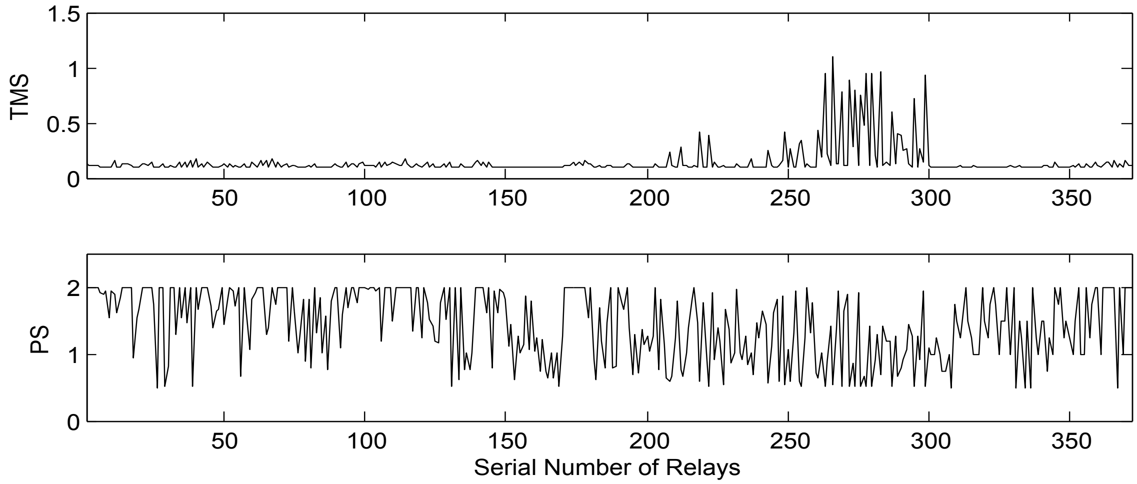

Figure 3.8: Optimum relays settings for the IEEE 118-bus system.

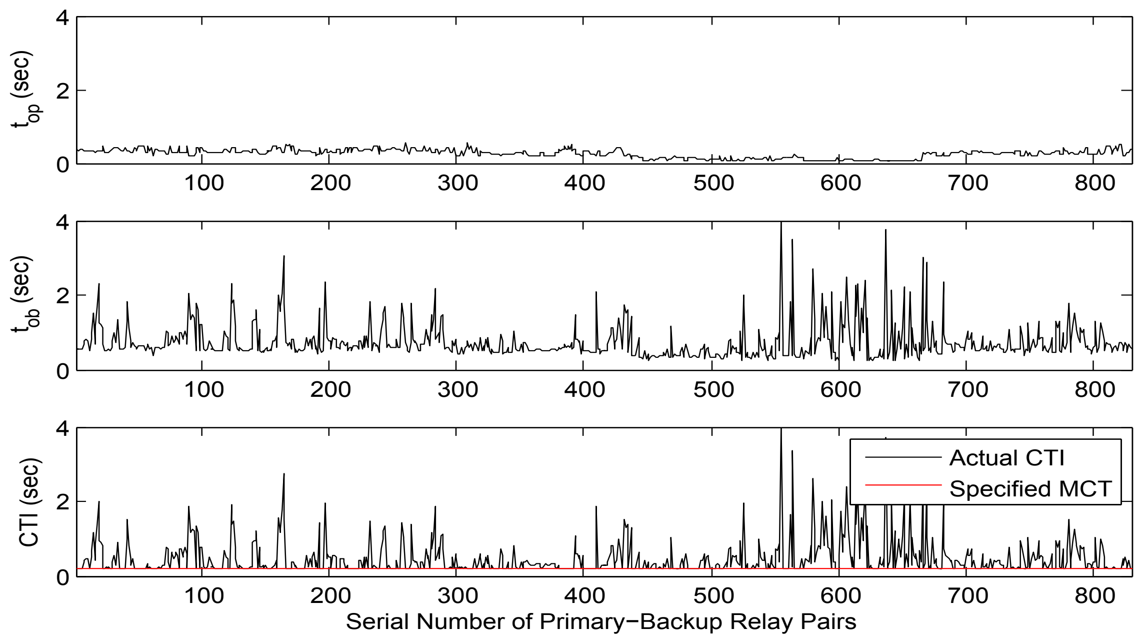

Figure 3.9: Operating times of primary relays, backup relays and CTI in the IEEE 118-bus system.

further study, as considered in the 14 and 30-bus systems, a case has also been considered in this system in which all generator feeders are equipped with DOCRs. As there are 54 generator buses in this system, a total of 54 extra DOCRs have now been considered. Each of these DOCRs has been assumed to be a numerical relay of type EIN. Further, as there are a total of 206 lines connected to the generator buses (as shown in Figure 3.10), 206 extra primary-backup pairs also

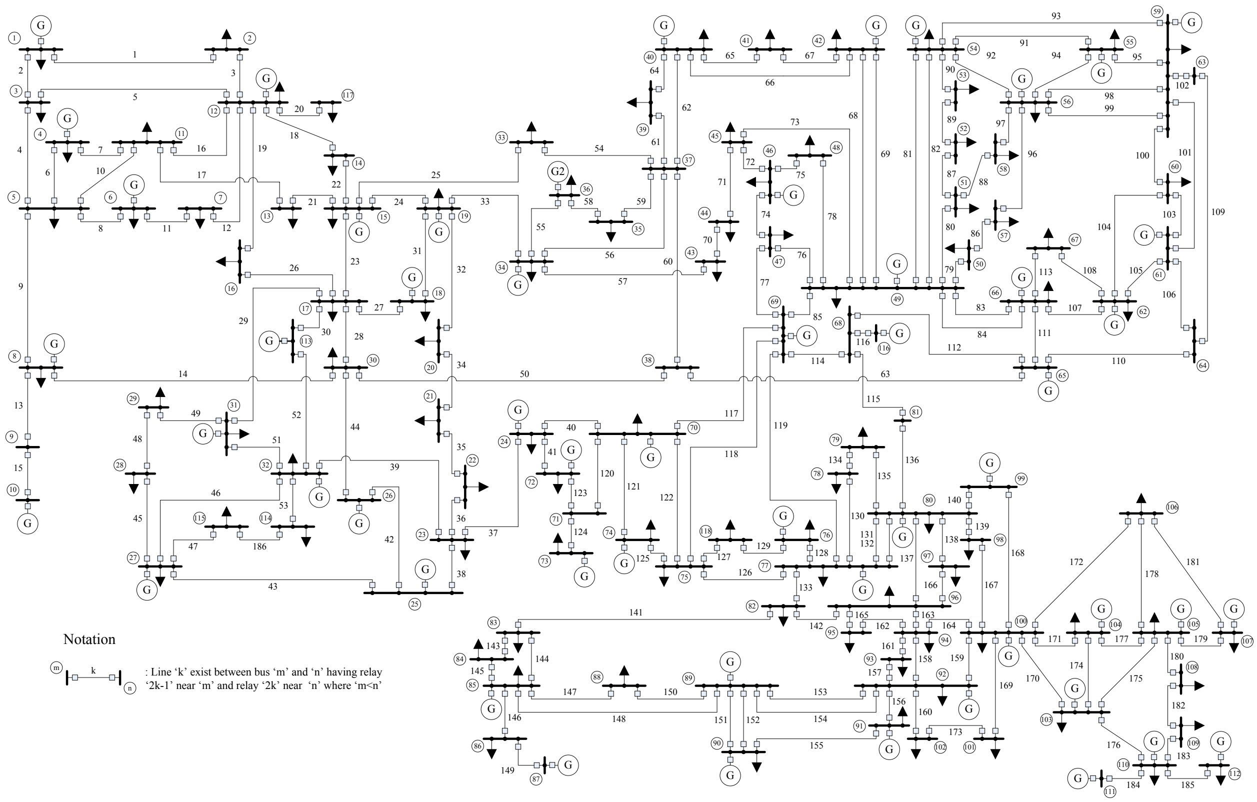

Figure 3.10: IEEE 118-bus system having a DOCR at each generator feeder.

need to be considered. Therefore, the augmented protection scheme of this system comprises of 426 DOCRs having 1036 primary-backup pairs among them. Again, for co-ordination of these relays, the maximum load currents and various fault currents have been calculated using the same procedure as discussed in Section 3.3.1.

The co-ordination problem of this augmented protection scheme has again been solved for the combination of NOF and IPM-IPM method (as this combination gives the best co-ordination result as shown in Tables 3.11 and 3.12). The optimum relay settings for all these 426 relays are shown in Figure 3.11. Comparison of the numerical values of Figures 3.8 and 3.11 shows that the TMS values of 124 relays (out of the original 372 relays) have changed while those of the remaining 248 relays remain the same. Out of the 124 changes in TMS values, values of TMS for 28 relays have increased while TMS values for 96 relays have reduced. Similarly, the PS values of 95 relays have increased, 100 relays have reduced and those of the remaining 177 relays remained same. Also, for 149 relays, both TMS and PS values did not change (i.e. for 99 relays, PS values changed but TMS values did not change while for 28 relays, TMS values changed but PS values did not change).

These changes in TMS and PS settings of the original 372 relays are shown in Figure 3.12. From Figure 3.12 it is observed that the maximum change in TMS and PS values is limited below 0.4 and 1, respectively, which shows that the presence of DOCRs on generator feeders does not change the relays settings appreciably. Lastly, the operating times of all primary relays, backup relays and CTI corresponding to all 1036 pairs are shown in Figure 3.13. Comparison of Figures 3.9 and 3.13 shows that for this system also, the presence of DOCRs on the generator feeders changes the operating times of the relays marginally.

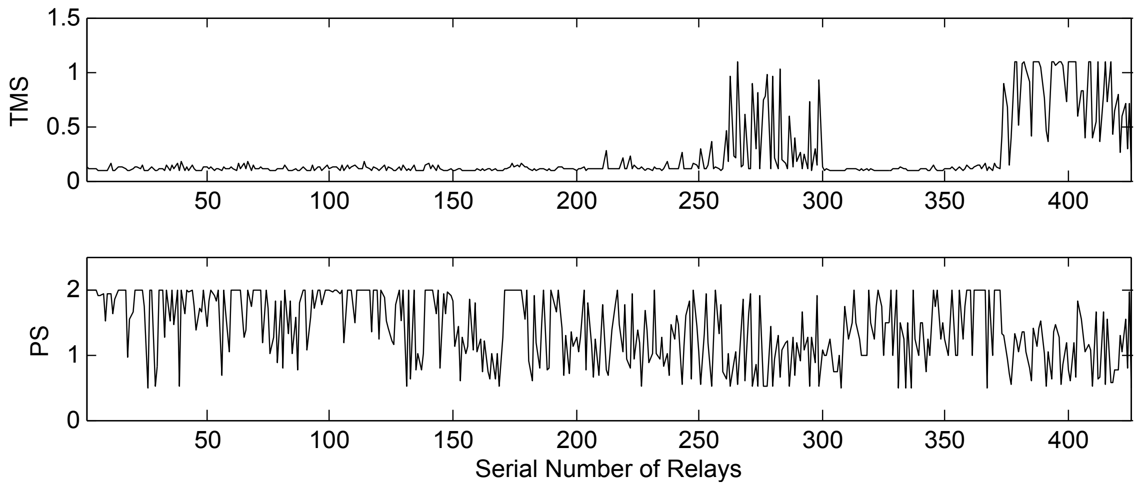

Figure 3.11: Optimum relays settings for the IEEE 118-bus augmented protection system.

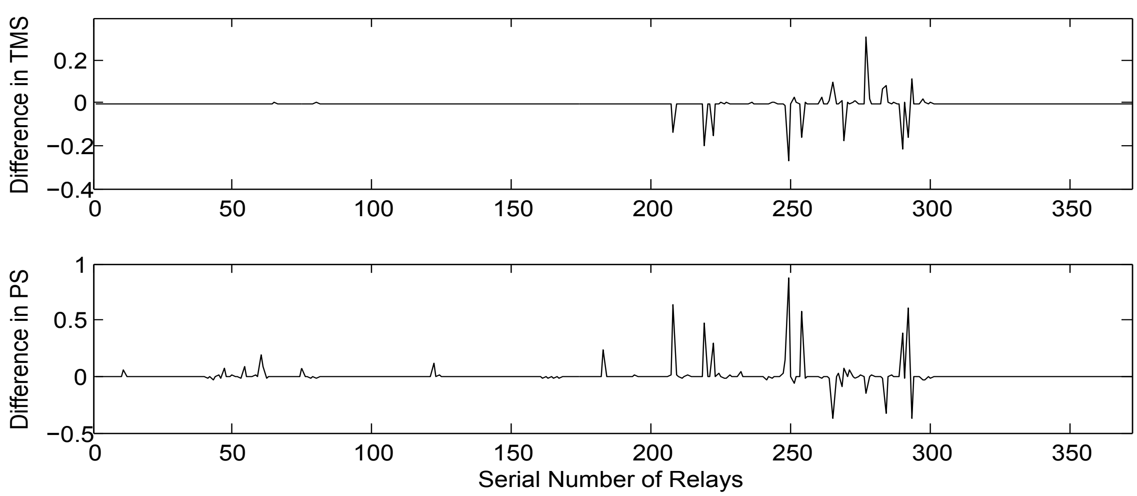

Figure 3.12: Differences in TMS and PS in the IEEE 118-bus augmented protection system.

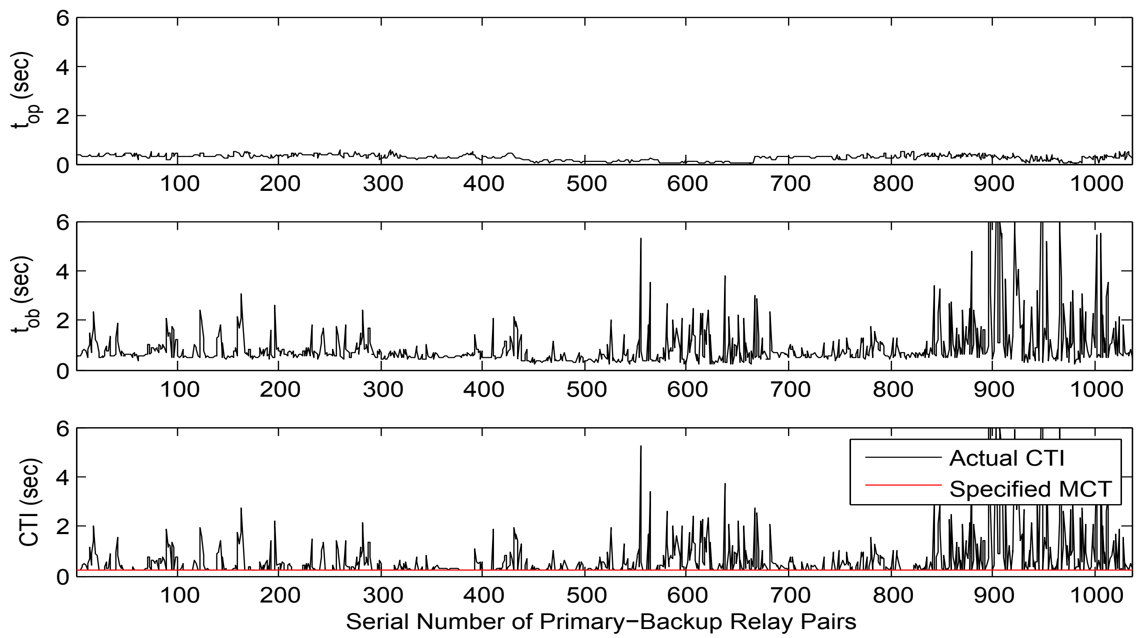

Figure 3.13: Operating times of primary relays, backup relays and CTI in the IEEE 118-bus augmented protection system.

3.5 Conclusion

In this chapter, two distinct two-stage optimization based methods are proposed for the coordination of directional overcurrent relays for meshed networks. Further, to minimize the operating times of the primary and backup relays simultaneously, a new objective function has been developed. Based on detailed investigation on two test systems, following conclusions can be drawn:

(i) Between the two proposed approaches, IPM-IPM method is better than the IPM-BBM method.

(ii) IPM-IPM approach is also better than the two metaheuristic methods and two hybrid approaches considered in this work.

(iii) The proposed IPM-IPM solution method always gives acceptable solution to the coordination problem of DOCRs efficiently without any constraint violation.

(iv) The proposed objective function ensures that the operating times of both primary and backup relays are minimized.

In the next chapter, protection coordination of DOCRs considering multiple network topologies is discussed.

Chapter 4

Robust Protection Coordination of Directional Overcurrent Relays Under Multiple Network Topologies

Abstract

This chapter proposes a contingency constrained robust protection coordination scheme of directional overcurrent relays (DOCRs). The robust protection coordination scheme provides single settings of DOCRs which will be valid for the credible (N-1) topologies created after outage of any element. For selecting the feasible contingencies, a composite security index has been used. The robust protection coordination scheme has been posed as an optimization problem and solved using an interior point method based algorithm. The feasibility of the proposed formulation and solution algorithm has been demonstrated on IEEE 14, 30 and 118-bus power system networks.

4.1 Introduction

IN the previous two chapters, the protection coordination problem has been solved for a fixed topology of the network. However, as discussed in Chapter 1, a power system may operate in different topologies due to outages of transmission lines, transformers and generating units. Under such circumstances, the changes in the network topology may lead to mis-coordination of DOCRs [56, 88, 107–116]. To address this issue, this chapter poses the coordination problem of DOCRs, under variation of topology, as a robust MINLP problem and the formulated problem has been solved by an interior point method (IPM) based algorithm. The variation in topology is incorporated in the formulated problem by considering the credible (N-1) contingencies of the system under study. The solution of the formulated problem gives the settings of the DOCRs which will be valid for the credible (N-1) topologies created after outage of any single line, transformer or a generator. The feasibility of the proposed formulation and solution algorithm has been demonstrated on IEEE 14, 30 and 118-bus power system networks.

4.2 Problem formulation for the system under contingency

In this case, the formulated problem considers all network configurations when the system is running successfully under (N-1) contingency. Here, the protection coordination problem can be formulated as the minimization of the sum of the operating times of all the DOCRs for the maximum fault current (passing through the primary relays) while maintaining CTI between all possible primary-backup relay pairs under the contingency. The corresponding objective function under contingency (OFC) can be expressed as,

$$\mathit{OFC} = \min \sum_{l=1}^{nc} \sum_{i=1}^{m} t_{op,il} \tag{4.1}$$

where

$$t_{op,il} = \frac{\lambda \times \mathit{TMS}_i}{(I_{Fil}/\mathit{PS}_i)^{\eta} - 1} + L;\ \forall i\, \forall l \tag{4.2}$$

subjected to:

$$t_{ob,jl} - t_{op,il} \geq \mathit{CTI};\ \forall i\, \forall j\, \forall l \tag{4.3}$$

$$t_{i,min} \leq t_{op,il} \leq t_{i,max};\ \forall i\, \forall l \tag{4.4}$$

$$\mathit{TMS}_{i,min} \leq \mathit{TMS}_i \leq \mathit{TMS}_{i,max} \tag{4.5}$$

$$\mathit{PS}_{i,min} \leq \mathit{PS}_i \leq \mathit{PS}_{i,max} \tag{4.6}$$

In eqns. (4.1)-(4.4), nc is the total number of (N-1) contingencies under which the system under study is running successfully and m is the number of relays in the system. Further, I_{Fil} denotes the fault current through relay R_i in l^{th} configuration and $t_{op,il}$ is the operating time of relay R_i in l^{th} configuration.

Further, as discussed earlier, if PS_i in eqn. (4.2) of relay R_i is considered to be previously known, then $t_{op,i}$ will be a linear function in TMS_i. Thus, actual NLP protection coordination problem given in eqn. (4.1) can be converted into an approximate LP problem [57, 58].

Similar to NOF discussed in the previous chapter, for simultaneously minimizing the operating times of primary and backup relays, a new objective function under contingency (NOFC) has been developed in this work which can be expressed as,

$$\mathit{NOFC} = \min \sum_{l=1}^{nc} \left(\alpha_1 \sum_{i=1}^{m} (t_{op,il})^2 + \alpha_2 \sum_{j=1}^{n} (t_{ob,jl} - \mathit{MCT})^2 \right) \tag{4.7}$$

This NOFC is minimized subjected to the constraints given in eqns. (4.3)-(4.6). It can be observed that the problem formulated in this section is twice continuously differentiable for continuous values of TMS and PS within their respective ranges. It is to be noted that eqn. (4.3) ensures that all the coordination constraints are satisfied in the obtained solution.

Now, in any system, the number of possible (N-1) contingencies can be quite high. However, for protection coordination, only the credible contingencies (out of the all possible contingencies) need to be considered. For selecting the credible contingencies, the composite security index, as discussed in the next section, has been followed in this work.

4.3 An overview of composite security index

The composite security index (CSI) provides an efficient method for contingency selection and ranking. It is defined in terms of the limit violations of bus voltages and line power flows. Two types of limits are defined for both bus voltages and line power flows, namely ”alarm limit” and ”security limit”. The alarm limit gives an indication of closeness to limit violations. The security limit is the maximum limit specified for the bus voltages and line power flows. In this study, alarm and security limits on the bus voltages have been taken as $\pm 5\%$ and $\pm 7\%$ variation from the desired value (1.0 p.u.), respectively, whereas 80% of the specified thermal limit of line power flow has been taken as the alarm limit of the line power flow [117, 118].

The CSI selects only credible cases and ranks them in the order of severity. The CSI has two components: a) bus voltage security index and b) line power flow security index. These components and the CSI as suggested in [118–120], have been adopted in this work and are discussed below.

The normalized lower and upper voltage limit violations beyond the alarm limits are expressed as,

$$
\begin{aligned}
r^{l}_{v,ib} &= \frac{[V^{la}_{ib} - V_{ib}]}{[V^{la}_{ib} - V^{ls}_{ib}]} \quad &; if\ V_{ib} < V^{la}_{ib} \\
r^{l}_{v,ib} &= 0 \quad &; if\ V_{ib} \geq V^{la}_{ib} \\
r^{u}_{v,ib} &= \frac{[V_{ib} - V^{ua}_{ib}]}{[V^{us}_{ib} - V^{ua}_{ib}]} \quad &; if\ V_{ib} > V^{ua}_{ib} \\
r^{u}_{v,ib} &= 0 \quad &; if\ V_{ib} \leq V^{ua}_{ib}
\end{aligned}
\tag{4.8}
$$

In eqn. (4.8), V^{la}_{ib}, V^{ua}_{ib}, V^{ls}_{ib} and V^{us}_{ib} represent the lower and the upper alarm and security limits of voltages of bus *ib*, respectively. By using eqn. (4.8), bus voltage security index (BVSI) can be defined as,

$$BVSI = \left[\sum_{ib}\left(r^{l}_{v,ib}\right)^2 + \sum_{ib}\left(r^{u}_{v,ib}\right)^2\right]^{1/2} \tag{4.9}$$

For line power flow, only the maximum power flow limit of each line needs to be specified. The normalized upper line power flow limit violations beyond the alarm limits are expressed as,

$$\begin{aligned} r^{u}_{p,jk} &= \frac{\left[|P_{jk}| - P^{ua}_{jk}\right]}{\left[P^{us}_{jk} - P^{ua}_{jk}\right]} \quad ; if\ P_{jk} > P^{ua}_{jk} \\ r^{u}_{p,jk} &= 0 \quad ; if\ P_{jk} \le P^{ua}_{jk} \end{aligned} \tag{4.10}$$

In eqn. (4.10), P^{ua}_{jk} and P^{us}_{jk} represent the alarm and the security limits of each line *jk*. By using eqn. (4.10) line power flow security index (LPFSI) can be defined as,

$$LPFSI = \left[\sum_{jk}\left(r^{u}_{p,jk}\right)^2\right]^{1/2} \tag{4.11}$$

Using eqns. (4.9) and (4.11) the composite security index (CSI) is defined as,

$$CSI = \left[BVSI^2 + LPFSI^2\right]^{1/2} \tag{4.12}$$

Depending on the value of CSI from eqn. (4.12), the following conclusions can be drawn about the state of the system,

a) insecure state if $CSI > 1$

b) alarm state if $0 < CSI \le 1$

c) secure if $CSI = 0$.

In this work, the composite security index defined by eqn. (4.12) has been considered for contingency ranking.

It is well known that on-load tap changers (OLTC) in transmission and distribution systems try to maintain bus voltages within the specified limits. In this work, the contingency screening has been performed considering the presence of OLTC in the system and for this purpose, the effect of OLTC has been included in the NRLF method as discussed below [121, 122].

Let us assume that in a *nb* bus, *ng* generator power system, an OLTC is connected between bus *u* and bus *v*, having a tap ratio of $1 : t$ and total admittance y_0, as shown in Figure 4.1. The OLTC controls the bus voltage magnitude at bus v. Further, assume that the generators are connected at the first *ng* buses with bus 1 being the slack bus.

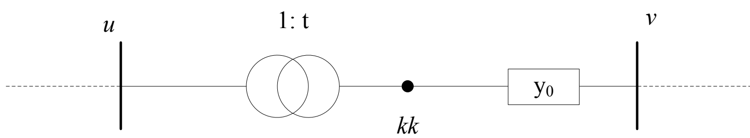

Figure 4.1: Representation of OLTC

The power flow equations for nodes u and v can be expressed as [123]

$$\begin{aligned} P_u = V_u^2 G_{uu} + V_u V_v(-ty_0)cos(\theta_u - \theta_v - \alpha_{uv}) \\ + \sum_{l=1,\neq u,v}^{nb} V_u V_l Y_{u,l} cos(\theta_u - \theta_l - \alpha_{ul}) \end{aligned} \tag{4.13}$$

$$\begin{aligned} P_v = V_v^2 G_{vv} + V_v V_u(-ty_0)cos(\theta_v - \theta_u - \alpha_{vu}) \\ + \sum_{l=1,\neq u,v}^{nb} V_v V_l Y_{v,l} cos(\theta_v - \theta_l - \alpha_{vl}) \end{aligned} \tag{4.14}$$

$$\begin{aligned} Q_u = V_u^2 (B_{uu} - t^2 y_0) + V_u V_v(-ty_0)sin(\theta_u - \theta_v - \alpha_{uv}) \\ + \sum_{l=1,\neq u,v}^{nb} V_u V_l Y_{u,l} sin(\theta_u - \theta_l - \alpha_{ul}) \end{aligned} \tag{4.15}$$

$$\begin{aligned} Q_v = V_v^2 B_{vv} + V_v V_u(-ty_0)sin(\theta_v - \theta_u - \alpha_{vu}) \\ + \sum_{l=1,\neq u,v}^{nb} V_v V_l Y_{v,l} sin(\theta_v - \theta_l - \alpha_{vl}) \end{aligned} \tag{4.16}$$

In eqns. (4.13))-(4.16)), P_u, Q_u, P_v and Q_v represent the real and reactive power flow into bus u and bus v, respectively, V_u, θ_u, V_v and θ_v are the magnitude and angle of voltage at buses u and v, respectively, Y_{uv} and α_{uv} are the magnitude and angle of $(u, v)^{th}$ element of bus admittance matrix (Y_{bus}), G_{uu}, B_{uu}, G_{vv} and B_{vv} are the real and imaginary parts of Y_{bus} corresponding to bus u and v, respectively, without considering the presence of OLTC and nb is the total number of buses in the system.

Partially differentiating eqns. (4.13))-(4.16)) with respect to t, the following four equations are obtained

$$\frac{\partial P_u}{\partial t} = -V_v V_u y_0 cos(\theta_u - \theta_v - \alpha_{uv}) \tag{4.17}$$

$$\frac{\partial P_v}{\partial t} = -V_v V_u y_0 cos(\theta_v - \theta_u - \alpha_{vu}) \tag{4.18}$$

$$\frac{\partial Q_u}{\partial t} = -2tV_u^2y_0 - V_uV_vy_0sin(\theta_u - \theta_v - \alpha_{uv}) \tag{4.19}$$

$$\frac{\partial Q_v}{\partial t} = -V_vV_uy_0sin(\theta_v - \theta_u - \alpha_{vu}) \tag{4.20}$$

In the NRLF formulation, the specified vector remains the same, while in the solution vector, quantity V_v is replaced by the quantity t. Also, the size of the Jacobian matrix remains unaltered. However, the column corresponding to V_v is replaced by a now column, in which only 4 elements are non-zero and rest of the elements are zero. These non-zero elements are given by eqns. (4.17)-(4.20). For incorporating multiple OLTCs, similar changes in Jacobian matrix can be made.

4.4 Fault current calculations for the system under contingency

In this chapter, various currents under contingency have been calculated using the following procedures. The maximum load current (I_{Lmax}) has been calculated using Newton-Raphson load flow (NRLF) analysis. The fault current calculations have been carried out using bus impedance matrix (Z_{bus}) approach [95]. Three-phase-to-ground solid faults and line-to-line faults with a fault impedance of 0.1 p.u. [31] have been considered for calculating the maximum fault current (I_{fmax}) and the minimum fault current (I_{fmin}) passing through each relay, respectively. In this study, the faults have been applied at the middle of each line. It is to be noted that the same procedure as discussed in the previous chapter has been adopted for calculating various load and fault currents under each credible contingency. Thus, the maximum load current is the maximum value of the load current passing through various relays under all the credible contingencies. Similarly, the minimum and the maximum fault current is the minimum and the maximum values of the fault currents passing through various relays, respectively, under all credible contingencies.

4.5 Calculation of current transformer ratio for the system under contingency

For calculating the CT ratio of i^{th} relay, following procedure has been adopted. Let there be a total of N credible configurations in a system. Corresponding to any k^{th} configuration ($1 \leq k \leq N$), the load current passing through the relay ($i_{Lk,i}$) and the fault current passing through the relay ($i_{fk,i}$) is calculated. Subsequently, $i_{LmaxA,i}$ and $i_{fmaxA,i}$ are calculated as; $i_{LmaxA,i} = max(i_{L1,i}, i_{L2,i}, ..., i_{LN,i})$ and $i_{fmaxA,i} = max(i_{f1,i}, i_{f2,i}, ..., i_{fN,i})$. Finally, the primary side rating of the CT corresponding to relay R_i is calculated as [60],

$$\mathit{CTR}_i = \max\left(I_{LmaxA,i}, \frac{I_{fmaxA,i}}{20}\right) \tag{4.21}$$

Once CTR is calculated it remains fixed in all configurations of the system. With this calculated CTR_i, the ratio of the current transformer used in this work is CTR_i:1. These current transformer ratios are kept fixed for all configurations of the system.

4.6 Proposed optimization algorithm

In this work, an interior point method (IPM) [124] based algorithm has been developed to solve the optimization problem described in Section 4.2.

The protection coordination problem of DOCRs, formulated in Section 4.2, can be categorized into two classes as,

1) NLP problem: *only numerical/digital relays*

2) MINLP problem: *static or electromechanical relays in addition to numerical/digital relays*

It is to be noted that both TMS and PS can have any continuous values within their ranges for numerical/digital type relays whereas, TMS can have any continuous value and PS can only have certain fixed discrete values for static or electromechanical type relays within their respective ranges [40]. Consequently, the optimum coordination problem of DOCRs can be termed as an NLP problem if all the relays considered in the system are of numerical/digital type. If static or electromechanical relays are also considered in addition to the numerical/digital relays, then the optimum relay coordination problem can be termed as MINLP problem.

The NLP problem can directly be solved using IPM whereas MINLP problem needs special approach to solve it. In this chapter, IPM-IPM algorithm developed in Chapter 3 is used to solve MINLP problem of DOCRs. A flowchart with detailed information of the proposed overall approach used in this chapter is shown in Figure 4.2.

4.7 Simulation results and discussion

The proposed IPM based algorithm has been tested successfully for determining optimum settings of DOCRs of IEEE 14, 30 and 118-bus systems [94]. The IEEE 14-bus system has 20 lines, 3 transformers (out of which 2 have OLTC installed), and 5 generators. The IEEE 30-bus system

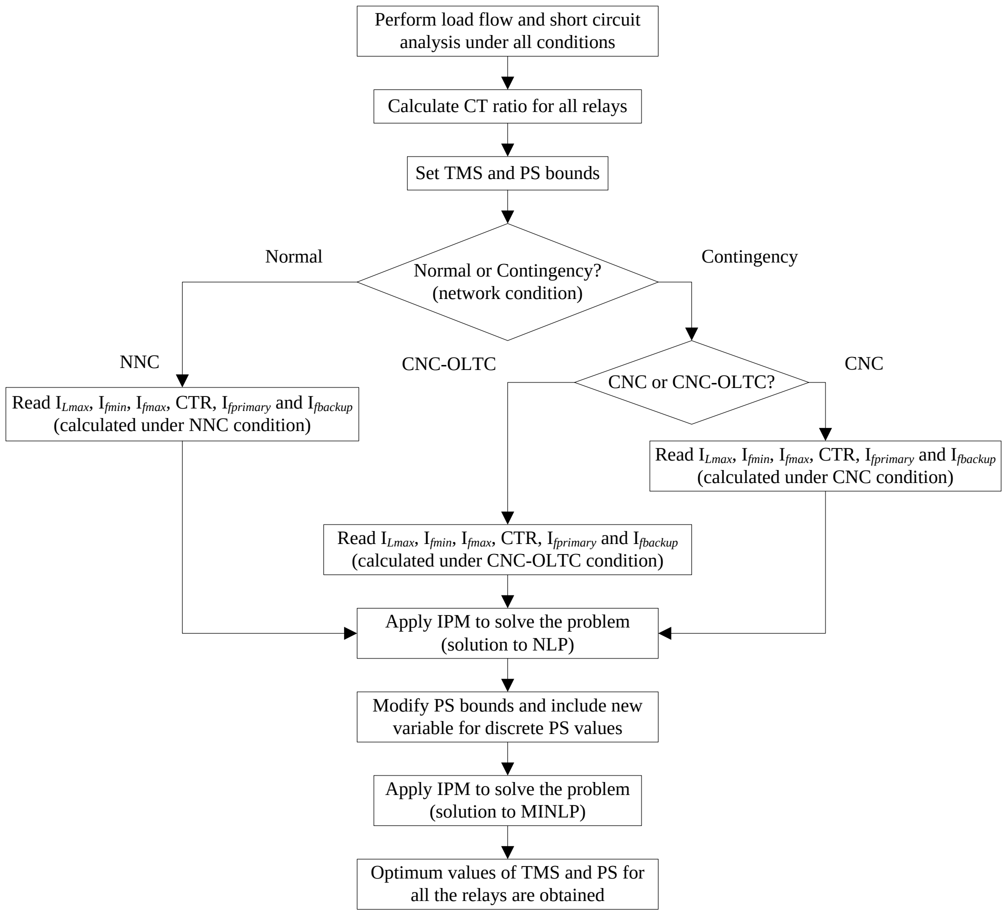

Figure 4.2: Flowchart of the overall approach for robust protection coordination.

has 41 lines, 4 transformers (out of which 3 have OLTC installed), and 6 generators. The IEEE 118-bus system has 186 lines, 9 transformers (out of which 5 are having OLTC facility), and 54 generators. To protect the IEEE 14-bus system using DOCRs, a total of 40 DOCRs (two DOCRs for each line) need to be used and coordinated with each other, whereas to protect the IEEE 30-bus system, a total of 82 DOCRs need to be used and coordinated with each other. In these two systems, static and electromechanical types of relays with standard IDMT characteristic curve have been considered. To protect the IEEE 118-bus system, a total of 372 DOCRs need to be installed and coordinated with each other in the system. In this system, numerical/digital, static and electromechanical types of relays with three different characteristic curves (standard IDMT, VIN and EIN) have been considered. For each test system, the following three scenarios have been considered. It is to be noted that the characteristics of relays are pre-specified.

1) Normal network configuration (NNC)

2) (N-1) contingency network configuration (CNC)

3) CNC in the presence of OLTC (CNC-OLTC)

In NNC scenario, all the DOCRs are expected to coordinate properly for that particular network configuration. In CNC scenarios (CNC and CNC-OLTC), the DOCRs are expected to coordinate properly for all credible (N-1) contingency network configurations (i.e. with $CSI<1$). In this case, initially, the ranking of all (N-1) contingencies is carried out on the basis of the values of CSI (discussed in Section 4.3). Subsequently, all the network configurations with $CSI<1$ are considered to be feasible, which are to be protected using DOCRs. After that, the steady state currents and various fault currents are calculated for all these feasible configurations.

For both cases, following quantities have been considered. The minimum and the maximum limits on TMS, PS and t_{op} of each relay has been considered as discussed in Chapter 3. However, the value of CTI considered for numerical/digital relays is 0.1 seconds whereas for electromechanical and static relays, it is 0.3 seconds [31, 40].

The proposed algorithm has been simulated in AMPL environment [75]. It is to be noted that under NNC, the objective function is given by eqn. (3.10) whereas for CNC cases, the objective function is given by eqn. (4.7). It is to be noted that while simulating outage of a generator, the generation levels of the remaining generators are increased in proportion to their MVA ratings to compensate for the lost generation.

4.7.1 A motivating example

Figure 4.3 shows a typical example of a 4-bus system supplied by an external system (equivalent system) at bus 1 and a generating source at bus 2. To provide complete protection of the system, a total of 8 DOCRs are needed. In this example, all the relays are assumed to be of numerical/digital type with standard IDMT characteristic. For a fault on line L2, Table 4.1 gives the information regarding the primary-backup relay pair along with the corresponding fault currents considering power supplied by the equivalent system with (a) G in-service and (b) G out-of-service. It is to be noted that the selected relay pair 3-1 has completely different fault current patterns in network configurations (a) and (b). This situation is critical for protection coordination problem of the system.

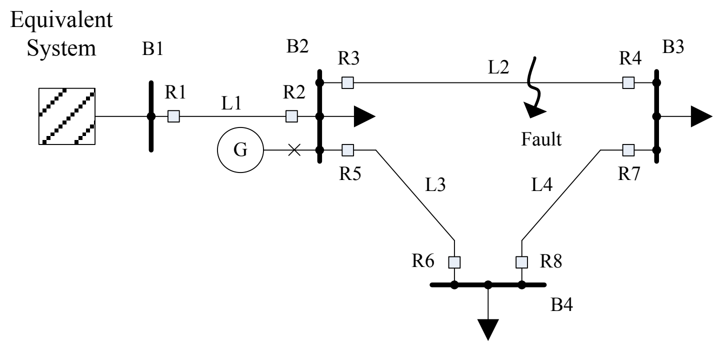

Figure 4.3: Example of a 4-bus system.

Table 4.1: Fault currents through primary relay R3 and backup relay R1 for fault on line L2 in two different situation

Fault Zone	Primary Relay	Backup Relay	G in-service		G out-of-service	
			I_{prim}	I_{back}	I_{prim}	I_{back}
L2	3	1	7778	5240	5549	6775

The optimum settings (TMS and PS) with corresponding operating times (t_R) of relay R1 and R3, including actual CTI of the pair in three different situations, are given in Table 4.2. In Table 4.2, column (1) and column (2) give the values of TMS, PS and t_R of relays R1 and R3 for network configurations (a) and (b), respectively, (as in NNC case) whereas, column (3) gives the values of TMS and PS of relay R1 and R3 for network configurations (a) and (b) simultaneously (as in CNC case) and the operating times of relays R1 and R3.

Table 4.2: Optimum settings with corresponding operating times of relays R1 and R3 as well as CTI of the pair

Relays	G in-service (1)			G out-of-service (2)			Both (1) and (2) (3)			
	TMS	PS	t_R	TMS	PS	t_R	TMS	PS	t_R in (a)	t_R in (b)
1	0.1731	2	1.0093	0.1750	2	0.8366	0.2906	1.5	1.3598	1.1550
3	0.2063	2	0.6897	0.1335	2	0.5360	0.2128	2	0.7114	0.8545
CTI			0.3196			0.3006			0.6484	0.3005

From columns (1) and (2) of Table 4.2, it is to be noted that the optimum settings obtained for situations (a) and (b) are quite different for relay R3. Therefore, for maintaining selectivity, the TMS setting of relay R3 needs to be changed depending on the network configuration. On the other hand, the optimum TMS settings of the relays shown in column (3) have been obtained considering both the situations discussed in (a) and (b) simultaneously. Further, from column (3) it is observed that, even when the settings are kept same (irrespective of the system configuration), the selectivity of the relays is always maintained in any of the configurations. As a result, the relay settings obtained in this case are able to coordinate properly in any of the above two configurations as CTI is maintained for both the situations.

Further, to study the effect of OLTC on the settings of DOCRs, an OLTC transformer has been placed between bus 2 and bus 4 of the 4-bus system as shown in Figure 4.4. The presence of OLTC regulates the voltage of bus 4. Now, a fault on line L2 is applied with G-in-service.

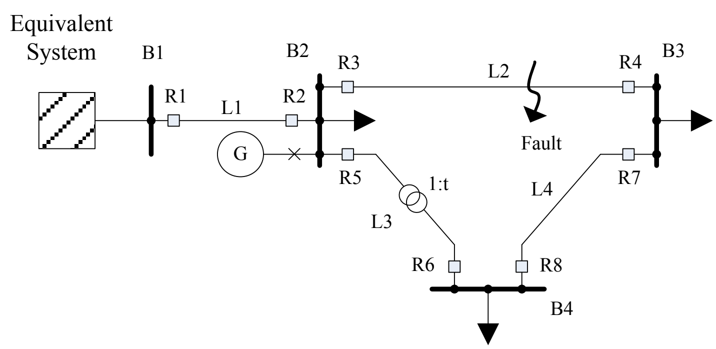

Figure 4.4: Example of a 4-bus system with OLTC.

Table 4.3 gives the information regarding the primary-backup relay pair along with the corresponding fault currents for two cases; (c) without OLTC and (d) with OLTC. It is to be noted that the presence of OLTC significantly changes the fault current value seen by the relay pair 4-8. This situation may affect the protection coordination of the system.

Table 4.3: Fault currents through primary relay R4 and backup relay R8 for fault on line L2 without and with OLTC

Fault Zone	Primary Relay	Backup Relay	without OLTC		with OLTC	
			I_{prim}	I_{back}	I_{prim}	I_{back}
L2	4	8	2208	1190	2179	1786

The optimum settings (TMS and PS) with corresponding operating times (t_R) of relay R4 and R8 including actual CTI of the pair in two different situations are given in Table 4.4.

Table 4.4: Optimum settings with corresponding operating times of relays R4 and R8 as well as CTI of the pair without and with OLTC

Relays	without OLTC			with OLTC		
	TMS	PS	t_R	TMS	PS	t_R
4	0.4084	0.5	1.0653	0.3964	0.5	1.0457
8	0.2315	2.0	0.7647	0.1549	2.0	0.7450
CTI			0.3006			0.3007

From Table 4.4, it is observed that the optimum settings of relays R4 and R8 are different in these two cases (with and without OLTC). This difference is because of the change in fault currents passing through the relay pair in these two cases (Table 4.3).

4.7.2 Selection of α_1 and α_2 for NOF/NOFC

For the selection of α_1 and α_2 the following procedure has been adopted. Corresponding to the various values of α_1 and α_2, the optimized value of the sum of the operating times of the primary and backup relays (SOTPBR) has been calculated in NNC of IEEE 14-bus system. The values of SOTPBR for different values of α_1 and α_2 are given in Table 4.5. From this table, it can be observed that $\alpha_1 = 0.6$ and $\alpha_2 = 0.4$ give the lowest value of the SOTPBR. However, for CNC case of the IEEE 14-bus system, the lowest value of SOTPBR is obtained for $\alpha_1 = 0.9$ and $\alpha_2 = 0.1$. Further, for the IEEE 30 and 118-bus systems, the values of α_1 and α_2 are identical to those found for NNC and CNC cases of the IEEE 14-bus system. Hence, these values of α_1 and α_2 have been used for calculating NOF (eq. 3.10)) and NOFC (eq. (4.7)). Also, the values of α_1 and α_2 for CNC-OLTC case are the same as obtained for CNC case in both the systems.

Table 4.5: Selection of optimum values of α_1 and α_2 for NOF

α_1	0	0.1	0.2	0.3	0.4	0.5	**0.6**	0.7	0.8	0.9	1
α_2	1	0.9	0.8	0.7	0.6	0.5	**0.4**	0.3	0.2	0.1	0
SOTPBR	97.858	96.729	96.729	96.729	96.729	96.812	**96.428**	96.429	96.575	97.727	102.578

4.7.3 Results on the IEEE 14-bus system

Figure 4.5 shows the single-line diagram of IEEE 14-bus system with 40 DOCRs placed on 20 lines (two on each line). This system has 93 primary-backup relay pairs. All these pairs are given in Table A.10. It is to be noted that L9 and L10 in this figure are equipped with OLTC. However, only the first OLTC at L9 is used to control bus voltage at bus 9 (B9) and second OLTC is not used to control bus voltage at bus 6 (B6) as G5 controls the voltage at B6.

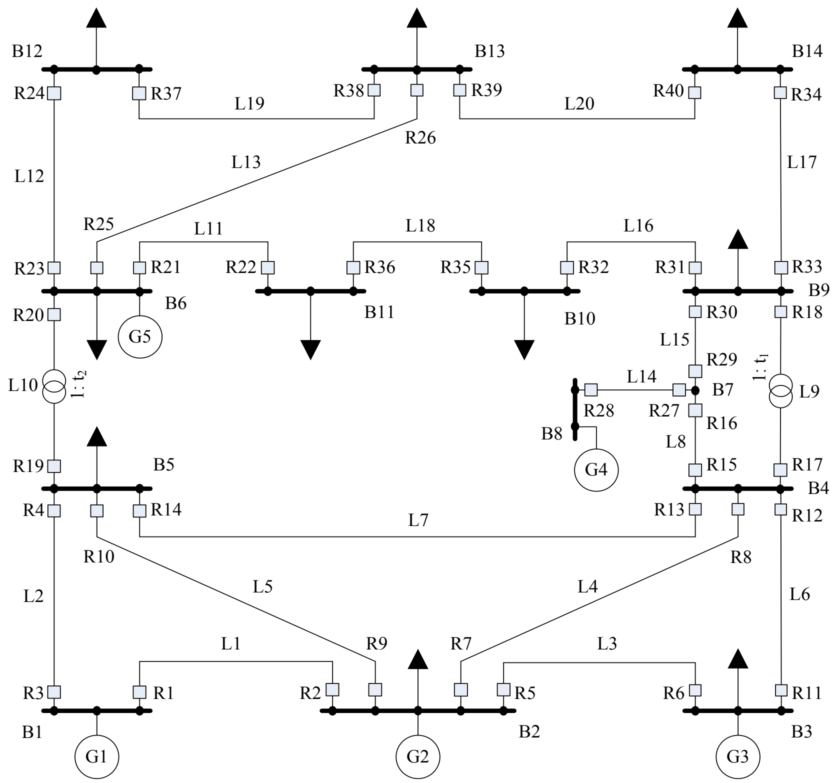

Figure 4.5: IEEE 14-bus system with OLTC.

4.7.3.1 Normal network configuration (NNC)

In this scenario, there are total 93 primary-backup relay pairs among all the 40 relays. It is to be noted that only 70 relay pairs have been considered in the optimization problem as the other 23 relay pairs are satisfying eqn. (3.14) in which coordination constraints always remain satisfied.

4.7.3.2 (N-1) contingency network configuration (CNC)

In this system, there are 20 lines and 5 generators, i.e., a total of 25 elements which can experience contingency. Therefore, under CNC scenario, there are a total of 25 configurations generated by (N-1) contingencies. Out of these 25 contingencies, 23 contingencies have $CSI < 1$ and hence, these configurations are considered as feasible system topologies. Therefore, for deciding the parameters of the relays, a total of 24 configurations (23 contingency configurations and one normal configuration) are considered. As each configuration has 93 primary-backup relay pairs, total number of primary-backup relay pairs considered under contingency is 2232 ($= 24 \times 93$). It is to be noted that, out of these 2232 relay pairs, only 1167 relay pairs have been considered in the optimization problem, as remaining 1065 relay pairs satisfy eqn. (3.14) thereby, ensuring that the coordination constraints are always satisfied for these relay pairs.

4.7.3.3 CNC in the presence of OLTC (CNC-OLTC)

In this scenario, out of the 25 contingencies, 20 contingencies have $CSI < 1$ and hence, these configurations are considered as feasible system topologies. Therefore, for deciding the parameters of the relays, a total of 21 configurations are considered. The total number of primary-backup relay pairs considered under contingency is 1953. It is to be noted that only 1069 relay pairs have been considered in the optimization problem in this scenario, as remaining 884 relay pairs satisfy eqn. (3.14) and therefore, the coordination constraints are always satisfied for these relay pairs.

The optimum settings of the relays obtained in all the three cases (NNC, CNC and CNC-OLTC) using the proposed IPM based algorithm are given in Table 4.6. Further, for these three cases, the optimized CTI between the operating times of primary and backup relay pairs are shown in Figures 4.6, 4.7 and 4.8, respectively. From these figures, it is observed that the minimum CTI is always maintained for any primary-backup relay pair, thereby ensuring the selectivity of the relays. Further, to test the effectiveness of the proposed NLP model (NOF), the optimum settings of the relays obtained in all the three cases considering approximate LP model proposed in [57, 58] and using the proposed IPM algorithm are given in Table 4.6.

From Table 4.6, it is observed that the sum of the operating times of all the relays in NNC scenario is 17.9778 seconds whereas the sum of the operating times of all the relays in CNC scenario is 26.5592 seconds. Further, the sum of the operating times of all the relays in CNC-OLTC scenario is 29.6404 seconds. It is also observed that 316 (i.e., 27.08%) coordination constraints of CNC and 276 (i.e., 25.82%) coordination constraints of CNC-OLTC are violated with the relay settings as obtained using NNC. Subsequently, from Table 4.6, it is observed that the sum of the operating times of all the 40 relays are more for CNC and CNC-OLTC cases than those for NNC. The reason for this is the fact that the relay settings obtained for CNC and CNC-OLTC are robust as these can maintain protection coordination under all the credible (N-1) contingencies of the

Table 4.6: Optimum settings of the relays obtained using the proposed algorithm for the IEEE 14-bus system

Relays	Approximate LP model						Proposed NLP model (NOF)					
	NNC		CNC		CNC-OLTC		NNC		CNC		CNC-OLTC	
	TMS	PS	TMS	PS	TMS	PS	TMS	PS	TMS	PS	TMS	PS
1	0.1	1.5	0.1	1.5	0.1	1.5	0.1	0.75	0.1139	1	0.1	1.25
2	0.1	1	0.4011	1	0.4016	1	0.1	0.5	0.2059	2	0.2059	2
3	0.1	2	0.128	1.5	0.128	1.5	0.1017	1.25	0.1	1.5	0.1	1.5
4	0.1	1	0.1	1	0.1	1	0.1	0.5	0.1	0.5	0.1	0.5
5	0.1	2	0.1	2	0.1	2	0.1	1.25	0.1162	1.25	0.1	1.5
6	0.1219	1	0.4599	1	0.4618	1	0.1	1.25	0.5365	0.5	0.5404	0.5
7	0.1	2	0.1	2	0.1	2	0.1287	1	0.152	1	0.1689	1
8	0.1014	1	0.3569	1	0.354	1	0.1034	1	0.2999	1	0.4484	0.5
9	0.1121	2	0.1	2	0.1017	2	0.1596	1	0.1296	1.25	0.1724	1
10	0.1	1	0.3535	1	0.3508	1	0.1	1	0.2109	1.5	0.2085	1.5
11	0.2415	1	0.4462	1	0.4844	1	0.2648	0.5	0.4616	0.5	0.5111	0.5
12	0.1013	2	0.1	1.5	0.1	1.5	0.1	2	0.1	0.75	0.1	0.75
13	0.1833	1	0.2987	1	0.3324	1	0.1	2	0.1785	1.5	0.2276	1.25
14	0.1	2	0.1	1.5	0.1	1.5	0.1089	1	0.1068	1	0.1068	1
15	0.1022	2	0.1	2	0.1238	2	0.105	1.75	0.135	1.25	0.1099	2
16	0.1	1	0.1	1	0.1	1	0.1	0.5	0.1	0.5	0.1	0.5
17	0.152	2	0.1	2	0.1237	2	0.1258	2	0.12	1.75	0.1726	1.5
18	0.1388	1	0.2276	1	0.2462	1	0.1	1.5	0.1917	1	0.1483	1.5
19	0.1	2	0.1	2	0.1	2	0.104	1.5	0.1377	1.25	0.1409	1.25
20	0.1	1	0.2826	1	0.281	1	0.1	0.5	0.3208	0.5	0.3183	0.5
21	0.3885	1	0.2793	2	0.3208	2	0.2334	2	0.2895	2	0.3118	2
22	0.3367	1	0.1488	2	0.5122	1	0.1935	2	0.1416	2	0.3312	2
23	0.2571	1.5	0.2746	2	0.3131	2	0.1547	2	0.2763	2	0.2864	2
24	0.2778	1	0.3268	1	0.3643	1	0.3274	0.5	0.366	0.75	0.4679	0.5
25	0.2437	2	0.2024	2	0.2347	2	0.1914	2	0.2121	1.75	0.2013	2
26	0.2814	1	0.1916	2	0.4826	1	0.1316	2	0.2873	1.25	0.597	0.5
27	0.1	2	0.1	2	0.1	2	0.1	1.25	0.1	1	0.1	1.25
28	0.4148	1	0.4705	1	0.6263	1	0.4535	0.5	0.5977	0.5	0.7062	0.5
29	0.1	2	0.1	1	0.1	2	0.1	1	0.1	0.5	0.1	1
30	0.2414	1	0.1795	1.5	0.2076	1.5	0.1361	2	0.149	2	0.2548	1.25
31	0.4225	1	0.1868	2	0.4121	1.5	0.2489	2	0.2509	1.25	0.4749	0.75
32	0.3229	1	0.2358	2	0.3004	2	0.3466	0.5	0.3427	1	0.3062	1.75
33	0.2702	1.5	0.1421	2	0.2843	2	0.1795	2	0.1395	2	0.2557	2
34	0.4048	1	0.5371	1	0.6758	1	0.227	2	0.3849	1.75	0.4047	2
35	0.38	1	0.1537	2	0.4878	1	0.2215	2	0.148	2	0.2962	2
36	0.3912	1	0.2451	2	0.2942	2	0.2513	2	0.2571	2	0.2835	2
37	0.3037	1	0.3214	2	0.3771	2	0.1393	2	0.4136	1.25	0.3958	1.5
38	0.2692	1	0.2729	1	0.2953	1	0.1654	2	0.1662	2	0.1817	2
39	0.3839	1	0.2262	2	0.2732	2	0.2051	2	0.206	2	0.2246	2
40	0.3232	1	0.2084	2	0.4937	1	0.175	2	0.2033	2	0.3194	2
$\sum_{i=1}^{40} t_{op,i}$	22.7031		29.0352		33.8155		**17.9778**		**26.5592**		**29.6404**	

system. Therefore, it can be concluded that the price of robustness is an increase in total operating time of the relays. Further, it is to be noted that in case of CNC-OLTC, the change in voltage profile of the system is causing a change in the fault currents which ultimately decides the different operating times of all the relays. As a results, the sum of operating times of all the relays in CNC-OLTC are different than those obtained in CNC. Further, from Figures 4.6-4.8, it is observed

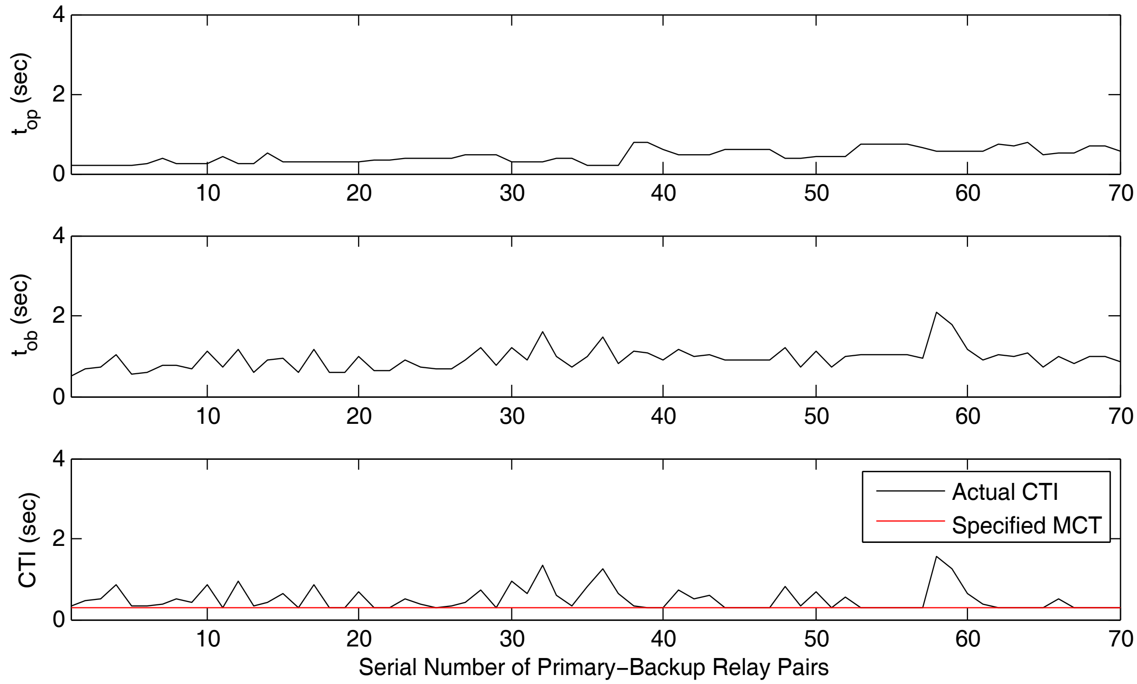

Figure 4.6: Optimized CTI in NNC of the IEEE 14-bus system.

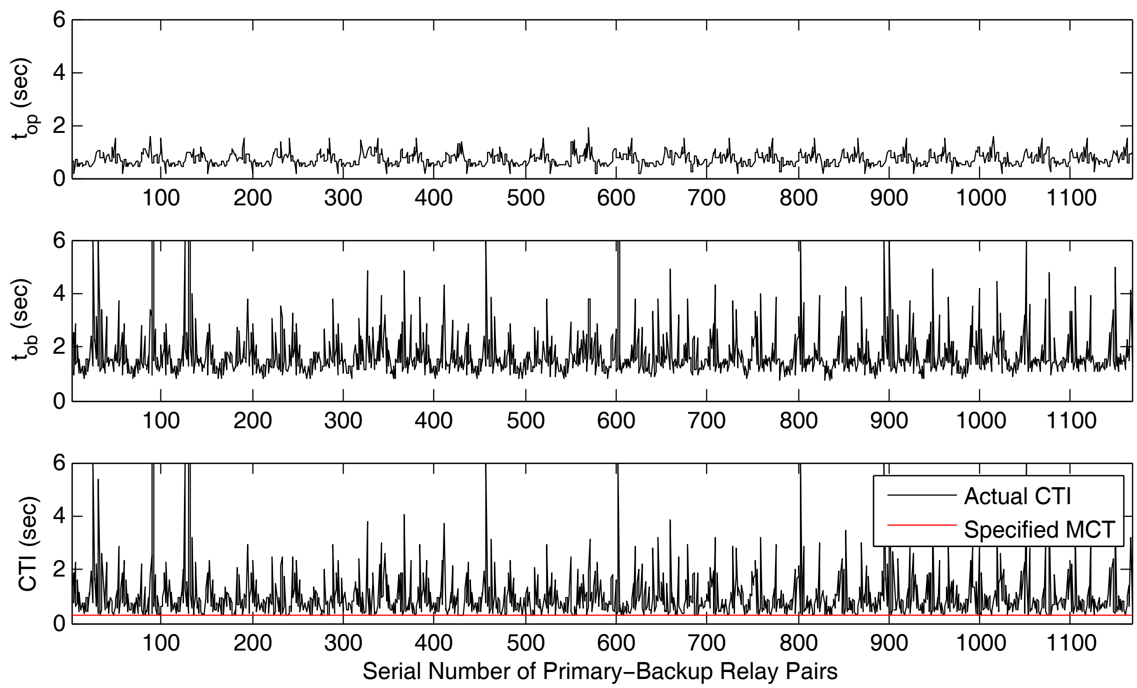

Figure 4.7: Optimized CTI in CNC of the IEEE 14-bus system.

that the minimum CTI requirement is always maintained in all the three scenarios of the system. Therefore, the settings obtained under the CNC and CNC-OLTC scenario are able to maintain the

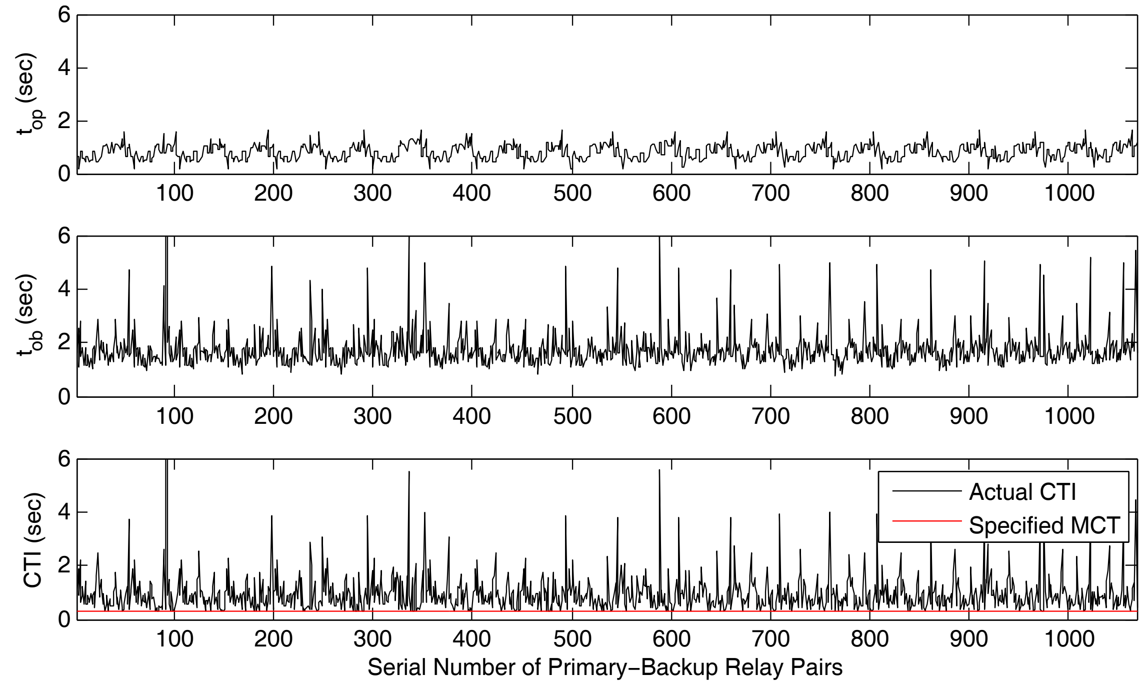

Figure 4.8: Optimized CTI in CNC-OLTC of the IEEE 14-bus system.

relay coordination properly under all the credible configurations of the system.

Further, the protection coordination problem has also been solved by considering a fixed PS for each relay in which case the coordination problem becomes an approximate linear programming (LP) problem [57, 58]. The results are shown in Table 4.6 from which, it is observed that the sum of operating times of all the relays in all the three cases (NNC, CNC and CNC-OLTC) are significantly lower in the proposed MINLP model (NOF) than those in the approximate LP model which has also been solved using the proposed IPM based algorithm. This shows the superiority of the proposed MINLP model over the approximate LP model.

4.7.4 Results on the IEEE 30-bus system

Figure 4.9 shows the single-line diagram of IEEE 30-bus system having 82 DOCRs placed on 41 lines (two on each line). This system has 195 primary-backup relay pairs. All these pairs are given in Table A.11. It is to be noted that L8, L13 and L38 of this system are equipped with OLTC. However, only the second and the third OLTCs at L13 and L38 are used to control bus voltages at bus 10 (B9) and at bus 27 (B27), respectively, whereas, the first OLTC is not used to control bus voltage at bus 12 (B12) as the generator at bus 13 controls the voltage.

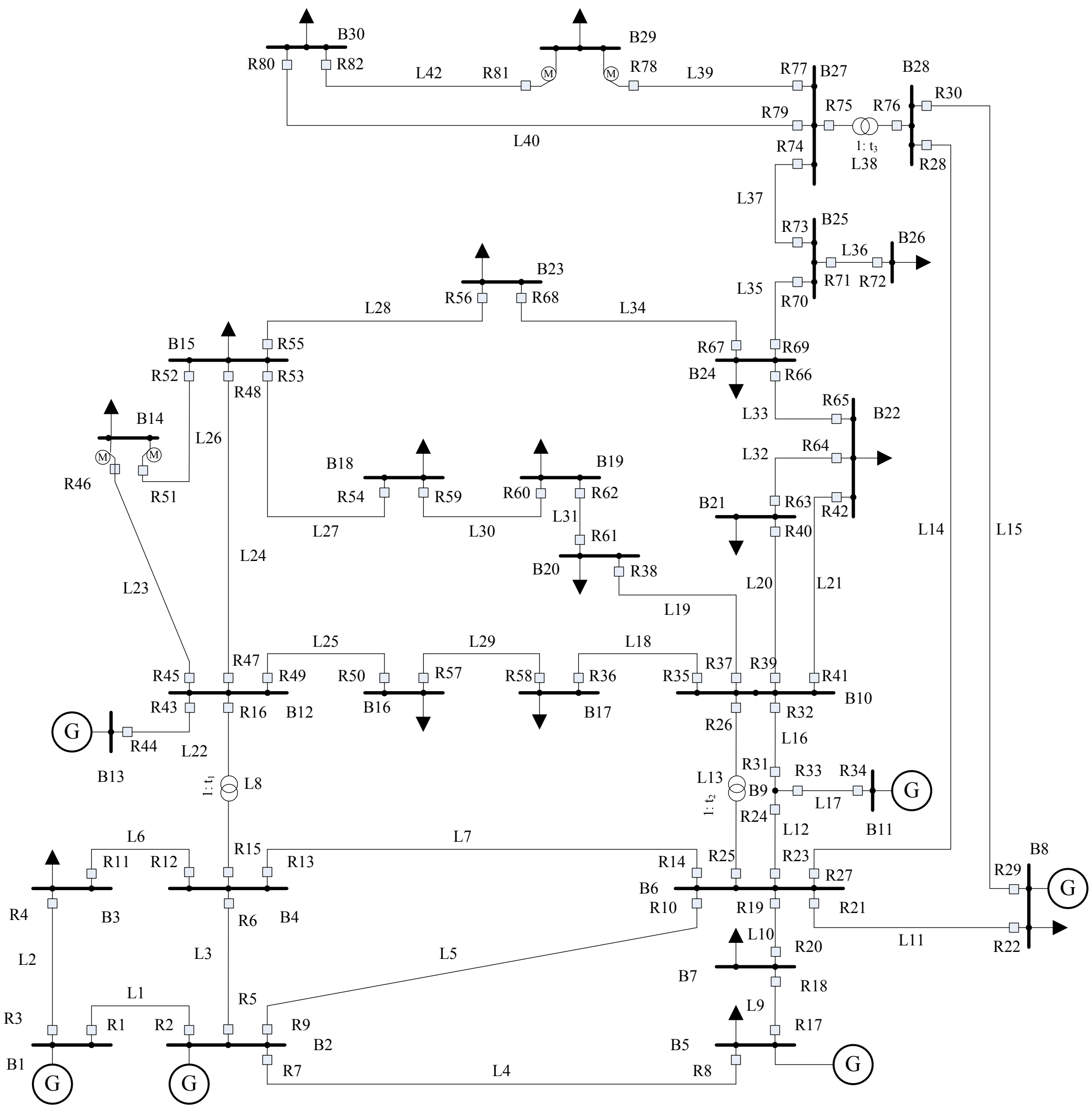

Figure 4.9: IEEE 30-bus system with OLTC.

4.7.4.1 Normal network configuration (NNC)

In this scenario, there are total 195 primary-backup relay pairs among all the 82 relays. It is to be noted that only 159 relay pairs have been considered in the optimization problem as the other 36 relay pairs are satisfying eqn. (3.14) in which coordination constraints always remain satisfied.

4.7.4.2 (N-1) contingency network configuration (CNC)

In this system, there are 41 lines and 6 generators, i.e., a total of 47 elements which can experience contingency. Therefore, under CNC scenario, there are a total of 47 configurations generated by

(N-1) contingencies. Out of these 47 contingencies, 33 contingencies have $CSI < 1$ and hence, these configurations are considered as feasible system topologies. Therefore, for deciding the parameters of the relays, a total of 34 configurations (33 contingency configurations and one normal configuration) are considered. As each configuration has 195 primary-backup relay pairs, total number of primary-backup relay pairs considered under contingency is 6630 ($= 34 \times 195$). It is to be noted that, out of these 6630 relay pairs, only 4076 relay pairs have been considered in the optimization problem in this scenario, as remaining 2554 relay pairs satisfy eqn. (3.14) thereby, ensuring that the coordination constraints are always satisfied for these relay pairs.

4.7.4.3 CNC in the presence of OLTC (CNC-OLTC)

In this scenario, out of the 47 contingencies, 38 contingencies have $CSI < 1$ and hence, these configurations are considered as feasible system topologies. Therefore, for deciding the parameters of the relays, a total of 39 configurations are considered. The total number of primary-backup relay pairs considered under contingency is 7605. However, only 4741 relay pairs have been considered in the optimization problem in this scenario, as remaining 2864 relay pairs satisfy eqn. (3.14).

The optimum settings of the relays obtained in all the three cases (NNC, CNC and CNC-OLTC) using the proposed IPM based algorithm are given in Table 4.7. Further, for these three cases, the optimized CTI between the operating times of primary and backup relay pairs are shown in Figures 4.10, 4.11 and 4.12, respectively. From these figures, it is observed that the minimum CTI is always maintained for any primary-backup relay pair, thereby ensuring the selectivity of the relays. Further, to test effectiveness of the proposed NLP model (NOF), the optimum settings of the relays obtained in all the three cases considering approximate LP model proposed in [57, 58] and using the proposed IPM algorithm are given in Table 4.7.

Table 4.7: Optimum settings of the relays obtained using the proposed algorithm for the IEEE 30-bus system

Relays	Approximate LP model						Proposed NLP model (NOF)					
	NNC		CNC		CNC-OLTC		NNC		CNC		CNC-OLTC	
	TMS	PS	TMS	PS	TMS	PS	TMS	PS	TMS	PS	TMS	PS
1	0.1	1.5	0.1	1.25	0.1	1.25	0.1	1	0.1	0.75	0.1	0.75
2	0.1	1.25	0.1	1.25	0.5929	1.25	0.1	0.5	0.1	0.5	0.3167	2
3	0.1401	1.5	0.2393	1.5	0.2905	1.25	0.1007	2	0.1222	2	0.3169	0.75
4	0.1	1.25	0.1	1.25	0.1	1.25	0.1	0.5	0.1032	0.75	0.1032	0.75
5	0.1573	1.5	0.2066	1.5	0.2076	1.5	0.1756	1.25	0.2081	1.25	0.2081	1.25
6	0.1	1.25	0.1044	1.25	0.3448	1.25	0.1055	0.75	0.1	1.25	0.2099	1.5

Continued on next page

Table 4.7 – continued from previous page

Relays	Approximate LP model						Proposed NLP model (NOF)					
	NNC		CNC		CNC-OLTC		NNC		CNC		CNC-OLTC	
	TMS	PS	TMS	PS	TMS	PS	TMS	PS	TMS	PS	TMS	PS
7	0.1	1.5	0.1	1.5	0.1	1.25	0.1	1.5	0.1	1	0.1	0.75
8	0.1253	1.25	0.1612	1.25	0.458	1.25	0.1	1.5	0.1012	1.75	0.5068	0.5
9	0.1093	1.5	0.1441	1.5	0.1856	1.25	0.1205	1.25	0.1744	1	0.2223	0.75
10	0.1	1.25	0.1105	1.25	0.365	1.25	0.1	1	0.1636	0.5	0.3594	0.75
11	0.1105	1.25	0.243	1.25	0.2444	1.25	0.1086	1.25	0.1436	1.5	0.1104	1.75
12	0.159	1.25	0.1591	1.25	0.1591	1.25	0.1056	2	0.1127	2	0.1127	2
13	0.1273	1.5	0.2144	1.25	0.2158	1.25	0.1369	1.25	0.2407	0.75	0.2407	0.75
14	0.2384	1.25	0.2455	1.25	0.2734	1.25	0.1683	2	0.3287	0.5	0.3343	0.5
15	0.1786	1.5	0.1608	1.5	0.1608	1.5	0.1799	1.25	0.1272	1.5	0.1304	1.5
16	0.1023	1.25	0.1962	1.25	0.2427	1.25	0.1	1.25	0.242	0.75	0.3129	0.5
17	0.3389	1.25	0.446	1.5	0.4484	1.5	0.2553	2	0.3051	2	0.3051	2
18	0.1431	1.5	0.1	1.25	0.1	1.25	0.1082	2	0.1	0.75	0.1	0.75
19	0.1774	1.5	0.1209	1.25	0.1209	1.25	0.136	2	0.1188	1	0.1492	0.75
20	0.3061	1.25	0.4885	1.25	0.4918	1.25	0.3893	0.5	0.4513	0.75	0.4513	0.75
21	0.143	1.25	0.3739	1.5	0.377	1.5	0.1008	1.75	0.2197	2	0.2197	2
22	0.2868	1.25	0.3897	1.25	0.3897	1.25	0.3716	0.5	0.3765	1	0.3765	1
23	0.2015	1.5	0.3328	1.5	0.3328	1.5	0.2021	1.25	0.2728	1.5	0.2728	1.5
24	0.1	1.25	0.1	1.25	0.1	1.25	0.1	0.5	0.1	0.5	0.1	0.5
25	0.2566	1.5	0.3289	1.5	0.3289	1.5	0.1881	1.75	0.3288	1.25	0.3288	1.25
26	0.1614	1.25	0.2893	1.25	0.2893	1.25	0.1	2	0.4145	0.5	0.4145	0.5
27	0.1657	1.25	0.2705	1.5	0.2705	1.5	0.1272	1.5	0.23	1.5	0.2819	1.25
28	0.1378	1.25	0.3517	1.25	0.3762	1.25	0.1032	1.5	0.4735	0.5	0.479	0.5
29	0.1363	1.25	0.5502	1.25	0.5502	1.25	0.1059	1.5	0.3025	2	0.3025	2
30	0.1259	1.25	0.1	1.5	0.1	1.5	0.1	1.5	0.1	1	0.1	1
31	0.1	1.5	0.1	1.75	0.1	1.75	0.1	1.25	0.1	1.5	0.1	1.5
32	0.2192	1.25	0.3411	1.5	0.3411	1.5	0.1226	2	0.4068	1	0.4068	1
33	0.1	1.5	0.1	1.5	0.1	1.5	0.1	1	0.1	1.25	0.1	1.25
34	0.4088	1.25	0.863	1.25	0.863	1.25	0.5125	0.5	1.0084	0.5	1.0084	0.5
35	0.3893	1.25	0.5544	1.25	0.5544	1.25	0.2461	2	0.5479	0.75	0.5525	0.75
36	0.475	1.25	0.8229	1.5	0.8229	1.5	0.3995	1.25	0.8089	1	0.8089	1
37	0.4792	1.25	0.8008	1.5	0.8008	1.5	0.3192	2	0.7929	1	0.8027	1
38	0.4456	1.25	0.8755	1.25	0.8755	1.25	0.2891	2	0.5417	2	0.5417	2
39	0.4088	1.5	0.6733	1.5	0.6733	1.5	0.287	2	0.5856	1.25	0.5856	1.25
40	0.3978	1.25	0.7783	1.25	0.7783	1.25	0.3624	1	0.8688	0.5	0.8688	0.5
41	0.3219	1.25	0.5485	1.5	0.5485	1.5	0.2012	2	0.3555	2	0.3555	2
42	0.2837	1.25	0.6112	1.25	0.6112	1.25	0.4054	0.5	0.7757	0.5	0.7757	0.5
43	0.1	1.25	0.1	1.5	0.1	1.5	0.1	0.5	0.1	1	0.1	1
44	0.4563	1.25	0.7523	1.25	0.7523	1.25	0.2972	2	0.6012	1.25	0.4804	2
45	0.3027	1.25	0.6534	1.5	0.6534	1.5	0.183	2	0.4775	2	0.4775	2
46	0.2332	1.25	0.5236	1.25	0.5236	1.25	0.2326	1	0.7027	0.5	0.7027	0.5
47	0.3663	1.5	0.5643	1.5	0.5643	1.5	0.2515	2	0.3644	2	0.406	1.75
48	0.2847	1.25	0.5818	1.25	0.5818	1.25	0.1535	2	0.735	0.5	0.735	0.5
49	0.4573	1.25	0.7124	1.5	0.7124	1.5	0.3005	2	0.5044	2	0.5044	2
50	0.389	1.25	0.5767	1.25	0.5767	1.25	0.2431	2	0.4127	1.5	0.4182	1.5
51	0.3763	1.25	0.6861	1.5	0.6861	1.5	0.2818	1.5	0.7196	1	0.7196	1
52	0.2457	1.25	0.4066	1.25	0.4066	1.25	0.1717	2	0.2854	2	0.2854	2
53	0.5327	1.25	0.6782	1.5	0.6782	1.5	0.3564	2	0.6671	1	0.6671	1
54	0.3769	1.25	0.9529	1.25	0.9529	1.25	0.2382	2	0.7149	1.5	0.7847	1.25
55	0.4163	1.25	0.7427	1.5	0.7427	1.5	0.2725	2	0.501	2	0.501	2
56	0.4546	1.25	0.9501	1.25	0.9501	1.25	0.2882	2	0.6101	2	0.6101	2
57	0.5081	1.25	0.7223	1.5	0.7223	1.5	0.3488	2	0.5081	2	0.5081	2
58	0.3762	1.25	0.5695	1.25	0.5695	1.25	0.235	2	0.3555	2	0.3594	2
59	0.5223	1.25	0.6934	1.5	0.6934	1.5	0.3515	2	0.4606	2	0.4606	2
60	0.4059	1.25	0.8471	1.25	0.8471	1.25	0.2627	2	0.5404	2	0.5493	2
61	0.4798	1.25	0.8052	1.25	0.8052	1.25	0.3176	2	0.4915	2	0.4915	2
62	0.4703	1.25	0.8092	1.5	0.8092	1.5	0.3148	2	0.567	2	0.5749	2
63	0.4476	1.25	0.7816	1.25	0.7816	1.25	0.2863	2	0.4923	2	0.4923	2

Continued on next page

Table 4.7 – continued from previous page

Relays	Approximate LP model						Proposed NLP model (NOF)					
	NNC		CNC		CNC-OLTC		NNC		CNC		CNC-OLTC	
	TMS	PS	TMS	PS	TMS	PS	TMS	PS	TMS	PS	TMS	PS
64	0.3977	1.25	0.4483	1.5	0.4483	1.5	0.2705	2	0.4272	1.25	0.4272	1.25
65	0.4275	1.25	0.6252	1.5	0.6252	1.5	0.2681	2	0.4116	2	0.4116	2
66	0.4505	1.25	0.928	1.5	0.928	1.5	0.3116	2	0.8424	1.25	0.8424	1.25
67	0.3931	1.25	0.8569	1.5	0.8569	1.5	0.2569	2	0.5871	2	0.5871	2
68	0.4649	1.25	0.7871	1.25	0.7871	1.25	0.2975	2	0.4838	2	0.4838	2
69	0.2496	1.25	0.5222	1.25	0.5441	1.25	0.1746	2	0.5164	0.75	0.5195	0.75
70	0.3272	1.5	0.7853	1.5	0.7853	1.5	0.233	2	0.4883	2	0.4883	2
71	0.1	1.25	0.1	1.25	0.1	1.25	0.1	0.5	0.1	0.75	0.1	0.75
72	0.1	1.25	0.1	1.25	0.1	1.25	0.1	0.5	0.1	0.5	0.1	0.5
73	0.2	1.25	0.5435	1.25	0.5712	1.25	0.1395	2	0.4411	1	0.4445	1
74	0.4452	1.5	0.8314	1.5	0.8314	1.5	0.3341	2	0.5263	2	0.5263	2
75	0.1389	1.25	0.5698	1.25	0.6047	1.25	0.1	1.75	0.3357	1.75	0.339	1.75
76	0.2522	1.5	0.4858	1.5	0.4858	1.5	0.2584	1.25	0.4468	1.25	0.4468	1.25
77	0.139	1.5	0.139	1.5	0.139	1.5	0.1	2	0.1	2	0.1	2
78	0.1	1.25	0.1	1.25	0.1	1.25	0.1	0.5	0.1	0.5	0.1	0.5
79	0.1	1.5	0.1	1.5	0.1	1.5	0.1	1	0.1	1	0.1	1
80	0.1	1.25	0.1	1.25	0.1	1.25	0.1	0.5	0.1	0.5	0.1	0.5
81	0.1	1.5	0.1	1.5	0.1	1.5	0.1	1	0.1	1	0.1	1
82	0.1	1.25	0.1	1.25	0.1	1.25	0.1	0.5	0.1	0.5	0.1	0.5
$\sum_{i=1}^{82} t_{op,i}$	58.5682		107.5829		111.5326		**48.4711**		**86.8552**		**89.7729**	

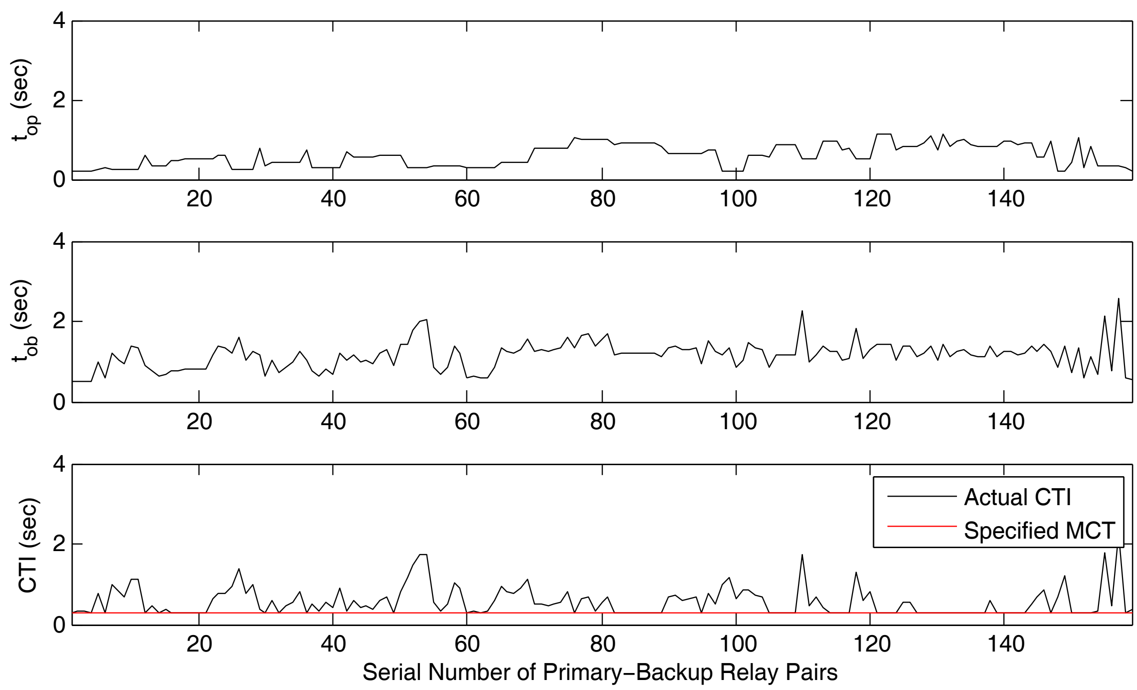

Figure 4.10: Optimized CTI in NNC of the IEEE 30-bus system.

From Table 4.7, it is observed that the sum of the operating times of all the relays in NNC scenario is 48.4711 seconds whereas the sum of the operating times of all the relays in CNC

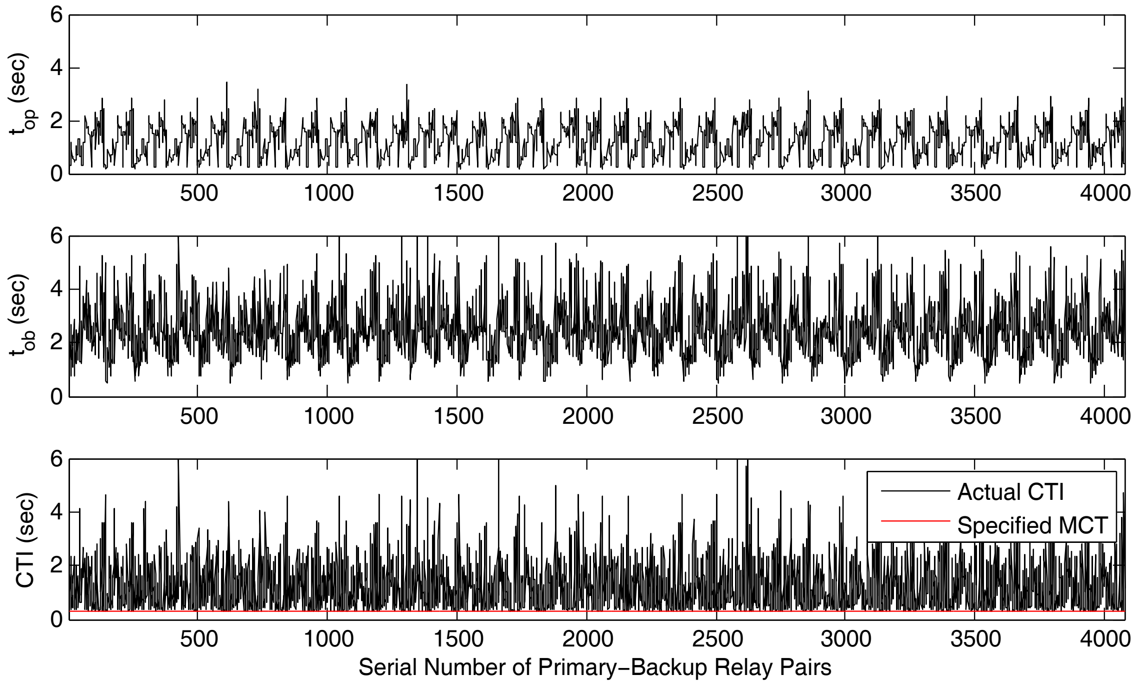

Figure 4.11: Optimized CTI in CNC of the IEEE 30-bus system.

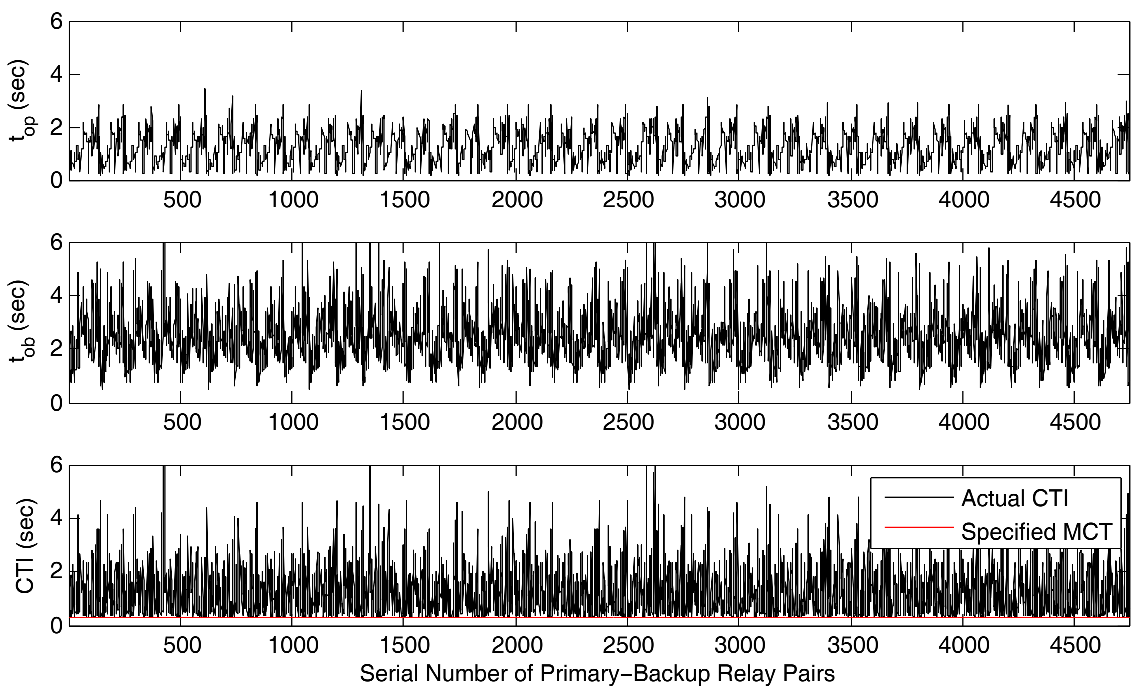

Figure 4.12: Optimized CTI in CNC-OLTC of the IEEE 30-bus system.

scenario is 86.8552 seconds. Further, the sum of the operating times of all the relays in CNC-OLTC scenario is 89.7729 seconds. It is also observed that 404 (i.e., 9.91%) coordination constraints of

CNC and 465 (i.e., 9.81%) coordination constraints of CNC-OLTC are violated with the relay settings as obtained using NNC. Subsequently, from Table 4.7, it is observed that the sum of the operating times of all the 82 relays are more for CNC and CNC-OLTC cases than those for NNC. This is because the relay settings obtained in these two cases are robust and thus can maintain protection coordination under all the credible (N-1) contingencies of the system thereby again demonstrating that the price of robustness is an increase in total operating time of the relays. Further, it is to be noted that in case of CNC-OLTC, the change in voltage profile of the system causes a change in the fault currents which ultimately decides the different operating times of all the relays. As a result, the sum of operating times of all the relays in CNC-OLTC are different than those obtained in CNC. Further, from Figures 4.10-4.12, it is observed that the minimum CTI requirement is always maintained in all the three scenarios of the system. Therefore, the settings obtained under the CNC and CNC-OLTC scenario are able to maintain the relay coordination properly under all credible configurations of the system.

Further, the protection coordination problem has also been solved by considering a fixed PS for each relay in which case the coordination problem becomes an approximate linear programming (LP) problem [57, 58]. The results are shown in Table 4.7 from which, it is observed that the sum of operating times of all the relays in all the three cases (NNC, CNC and CNC-OLTC) are significantly lower in the proposed MINLP model (NOF) than those in the approximate LP model which has also been solved using the proposed IPM based algorithm. This shows the superiority of the proposed MINLP model over the approximate LP model.

4.7.5 Results on the IEEE 118-bus system

Figure 4.13 shows the single-line diagram of the IEEE 118-bus system having 372 DOCRs placed on 186 lines (two on each line). It is to be noted that L28, L60, L102, L106 and L136 in this system are equipped with OLTC. This system has 1184 primary-backup relay pairs which are given in Table A.12. The various types of DOCRs with different characteristic curves as considered in Chapter 3 have again been considered which are as follows;

1) R1-R200: numerical/digital type (IDMT characteristics)

2) R201-R260: numerical/digital type (VIN characteristics)

3) R261-R300: numerical/digital type (EIN characteristics)

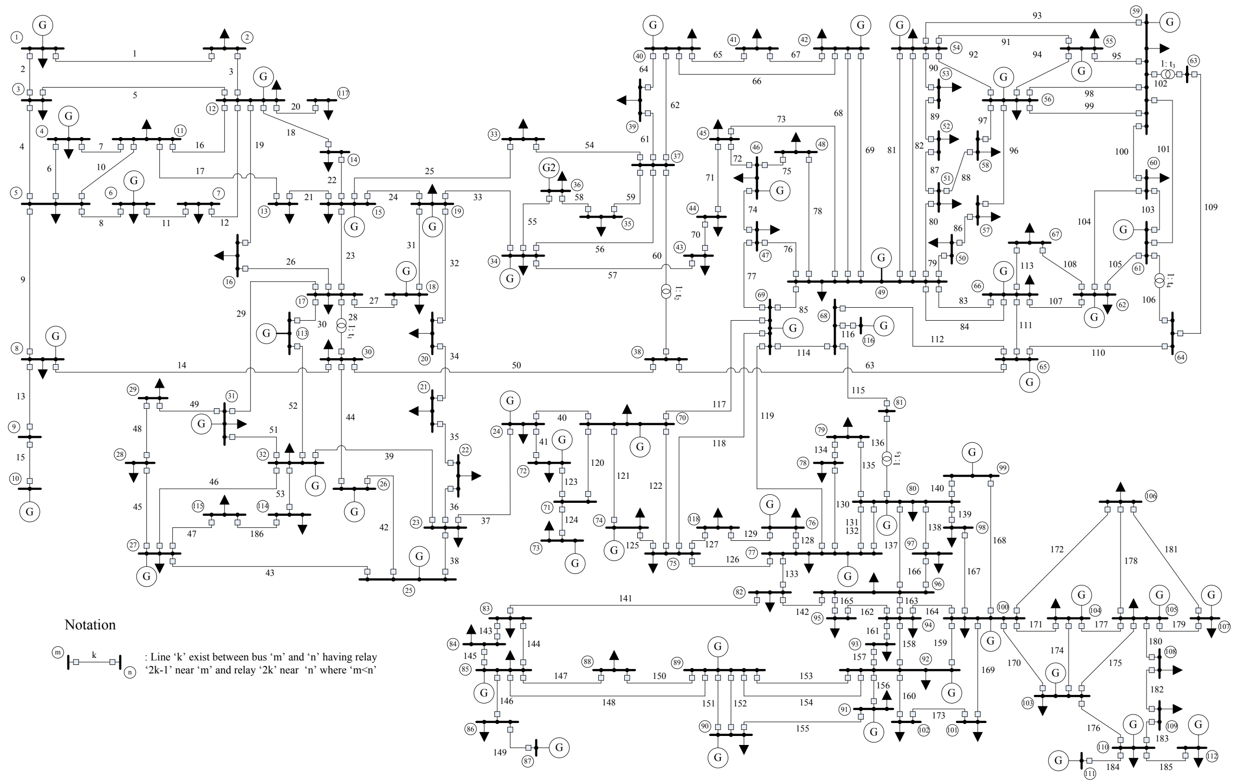

Figure 4.13: IEEE 118-bus system with OLTC.

4) R301-R372: static or electromechanical type (IDMT characteristics)

Now, the optimum settings of the relays obtained for NNC, CNC and CNC-OLTC are discussed below for this case.

4.7.5.1 Normal network configuration (NNC)

In this scenario, there are a total of 1184 primary-backup relay pairs among all the 372 relays. It is to be noted that only 829 relay pairs have been considered in the optimization problem as the other relay pairs are satisfying eqn. (3.14) in which the coordination constraints always remain satisfied.

4.7.5.2 (N-1) contingency network configuration (CNC)

In this system, there are a total of 240 network elements (186 lines and 54 generators) which can undergo contingency. Out of the total 240 configurations created by (N-1) contingencies, 220 configurations are considered feasible as they have $CSI < 1$. Thus, a total of 221 configurations are considered for robust relay settings (220 contingency configurations and one normal configuration), resulting into a total of 261664 ($= 221 \times 1184$) primary-backup relay pairs to be taken into account. It is to be noted that only 32940 relay pairs (out of 261664 pairs) have been considered in this case, as the remaining relay pairs are satisfying eqn. (3.14) implying that the coordination constraints always remain satisfied for these relay pairs.

4.7.5.3 CNC in the presence of OLTC (CNC-OLTC)

In this scenario, out of the total 240 configurations created by (N-1) contingencies, 218 configurations are considered feasible as they have $CSI < 1$. Thus a total of 219 configurations are considered for robust relay settings, resulting into a total of 259296 primary-backup relay pairs to be taken into account. However, only 35593 relay pairs (out of 259296 pairs) have been considered in this case, as the remaining relay pairs are satisfying eqn. (3.14).

The optimum settings of the relays obtained in all the three cases (NNC, CNC and CNC-OLTC) using the proposed IPM based algorithm are shown in Figures 4.14, 4.15 and 4.16, respectively. Also, for these three cases, the optimized CTI between the operating times of primary and backup relay pairs are displayed in Figures 4.17, 4.18 and 4.19, respectively.

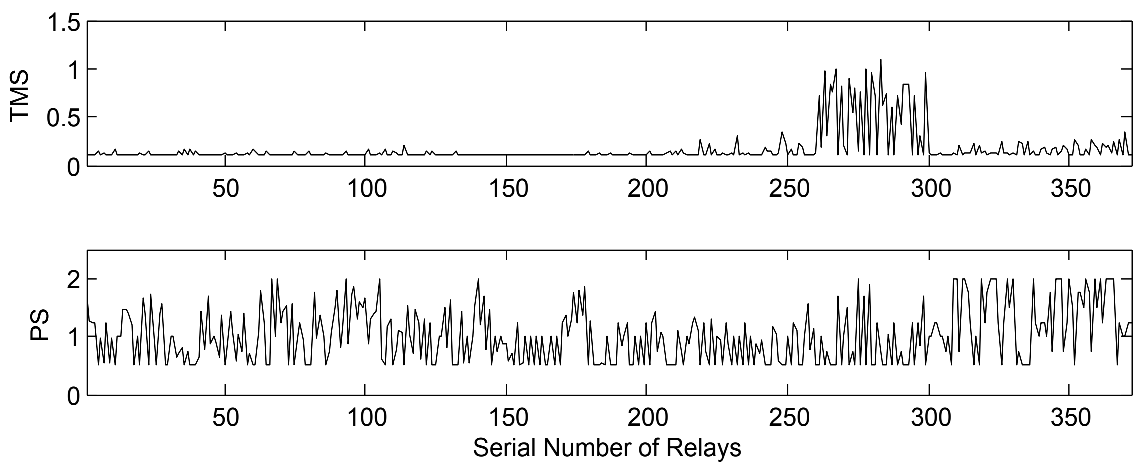

Figure 4.14: Optimum relays settings in NNC for the IEEE 118-bus system.

Further, the sum of the operating times of all the 372 relays in NNC is 88.4653 seconds whereas the sum of the operating times of all the 372 relays in CNC is 119.9244 seconds. Also, the sum of the operating times of all the 372 relays in CNC-OLTC is 119.6043 seconds. It is also found that 20628 (i.e., 62.62%) coordination constraints of CNC and 21954 (i.e., 61.68%) coordination constraints of CNC-OLTC are violated with the relay settings obtained using NNC. Further, the

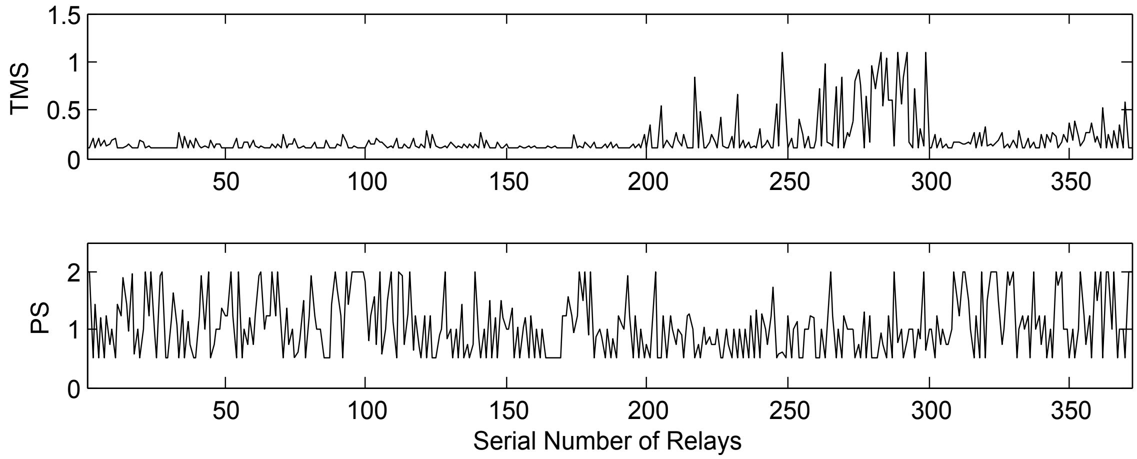

Figure 4.15: Optimum relays settings in CNC for the IEEE 118-bus system.

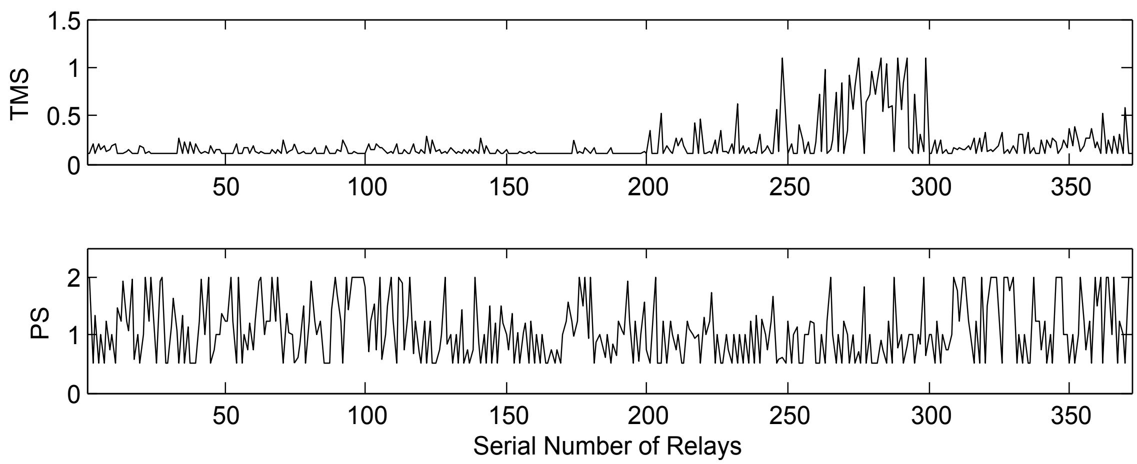

Figure 4.16: Optimum relays settings in CNC-OLTC for the IEEE 118-bus system.

sum of the operating times of all the 372 relays are more for CNC and CNC-OLTC cases than those for NNC as in the case for IEEE 14 and 30-bus systems. The reason for this is the fact that the relay settings obtained for CNC and CNC-OLTC cases are robust as these can maintain protection coordination under all the credible (N-1) contingencies of the system. Thus, it again corroborates the fact that the price of robustness is an increase in the total operating time of the relays. Also, the difference in the sum of operating times of all the relays in CNC and CNC-OLTC is because of change in the fault currents caused by change in the voltage profile in these two configurations. Also, from Figures 4.17-4.19, it is observed that the CTI requirements of 0.1 seconds (for numerical/digital relays) and 0.3 seconds (electromechanical and static relays) are always maintained in NNC, CNC and CNC-OLTC scenarios of the system. Thus, the selectivity

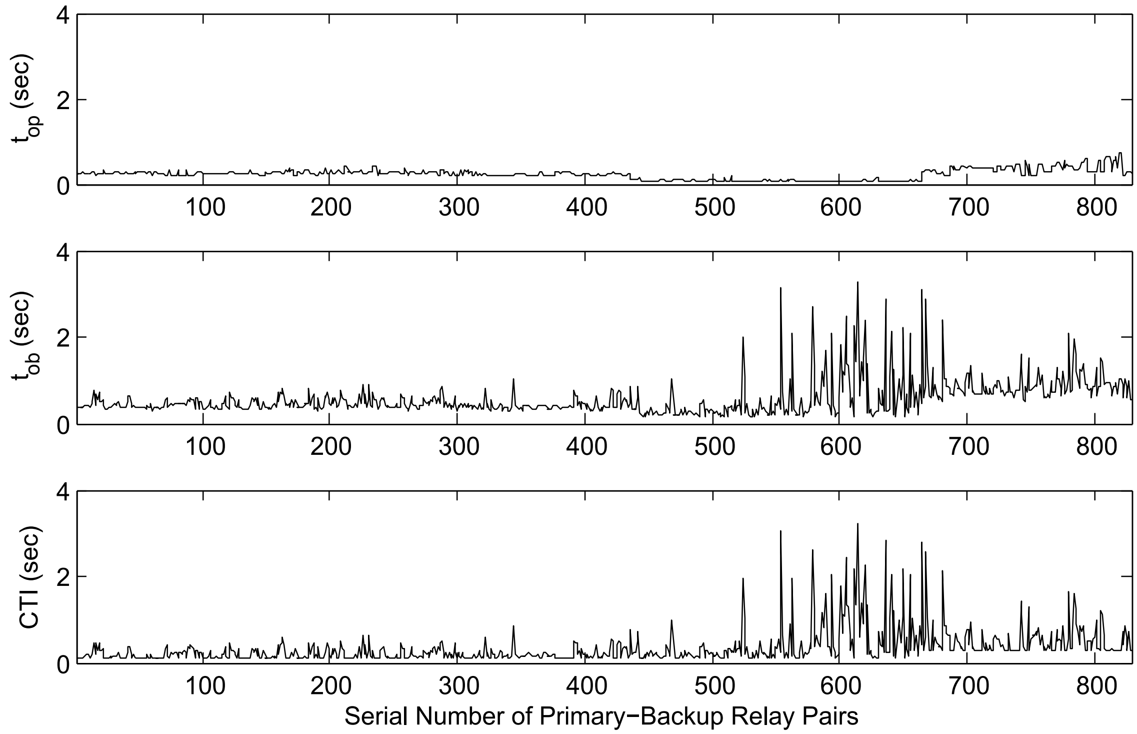

Figure 4.17: Optimized CTI in NNC of the IEEE 118-bus system.

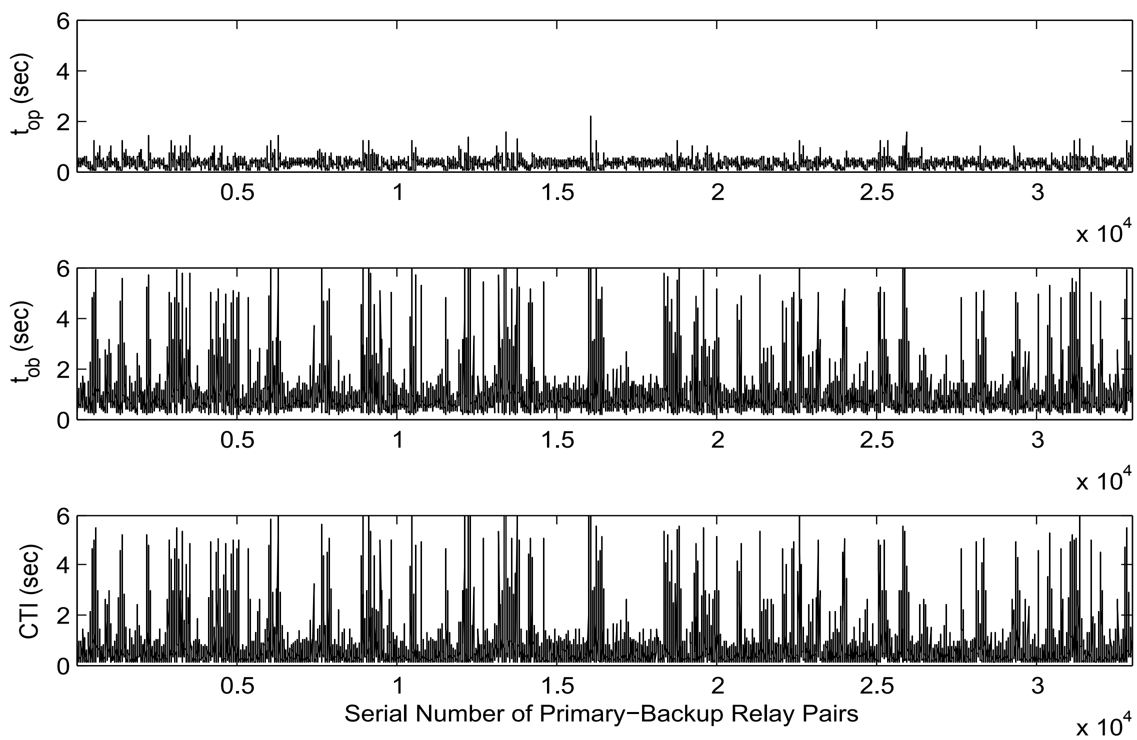

Figure 4.18: Optimized CTI in CNC of the IEEE 118-bus system.

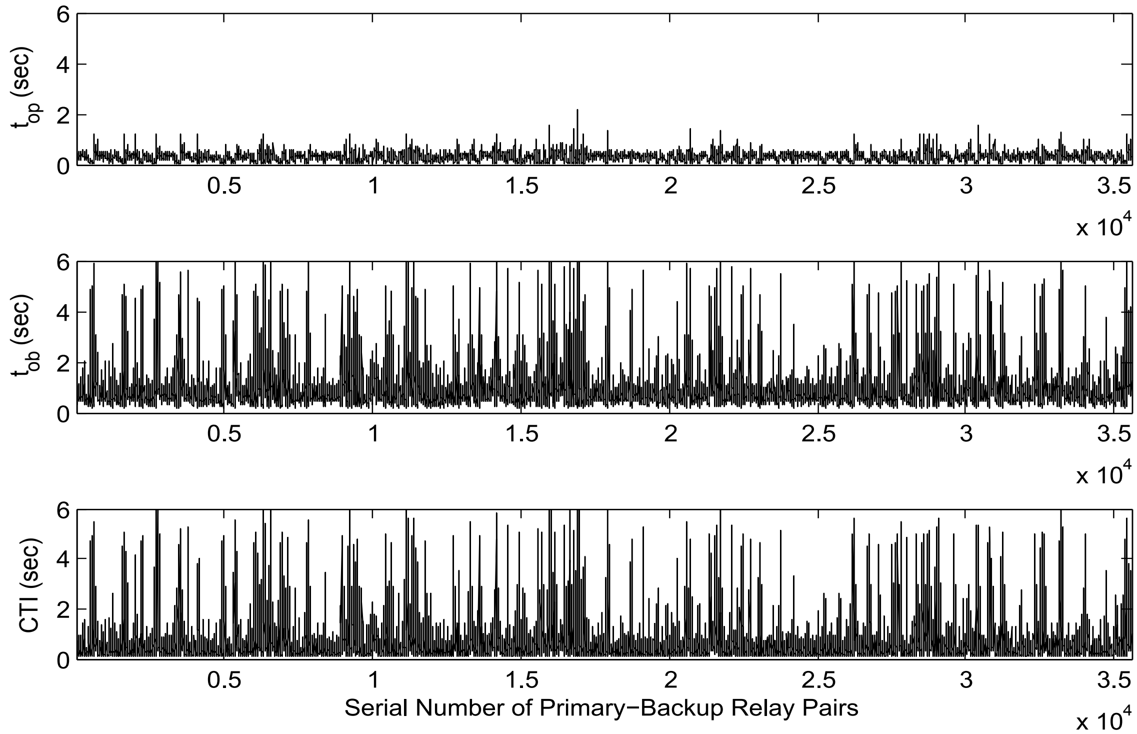

Figure 4.19: Optimized CTI in CNC-OLTC of the IEEE 118-bus system.

of the relays is always maintained under all credible configurations of the system.

Further, in this case also, the protection coordination problem has been solved as an approximate LP problem by considering PS of each relay to be known [57, 58]. It was found that the sum of the operating times of all the relays obtained with the approximate LP model (solved using the proposed IPM based algorithm) in all the three cases NNC, CNC and CNC-OLTC are 108.8214, 144.4899 and 144.2273 seconds, respectively. So, as in the previous two test systems, the sum of operating times of all the relays in all the three cases are significantly lower in the proposed MINLP model (NOF) than those in the approximate LP model. Thus, the MINLP model is superior to the approximate LP model.

4.8 Comparative studies of IPM based algorithm in AMPL and MATLAB environments

In this section, comparative summary of the results obtained after 100 independent runs of the proposed IPM based algorithm implemented in AMPL and MATLAB environments using NOF on all the three test systems is presented. Table 4.8 gives the detailed summary of the results which includes the best, mean and worst values of objective function along with standard deviation and average run time taken by the both environments under the three cases (NNC, CNC, CNC-OLTC) of the IEEE 14, 30 and 118-bus systems discussed earlier in this chapter.

Table 4.8: Summary of the results obtained after 100 independent runs by the proposed IPM based algorithm implemented in AMPL and MATLAB environments

Test systems	Various cases	Environments	Objective function values			Standard deviation	Average run time
			Best	Mean	Worst		
14-bus	NNC	AMPL	17.9778	17.9778	17.9778	0	0.2505
	NNC	MATLAB	17.9781	17.9782	17.9783	0.0001	17.0447
	CNC	AMPL	26.5592	26.5592	26.5592	0	0.6295
	CNC	MATLAB	26.5586	26.5586	26.5586	0	243.58
	CNC-OLTC	AMPL	29.6404	29.6404	29.6404	0	0.5118
	CNC-OLTC	MATLAB	29.5849	29.5849	29.585	0	231.1638
30-bus	NNC	AMPL	48.4711	48.4711	48.4711	0	0.5013
	NNC	MATLAB	48.4697	48.4697	48.4698	0	95.0155
	CNC	AMPL	86.8552	86.8552	86.8552	0	3.4315
	CNC	MATLAB	86.8554	86.8554	86.8554	0	2791.0045
	CNC-OLTC	AMPL	89.7729	89.7729	89.7729	0	4.2575
	CNC-OLTC	MATLAB	89.7731	89.7731	89.7732	0.0001	3013.5119
118-bus	NNC	AMPL	88.4653	88.4653	88.4653	0	1.5424
	NNC	MATLAB	88.4464	88.5178	88.7282	0.1181	4522.6375
	CNC	AMPL	119.9244	119.9244	119.9244	0	135.5387
	CNC	MATLAB	119.9244	119.9244	119.9244	0	4781.3246
	CNC-OLTC	AMPL	119.6043	119.6043	119.6043	0	145.4078
	CNC-OLTC	MATLAB	119.6043	119.6043	119.6043	0	4937.7628

From Table 4.8, it can be observed that the optimum values of the sum of operating times of all the relays obtained in AMPL and MATLAB environments under various cases in the three test systems are very close to each other. However, the average run time taken by AMPL is much lower than that obtained by MATLAB. This is the reason behind adopting AMPL based IPM algorithm in this chapter.

4.9 Conclusion

In this chapter, a method for robust protection coordination settings of directional overcurrent relays, considering (N-1) contingencies, is proposed. An algorithm suitable for solving mixed-integer non-linear programming problems based on interior point method has been suggested for solving this optimization problem. The feasible system configurations under (N-1) contingencies have been selected using a composite security index. Based on the detailed investigation on three IEEE test systems, following conclusions can be drawn:

(i) Robust settings obtained are suitable for coordinating DOCRs properly under all credible (N-1) contingencies.

(ii) The developed objective function ensures that the operating times of both primary and backup relays are minimized.

(iii) Proposed IPM based technique is efficient and robust in solving large scale MINLP problems.

(iv) For practical application it is desirable to implement the relay settings as obtained using CNC and CNC-OLTC based approach.

(v) AMPL environment based IPM algorithm is superior to MATLAB environment based IPM algorithm.

In the next chapter, optimum protection coordination of recloser and fuses in the presence of multiple DGs is discussed.

Chapter 5

Optimum Recloser-fuse Coordination in Radial Distribution Systems in the Presence of Multiple Distributed Generations

Abstract

In this chapter, optimum recloser-fuse coordination scheme is proposed in the presence of multiple distributed generators (DGs) in a radial distribution network. The proposed approach formulates optimum recloser-fuse coordination problem as an optimization problem and applies interior point method (IPM) to solve this optimization problem for obtaining the optimum recloser and fuse settings. The proposed scheme gives a single set of settings of the recloser and fuses which is robust enough to be able to coordinate the operations of the recloser and fuses properly without and in the presence of single/multiple DGs in the system. The proposed approach has been tested on the IEEE 33 and 69-bus systems for three different scenarios: i) no DG in the system, ii) a single DG in the system and iii) multiple DGs in the system. The test results prove the robustness and effectiveness of the presented scheme.

5.1 Introduction

AS discussed in Chapter 1, in radial distribution systems, the feeders are protected by means of reclosers and fuses. Fuses are placed at laterals which are at a more remote position from the substation. Whenever a temporary fault occurs in any feeder, the corresponding fuse does not melt because the fast operation of recloser allows the temporary fault to self-clear. But, whenever a permanent fault occurs, the concerned fuse must melt just before the final trip operation of the recloser in order to prevent the loads between the recloser and the fuse from being interrupted [125–127]. In radial distribution systems, the flow of currents are unidirectional whereas in the presence of distributed generators (DGs) in the system, the flow of currents no longer remains unidirectional [128–130]. Further, integration of DGs at multiple locations can completely alter the flow of currents in the feeder sections during the fault. As a result, there are always chances of miscoordination in the operation of recloser and fuses in the presence of DGs [131–134].

To address the issues discussed above, in this chapter an optimum protection coordination scheme for recloser and fuses is proposed. Towards this goal, the coordination problem has been posed as an optimization problem and subsequently, interior point method (IPM) has been used to solve the formulated optimization problem in order to achieve a fixed characteristics of recloser and fuses which can coordinate properly under various operating conditions and locations of DGs in radial distribution systems. The proposed approach has been tested on the IEEE 33 and 69-bus systems for three different scenarios: i) no DG in the system, ii) a single DG in the system and iii) multiple DGs in the system.

5.2 Recloser-fuse coordination philosophy

For coordination of recloser and fuses in a radial distribution system, fuse saving and fuse blowing approaches are employed. During recloser fast mode of operation, fuse saving approach is adopted in order to avoid permanent disconnection of supply to the customers for temporary faults. However, for a permanent fault, before the last slow mode of operation of the recloser, the nearest fuse must blow in order to avoid unnecessary operation of recloser (and thereby disconnection of supply to a large set of customers). These features are most desirable in coordination of recloser and fuses to avoid unnecessary outages in the system.

5.3 Time-current characteristics of reclosers and fuses

Normally, reclosers are made to follow extremely inverse characteristic curves whereas characteristics of downstream fuses are represented as straight lines on log-log graph paper [67, 135–137]. Mathematically these characteristics can be expressed as given below;

5.3.1 Recloser characteristics

The characteristics of recloser is expressed as following [67];

$$t_{opR} = \mathit{TDS} \times \left[\frac{A}{(I_{FR}/\mathit{PCS})^p - 1} + B \right] \tag{5.1}$$

In eqn. (5.1), t_{opR} is the operating time of the recloser, I_{FR} is the fault current passing through the recloser, *PCS* is the pickup current setting for the recloser whereas, A, B and p are the coefficients of the recloser characteristics.

5.3.2 Fuse characteristics

The characteristics of fuse is expressed using log-log function as follows [67];

$$log(t_{opF}) = a \times log(I_{FF}) + b \tag{5.2}$$

In eqn. (5.2), t_{opF} is the operating time of the fuse, I_{FF} is the fault current passing through the fuse whereas, a and b are the fuse characteristic coefficients, i.e., fuse constants.

5.4 Conventional recloser-fuse coordination approach

In conventional method of coordination of recloser and fuses, initially, recloser settings are fixed and subsequently, the operating times of all the downstream fuses are calculated using the concept of time grading between two consecutive fuses. After computing the operating times of all the fuses, their characteristic constants (a and b) are calculated. The overall conventional approach is discussed below.

5.4.1 Calculation of recloser settings

Recloser settings are obtained by fixing the values of time dial setting (*TDS*) and pickup current setting (*PCS*). It is to be noted that two *TDSs* (one for fast mode and one for slow mode of operation of recloser) and only one *PCS* are required. The following equation is used to fix *PCS* of the recloser [67].

$$PCS = OLF \times I_{Lmax} \tag{5.3}$$

In eqn. (5.3), *OLF* is the overload factor and I_{Lmax} is the maximum value of the load current passing through the recloser. For fixing *TDSs* of the recloser, a certain minimum time gap is maintained between the operation of the recloser in the fast and slow modes of operation. Typically the minimum gap should be sufficient enough to allow all the downstream fuses to operate in order to clear any permanent fault in the protective zone before the recloser slow mode of operation. Further, if more than one fuse is placed in any lateral to the downstream of the recloser then some additional gap needs to be considered in order to allow the fuse-fuse coordination before the recloser slow mode of operation. The minimum time gap required between the operating times (fast and slow modes) of recloser is known as minimum recloser coordination time interval (MRCTI) whereas the minimum time gap required between the operating times of two fuses is known as minimum fuse coordination time interval (MFCTI). Two fuses placed consecutively in any lateral must have a time gap at least equal to MFCTI of the first fuse responsible for clearing a permanent fault. It is to be noted that MFCTI compensates for effects such as load current and ambient temperature, or fatigue in the fuse element caused by the heating effect of fault currents which have passed through the fuse to a fault downstream but which were not sufficiently large enough to melt the fuse [138]. Further, recloser in its slow mode of operation must allow the fuse nearest to the recloser to completely operate for a permanent fault in order to maintain fuse-recloser coordination.

In conventional recloser and fuse coordination approach, TDS for the fast mode of operation of the recloser is selected in such a way that it should react as fast as possible for any fault. However, TDS for the slow mode of operation of the recloser is selected in such a way that it should allow all the downstream fuses to clear any permanent fault while maintaining the coordination between them. A trial and error procedure is adopted to select the two TDSs and after that the time grading for the operation of the fuses is carried out [67, 135].

5.4.2 Calculation of settings of the fuses

The following procedure is followed to obtain the graded operating times of all the fuses downstream of the recloser [67].

$$t_{opF,i} = t_{opR,fm} + \frac{i \times (t_{opR,sm} - t_{opR,fm})}{n+1} \tag{5.4}$$

In eqn. (5.4), $t_{opR,fm}$ and $t_{opR,sm}$ are the operating times of the recloser in its fast and slow mode of operation, respectively, $t_{opF,i}$ is the operating time of fuse i in the faulted path where $i = 1$ represents the fuse closest to the faulted point and n is the total number of fuses in the fault path to the sub-station. After computing the operating times of all the fuses and the recloser, performance testing of the coordinated operation is carried out by checking correct sequence of operation of the protective devices [67] for maintaining the minimum time requirement (i.e., MFCTI/MRCTI) for proper coordination between them. If any coordination failure is observed, the TDSs of the recloser are changed and the time grading of the fuses needs to be recalculated to check the coordination requirement. Once the correct time grading which maintains the coordination properly is obtained then the fuse constants are calculated for all the fuses using eqn. (5.2).

5.5 Miscoordination in the presence of distributed generations

In radial distribution systems, current flow is unidirectional from the sub-station to the load points. Further, during any fault in the system, the direction of flow of the fault current remains the same from sub-station to the fault point. Also, in the absence of DGs, the fault current passing through various protective devices in the faulted path (from fault point to the sub-station) either increases gradually or remains the same (depending on loading level during the fault). In such radial networks, coordination of recloser and fuses obtained by the conventional approach works well [67].

However, the presence of a DG anywhere in the system (except substation) completely changes the pattern of fault currents flowing through different protective devices in the system. In some cases, the fault currents passing through a recloser becomes much smaller than that flowing through its downstream fuses because of the presence of DG in the fault path. In some other cases, in the presence of DGs, the direction of fault current through some fuses reverses (vis-a-vis the direction of fault current in the absence of any DG). More details of these cases can be found in [15, 64, 66–68]. Further, increased penetration of variable renewable distributed generation (RDG) makes this coordination problem more complex [139]. Under these circumstances, it is quite difficult to obtain a common settings of recloser and fuses which will be able to coordinate properly irrespective of the presence of DG in the radial distribution system [64, 65]. Further, the presence of multiple DGs in the system makes the coordination of recloser and fuses very complex.

A new optimization based approach is proposed in this thesis to solve this complex problem and to obtain a proper coordination of recloser and fuses in the presence of DGs in a distribution system.

5.6 Proposed optimum recloser-fuse coordination approach

With a properly coordinated reclosers and fuses in a radial distribution system, the operating times of all the fuses are selected in such a way that they should operate as fast as possible for any permanent fault in their respective protective zones. Further, if the nearest fuse to the fault point fails to clear the fault, the next responsible protective device (fuse or recloser in its slow mode) should operate just after MFCTI of the nearest fuse. Similarly, recloser in its fast mode must operate as fast as possible for any fault (temporary/permanent) in the protective zone and reclose the contacts after its pre-defined sequence of operation. If fault persists (i.e., a permanent fault), then the nearest fuse to the fault point should operate just after the contacts of the reclosers are closed.

From the above observations, it can be concluded that the problem of protection coordination of recloser and fuses can be formulated as an optimization problem whose objective is to minimize the sum of operating times of all the fuses and the recloser (in its both modes of operations), while simultaneously maintaining the correct operating sequence with certain minimum time gap between them. Mathematically, this problem can be expressed with the following objective function (OF) as given below;

$$OF = \min \sum_{j=1}^{m} (t_{opR,fm,j} + t_{opR,sm,j} + \sum_{k=1}^{N_j} t_{opF,jk}) \tag{5.5}$$

Subjected to:

$$t_{opF,jk} - t_{opR,fm,j} > MRCTI/2; \;\; \forall j = 1, 2, ..., m; \; \forall k = 1, 2, ..., N_j \tag{5.6}$$

$$t_{opF,j(k+1)} - t_{opF,jk} > MFCTI; \;\; \forall j = 1, 2, ..., m; \; \forall k = 1, 2, ..., N_j \tag{5.7}$$

$$t_{opR,sm,j} - t_{opF,jk} > MRCTI/2; \;\; \forall j = 1, 2, ..., m; \; \forall k = 1, 2, ..., N_j \tag{5.8}$$

$$t_{opR,sm,j} - t_{opR,fm,j} > MRCTI; \;\; \forall j = 1, 2, ..., m \tag{5.9}$$

$$TDS_{min} \leq TDS_{fm} \leq TDS_{max} \tag{5.10}$$

$$TDS_{min} \leq TDS_{sm} \leq TDS_{max} \tag{5.11}$$

In eqn. (5.5), $t_{opR,fm,j}$ and $t_{opR,sm,j}$ are the operating times of the recloser in its fast and slow mode of operation, respectively, for fault at node j; $t_{opF,jk}$ is the operating time of fuse k for fault at node j; m is the total number of nodes; N_j is the total number of fuses in the faulted path from node j to the recloser. In eqns. (5.10) and (5.11), TDS_{min} and TDS_{max} are the minimum and maximum limits, respectively, on TDS of recloser whereas TDS_{fm} and TDS_{sm} are the values of TDS for recloser fast and slow mode of operation, respectively. It is to be noted that half of the MRCTI has been considered as the time gap between the operating times of the recloser (either fast and slow mode of operation) and any fuse.

The operating times of recloser in fast and slow mode of operation are defined as follows [60, 67];

$$t_{opR,fm,j} = TDS_{fm} \times \left[\frac{A}{(I_{FR,j}/PCS)^p - 1} + B \right] \tag{5.12}$$

$$t_{opR,sm,j} = \textit{TDS}_{sm} \times \left[\frac{A}{(I_{FR,j}/\textit{PCS})^p - 1} + B \right] \tag{5.13}$$

In eqns. (5.12) and (5.13), $I_{FR,j}$ is the fault current passing through the recloser for fault at node j and *PCS* is the pick-up current setting for the recloser defined in eqn. (5.3).

The operating times of fuses are defined as follows [67];

$$t_{opF,jk} = exp(a_k \times log(I_{FF,jk}) + b_k) \tag{5.14}$$

In eqn. (5.14), $I_{FF,jk}$ is the fault current passing through fuse k when fault occurs at node j and coefficients a_k and b_k are the characteristic constants of fuse k.

It is to be noted that the solution of this problem gives the optimum values of TDSs ($\textit{TDS}_{fm}$ and $\textit{TDS}_{sm}$) for the recloser and the optimum values of fuse constants a and b for the fuses (a_k and b_k for $k = 1, 2, ..., N$ where N is the total number of fuses).

5.7 Steady-state and short-circuit current calculations

In this work, the maximum fault current passing through all the protective devices have been calculated using bus incidence matrix (Zbus) approach [15]. Under this, bolted three-phase to ground faults at each bus has been applied and the currents passing through each protective devices have been calculated. The pre-fault voltages required in each reconfigurable configuration have been calculated using backward-forward sweep method (BFSM) [140]. Further, the maximum load current passing through each protective device has been calculated using BFSM.

5.8 Proposed approach for solving the optimum recloser-fuse coordination problem

It can easily be observed that the above formulated recloser and fuse coordination problem has twice continuously differentiable objective function and constraints in term of its control variables ($\textit{TDS}_{fm}$, $\textit{TDS}_{sm}$, a_k and b_k for all $k \in 1, 2, ..., N$). This property allows the application of any mathematical optimization approach to solve this problem to obtain the optimum settings. So, in this work, interior point method (IPM) has been utilized to obtain the optimum coordination results, which has been implemented using MATLAB Optimization Toolbox [74].

Overall, the following procedure has been adopted. Initially, steady state load flow analysis using BFSM has been performed to calculate various load currents passing through each protective device [140]. Subsequently, bolted three-phase-to-ground short circuit analysis using bus-incidence matrix (Zbus) approach has been carried out to calculate the maximum fault currents passing through each protective device of the system [15] and PCS of the recloser is calculated using eqn. (5.3). After that, IPM is applied to solve the formulated optimization problem to obtain the optimum values of TDSs of the recloser and fuse constants for all the fuses. The steps of the solution procedure are as follows:

1. Perform steady-state and short-circuit analysis.

2. Calculate the fault currents to be interrupted by the recloser and the fuses caused by faults on various nodes.

3. Set PCS of recloser using eqn. (5.3).

4. Apply IPM to solve the formulated problem to obtain the optimum values of recloser settings (TDSs) and fuse constants (a and b for all the fuses).

A flowchart with detailed information of the proposed overall approach used in this chapter is shown in Figure 5.1.

5.9 Results and discussion

The effectiveness of the proposed methodology has been investigated on two radial distribution systems. These two systems are IEEE 33 and 69-bus radial distribution systems. The detailed information about these two systems can be obtained in [72, 141–145].

The following points have been considered while solving the protection coordination problem of recloser and fuses [138]:

1. Two fast and two slow modes of operation of the recloser have been considered.

2. The optimum settings of TDSs have been obtained for the second fast mode and the first slow mode of operation of the recloser while maintaining the requirement of MFCTI/MRCTI between the operation of the recloser in these two modes.

3. The operating times of all the fuses have been considered within these two operating times of the recloser separated by MFCTI from each other.

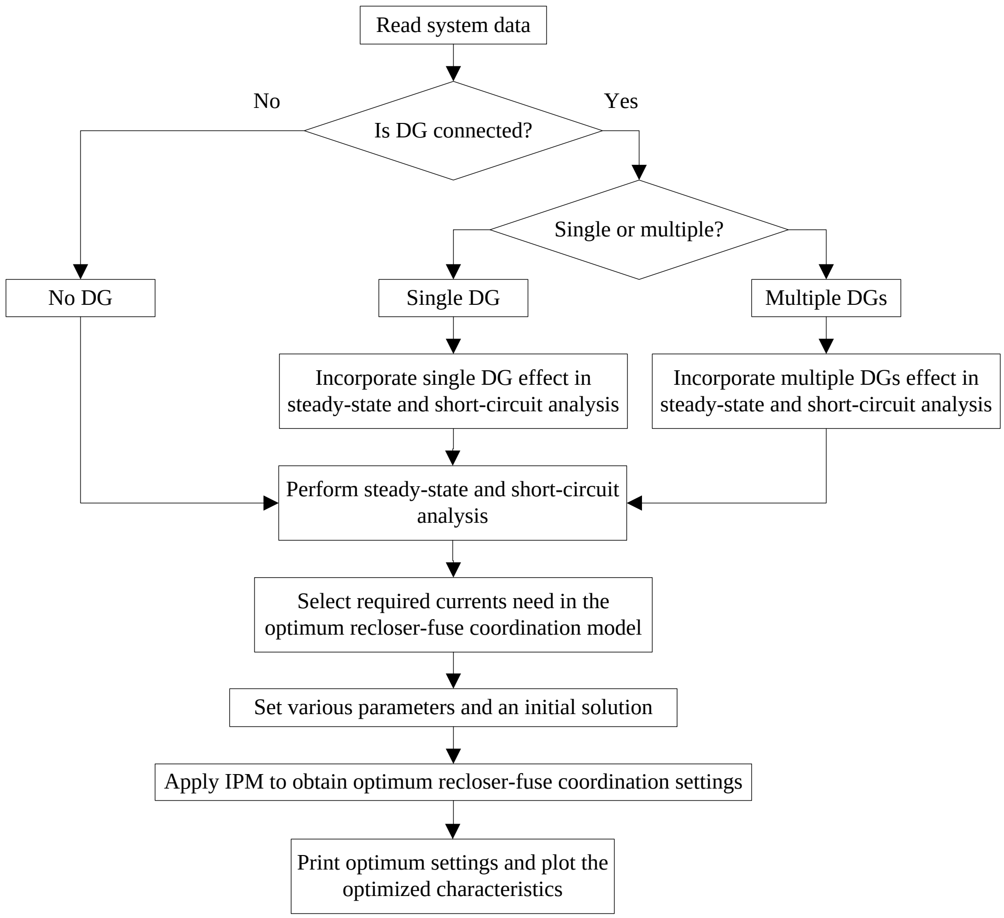

Figure 5.1: Flowchart of the overall approach for recloser-fuse coordination.

4. TDSs for the first fast mode and the second slow mode of operation of the recloser have been obtained depending on the optimum settings of TDSs for the second fast mode and the first slow mode of operation of the recloser.

5. For the first fast mode of operation of recloser, TDS has been considered as one step less than the optimum value of TDS obtained for the fast mode of operation whereas, for the second slow mode of operation of recloser, TDS has been considered as one step higher than the optimum value of TDS obtained for the slow mode of operation.

The values of A, B and p for recloser have been considered as 28.2, 0.1217 and 2, respectively, [67]. The minimum and the maximum value of TDS for optimum coordination have been considered as 0.5 and 10, respectively, [60]. The MFCTI for the fuses has been taken as 0.2 seconds and MRCTI between the second fast mode and the first slow mode of operation of the recloser has been taken as 0.5 seconds whereas, overloading factor for recloser has been considered as 1.25 [60]. The value of fuse constant a for all the fuses has been considered to be the same in any particular network condition. This condition is practically acceptable because all fuses in the system should be of the same type [67].

5.9.1 Results on the IEEE 33-bus system

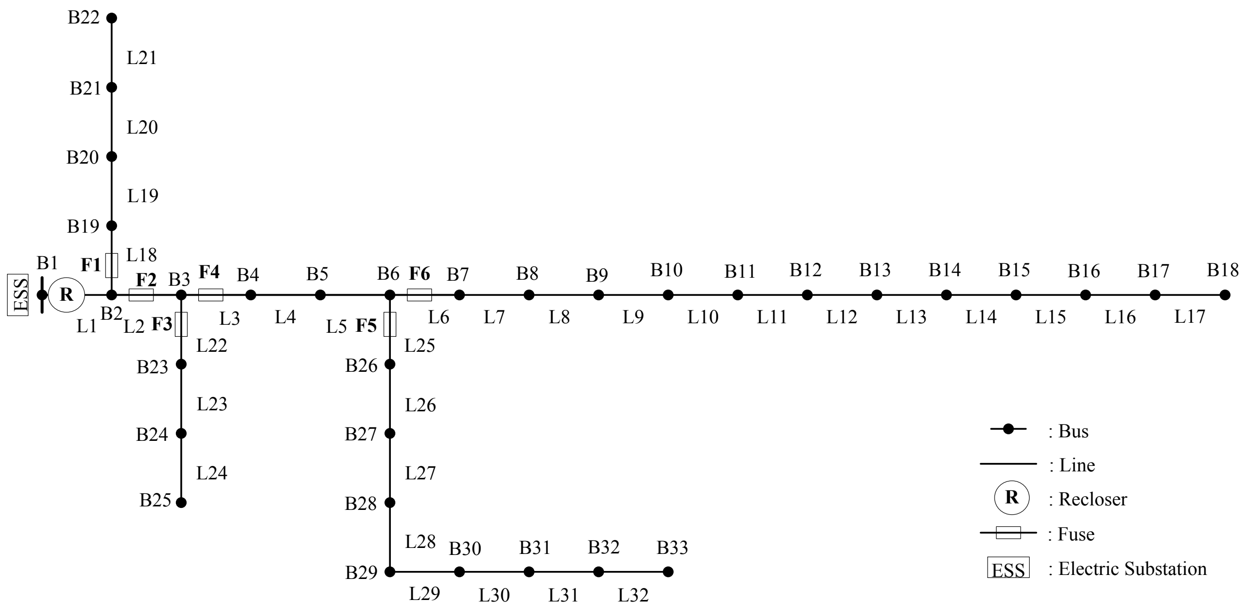

Figure 5.2: IEEE 33-bus radial distribution system network.

Figure 5.2 shows the single-line diagram of the IEEE 33-bus radial distribution system. This system has 32 branches and is energised at bus 1 by a substation with a short-circuit capacity of 100 MVA. The detailed information about the system is available in [146]. For providing complete protection using recloser and fuses, one recloser and six fuses are required, which are shown in Figure 5.2. The recloser is placed close to the substation which provides protection to the entire network from any temporary fault in the system and also provides overall backup protection for any permanent fault in the system. Fuses have been placed, downstream to the recloser, on each branch after any node, to provide primary protection against any permanent fault in that particular branch. It is to be noted that placement of fuse at each branch rather than at each lateral provides complete protection against any permanent fault in the main feeder (B1, B2, ..., B18).

With six fuses and two modes of operation of the recloser (fast and slow), there are a total of seven correct operating sequences of the protecting devices for a fault occurring anywhere in the system. These operating sequences are given in Table 5.1. The correct sequence of operation of protective devices will be decided by the location of the fault in the network. As an example, for fault at node 10, the correct operating sequence of the protective devices is given by the serial no. 7 in Table 5.1, where recloser in its fast mode (R_{FM}) will operate first. If the fault is a permanent fault, then fuse no. 6 (F6) should operate to isolate the fault. In case F6 fails to operate, fuse no. 4 (F4), which acts as the backup protection for F6, should operate. If F4 also fails, then its backup protection device (F2) should operate. Finally, if all these devices fail to clear the fault then the recloser in its slow mode of operation (R_{SM}) will operate to isolate the whole network. From Table 5.1, it is observed that F2 provides backup protection for F3 and F4 whereas F4 provides backup protection for F5 and F6. Further, it is also observed that F1, F3, F5 and F6 work only as a primary protection device for any permanent fault in their respective protection zones.

Table 5.1: Correct operating sequences of the various protective devices for a fault anywhere in the IEEE 33-bus system

Sl. No.	Correct operating sequences
1	$R_{FM} - R_{SM}$
2	$R_{FM} - F1 - R_{SM}$
3	$R_{FM} - F2 - R_{SM}$
4	$R_{FM} - F3 - F2 - R_{SM}$
5	$R_{FM} - F4 - F2 - R_{SM}$
6	$R_{FM} - F5 - F4 - F2 - R_{SM}$
7	$R_{FM} - F6 - F4 - F2 - R_{SM}$

5.9.1.1 Optimum recloser settings and fuse constants without considering the presence of DG in the IEEE 33-bus system

Table 5.2 gives the values of the maximum fault current passing through each protective device for faults on various nodes of the system shown in Figure 5.2. It is to be noted that the recloser has to operate for the maximum fault currents in both fast and slow mode of operation. It also has to maintain a certain MRCTI between its two operating modes as well as some additional margin i.e., MFCTI with downstream fuses responsible for clearing any permanent fault. Thus, for the same fault current recloser has to work either as the primary protection or the backup protection (in case the fuses fail to operate) while maintaining sufficient coordination time interval. Further, there are total 32 operating sequences (due to 32 possible fault location for 32 feeder system) of the protective devices under which recloser-fuse and fuse-fuse coordinations need to be maintained. It is to be noted that the number of the actual operating sequence is only 7, however, because of different values of fault currents, there is a total of 32 cases of operation for faults on all the nodes. Further, it is to be noted that symbol '$-$' in various tables represent that the value of fault current for that particular fuse is of no interest (because the current does not pass through them).

Table 5.2: Maximum fault currents passing through various protective devices for faults on different nodes without a DG in the IEEE 33-bus system

	Fault currents passing through various protective devices (A)						
Faulted node	Recloser	Fuse 1	Fuse 2	Fuse 3	Fuse 4	Fuse 5	Fuse 6
2	4410	-	-	-	-	-	-
3	3613	-	3612	-	-	-	-
4	3111	-	3109	-	3108	-	-
5	2683	-	2681	-	2679	-	-
6	1894	-	1891	-	1889	-	-
7	1620	-	1616	-	1614	-	1609
8	1417	-	1413	-	1410	-	1405
9	1134	-	1130	-	1127	-	1120
10	944	-	939	-	936	-	928
11	921	-	917	-	914	-	905
12	882	-	877	-	874	-	865
13	720	-	715	-	712	-	703
14	663	-	658	-	655	-	645
15	621	-	616	-	613	-	603
16	579	-	575	-	571	-	561
17	504	-	499	-	496	-	486
18	478	-	473	-	469	-	459
19	3994	3993	-	-	-	-	-
20	2012	2009	-	-	-	-	-
21	1718	1714	-	-	-	-	-
22	1350	1346	-	-	-	-	-
23	2937	-	2935	2934	-	-	-
24	2038	-	2035	2033	-	-	-
25	1556	-	1553	1550	-	-	-
26	1793	-	1790	-	1787	1783	-
27	1665	-	1662	-	1659	1654	-
28	1240	-	1236	-	1233	1227	-
29	1038	-	1034	-	1030	1023	-
30	959	-	955	-	952	944	-
31	813	-	809	-	805	797	-
32	773	-	768	-	765	756	-
33	728	-	724	-	721	712	-
I_{Lmax}	210	18	187	48	135	65	58

The optimum settings of TDSs for recloser and constants for all the fuses obtained using the proposed approach for the network without considering DG are given in Table 5.3. The corresponding time-current characteristic (TCC) curves of the recloser and the fuses are shown in Figure 5.3.

Table 5.3: Optimum values of TDSs of the recloser and constants of all fuses without a DG in the IEEE 33-bus system

Recloser settings			Fuse settings						
Modes	PCS (A)	TDS	Constants	F1	F2	F3	F4	F5	F6
Fast	275	0.5000	*a*	-1.5941	-1.5941	-1.5941	-1.5941	-1.5941	-1.5941
Slow	275	3.4455	*b*	12.2461	12.1565	11.8965	11.9565	11.5037	11.7565

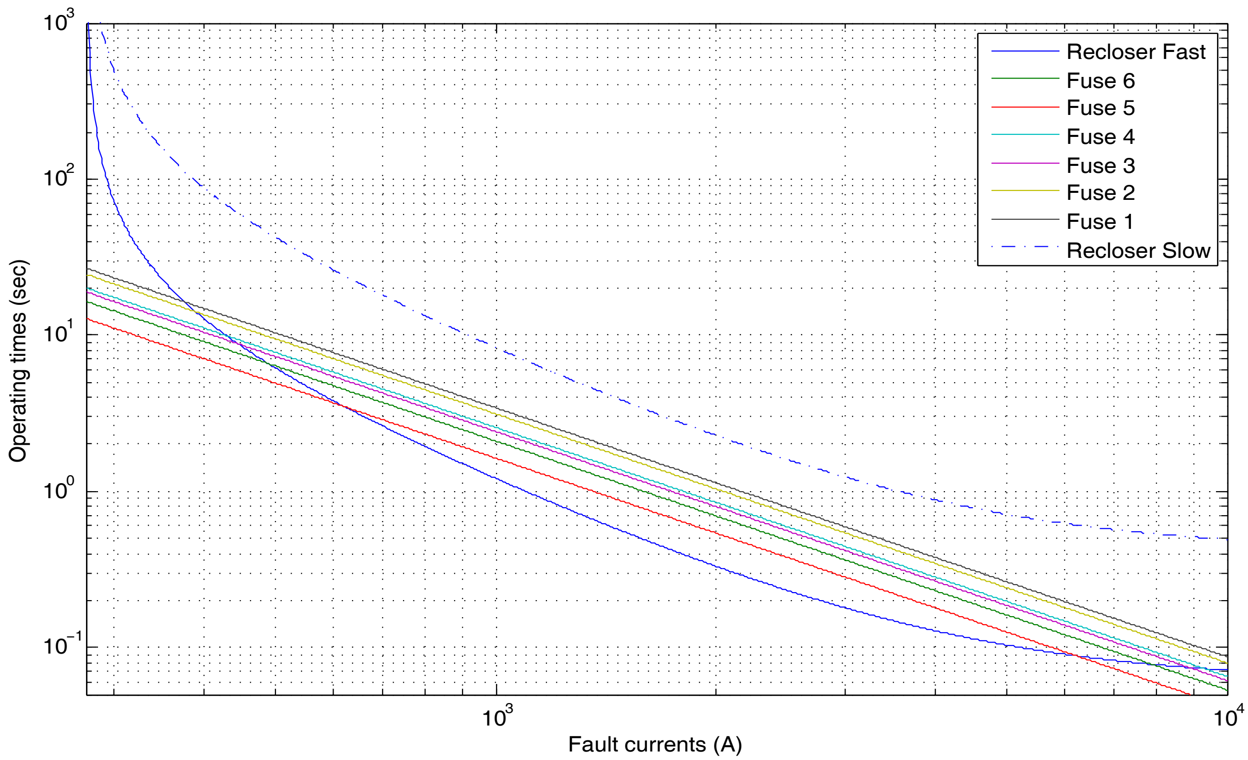

Figure 5.3: TCC curves of the protective devices for the optimum coordination without a DG in the IEEE 33-bus system.

From Table 5.3, it is observed that the value of constant b for F4 is higher than that for F5 and F6, while that for F2 is higher than those for F3 and F4. From eqn. 5.2, higher value of constant b results into higher operating time and therefore, F2 provides backup protection to F3 and F4 while F4 provides backup protection to F5 and F6. From Figure 5.3, it is observed that the optimum coordinated characteristic curves of fuses lie well inside the operating times of recloser fast and slow modes of operation. Further, the operating sequences and MFCTI are correctly maintained among the fuses.

5.9.1.2 Optimum recloser settings and fuse constants in the presence of a single DG in the IEEE 33-bus system

In this case, a single DG at bus 6 has been considered. The DG has a short circuit capacity of 25 MVA while its real power output and operating power factor have been taken as 2.48 MW and unity, respectively, [147–149].

Table 5.4 gives the values of the maximum fault current passing through each protective device for faults on various nodes in this case. From Tables 5.2 and 5.4, it is observed that in the presence of DG, the fault currents passing through F1, F3, F5 and F6 increase for faults anywhere in the system. However, depending on the location of the fault, the fault current through recloser, F2 and F4 either increases or decreases (as compared to the results of Table 5.2). If the settings of recloser and fuses obtained in the previous subsection are adopted, then such variation in the fault currents due to the presence of DG in the network causes incorrect sequence of operation of the protective devices (recloser and fuses) resulting in their miscoordination. It can also be observed from Table 5.2, Table 5.4 and Figure 5.2 that the current through F2 reverses for fault at bus 2, 19, 20, 21 and 22 and that through F4 reverses for faults at bus 2, 3, 19, 20, 21, 22, 23, 24 and 25. These reversals of current directions take place because of the presence of DG at bus 6.

Through application of the proposed methodologies, the optimum values of TDSs of the recloser and constants for all the fuses have been calculated and are given in Table 5.5. The resulting time-current characteristic curves of the recloser and the fuses are shown in Figure 5.4.

From Table 5.5, it is observed that the fuse constant b for F4 is higher than that for F5 and F6, while the constant b for F2 is higher than those for F3 and F4. Thus, F2 provides backup protection to F3 and F4 while F4 provides backup protection to F5 and F6. Further, from Figure 5.4, it is observed that the optimum coordinated characteristic curves of the fuses lie well inside the operating times of recloser fast and slow modes of operation and also all the operating sequences given in Table 5.1 are correctly maintained.

Table 5.4: Maximum fault currents passing through various protective devices for faults on different nodes in the presence of single DG at bus 6 in the IEEE 33-bus system

Faulted node	Fault currents passing through various protective devices (A)						
	Recloser	Fuse 1	Fuse 2	Fuse 3	Fuse 4	Fuse 5	Fuse 6
2	4417	-	932	-	932	-	-
3	3648	-	3647	-	971	-	-
4	3161	-	3159	-	3158	-	-
5	2743	-	2741	-	2739	-	-
6	1964	-	1961	-	1959	-	-
7	1551	-	1547	-	1544	-	2340
8	1322	-	1320	-	1317	-	1993
9	993	-	996	-	992	-	1499
10	789	-	795	-	792	-	1195
11	767	-	773	-	769	-	1161
12	727	-	734	-	731	-	1102
13	568	-	579	-	576	-	867
14	514	-	527	-	523	-	789
15	475	-	490	-	486	-	733
16	436	-	454	-	450	-	678
17	369	-	390	-	386	-	582
18	346	-	369	-	365	-	551
19	3907	4715	824	-	824	-	-
20	1783	2148	375	-	375	-	-
21	1507	1814	316	-	316	-	-
22	1170	1406	245	-	245	-	-
23	2828	-	2825	3573	752	-	-
24	1842	-	1838	2323	488	-	-
25	1363	-	1359	1713	359	-	-
26	1829	-	1825	-	1822	2764	-
27	1660	-	1656	-	1654	2507	-
28	1119	-	1117	-	1114	1683	-
29	895	-	894	-	890	1342	-
30	813	-	813	-	810	1219	-
31	659	-	667	-	663	1000	-
32	619	-	629	-	626	943	-
33	573	-	587	-	584	881	-
I_{Lmax}	124	18	106	48	0	63	56

Table 5.5: Optimum values of TDSs of the recloser and constants of all fuses in the presence of a single DG in the IEEE 33-bus system

Recloser settings			Fuse settings						
Modes	PCS (A)	TDS	Constants	F1	F2	F3	F4	F5	F6
Fast	275	0.5000	a	-2.1271	-2.1271	-2.1271	-2.1271	-2.1271	-2.1271
Slow	275	4.4347	b	17.0272	17.0241	16.5934	16.8241	16.4050	16.6241

5.9.1.3 Optimum recloser settings and fuse constants in the presence of multiple DGs in the IEEE 33-bus system

In this case, three DGs at bus 17, 18 and 33 with real power outputs of 0.107 MW, 0.5724 MW and 1.0462 MW, respectively, at unity power factor have been considered [150]. The short-circuit

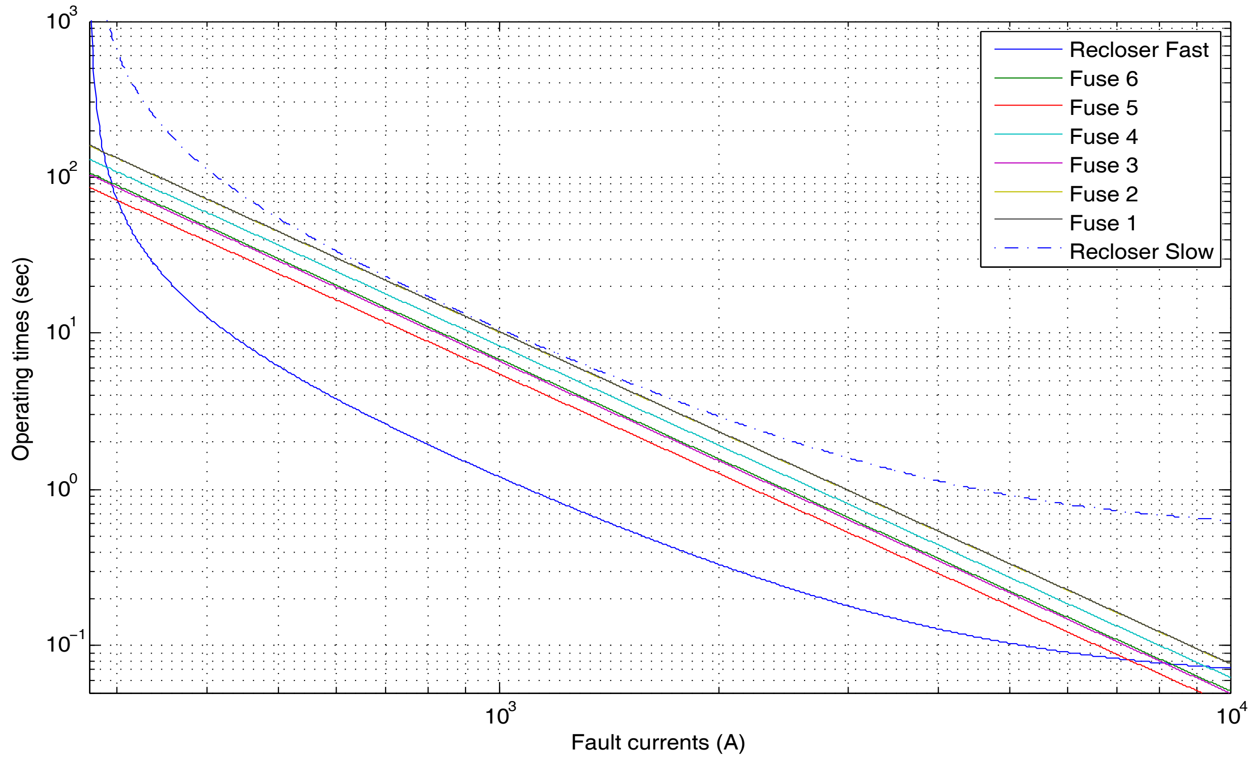

Figure 5.4: TCC curves of the protective devices for the optimum coordination in the presence of a single DG in the IEEE 33-bus system.

capacities of these three DGs have been considered as 2 MVA, 6 MVA and 10 MVA, respectively.

Table 5.6 gives the values of the maximum fault current passing through each protective device for faults on various nodes in this case. From Tables 5.2 and 5.6, it is observed that the fault currents passing through the recloser and fuses change quite randomly (increase for some faults and decrease for some other faults). Further, from Table 5.2, Table 5.6 and Figure 5.2 it can be seen that for some faults, the direction of fault currents through F2, F4, F5 and F6 reverses. Such pattern of fault currents in the network causes incorrect sequence of operation of the protective devices (recloser and fuses) resulting into miscoordination, if the settings of recloser and fuses obtained in the previous subsections are adopted.

The optimum settings of TDSs of recloser and constants for all the fuses are given in Table 5.7 for this case. From this table it is again confirmed that F4 provides backup protection for F5 and F6 while backup protection for F3 and F4 is provided by F2. The resulting time-current characteristic curves of recloser and fuses in the presence of multiple DGs are shown in Figure 5.5 which indicates that all the operating sequences given in Table 5.1 are correctly maintained.

Table 5.6: Maximum fault currents passing through various protective devices for faults on different nodes in the presence of multiple DGs in the IEEE 33-bus system

	Fault currents passing through various protective devices (A)						
Faulted node	Recloser	Fuse 1	Fuse 2	Fuse 3	Fuse 4	Fuse 5	Fuse 6
2	4415	-	540	-	540	318	223
3	3638	-	3637	-	553	325	228
4	3147	-	3145	-	3144	331	233
5	2726	-	2724	-	2722	338	238
6	1944	-	1941	-	1939	362	254
7	1619	-	1616	-	1613	301	1889
8	1402	-	1400	-	1397	260	1634
9	1098	-	1100	-	1097	203	1279
10	901	-	906	-	902	165	1048
11	878	-	883	-	880	161	1022
12	837	-	844	-	840	153	974
13	673	-	684	-	680	122	784
14	616	-	629	-	625	112	719
15	574	-	588	-	584	104	671
16	532	-	548	-	545	96	623
17	456	-	476	-	472	82	537
18	427	-	449	-	445	76	505
19	3941	4399	482	-	482	283	199
20	1872	2086	228	-	228	134	94
21	1589	1770	194	-	194	114	80
22	1240	1379	151	-	151	88	62
23	2871	-	2868	3302	436	256	180
24	1917	-	1914	2202	290	171	120
25	1437	-	1433	1646	216	127	89
26	1832	-	1829	-	1826	2052	240
27	1694	-	1691	-	1688	1894	221
28	1236	-	1234	-	1231	1378	161
29	1028	-	1026	-	1023	1142	133
30	947	-	947	-	943	1052	122
31	793	-	800	-	796	885	102
32	752	-	760	-	757	839	97
33	704	-	716	-	712	789	90
I_{Lmax}	144	18	123	48	80	0	31

Table 5.7: Optimum values of TDSs of the recloser and constants of all fuses in the presence of multiple DGs in the IEEE 33-bus system

Recloser settings			Fuse settings						
Modes	PCS (A)	TDS	Constants	F1	F2	F3	F4	F5	F6
Fast	275	0.5000	a	-1.8370	-1.8370	-1.8370	-1.8370	-1.8370	-1.8370
Slow	275	3.6196	b	14.4431	14.2664	14.0664	14.0664	13.5575	13.8664

5.9.1.4 Common optimum recloser settings and fuse constants without and with presence of DG in the IEEE 33-bus system

In the above three case studies, it is observed that recloser and fuses settings are different in the same network depending on integration and location of DGs. Thus, the settings obtained in one

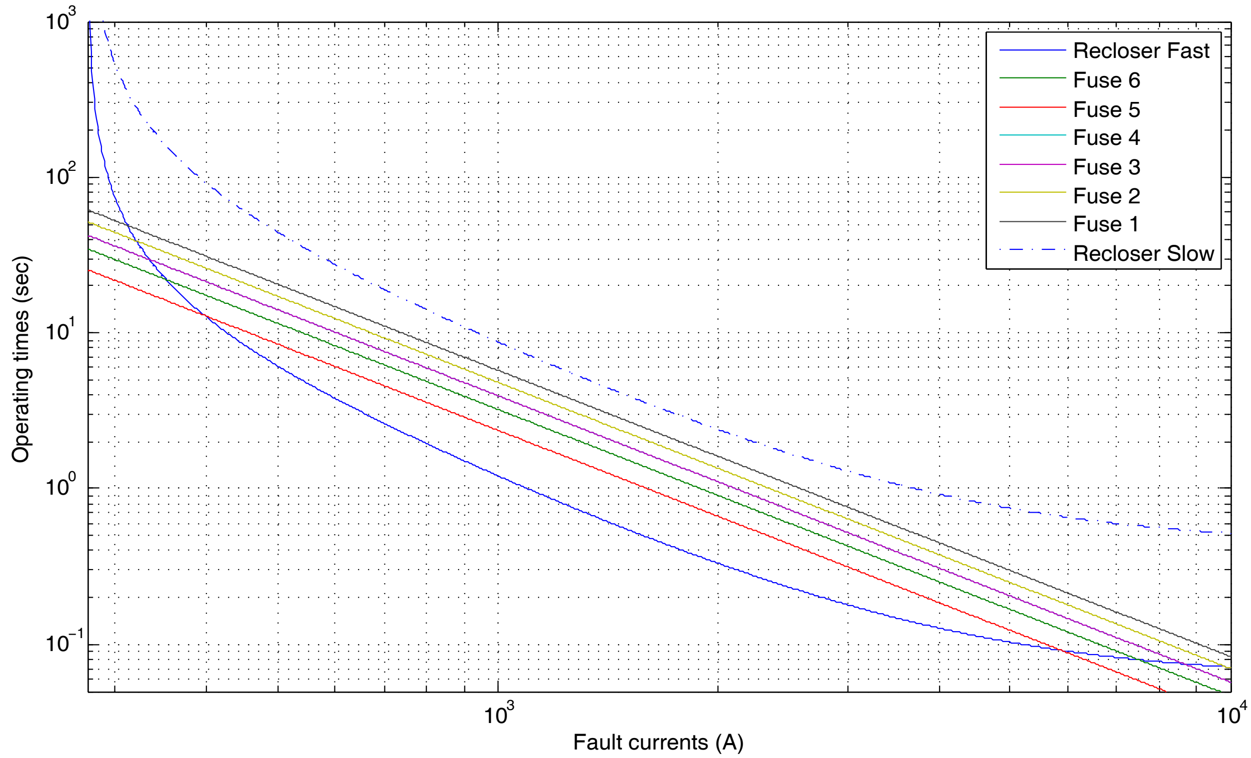

Figure 5.5: TCC curves of the protective devices for the optimum coordination in the presence of multiple DGs in the IEEE 33-bus system.

particular case cannot coordinate properly in another case. So, it is necessary to obtain appropriate settings of recloser and fuses so that they can coordination properly in all the three above cases.

To obtain common optimum settings of recloser and fuses, the fault currents in the above three situations have been considered together and then the proposed approach has been applied. The common optimum settings of TDSs of the recloser and constants for all the fuses obtained are given in Table 5.8. As observed from Table 5.8, in this case also, F4 provides backup protection to F5 and F6 while backup protection for F3 and F4 is provides by F2. Moreover, the correct operating sequences are maintained while satisfying the MFCTI requirements between the fuses. The corresponding time-current characteristic curves of recloser and fuses are shown in Figure 5.6.

In the above four sub-sections, four different cases of recloser-fuse coordination have been studied. A comparative assessment of these four coordination results is provided later in Section 5.10.

Table 5.8: Common optimum values of TDSs of the recloser and constants of all fuses in the IEEE 33-bus system

Recloser settings			Fuse settings						
Modes	PCS (A)	TDS	Constants	F1	F2	F3	F4	F5	F6
Fast	275	0.5000	a	-2.1301	-2.1301	-2.1301	-2.1301	-2.1301	-2.1301
Slow	275	4.4540	b	17.0527	17.0431	16.6180	16.8431	16.4288	16.6431

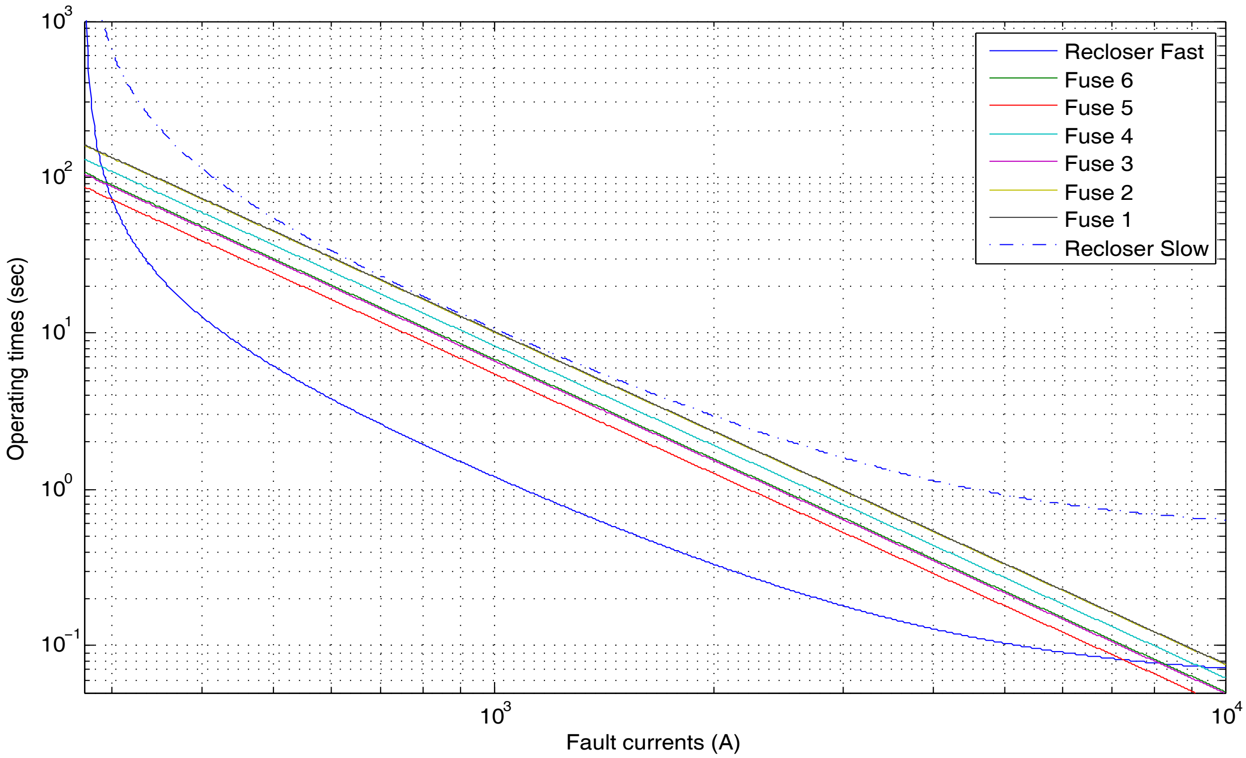

Figure 5.6: TCC curves of the protective devices for the common optimum coordination results obtained in the IEEE 33-bus system.

5.9.2 Results on the IEEE 69-bus system

Figure 5.7 shows the single-line diagram of the IEEE 69-bus radial distribution system. This system has 68 branches and is energised at bus 1 by a substation with a short-circuit capacity of 100 MVA. The detailed information about the system is available in [151]. For providing complete protection using recloser and fuses, one recloser and 13 fuses are required, which are shown in Figure 5.7. With 13 fuses and two modes of operation of the recloser (fast and slow), there are a total of 14 correct operating sequences of the protecting devices for a fault occurring anywhere in the system. These operating sequences are given in Table 5.9.

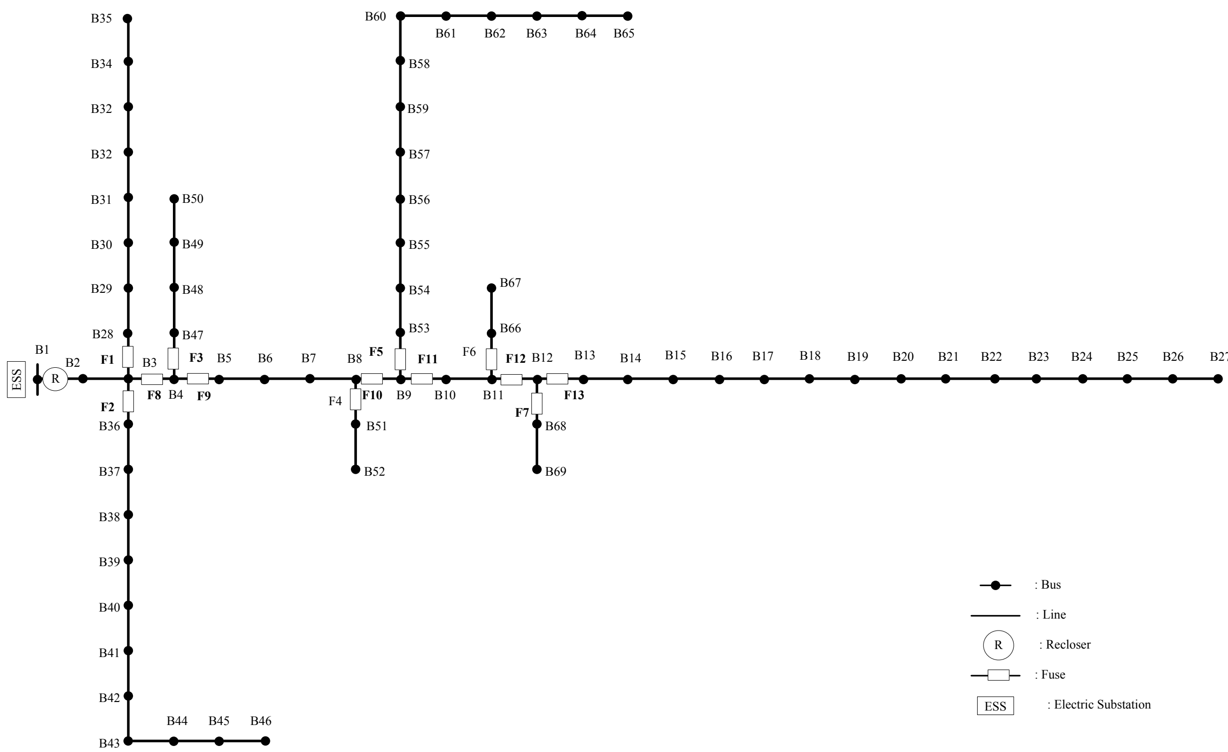

Figure 5.7: IEEE 69-bus radial distribution system network.

It is to be noted that only one of the sequences of the protective devices is responsible to operate for fault at anywhere in the network. As an example, for fault at node 60, the correct operating sequence of the protective devices is given by the serial no. 9 in Table 5.9 where recloser in its fast mode (R_{FM}) will operate first. If the fault is a permanent fault, then fuse no. 5 (F5) should operate to isolate the fault. In case F5 fails to operate, fuse no. 10 (F10), which acts as the backup protection for F5, should operate. Similarly, if F10 fails, then its backup fuse no. 9 (F9) should operate. Even if F9 fails, then its backup fuse no. 8 (F8) should operate. Finally, if all these devices fail to clear the fault then the recloser in its slow mode of operation (R_{SM}) will operate to isolate the whole network. From Table 5.9, it is observed that fuse 8 provides backup protection for fuse 3 and fuse 9, fuse 9 provides backup for fuse 4 and fuse 10, fuse 10 provides backup for fuse 5 and fuse 11, fuse 11 provides backup for fuse 6 and fuse 12, whereas fuse 12 provides backup protection for fuse 7 and fuse 13, respectively. Further, it is also observed that fuses 1 to 7 and fuse 13 work only as a primary protection device for any permanent fault in their respective protection zones.

Table 5.9: Correct operating sequences of the various protective devices for a fault anywhere in the IEEE 69-bus system

Sl. No.	Correct operating sequences
1	$R_{FM} - R_{SM}$
2	$R_{FM} - F1 - R_{SM}$
3	$R_{FM} - F2 - R_{SM}$
4	$R_{FM} - F8 - R_{SM}$
5	$R_{FM} - F3 - F8 - R_{SM}$
6	$R_{FM} - F9 - F8 - R_{SM}$
7	$R_{FM} - F4 - F9 - F8 - R_{SM}$
8	$R_{FM} - F10 - F9 - F8 - R_{SM}$
9	$R_{FM} - F5 - F10 - F9 - F8 - R_{SM}$
10	$R_{FM} - F11 - F10 - F9 - F8 - R_{SM}$
11	$R_{FM} - F6 - F11 - F10 - F9 - F8 - R_{SM}$
12	$R_{FM} - F12 - F11 - F10 - F9 - F8 - R_{SM}$
13	$R_{FM} - F7 - F12 - F11 - F10 - F9 - F8 - R_{SM}$
14	$R_{FM} - F13 - F12 - F11 - F10 - F9 - F8 - R_{SM}$

5.9.2.1 Optimum recloser settings and fuse constants without considering the presence of DG in the IEEE 69-bus system

Table 5.10 gives the values of the maximum fault current passing through each protective device for faults on various nodes of the system shown in Figure 5.7. It is to be noted that there are total 68 cases of operation (due to 68 possible fault location for 68 feeder system) of the protective devices under which recloser-fuse, fuse-fuse and fuse-recloser coordinations need to be maintained. Although, the number of the actual operating sequence is only 14, because of different values of fault currents, there is a total of 68 cases of operation for faults on all the nodes.

Table 5.10: Maximum fault currents passing through various protective devices for faults on different nodes without a DG in the IEEE 69-bus system

Faulted node	Fault currents passing through various protective devices (A)													
	Recloser	Fuse 1	Fuse 2	Fuse 3	Fuse 4	Fuse 5	Fuse 6	Fuse 7	Fuse 8	Fuse 9	Fuse 10	Fuse 11	Fuse 12	Fuse 13
2	4557	-	-	-	-	-	-	-	-	-	-	-	-	-
3	4553	-	-	-	-	-	-	-	-	-	-	-	-	-
4	4543	-	-	-	-	-	-	-	4543	-	-	-	-	-
5	4457	-	-	-	-	-	-	-	4457	4457	-	-	-	-
6	3877	-	-	-	-	-	-	-	3877	3877	-	-	-	-
7	3316	-	-	-	-	-	-	-	3316	3316	-	-	-	-
8	3193	-	-	-	-	-	-	-	3193	3193	-	-	-	-
9	3130	-	-	-	-	-	-	-	3130	3130	3130	-	-	-
10	2429	-	-	-	-	-	-	-	2429	2429	2427	2426	-	-
11	2298	-	-	-	-	-	-	-	2298	2298	2296	2295	-	-
12	1897	-	-	-	-	-	-	-	1897	1897	1894	1893	1891	-
13	1501	-	-	-	-	-	-	-	1501	1501	1497	1496	1492	1490
14	1232	-	-	-	-	-	-	-	1232	1232	1227	1226	1221	1218
15	1040	-	-	-	-	-	-	-	1040	1040	1035	1034	1028	1024

Continued on next page

Table 5.10 – continued from previous page

	Fault currents passing through various protective devices (A)													
Faulted node	Recloser	Fuse 1	Fuse 2	Fuse 3	Fuse 4	Fuse 5	Fuse 6	Fuse 7	Fuse 8	Fuse 9	Fuse 10	Fuse 11	Fuse 12	Fuse 13
16	1012	-	-	-	-	-	-	-	1012	1012	1007	1005	999	995
17	959	-	-	-	-	-	-	-	959	959	954	953	947	942
18	959	-	-	-	-	-	-	-	959	959	954	953	947	942
19	919	-	-	-	-	-	-	-	919	919	914	913	906	902
20	895	-	-	-	-	-	-	-	895	895	890	888	882	877
21	858	-	-	-	-	-	-	-	858	858	852	851	844	839
22	857	-	-	-	-	-	-	-	857	857	851	850	843	839
23	841	-	-	-	-	-	-	-	841	841	836	834	828	823
24	809	-	-	-	-	-	-	-	809	809	804	802	795	790
25	747	-	-	-	-	-	-	-	747	747	742	740	733	728
26	725	-	-	-	-	-	-	-	725	725	719	718	711	705
27	712	-	-	-	-	-	-	-	712	712	707	705	698	693
28	4523	4523	-	-	-	-	-	-	-	-	-	-	-	-
29	4120	4120	-	-	-	-	-	-	-	-	-	-	-	-
30	4076	4076	-	-	-	-	-	-	-	-	-	-	-	-
31	4454	4454	-	-	-	-	-	-	-	-	-	-	-	-
32	4133	4133	-	-	-	-	-	-	-	-	-	-	-	-
33	3520	3520	-	-	-	-	-	-	-	-	-	-	-	-
34	2636	2636	-	-	-	-	-	-	-	-	-	-	-	-
35	2843	2843	-	-	-	-	-	-	-	-	-	-	-	-
36	4523	-	4523	-	-	-	-	-	-	-	-	-	-	-
37	4120	-	4120	-	-	-	-	-	-	-	-	-	-	-
38	3838	-	3838	-	-	-	-	-	-	-	-	-	-	-
39	3762	-	3762	-	-	-	-	-	-	-	-	-	-	-
40	3758	-	3758	-	-	-	-	-	-	-	-	-	-	-
41	2488	-	2488	-	-	-	-	-	-	-	-	-	-	-
42	2160	-	2160	-	-	-	-	-	-	-	-	-	-	-
43	2123	-	2123	-	-	-	-	-	-	-	-	-	-	-
44	2114	-	2114	-	-	-	-	-	-	-	-	-	-	-
45	2016	-	2016	-	-	-	-	-	-	-	-	-	-	-
46	2015	-	2015	-	-	-	-	-	-	-	-	-	-	-
47	4519	-	-	4519	-	-	-	-	4519	-	-	-	-	-
48	4009	-	-	4009	-	-	-	-	4009	-	-	-	-	-
49	2846	-	-	2846	-	-	-	-	2846	-	-	-	-	-
50	2629	-	-	2629	-	-	-	-	2629	-	-	-	-	-
51	3082	-	-	-	3082	-	-	-	3082	3082	-	-	-	-
52	2783	-	-	-	2781	-	-	-	2783	2783	-	-	-	-
53	2925	-	-	-	-	2924	-	-	2925	2925	2924	-	-	-
54	2708	-	-	-	-	2706	-	-	2708	2708	2706	-	-	-
55	2444	-	-	-	-	2441	-	-	2444	2444	2442	-	-	-
56	2222	-	-	-	-	2219	-	-	2222	2222	2219	-	-	-
57	1487	-	-	-	-	1482	-	-	1487	1487	1483	-	-	-
58	1263	-	-	-	-	1258	-	-	1263	1263	1259	-	-	-
59	1191	-	-	-	-	1186	-	-	1191	1191	1187	-	-	-
60	1112	-	-	-	-	1106	-	-	1112	1112	1107	-	-	-
61	1011	-	-	-	-	1005	-	-	1011	1011	1006	-	-	-
62	996	-	-	-	-	990	-	-	996	996	991	-	-	-
63	975	-	-	-	-	969	-	-	975	975	970	-	-	-
64	883	-	-	-	-	876	-	-	883	883	878	-	-	-
65	781	-	-	-	-	775	-	-	781	781	776	-	-	-
66	2176	-	-	-	-	-	2172	-	2176	2176	2173	2173	-	-
67	2173	-	-	-	-	-	2169	-	2173	2173	2170	2170	-	-
68	1600	-	-	-	-	-	-	1590	1600	1600	1596	1595	1591	-
69	1598	-	-	-	-	-	-	1588	1598	1598	1594	1593	1589	-
I_{Lmax}	224	5	10	48	3	105	2	3	208	160	151	44	32	20

The optimum settings of TDSs for recloser and constants for all the fuses obtained using the proposed approach for the network without considering DG for the IEEE 69-bus radial system are given in Table 5.11. The time-current characteristic curves of the recloser and the fuses using these optimum coordination results are shown in Figure 5.8.

Table 5.11: Optimum values of TDSs of the recloser and constants of all fuses without a DG in the IEEE 69-bus system

Recloser settings			Fuse settings													
Modes	PCS (A)	TDS	Constants	F1	F2	F3	F4	F5	F6	F7	F8	F9	F10	F11	F12	F13
Fast	300	0.5000	*a*	-1.308	-1.308	-1.308	-1.308	-1.308	-1.308	-1.308	-1.308	-1.308	-1.308	-1.308	-1.308	-1.308
Slow	300	7.4544	*b*	10.6854	10.6854	10.5356	9.9898	9.7671	9.4228	9.2488	10.7356	10.5204	10.3204	10.1204	9.9204	9.7204

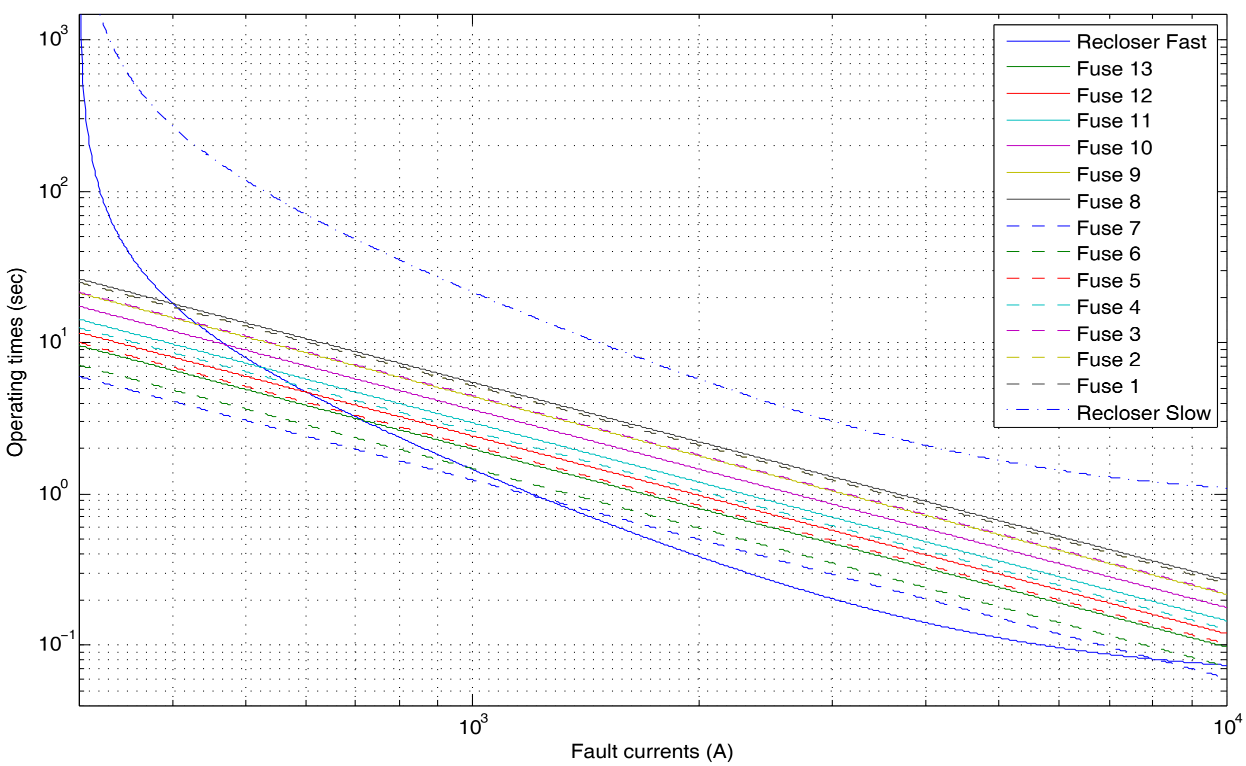

Figure 5.8: TCC curves of the protective devices for the optimum coordination without a DG in the IEEE 69-bus system.

From Table 5.11, it is observed that the value of constant b for F12 is higher than that for F7 and F13. Similarly, the fuse constant b for F11 is higher than that for F6 and F12, the fuse constant

b for F10 is higher than that for F5 and F11, the fuse constant b for F9 is higher than that for F4 and F10 while that for F8 is higher than those for F3 and F9. From eqn. (5.2), higher value of constant b results into higher operating time and therefore, F8 provides backup protection to F3 and F9. Similarly, F9 provides backup protection to F4 and F10, F10 provides backup protection to F5 and F11, F11 provides backup protection to F6 and F12 while F12 provides backup protection to F7 and F13. From Figure 5.8, it is observed that the optimum coordinated characteristic curves of fuses lie well inside the operating times of recloser fast and slow modes of operation. Further, the operating sequences and MFCTI are correctly maintained among the fuses.

5.9.2.2 Optimum recloser settings and fuse constants in the presence of a single DG in the IEEE 69-bus system

In this case, a single DG at bus 61 has been considered as suggested in [72]. The DG has a short circuit capacity of 20 MVA while its real power output and operating power factor have been taken as 1.81 MW and unity, respectively, [147, 148].

Table 5.12 gives the values of the maximum fault current passing through each protective device for faults on various nodes in this case. From Tables 5.10 and 5.12, it is observed that in the presence of DG, the fault currents passing through F1, F2, F3, F4, F6, F7, F11, F12 and F13 increases for a fault anywhere in the system. However, depending on the location of the fault, the fault current through recloser, F5, F8, F9 and F10 either increases or decreases (as compared to the results of Table 5.10). Such variation of fault currents in the presence of DG in the network causes incorrect sequence of operation of the protective devices (recloser and fuses) resulting into mis-coordination, if the settings of recloser and fuses obtained in the previous subsection are adopted. It can also be observed from Table 5.10, Table 5.12 and Figure 5.7 that the current through F2 reverses for fault at bus 2 to 52 and 66 to 69. Similarly, the current through F8 reverses for fault at bus 2 to 3 and 28 to 46, the current through F9 reverses for fault at bus 2 to 4 and 28 to 46 while the current through F10 reverses for fault at bus 2 to 8 and 28 to 46. These reversals of current directions take place because of the presence of DG at bus 61.

Table 5.12: Maximum fault currents passing through various protective devices for faults on different nodes in the presence of a single DG in the IEEE 69-bus system

	Fault currents passing through various protective devices (A)													
Faulted node	Recloser	Fuse 1	Fuse 2	Fuse 3	Fuse 4	Fuse 5	Fuse 6	Fuse 7	Fuse 8	Fuse 9	Fuse 10	Fuse 11	Fuse 12	Fuse 13
2	4557	-	-	-	-	646	-	-	646	646	646	-	-	-
3	4553	-	-	-	-	646	-	-	646	646	646	-	-	-
4	4543	-	-	-	-	646	-	-	4543	646	646	-	-	-
5	4458	-	-	-	-	648	-	-	4458	4458	648	-	-	-
6	3896	-	-	-	-	665	-	-	3896	3896	665	-	-	-
7	3348	-	-	-	-	683	-	-	3348	3348	683	-	-	-
8	3228	-	-	-	-	688	-	-	3228	3228	688	-	-	-
9	3166	-	-	-	-	690	-	-	3166	3166	3166	-	-	-
10	2331	-	-	-	-	508	-	-	2331	2331	2329	2836	-	-
11	2186	-	-	-	-	476	-	-	2186	2186	2183	2657	-	-
12	1752	-	-	-	-	381	-	-	1752	1752	1748	2128	2126	-
13	1350	-	-	-	-	292	-	-	1350	1350	1345	1636	1632	1630
14	1091	-	-	-	-	235	-	-	1091	1091	1086	1319	1313	1310
15	911	-	-	-	-	195	-	-	911	911	906	1099	1093	1089
16	884	-	-	-	-	189	-	-	884	884	879	1067	1061	1056
17	837	-	-	-	-	179	-	-	837	837	832	1008	1002	997
18	836	-	-	-	-	178	-	-	836	836	831	1008	1002	997
19	800	-	-	-	-	170	-	-	800	800	794	963	957	952
20	777	-	-	-	-	165	-	-	777	777	772	937	930	925
21	744	-	-	-	-	158	-	-	744	744	739	895	888	884
22	743	-	-	-	-	158	-	-	743	743	738	894	888	883
23	729	-	-	-	-	155	-	-	729	729	723	877	870	865
24	701	-	-	-	-	148	-	-	701	701	695	842	835	830
25	646	-	-	-	-	136	-	-	646	646	640	774	766	761
26	625	-	-	-	-	131	-	-	625	625	620	749	742	736
27	615	-	-	-	-	129	-	-	615	615	609	737	729	724
28	4518	5090	-	-	-	641	-	-	641	641	641	-	-	-
29	4062	4576	-	-	-	576	-	-	576	576	576	-	-	-
30	3958	4459	-	-	-	561	-	-	561	561	561	-	-	-
31	4428	4989	-	-	-	628	-	-	628	628	628	-	-	-
32	4027	4537	-	-	-	571	-	-	571	571	571	-	-	-
33	3327	3747	-	-	-	472	-	-	472	472	472	-	-	-
34	2414	2719	-	-	-	342	-	-	342	342	342	-	-	-
35	2620	2951	-	-	-	371	-	-	371	371	371	-	-	-
36	4518	-	5090	-	-	641	-	-	641	641	641	-	-	-
37	4062	-	4576	-	-	576	-	-	576	576	576	-	-	-
38	3744	-	4218	-	-	531	-	-	531	531	531	-	-	-
39	3660	-	4123	-	-	519	-	-	519	519	519	-	-	-
40	3655	-	4117	-	-	518	-	-	518	518	518	-	-	-
41	2322	-	2616	-	-	329	-	-	329	329	329	-	-	-
42	1997	-	2250	-	-	283	-	-	283	283	283	-	-	-
43	1961	-	2209	-	-	278	-	-	278	278	278	-	-	-
44	1952	-	2199	-	-	277	-	-	277	277	277	-	-	-
45	1857	-	2092	-	-	263	-	-	263	263	263	-	-	-
46	1856	-	2091	-	-	263	-	-	263	263	263	-	-	-
47	4515	-	-	5089	-	642	-	-	4515	642	642	-	-	-
48	3940	-	-	4440	-	560	-	-	3940	560	560	-	-	-
49	2701	-	-	3044	-	384	-	-	2701	384	384	-	-	-
50	2480	-	-	2795	-	352	-	-	2480	352	352	-	-	-
51	3093	-	-	-	3750	659	-	-	3093	3093	659	-	-	-
52	2730	-	-	-	3309	581	-	-	2730	2730	581	-	-	-
53	2965	-	-	-	-	2964	-	-	2965	2965	2964	-	-	-
54	2753	-	-	-	-	2751	-	-	2753	2753	2751	-	-	-
55	2494	-	-	-	-	2491	-	-	2494	2494	2492	-	-	-
56	2275	-	-	-	-	2272	-	-	2275	2275	2272	-	-	-

Continued on next page

Table 5.12 – continued from previous page

Faulted node	Fault currents passing through various protective devices (A)													
	Recloser	Fuse 1	Fuse 2	Fuse 3	Fuse 4	Fuse 5	Fuse 6	Fuse 7	Fuse 8	Fuse 9	Fuse 10	Fuse 11	Fuse 12	Fuse 13
57	1555	-	-	-	-	1549	-	-	1555	1555	1550	-	-	-
58	1334	-	-	-	-	1329	-	-	1334	1334	1330	-	-	-
59	1264	-	-	-	-	1258	-	-	1264	1264	1259	-	-	-
60	1185	-	-	-	-	1179	-	-	1185	1185	1180	-	-	-
61	1085	-	-	-	-	1079	-	-	1085	1085	1080	-	-	-
62	1063	-	-	-	-	1057	-	-	1063	1063	1058	-	-	-
63	1032	-	-	-	-	1026	-	-	1032	1032	1027	-	-	-
64	899	-	-	-	-	892	-	-	899	899	893	-	-	-
65	759	-	-	-	-	752	-	-	759	759	753	-	-	-
66	2050	-	-	-	-	446	2491	-	2050	2050	2047	2492	-	-
67	2047	-	-	-	-	445	2488	-	2047	2047	2044	2489	-	-
68	1448	-	-	-	-	313	-	1750	1448	1448	1443	1755	1752	-
69	1446	-	-	-	-	313	-	1748	1446	1446	1441	1753	1750	-
I_{Lmax}	157	5	10	48	2	0	2	3	142	98	90	44	32	20

Through application of the proposed methodologies in this case, the optimum values of TDSs of the recloser and constants for all the fuses have been calculated and are given in Table 5.13. The resulting time-current characteristic curves of the recloser and the fuses are shown in Figure 5.9.

Table 5.13: Optimum values of TDSs of the recloser and constants of all fuses in the presence of a single DG in the IEEE 69-bus system

Recloser settings			Fuse settings													
Modes	PCS (A)	TDS	Constants	F1	F2	F3	F4	F5	F6	F7	F8	F9	F10	F11	F12	F13
Fast	300	0.5000	a	-1.4311	-1.4311	-1.4311	-1.4311	-1.4311	-1.4311	-1.4311	-1.4311	-1.4311	-1.4311	-1.4311	-1.4311	-1.4311
Slow	300	7.4544	b	11.8906	11.8906	11.7417	11.2577	10.7609	10.6288	10.4557	11.9417	11.7417	11.5417	11.3417	11.1417	10.9417

From Table 5.13, it is observed that the value of constant b for F12 is higher than that for F7 and F13. Similarly, the value of constant b for F11 is higher than that for F6 and F12, for F10 is higher than that for F5 and F11, for F9 is higher than that for F4 and F10 while that for F8 is higher than those for F3 and F9. Therefore, F8 provides backup protection to F3 and F9. Similarly, F9 provides backup protection to F4 and F10, F10 to F5 and F11, F11 to F6 and F12 while F12 provides backup protection to F7 and F13. From Figure 5.9, it is observed that the optimum coordinated characteristic curves of fuses lie well inside the operating times of recloser fast and slow modes of operation. Further, the operating sequences and MFCTI are correctly maintained among the fuses.

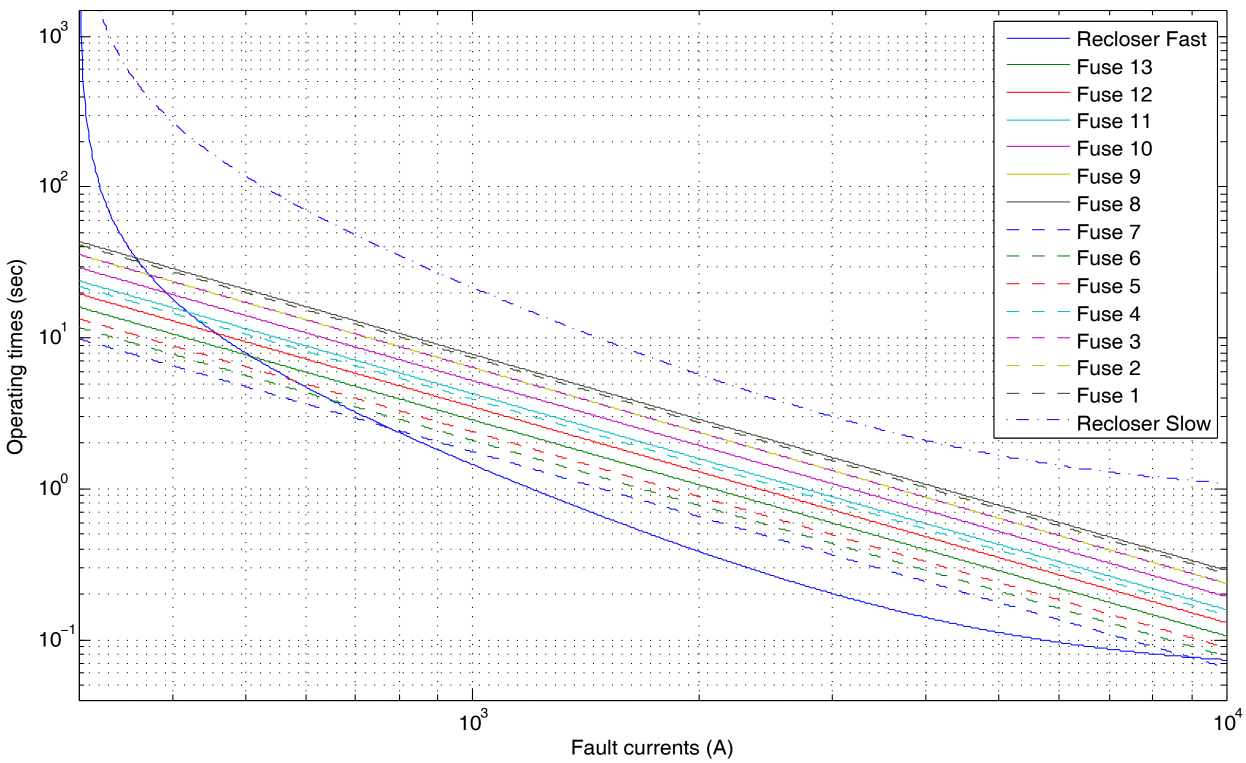

Figure 5.9: TCC curves of the protective devices for the optimum coordination in the presence of a single DG in the IEEE 69-bus system.

5.9.2.3 Optimum recloser settings and fuse constants in the presence of multiple DGs in the IEEE 69-bus system

In this case, three DGs at bus 65, 64 and 63 with real power outputs of 0.1018 MW, 0.3690 MW and 1.3024 MW, respectively, at unity power factor have been considered [150]. The short-circuit capacities of these three DGs have been considered as 5 MVA, 5 MVA and 10 MVA, respectively.

Table 5.14 gives the values of the maximum fault current passing through each protective device for faults on various nodes in this case. Similar to the previous case, from Tables 5.10 and 5.14, it is observed that in the presence of multiple DGs, the fault currents passing through F1, F2, F3, F4, F6, F7, F11, F12 and F13 increase for a fault anywhere in the system. However, depending on the location of the fault, the fault currents through recloser, F5, F8, F9 and F10 either increase or decrease (as compared to the results of Table 5.10). Such large variation of fault currents in the presence of multiple DGs in the network causes incorrect sequence of operation of the protective devices (recloser and fuses) resulting into miscoordination, if the settings of recloser and fuses obtained in the previous two subsections are adopted. Also, very similar to the previous case, it can also be observed from Table 5.10, Table 5.14 and Figure 5.7 that the current through F2 reverses for fault at bus 2 to 52 and 66 to 69. Similarly, the current through F8 reverses for fault at bus 2 to 3 and 28 to 46, the current through F9 reverses for fault at bus 2 to 4 and 28 to 46 and the current through F10 reverses for fault at bus 2 to 8 and 28 to 46. These reversals of current directions take place because of the presence of multiple DGs at bus 60, 61 and 62.

Table 5.14: Maximum fault currents passing through various protective devices for faults on different nodes in the presence of multiple DGs in the IEEE 69-bus system

Faulted node	Fault currents passing through various protective devices (A)													
	Recloser	Fuse 1	Fuse 2	Fuse 3	Fuse 4	Fuse 5	Fuse 6	Fuse 7	Fuse 8	Fuse 9	Fuse 10	Fuse 11	Fuse 12	Fuse 13
2	4557	-	-	-	-	822	-	-	822	822	822	-	-	-
3	4553	-	-	-	-	822	-	-	822	822	822	-	-	-
4	4543	-	-	-	-	822	-	-	4543	822	822	-	-	-
5	4458	-	-	-	-	825	-	-	4458	4458	825	-	-	-
6	3897	-	-	-	-	857	-	-	3897	3897	857	-	-	-
7	3349	-	-	-	-	892	-	-	3349	3349	892	-	-	-
8	3229	-	-	-	-	901	-	-	3229	3229	901	-	-	-
9	3167	-	-	-	-	906	-	-	3167	3167	3167	-	-	-
10	2285	-	-	-	-	653	-	-	2285	2285	2283	2930	-	-
11	2136	-	-	-	-	610	-	-	2136	2136	2133	2737	-	-
12	1698	-	-	-	-	484	-	-	1698	1698	1694	2173	2171	-
13	1300	-	-	-	-	368	-	-	1300	1300	1295	1659	1655	1653
14	1046	-	-	-	-	295	-	-	1046	1046	1041	1333	1327	1324
15	872	-	-	-	-	245	-	-	872	872	867	1109	1102	1098
16	847	-	-	-	-	237	-	-	847	847	841	1075	1069	1064
17	801	-	-	-	-	224	-	-	801	801	796	1016	1010	1005
18	800	-	-	-	-	224	-	-	800	800	795	1015	1009	1004
19	765	-	-	-	-	213	-	-	765	765	760	969	963	958
20	744	-	-	-	-	207	-	-	744	744	738	943	936	931
21	712	-	-	-	-	198	-	-	712	712	707	901	895	890
22	710	-	-	-	-	197	-	-	710	710	705	899	893	888
23	697	-	-	-	-	193	-	-	697	697	691	882	875	870
24	670	-	-	-	-	185	-	-	670	670	664	846	839	834
25	617	-	-	-	-	170	-	-	617	617	611	778	770	765
26	597	-	-	-	-	164	-	-	597	597	592	753	746	740
27	588	-	-	-	-	161	-	-	588	588	582	740	732	727
28	4517	5203	-	-	-	815	-	-	815	815	815	-	-	-
29	4048	4664	-	-	-	731	-	-	731	731	731	-	-	-
30	3919	4515	-	-	-	707	-	-	707	707	707	-	-	-
31	4419	5090	-	-	-	798	-	-	798	798	798	-	-	-
32	3992	4598	-	-	-	720	-	-	720	720	720	-	-	-
33	3271	3768	-	-	-	590	-	-	590	590	590	-	-	-
34	2359	2717	-	-	-	426	-	-	426	426	426	-	-	-
35	2563	2952	-	-	-	462	-	-	462	462	462	-	-	-
36	4517	-	5203	-	-	815	-	-	815	815	815	-	-	-
37	4048	-	4663	-	-	731	-	-	731	731	731	-	-	-
38	3721	-	4286	-	-	672	-	-	672	672	672	-	-	-
39	3634	-	4186	-	-	656	-	-	656	656	656	-	-	-
40	3629	-	4181	-	-	655	-	-	655	655	655	-	-	-
41	2285	-	2632	-	-	412	-	-	412	412	412	-	-	-
42	1962	-	2260	-	-	354	-	-	354	354	354	-	-	-

Continued on next page

Table 5.14 – continued from previous page

Faulted node	Fault currents passing through various protective devices (A)													
	Recloser	Fuse 1	Fuse 2	Fuse 3	Fuse 4	Fuse 5	Fuse 6	Fuse 7	Fuse 8	Fuse 9	Fuse 10	Fuse 11	Fuse 12	Fuse 13
43	1926	-	2218	-	-	347	-	-	347	347	347	-	-	-
44	1918	-	2209	-	-	346	-	-	346	346	346	-	-	-
45	1823	-	2100	-	-	329	-	-	329	329	329	-	-	-
46	1823	-	2099	-	-	328	-	-	328	328	328	-	-	-
47	4515	-	-	5203	-	817	-	-	4515	817	817	-	-	-
48	3924	-	-	4522	-	710	-	-	3924	710	710	-	-	-
49	2670	-	-	3077	-	483	-	-	2670	483	483	-	-	-
50	2450	-	-	2823	-	443	-	-	2450	443	443	-	-	-
51	3084	-	-	-	3934	860	-	-	3084	3084	860	-	-	-
52	2698	-	-	-	3441	752	-	-	2698	2698	752	-	-	-
53	2966	-	-	-	-	2965	-	-	2966	2966	2965	-	-	-
54	2754	-	-	-	-	2752	-	-	2754	2754	2752	-	-	-
55	2495	-	-	-	-	2492	-	-	2495	2495	2493	-	-	-
56	2277	-	-	-	-	2274	-	-	2277	2277	2274	-	-	-
57	1557	-	-	-	-	1551	-	-	1557	1557	1552	-	-	-
58	1336	-	-	-	-	1331	-	-	1336	1336	1332	-	-	-
59	1266	-	-	-	-	1260	-	-	1266	1266	1261	-	-	-
60	1188	-	-	-	-	1182	-	-	1188	1188	1183	-	-	-
61	1069	-	-	-	-	1063	-	-	1069	1069	1064	-	-	-
62	1048	-	-	-	-	1042	-	-	1048	1048	1043	-	-	-
63	1014	-	-	-	-	1008	-	-	1014	1014	1009	-	-	-
64	868	-	-	-	-	861	-	-	868	868	863	-	-	-
65	718	-	-	-	-	711	-	-	718	718	712	-	-	-
66	1998	-	-	-	-	570	2558	-	1998	1998	1995	2559	-	-
67	1995	-	-	-	-	569	2554	-	1995	1995	1992	2555	-	-
68	1396	-	-	-	-	396	-	1777	1396	1396	1391	1782	1779	-
69	1394	-	-	-	-	396	-	1775	1394	1394	1390	1780	1777	-
I_{Lmax}	155	5	10	48	2	0	2	3	140	97	89	44	32	20

By applying the proposed approach, the optimum values of TDSs of the recloser and constants for all the fuses have been calculated in this case and are given in Table 5.14. The resulting time-current characteristic curves of the recloser and the fuses are shown in Figure 5.10.

Table 5.15: Optimum values of TDSs of the recloser and constants of all fuses in the presence of multiple DGs in the IEEE 69-bus system

Recloser settings			Fuse settings													
Modes	PCS (A)	TDS	Constants	F1	F2	F3	F4	F5	F6	F7	F8	F9	F10	F11	F12	F13
Fast	300	0.5000	a	-1.4767	-1.4767	-1.4767	-1.4767	-1.4767	-1.4767	-1.4767	-1.4767	-1.4767	-1.4767	-1.4767	-1.4767	-1.4767
Slow	300	7.4544	b	12.3125	12.3125	12.1638	11.7053	11.1259	11.0536	10.8806	12.3638	12.1638	11.9638	11.7638	11.5638	11.3638

From Table 5.14, it is observed that the value of constant b for F12 is higher than that for F7 and F13. Similarly, the value of constant b for F11 is higher than that for F6 and F12, for F10 is higher than that for F5 and F11, for F9 is higher than that for F4 and F10 while that for F8 is higher than those for F3 and F9. Therefore, F8 provides backup protection to F3 and F9.

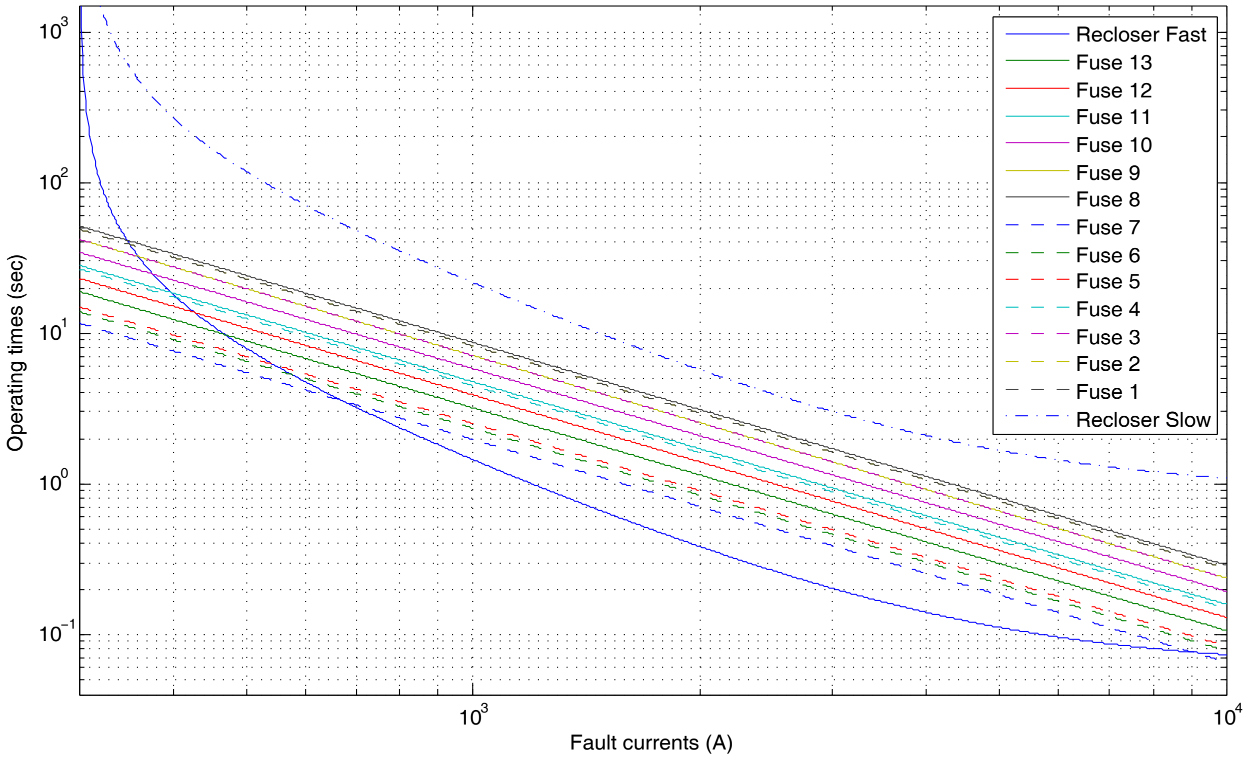

Figure 5.10: TCC curves of the protective devices for the optimum coordination in the presence of multiple DGs in the IEEE 69-bus system.

Similarly, F9 provides backup protection to F4 and F10, F10 to F5 and F11, F11 to F6 and F12 while F12 provides backup protection to F7 and F13. From Figure 5.10, it is observed that the optimum coordinated characteristic curves of fuses lie well inside the operating times of recloser fast and slow modes of operation. Further, the operating sequences and MFCTI are correctly maintained among the fuses. Thus, coordination among fuses with recloser is always maintained in the presence of multiple DGs in the IEEE 69-bus system.

5.9.2.4 Common optimum recloser settings and fuse constants without and with presence of DG in the IEEE 69-bus system

The common optimum settings of TDSs of the recloser and constants for all the fuses obtained are given in Table 5.16. As observed from Table 5.16, in this case also, F8 provides backup protection to F3 and F9. Similarly, F9 provides backup protection to F4 and F10, F10 to F5 and F11, F11 to F6 and F12 while F12 provides backup protection to F7 and F13. Moreover, the correct operating sequences are maintained while satisfying the MFCTI requirements between the fuses.

The corresponding time-current characteristic curves of recloser and fuses are shown in Figure 5.11. In this case study, it can be observed that combined settings are the same as the settings obtained in the presence of multiple DGs in the IEEE 69-bus system.

Table 5.16: Common optimum values of TDSs of the recloser and constants of all fuses in the IEEE 69-bus system

Recloser settings			Fuse settings													
Modes	PCS (A)	TDS	Constants	F1	F2	F3	F4	F5	F6	F7	F8	F9	F10	F11	F12	F13
Fast	300	0.5000	a	-1.4767	-1.4767	-1.4767	-1.4767	-1.4767	-1.4767	-1.4767	-1.4767	-1.4767	-1.4767	-1.4767	-1.4767	-1.4767
Slow	300	7.4544	b	12.3125	12.3125	12.1638	11.7053	11.1259	11.0536	10.8806	12.3638	12.1638	11.9638	11.7638	11.5638	11.3638

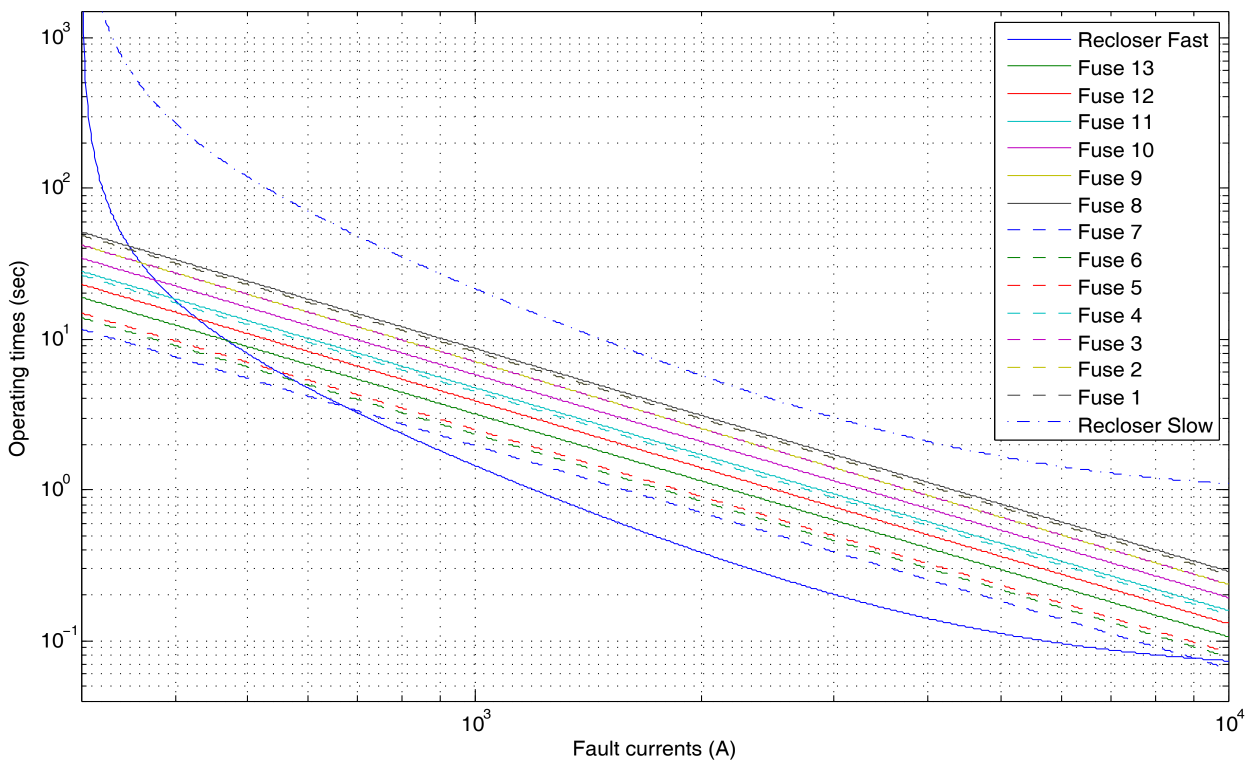

Figure 5.11: TCC curves of the protective devices corresponding to the common optimum coordination results in the IEEE 69-bus system.

In the above four sub-sections (for the two radial distribution systems), four different cases of recloser-fuse coordination have been studied. A comparative assessment of these four coordination results is provided below.

5.10 Comparative assessment of recloser-fuse coordination results

As discussed in the last section, in this work, three different network conditions have been considered. These are: i) no DG in the system, ii) a single DG in the system and iii) multiple DGs in the system. For investigating the performance of the recloser-fuse coordination results of these three cases, the number of mis-coordination has been calculated when the recloser and fuse settings obtained in any particular network condition is applied to all the three network conditions. Lastly, the number of mis-coordination has also been calculated when the common settings of the recloser and fuses (as obtained in Sections 5.9.1.4 and 5.9.2.4) are applied to all the three network conditions. Figures 5.12 and 5.13 show the results of this investigation for the IEEE 33 and 69-bus radial distribution system, respectively. In these two figures, each white bubble indicates a case when the co-ordination among the recloser and the fuses is maintained for a particular fault condition, while a black bubble indicates the case when this co-ordination does not hold.

In the IEEE 33-bus system, from Figure 5.12(a), it is observed that there are 14 and 6 mis-coordination cases when the co-ordination results obtained without any DG are applied to the networks with single DG and multiple DGs, respectively. Similarly, Figure 5.12(b) shows that when the co-ordination results obtained with a single DG are applied to the other two network conditions (without any DG and with multiple DGs), there are 12 mis-coordination results for each network condition. Further, from Figure 5.12(c) it can be seen that there are 11 and 12 mis-coordination cases when the co-ordination results obtained with multiple DGs are applied to the networks with single DG and without any DG, respectively. However, when the common co-ordination settings are applied to all the three network conditions, no single case of mis-coordination is observed (Figure 5.12(d)).

Similarly in the IEEE 69-bus system, from Figure 5.13(a), it is observed that there are 15 mis-coordination cases when the co-ordination results obtained without any DG are applied to the networks with single DG and multiple DGs, respectively. Similarly, Figure 5.13(b) shows that when the co-ordination results obtained with a single DG are applied to the other two network conditions (without any DG and with multiple DGs), there are 37 and 3 mis-coordination cases. However, from Figure 5.13(c) it can be seen that there is no constraint violation when the coordination results obtained with multiple DGs are applied to the other network conditions. The same

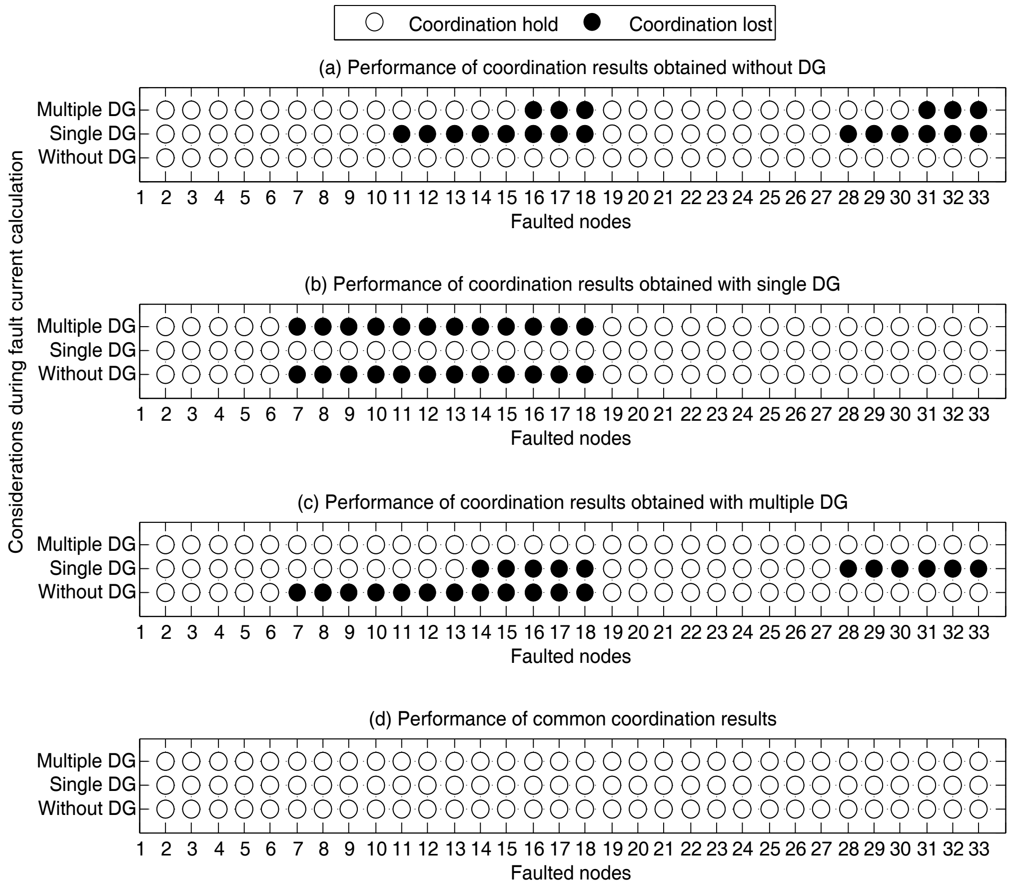

Figure 5.12: Performance of various settings of recloser and fuses for fault currents in different situations for the IEEE 33-bus system.

can also be observed when the common co-ordination settings are applied to all the three network conditions, i.e., there is not a single case of mis-coordination (Figure 5.13(d)).

Thus, the common settings are robust enough to maintain proper recloser-fuse co-ordination in any network condition considered in this work. It is to be noted that the approach discussed in Sections 5.9.1.4 and 5.9.2.4 can be extended in a straightforward manner for computing the robust settings of the recloser and fuses for any other netowrk condition(s) of the system under study.

5.11 Conclusion

In this chapter, an new approach for coordination of recloser and fuses has been proposed to achieve proper coordination in the presence of DGs in radial distribution systems. On the basis of detailed studies on IEEE 33 and 69-bus radial networks, it can be concluded that the proposed strategy can be used to obtain a common settings of the recloser and the fuses which would be able to maintain

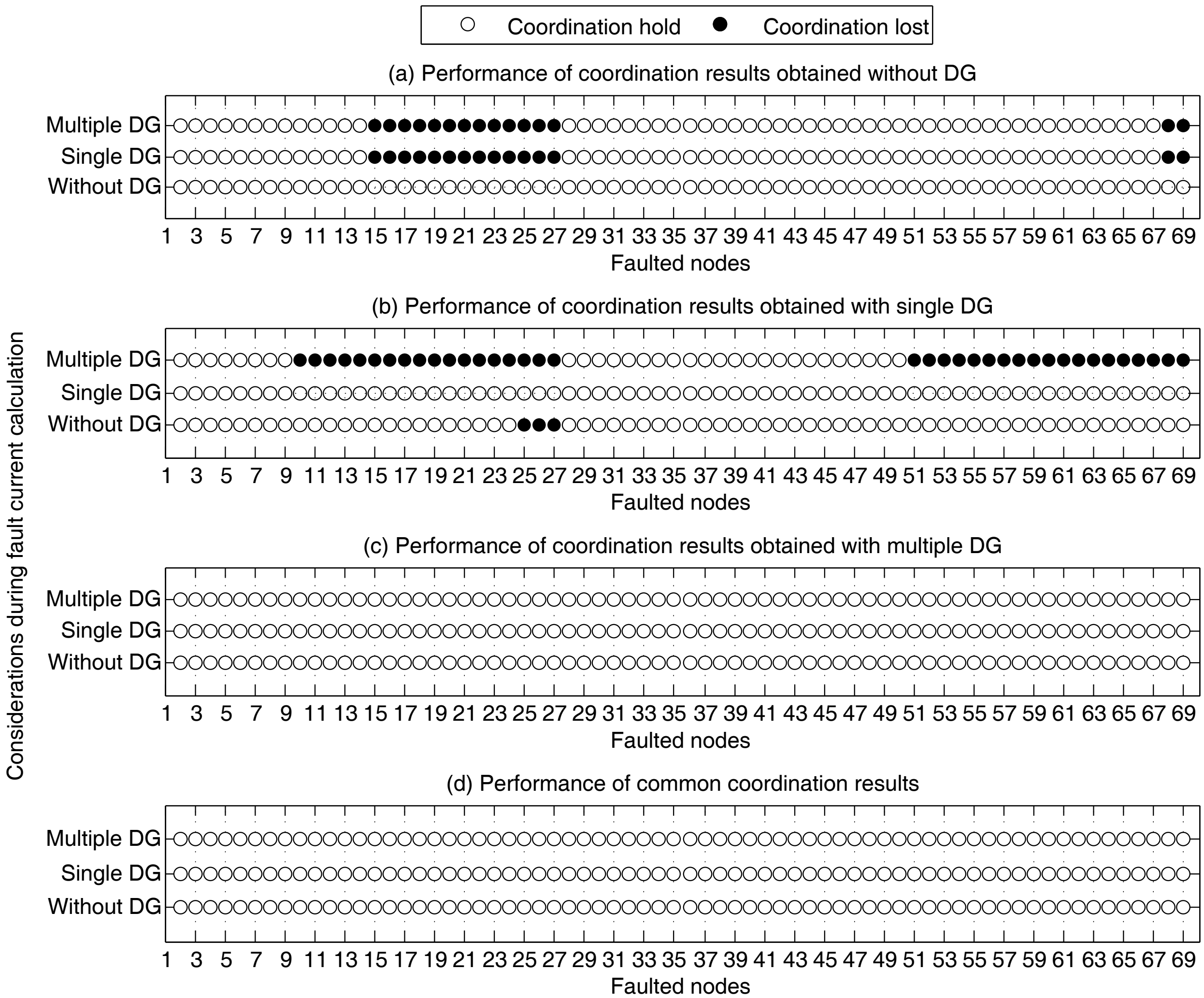

Figure 5.13: Performance of various settings of recloser and fuses for fault currents in different situations for the IEEE 69-bus system.

proper coordination for multiple network conditions simultaneously.

In the next chapter, a procedure to obtain the optimum recloser-fuse coordination in reconfigurable radial distribution systems in the presence of DG is described.

Chapter 6

Optimum Recloser-fuse Coordination in Reconfigurable Radial Distribution Systems in the Presence of Distributed Generation

Abstract

In this chapter, an optimum recloser-fuse coordination scheme in reconfigurable radial distribution systems in the presence of DG is proposed. In the proposed scheme, the problem of recloser-fuse coordination in reconfigurable radial distribution networks has been formulated as an optimization problem. The formulated recloser-fuse coordination problem has been solved using interior-point method (IPM) based algorithm. In order to obtain all possible reconfigurable radial network, a new graph theory based approach has been developed. The proposed approach has been applied to obtain optimum recloser-fuse settings in the IEEE 33 and 69-bus radial distribution systems in the presence of DG. The test results prove the effectiveness of the presented scheme.

6.1 Introduction

MODERN distribution networks have facilities to reconfigure their topology in order to achieve minimum loss and high reliability. In the previous chapter, the issue of miscoordination among reclosers and fuses in the presence of DGs has been studied in detail. However, the issue of miscoordination among reclosers and fuses owing to the variation of topology of the distribution network has not been studied [139, 152].

In this chapter, an optimum recloser-fuse coordination scheme in presence of DG in reconfigurable radial distribution systems is proposed. The problem of protection coordination of recloser and fuses has been formulated as an optimization problem. In order to obtain all possible configurations of the radial network, a new graph theory based approach has been developed. An IPM based algorithm has been used to solve this formulated optimization problem. The proposed approach has been tested on the IEEE 33 and 69-bus reconfigurable radial distribution systems for three different scenarios: i) no DG in the system, ii) a single DG in the system and iii) multiple

DGs in the system.

6.2 Miscoordination among protective devices in reconfigurable radial distribution systems in the presence of DG

Miscoordination among the protective devices are mostly because of the following two reasons which are discussed below.

6.2.1 Miscoordination in the presence of DGs

This issue has already been discussed in detail in the previous chapter.

6.2.2 Miscoordination with the change in configuration

In order to obtain minimum active power loss, better voltage profile and reliable operation, reconfiguration of distribution system is carried out regularly. However, it is quite difficult to maintain the protection coordination in reconfigurable networks as the directions of current through the feeder sections change with the change in configuration.

In order to obtain proper coordination in the presence of DGs in reconfigurable distribution systems, a new optimum coordination approach of recloser and fuses is developed in the next section.

6.3 Proposed optimum recloser and fuses coordination approach

The problem of optimum coordination of recloser and fuses can be formulated as an optimization problem whose objective function (OF) is to minimize the sum of operating times of all the fuses and the recloser (in its both modes of operations) subjected to the constraint that the correct operating sequence with certain minimum time gap between them in all feasible configurations of the system must be maintained. Mathematically, this problem can be expressed as follows;

$$OF = \min \sum_{i=1}^{NC} \left(\sum_{j=1}^{m} \left(t_{opR,fm,ij} + t_{opR,sm,ij} + \sum_{k=1}^{N_j} t_{opF,ijk} \right) \right) \tag{6.1}$$

Subjected to:

$$t_{opF,ijk} - t_{opR,fm,ij} > MRCTI/2; \forall i = 1,2,...,NC; \forall j = 1,2,...,m; \forall k = 1,2,...,N_j \quad (6.2)$$

$$t_{opF,ij(k+1)} - t_{opF,ijk} > MFCTI; \quad \forall i = 1,2,...,NC; \forall j = 1,2,...,m; \forall k = 1,2,...,N_j \quad (6.3)$$

$$t_{opR,sm,ij} - t_{opF,ijk} > MRCTI/2; \forall i = 1,2,...,NC; \forall j = 1,2,...,m; \forall k = 1,2,...,N_j \quad (6.4)$$

$$t_{opR,sm,ij} - t_{opR,fm,ij} > MRCTI; \quad \forall j = 1,2,...,m; \forall k = 1,2,...,N_j \quad (6.5)$$

$$TDS_{min} \leq TDS_{fm} \leq TDS_{max} \quad (6.6)$$

$$TDS_{min} \leq TDS_{sm} \leq TDS_{max} \quad (6.7)$$

In eqn. (6.1), $t_{opR,fm,ij}$ and $t_{opR,sm,ij}$ are the operating times of the recloser in its fast and slow mode of operation, respectively, for fault at node j in i^{th} configuration; $t_{opF,ijk}$ is the operating time of fuse k for fault at node j in i^{th} configuration; m is the total number of nodes; N_j is the total number of fuses in the faulted path from node j to the recloser. In eqns. (6.6) and (6.7), TDS_{min} and TDS_{max} are the minimum and maximum limits, respectively, on TDS of recloser whereas TDS_{fm} and TDS_{sm} are the values of TDS for recloser fast and slow modes of operation, respectively.

The operating times of recloser fast and slow modes of operation used in eqn. (6.1) are defined as follows;

$$t_{opR,fm,ij} = TDS_{fm} \times \left[\frac{A}{(I_{FR,ij}/PCS)^p - 1} + B \right] \quad (6.8)$$

$$t_{opR,sm,ij} = TDS_{sm} \times \left[\frac{A}{(I_{FR,ij}/PCS)^p - 1} + B \right] \quad (6.9)$$

In eqns. (6.8) and (6.9), $I_{FR,ij}$ is the fault current passing through the recloser when fault occurs at node j in i^{th} configuration and *PCS* is the pick-up current setting for the recloser defined in eqn. (5.3).

The operating times of fuses used in eqn. (6.1) are defined as follows;

$$t_{opF,ijk} = exp(a_k \times log(I_{FF,ijk}) + b_k) \quad (6.10)$$

In eqn. (6.10), $I_{FF,ijk}$ is the fault current passing through fuse k when fault occur at node j in i^{th} configuration and coefficients a_k and b_k are characteristic constants of fuse k. It is to be noted that the solution of this problem gives the optimum values of TDSs (TDS_{fm} and TDS_{sm}) for the recloser and the optimum values of fuse constants a and b for the fuses (a_k and b_k for $k = 1,2,...,N$ where

N is the total number of fuses). To determine all possible radial configurations of a distribution system, the procedure described in the next section has been adopted.

6.4 Determination of all possible radial configurations of a distribution system

Consider a distribution system which has N buses, M feeder sections and T tie-switches. It is to be noted that all the branches are considered to be equipped with sectionalising switches. As the original network is radial, $M = N - 1$. Let U represents the total number of the branches which is the sum of all feeder sections and all tie-switches i.e., $U = M + T$. For determining the total number of configurations of a radial network, initially the incidence matrix of the network is formed [153, 154]. Each row of this matrix represents the corresponding node of the graph while each column corresponds to a branch. When a graph has N nodes and U branches, the incident matrix [$\mathbf{A}_{inc}$] is a $N \times U$ rectangular matrix whose elements ($a_{i,j}$) are defined as

1. If branch j is incident at node i and is oriented away from the node, $a_{i,j} = 1$.
2. If branch j is incident at node i and is oriented towards node i, $a_{i,j} = -1$.
3. If branch j is not incident at node i, $a_{i,j} = 0$.

Once incident matrix $\mathbf{A}_{inc}$ of size $N \times U$ is formed using the above procedure, one row is removed to form reduced incident matrix **A** of size $(N - 1) \times U$. It is to be noted that selection of the row to be removed does not have any effect on further analysis [153]. In this study, the last row has been considered to be removed. The total number of all the possible radial configurations *TN* is defined as [153];

$$TN = det(\mathbf{A}\mathbf{A}^t) \tag{6.11}$$

In eqn. (6.11), matrix **A** represents row reduced incidence matrix of size $(N - 1) \times U$, t represents transpose operator on the matrix **A** and function $det(\mathbf{X})$ gives determinant of matrix **X**.

Now, to select a radial configuration from a distribution network of N buses, M feeder sections and T tie-lines, the following procedure is used. Any M columns from the row reduced incidence matrix **A** are selected to form another matrix **B** of size $(N - 1) \times M$. To determine whether matrix **B** represents a radial configuration or not, a quantity TNR is calculated as below: [153];

$$TNR = det(\mathbf{B}\mathbf{B}^t) \tag{6.12}$$

In eqn. (6.12), if *TNR* $= \pm 1$ then matrix **B** represents a redial network. Now, to select all the possible configurations of the radial network under study, the following procedure has been adopted. Initially, a matrix **MT** of size $TN \times U$ is initialized with zeros. After that, a binary string **R** of length U with M '1's and T '0's is generated randomly. A binary value '1' denotes that the branch corresponding to this bit position is present in the circuit (i.e. the switch on this feeder is 'ON'). On the other hand, a binary value '0' denotes that the branch corresponding to this bit position is not present in the circuit (i.e. the switch on this feeder is 'OFF'). This binary string is used to form matrix **B** to test the radiality nature of the string using eqn. (6.12). If the generated string qualifies the radiality test then its uniqueness is checked with each row of matrix **MT**. If the string does not exist as any row in matrix **MT** then it is included in the matrix in place of a zero row. This three step process (i.e. generation of a binary string, testing of radiality of the network represented by the string and determination of uniqueness of the string) continues till all the zero rows of matrix **MT** get replaced by the generated strings. Finally, matrix **MT** gives the sets of binary strings which represents all the possible radial configurations. Figure 6.1 gives a detailed flowchart of the procedure to select all possible radial configurations of a given distribution system.

6.5 Proposed approach for solving the optimum recloser-fuse coordination problem in reconfigurable radial distribution systems

To solve the proposed optimum coordination problem of recloser and fuses, the following approach has been adopted. Initially, steady state load flow analysis using BFSM has been performed to calculate various load currents passing through each protective device. Subsequently, bolted three-phase-to-ground short circuit analysis using Zbus approach has been carried out to calculate the maximum fault currents passing through each protective device under all possible configurations of the system [15, 140]. After that, PCS of the recloser is calculated using eqn. (5.3). Finally, IPM available in MATLAB [74] is applied to solve the problem to obtain the optimum values of TDSs for the recloser and fuse constants for all the fuses. The overall procedure can be described by the following steps:

1. Perform reconfiguration analysis and select feasible network topologies.

2. Perform load flow analysis for all feasible network topologies and select only those topologies for which load flow analysis converges.

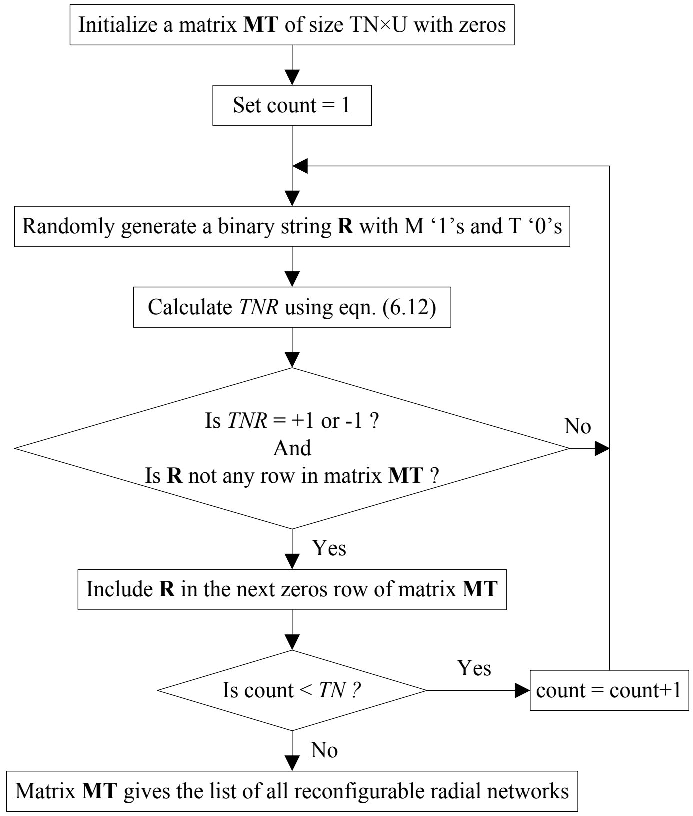

Figure 6.1: Flowchart for selection of all the possible radial configurations.

3. Perform steady-state and short-circuit analysis for all feasible network topologies.

4. Select the fault currents that need to be interrupted by the recloser and the fuses caused by faults on various nodes in all the feasible network topologies.

5. Set PCS of recloser using eqn. (5.3).

6. Apply IPM to solve the formulated problem to obtain the optimum values of recloser settings (TDSs) and fuse constants (a and b for all the fuses).

The following points have been considered while solving the protection coordination problems of recloser and fuses [60], [67], [138]:

1. Two fast and two slow modes of operation of the recloser have been considered.

2. Optimum characteristics of all fuses have been considered to reside between the optimum second fast mode and the first slow mode operations of recloser.

3. TDS for the second fast mode and the first slow modes of operation are optimized whereas TDS for the first fast mode and the second slow modes of operations are set one step lower than the optimized TDS for the second fast mode and one step higher than the optimized TDS for the first slow mode, respectively.

4. The values of A, B and p for recloser have been considered as 28.2, 0.1217 and 2, respectively.

5. The minimum and the maximum value of TDS for optimum coordination of recloser has been considered as 0.5 and 10, respectively.

6. The minimum and the maximum value of fuse constant a and b are considered in the range of [1.2, 2.4] and [2, 20], respectively.

7. The value of MFCTI and MRCTI are taken as 0.2 and 0.5 seconds, respectively.

8. Fuse constant a for all the fuses has been considered the same in any particular network condition.

A flowchart with detailed information of the proposed overall approach used in this chapter is shown in Figure 6.2.

6.6 Results and discussion

The effectiveness of the proposed methodology has been investigated on two reconfigurable radial distribution systems. These two systems are IEEE 33 and 69-bus. Detailed reconfiguration studies of these two systems are available in [70, 150, 151, 155–165].

6.6.1 Results on the IEEE 33-bus system

Figure 6.3 shows the IEEE 33-bus system having 32 branches and 5 tie-switches (a total of 37 line) and supplied by electric substation having a short-circuit capacity of 100 MVA. The detailed information about the system is available in [146]. For providing complete robust protection using recloser and fuses, one recloser and six fuses are required which are shown in the figure. The recloser is placed near to the substation which provides protection to the whole network from any temporary fault in the system and also provides overall backup protection for any permanent fault

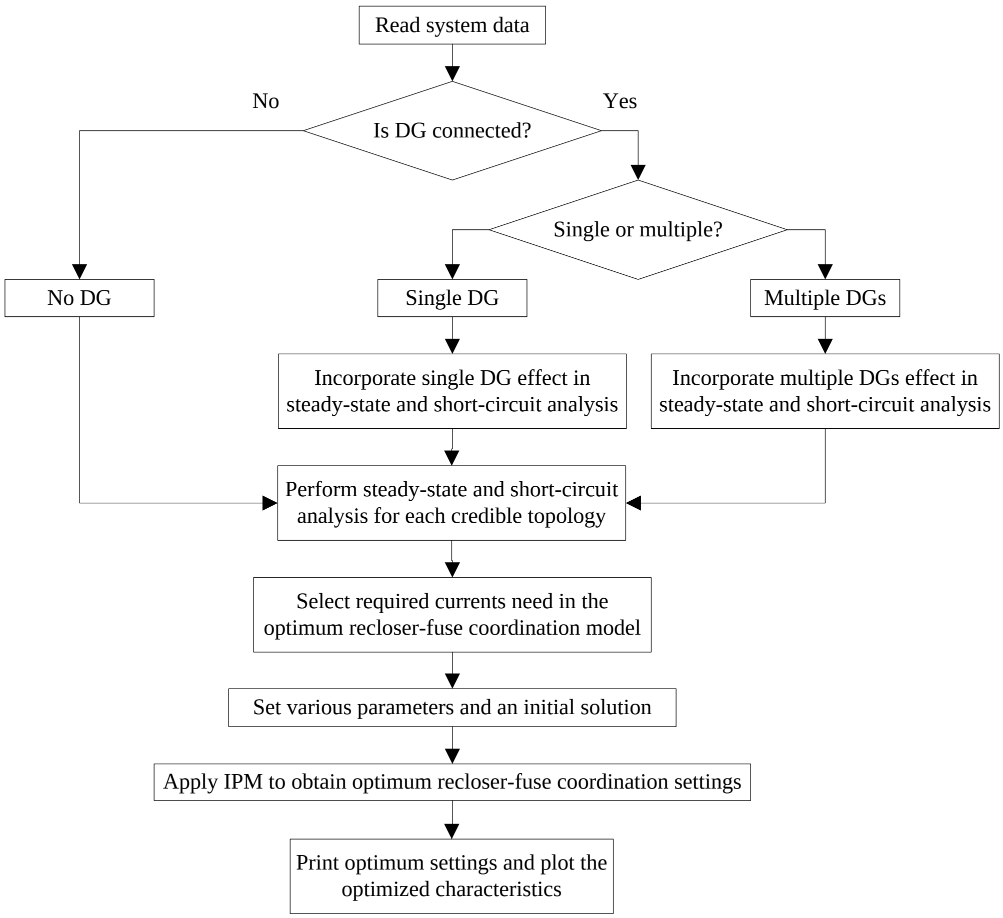

Figure 6.2: Flowchart of the overall approach.

in the system. Fuses are placed downstream of the recloser on every branch at each junction to provide primary protection against any permanent fault in the respective branch. It is to be noted that placing fuse at each branch rather than at each lateral provides additional selectivity for a fault in the main feeder. However, extra care must be taken in order to select the characteristic coefficients of the main feeder fuses.

With the six fuses and recloser fast and slow modes of operation there are a total of seven correct operating sequences of the protecting devices for a fault anywhere in the system under any configuration which are given in Table 6.1. It is to be noted that only one of the sequences of the protective devices is responsible to operate for a particular fault. As an example, for a fault at node 30 under the base case configuration (all switches are open), the correct operating sequence of the protective devices is given in serial no. 6 in Table 6.1 where recloser in its fast mode (R_{FM}) will operate first followed by fuse 5, fuse 4 and fuse 2. Further, if all these devices fail to clear the

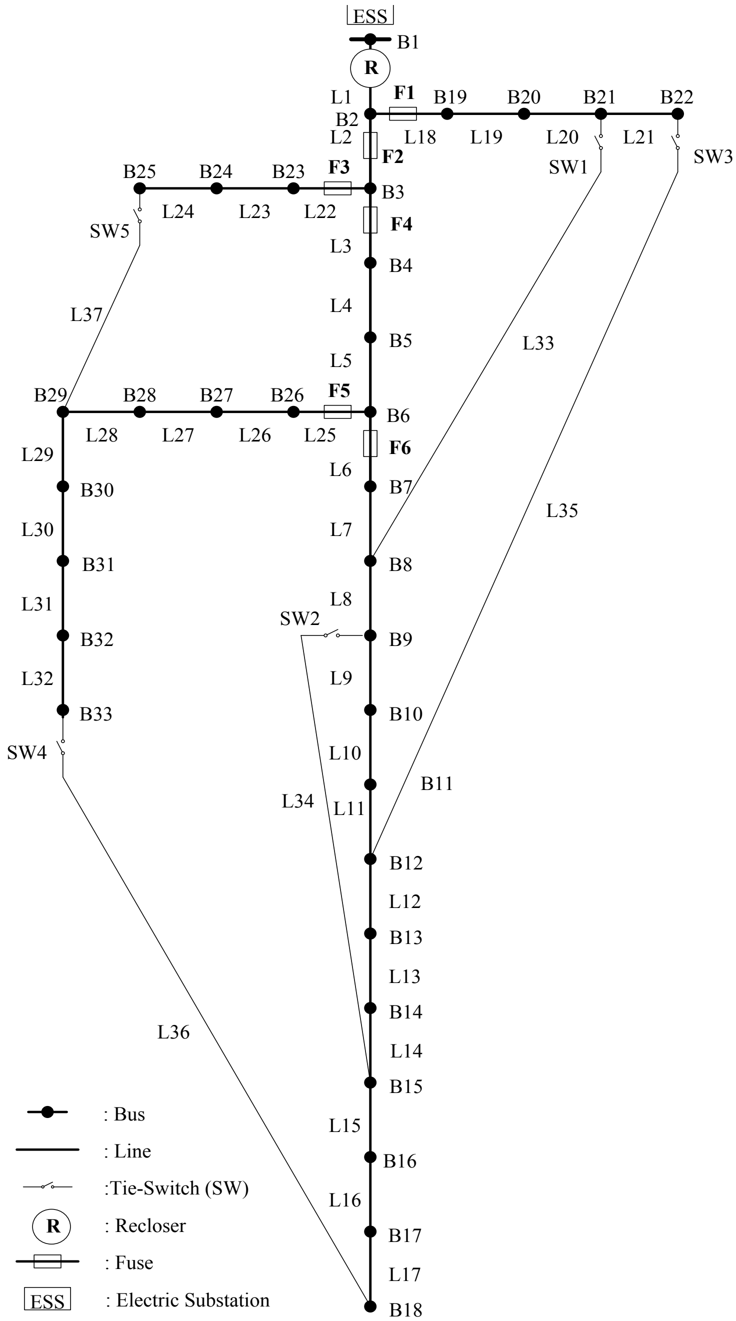

Figure 6.3: IEEE 33-bus system with tie-switches and protective devices.

fault then finally the recloser in its slow mode of operation (R_{SM}) will operate to isolate the whole network. From Table 6.1, it is observed that fuse 2 provides backup protection for fuse 3 and fuse 4 whereas fuse 4 provides backup protection for fuse 5 and fuse 6. Further, it is also observed that fuse 1, fuse 3, fuse 5 and fuse 6 work only as a primary protection for any permanent fault in their protection zones under any configuration. From Table 6.1, it is also observed that the sum of total number of operating devices in the seven protective devices (one recloser and six fuses) is 19.

Table 6.1: Correct operating sequences of the various protective devices in the IEEE 33-bus system

Sl. No.	Correct operating sequences	No. of operating devices
1	$R_{FM} - R_{SM}$	1
2	$R_{FM} - F1 - R_{SM}$	2
3	$R_{FM} - F2 - R_{SM}$	2
4	$R_{FM} - F3 - F2 - R_{SM}$	3
5	$R_{FM} - F4 - F2 - R_{SM}$	3
6	$R_{FM} - F5 - F4 - F2 - R_{SM}$	4
7	$R_{FM} - F6 - F4 - F2 - R_{SM}$	4

6.6.1.1 Selection of feasible configurations in the IEEE 33-bus system

In the IEEE 33-bus system there are a total of 50751 possible radial network configurations (obtained using the concepts discussed in Section 6.4). Out of 50751 possible radial network configurations, feasible power flow solutions are obtained (i.e., all bus voltages are within 0.9 p.u. and 1.1 p.u.) for only 14727 radial network configurations. Further, to prevent reverse power flow through all the fuses placed in the network, branches 1 to 5 are kept connected so that power flow from substation to the junction points in the network is always maintained which results in a reduction of 5339 configurations. Thus, the total number of credible radial network configurations are 9388 only.

From Table 6.1, it is to be noted that originally there are only seven primary-backup operating sequences among the seven protective devices (one recloser and six fuses) and thus only one sequence will be responsible to operate for fault at any node. However, it is possible that the values of fault current passing through various protective devices of the same operating sequence may be different for fault at different nodes. For example, the operating sequence 7 is responsible to operate for fault in any branch from node 7 to 18. Therefore, there are a total of 11 cases of operation with different values of fault currents (as there are 11 fault points) for this operating sequence (Sl. No. 7). As a result, corresponding to a fault on each node of a feasible radial network, there are 32 cases of operation with different values of fault currents in the seven original operating sequences of the protective devices given in Table 6.1. Hence, there are a total of 9388$\times$32 cases of operation in the seven operating sequences for coordination of recloser with downstream fuses (as there are

9388 feasible configurations) in all the possible configurations.

6.6.1.2 Constraints reduction strategy in reconfigurable radial networks in the IEEE 33-bus system

The constraint reduction strategy can easily be understood through an example. Figure 6.4 shows an example of a typical 4-bus radial distribution system. This system is protected by a recloser at substation and two fuses downstream of the recloser. Figure 6.5 shows typical time-current characteristic (TCC) plots of the recloser and two fuses. It is to be noted that, it is essential to maintain proper coordination among recloser and fuses at the maximum and minimum operating fault currents. Once the coordination is maintained for these critical fault currents, then for the other fault currents within the range (i.e. between minimum and maximum fault current) proper coordination would be maintained. Further, a minimum gap between the characteristics of recloser slow mode of operation and the nearest fuse curve needs to be maintained.

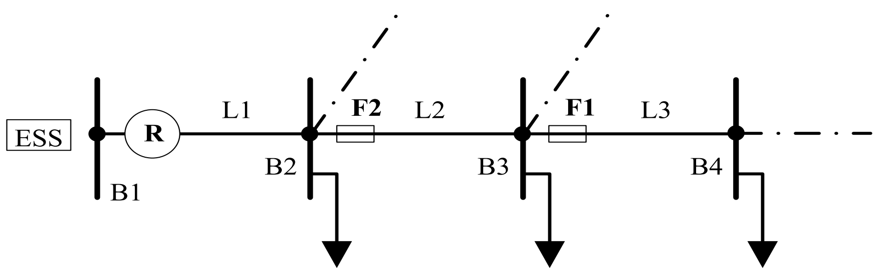

Figure 6.4: Example of a typical 4-bus radial system.

Now, if the network shown in Figure 6.4 is a part of a reconfigurable radial distribution system, then it is possible that the protective devices (R, F1 and F2) can have many sets of values of currents for faults on any other section which are contributed through this part of the network and also because of variation in the configuration. However, only two of them (maximum and minimum fault currents) for each protective device of the sequence are important for the purpose of protection coordination. If the coordination is maintained for these two values of fault currents then for the other values of fault currents coordination would be maintained (Figure 6.5). So, if there are three protective devices in an operating sequence then there are only six critical values of fault currents for which the protection co-ordination should be maintained. It will guarantee

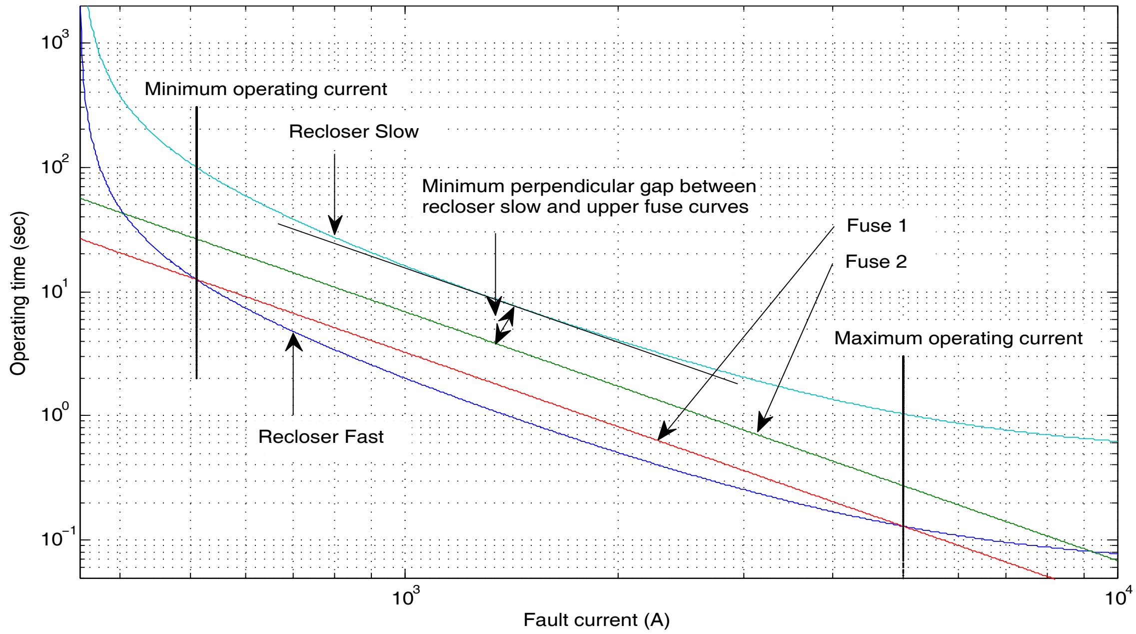

Figure 6.5: Typical TCC curves of the protective devices in the 4-bus system.

a proper coordination for any other fault currents of that sequence. Also, it is possible that the critical values of fault currents may be the same for the three protective devices in this sequence. Thus, the minimum and maximum number of critical values of fault currents in this example (of only one operating sequence) is two and six, respectively. Thus, each operating sequence can have a minimum of two critical values of fault currents and the maximum number of critical values of fault current is two times the number of protective devices present in that sequence.

In the IEEE 33-bus system, there is 7 operating sequences resulting into a total of 19 operating devices in these sequences (as can be observed from Table 6.1). Thus, the total number of critical values of fault currents in a given network configuration in this system is 38 ($= 2 \times 19$) as can be observed from Table 6.1. It is to be noted that the maximum possible number of the critical values is 38 as each protective device of a sequence has 2 critical values of fault currents whereas, the minimum possible number of the critical values of fault currents is 14 ($= 2 \times 7$) as each sequence can have only 2 critical values (which are same for all protective devices participating in that operating sequence).

In view of the above observations, although the total number of primary-backup operations is equal to 9388×32 in all the feasible configurations, the effective number of primary-backup operations is in between 14 to 38 depending on the network operating conditions.

6.6.1.3 Results without DG in the IEEE 33-bus system

In this case, only substation is supplying all the loads through bus 1. The critical values of fault currents passing through the protective devices obtained in all feasible configurations are given in Table 6.2. From this table, it is observed that there are only 14 critical cases of operation under all feasible network configurations. It is to be noted that symbol '$-$' in various tables represent that the value of fault current for that particular fuse is of no interest (because the current does not pass through them) for the fault on the corresponding node at that configuration.

Table 6.2: Critical values of fault currents through various protective devices in all feasible radial network configurations without DG in the IEEE 33-bus system

Sl. No.	Configuration (absent lines)	Faulted node	Fault currents passing through various protective devices (A)						
			Recloser	Fuse 1	Fuse 2	Fuse 3	Fuse 4	Fuse 5	Fuse 6
1	33, 34, 35, 36, 37	2	4410	-	-	-	-	-	-
2	28, 33, 34, 35, 36	2	4411	-	-	-	-	-	-
3	6, 21, 23, 31, 34	32	417	412	-	-	-	-	-
4	20, 34, 35, 36, 37	19	3995	3994	-	-	-	-	-
5	18, 34, 35, 36, 37	3	3607	-	3606	-	-	-	-
6	16, 14, 30, 35, 37	3	3637	-	3636	-	-	-	-
7	7, 11, 28, 34, 35	12	503	-	499	495	-	-	-
8	6, 14, 23, 30, 35	23	2964	-	2962	2961	-	-	-
9	11, 14, 19, 24, 31	6	1871	-	1868	-	1866	-	-
10	6, 14, 26, 30, 35	4	3153	-	3151	-	3150	-	-
11	6, 8, 11, 14, 37	11	451	-	447	-	443	433	-
12	3, 14, 26, 30, 35	26	1866	-	1863	-	1860	1856	-
13	11, 19, 32, 34, 35	33	430	-	426	-	422	-	412
14	7, 25, 30, 33, 34	7	1684	-	1680	-	1678	-	1673
I_{Lmax}			210	18	187	48	135	65	58

The optimum settings of TDSs for recloser and fuse constants for all the fuses obtained using the proposed approach for all feasible radial configurations without considering DG are given in Table 6.3. The resulting TCC curves of recloser and fuses using their optimum coordination results obtained without considering DG in all feasible radial configurations are shown in Figure 6.6.

Table 6.3: Optimum values of TDSs of the recloser and constants of all fuses without DG in the IEEE 33-bus system

Recloser settings			Fuse settings						
Modes	PCS (A)	TDS	Constants	F1	F2	F3	F4	F5	F6
Fast	275	0.5000	a	-1.6614	-1.6614	-1.6614	-1.6614	-1.6614	-1.6614
Slow	275	3.4268	b	12.8043	12.7127	12.4436	12.5127	12.2441	12.3127

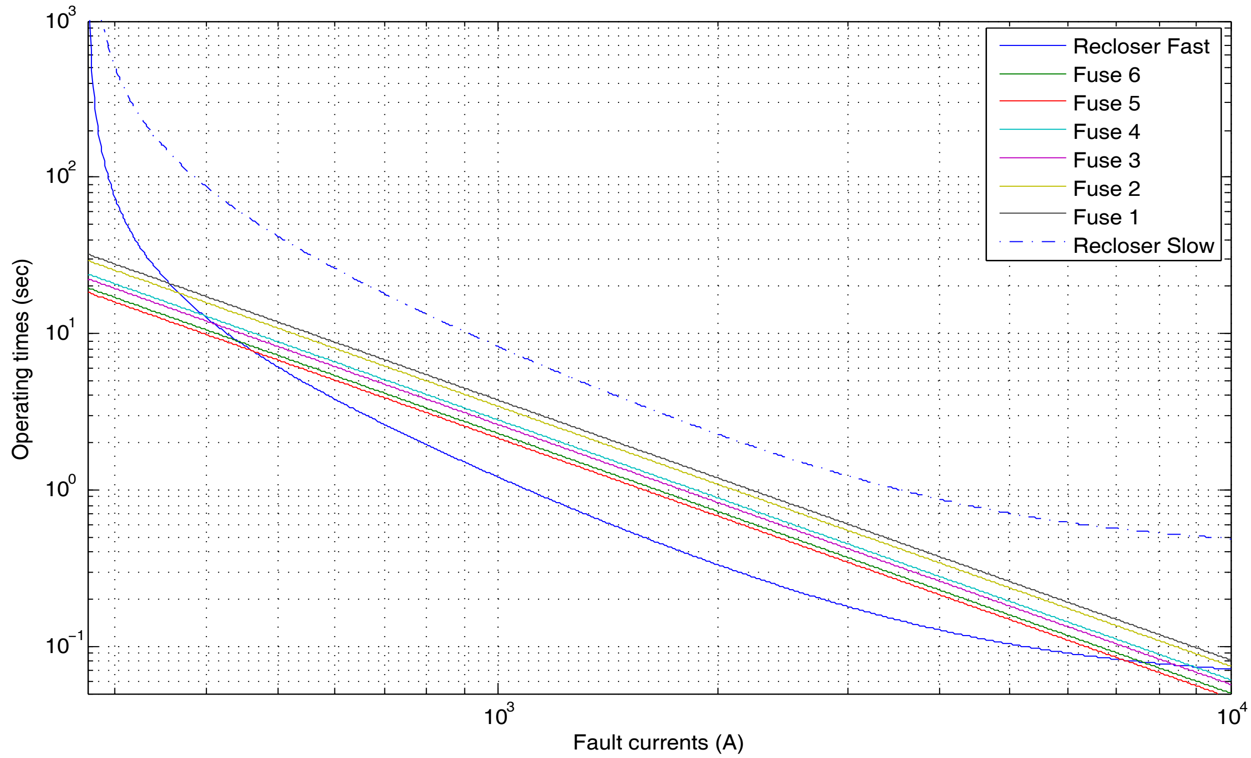

Figure 6.6: Optimum TCC curves of the protective devices without considering DG in the IEEE 33-bus system.

From Table 6.3, it is observed that the optimum values of TDSs for the fast and the slow modes of operation of the recloser for the network without DG are 0.5 and 3.4268, respectively. Further, from Table 6.3, it is observed that fuse constant a is -1.6614 for all the fuses. Also, fuse constant b for F4 is higher than that for F5 and F6, while for F2 fuse constant b is higher than that for F3 and F4 confirming the correct coordination sequences 1-7 as mentioned in Table 6.1.

From Figure 6.6, it is observed that the optimum coordinated characteristic curves of the fuses lie well inside the operating times of recloser fast and slow modes of operation. Further, the operating sequences of the fuses are also maintained as mentioned in Table 6.1 while maintaining MFCTI among the fuses.

The optimum DG locations and injections in the IEEE 33-bus system have been widely studied in the literature [147, 148, 150] for two cases. These cases are: i) DG at single location [147, 148] and ii) DGs at multiple locations [150]. The optimum location of the DG in the first case is at bus 6 with an optimum injection of 2.48 MW at unity power factor whereas, the optimum locations of the DGs in the second case are at buses 31, 32 and 33 with respective injections of 0.5586 MW, 0.5258

MW and 0.5840 MW at unity power factor. In subsequent subsections, coordination of recloser and fuses in the presence of DGs, for reconfigurable radial distribution system, is discussed.

6.6.1.4 Results in the presence of a single DG in the IEEE 33-bus system

In this case, one DG having a short circuit capacity of 25 MVA has been considered at bus 6 with 2.48 MW injections at unity power factor [147, 148].

The critical values of fault currents passing through the protective devices in all feasible configurations are given in Table 6.4. From Table 6.4, it is observed that the fault current pattern is very much different than that obtained without the presence of DG. Also, as in previous case, it is observed from this table that there are only 14 critical cases of operation under all credible network configurations.

Table 6.4: Critical values of fault currents through various protective devices in all feasible radial configurations in the presence of a single DG in the IEEE 33-bus system

Sl. No.	Configuration (absent lines)	Faulted node	Fault currents passing through various protective devices (A)						
			Recloser	Fuse 1	Fuse 2	Fuse 3	Fuse 4	Fuse 5	Fuse 6
1	33 , 34 , 35 , 36 , 37	2	4410	-	933	-	933	-	-
2	32 , 33 , 34 , 35 , 37	2	4411	-	934	-	934	-	-
3	11 , 15 , 19 , 25 , 33	32	354	418	-	-	-	-	-
4	9 , 13 , 20 , 27 , 31	19	3900	4727	844	-	844	-	-
5	9 , 13 , 18 , 25 , 30	3	3607	-	3606	-	1030	-	-
6	20 , 21 , 26 , 32 , 34	3	3637	-	3636	-	964	-	-
7	9 , 24 , 31 , 33 , 34	12	425	-	421	508	-	-	-
8	20 , 26 , 32 , 34 , 35	23	2822	-	2819	3591	775	-	-
9	8 , 9 , 15 , 18 , 25	6	1871	-	1868	-	1866	-	-
10	20 , 21 , 28 , 32 , 34	4	3153	-	3151	-	3150	-	-
11	17 , 20 , 21 , 25 , 34	11	341	-	336	-	332	472	-
12	20 , 21 , 26 , 32 , 34	26	1836	-	1832	-	1829	2771	-
13	8, 11 , 14 , 27 , 33	33	315	-	311	-	307	-	446
14	11 , 14 , 18 , 27 , 31	7	1554	-	1550	-	1547	-	2346
I_{Lmax}			215	100	208	140	174	117	102

The optimum settings of TDSs for recloser and fuse constants for all fuses considering all feasible radial configurations in the presence of single DG are given in Table 6.5. The resulting TCC curves of recloser and fuses corresponding to the optimum coordination results are shown in Figure 6.7.

From Table 6.5, it is observed that the optimum values of TDSs for the fast and the slow modes of operation of the recloser for the network for this case are 0.5 and 4.9913, respectively. Further, from Table 6.5, it is observed that fuse constant a is -2.1906 for all the fuses. From this table, it is

Table 6.5: Optimum values of TDSs of the recloser and constants of all fuses in the presence of single DG in the IEEE 33-bus system

Recloser settings			Fuse settings						
Modes	PCS (A)	TDS	Constants	F1	F2	F3	F4	F5	F6
Fast	275	0.5000	*a*	-2.1906	-2.1906	-2.1906	-2.1906	-2.1906	-2.1906
Slow	275	4.9913	*b*	17.5857	17.5857	17.1324	17.3857	16.9097	17.1857

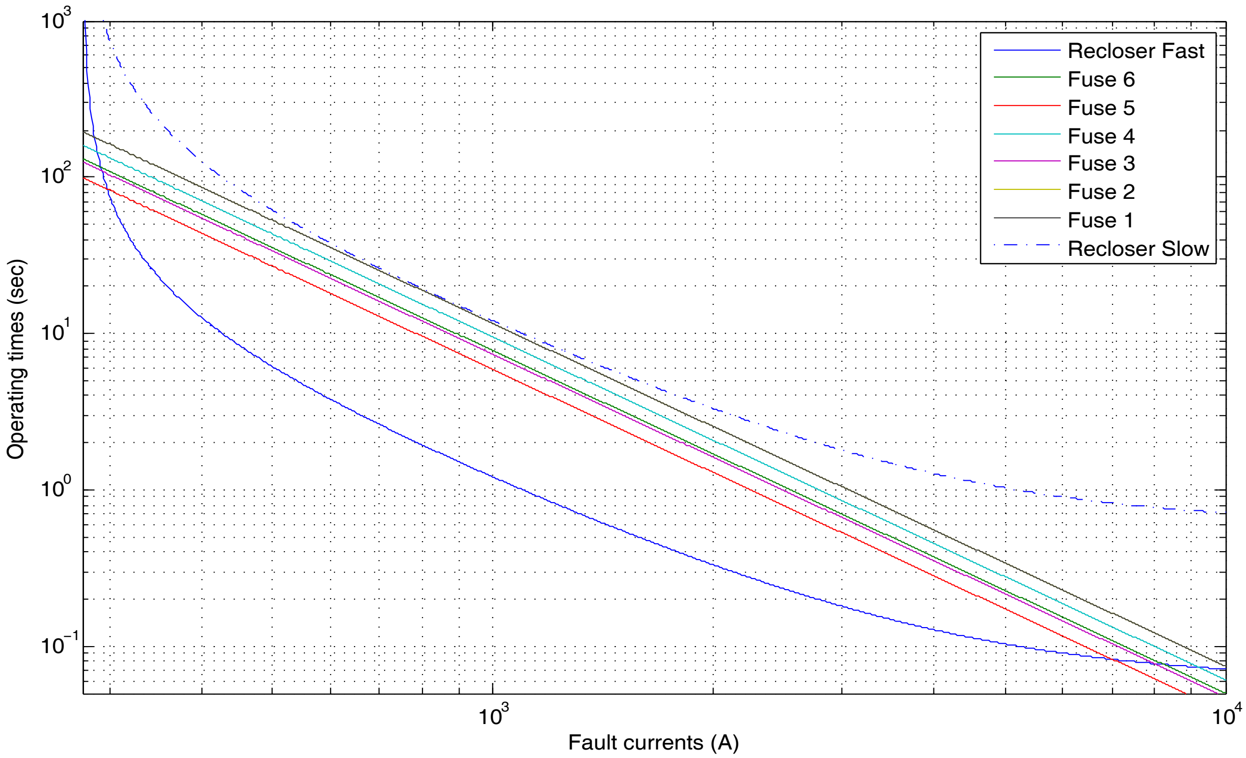

Figure 6.7: Optimum TCC curves of the protective devices in the presence of single DG in the IEEE 33-bus system.

observed that fuse constant b for F4 is higher than that for F5 and F6, while for F2, the constant b is higher than that for F3 and F4 confirming the correct operating sequences 1-7 mentioned in Table 6.1. Thus, the obtained results can provide proper coordination among the protective devices for any fault in the system under all feasible configurations in the presence of single DG.

Similar to the previous case, from Figure 6.7, it is observed that the optimum coordinated characteristic curves of fuses lie well inside the operating times of recloser fast and slow modes of operation. Additionally, the operating sequences of the fuses are also maintained as mentioned in Table 6.1. Thus, the obtained recloser settings and fuse constants can provide protection in all feasible radial configurations in the presence of a single DG.

6.6.1.5 Results in the presence of multiple DGs in the IEEE 33-bus system

In this case, multiple DGs are located at three different locations, i.e., bus 31, 32 and 33 with real power injections of 0.5586 MW, 0.5258 MW and 0.5840 MW, respectively. Further, it is assumed that all the DGs are operating at unity power factor with a short-circuit level of 10 MVA each.

The critical values of fault currents passing through the protective devices in the presence of multiple DGs are given in Table 6.6. This table shows 38 critical primary-backup cases of operation under all feasible network configurations. From Table 6.6, it is observed that the fault current pattern is very much different than that obtained in the presence of a single DG (Table 6.4) and without any DG (Table 6.2). It is to be noted that the fault current passing through the protective devices in Sl. Nos. 11, 13, 15, 23, 25, 27, and 29 are less than the corresponding load currents. So, these critical cases of operation need not be considered while calculating the optimum protection coordination settings because the recloser will not operate in these cases. Also, it has been observed that there are a total of 91 such cases of operation (among 9388$\times$32 operations) where fault currents passing through the recloser is less than the corresponding load currents. In such operating sequences, fuse will operate before the fast mode operation of recloser and remove the faulted portion of the network.

The optimum settings of TDSs for recloser and fuse constants for all the fuses in this case are given in Table 6.7. The resulting TCC curves of recloser and fuses are shown in Figure 6.8.

From Table 6.7, it is observed that the optimum values of TDSs for the fast and the slow modes of operation of the recloser for the network considering the presence of multiple DGs are 0.5 and 3.7889, respectively. Further, from Table 6.7, it is observed that fuse constant a is -1.9483 for all the fuses. Also, fuse constant b for F4 is higher than that for F5 and F6, while for F2, fuse constant b is higher than that for F3 and F4 confirming the correct operating sequences 1-7 mentioned in Table 6.1.

Similar to the previous cases, from Figure 6.8, it is observed that the optimum coordinated characteristic curves of fuses lie well inside the operating times of recloser fast and slow modes of operation and the operating sequences of the fuses are also maintained as mentioned in Table 6.1. Thus, the obtained protection coordination results can provide protection in all feasible radial

Table 6.6: Critical values of fault currents through various protective devices in all feasible radial configurations in the presence of multiple DGs in the IEEE 33-bus system

Sl. No.	Configuration (absent lines)	Faulted node	Fault currents passing through various protective devices (A)						
			Recloser	Fuse 1	Fuse 2	Fuse 3	Fuse 4	Fuse 5	Fuse 6
1	33 , 34 , 35 , 36 , 37	2	4410	-	770	770	-	-	-
2	32 , 33 , 34 , 35 , 37	2	4411	-	769	769	-	-	-
3	11 , 15 , 18 , 27 , 35	32	376	402	-	-	-	-	-
4	6 , 12 , 24 , 31 , 35	19	3988	3987	-	-	-	-	-
5	14 , 16 , 18 , 25 , 33	22	380	376	-	-	-	-	-
6	7 , 12 , 25 , 33 , 34	19	3900	4680	815	546	269	-	269
7	6 , 12 , 25 , 33 , 36	3	3541	333	3843	-	-	-	-
8	20 , 21 , 28 , 34 , 36	3	3630	-	3629	-	685	685	-
9	9 , 13 , 18 , 25 , 30	3	3607	-	3606	-	690	690	-
10	14 , 15 , 20 , 21 , 27	3	3547	366	3893	-	-	-	-
11	19 , 25 , 34 , 35 , 36	10	103	-	99	95	-	-	-
12	19 , 27 , 32 , 33 , 34	23	2938	-	2936	2935	-	-	-
13	19 , 25 , 32 , 34 , 35	10	103	-	98	95	-	-	-
14	14 , 19 , 27 , 30 , 35	23	2839	292	3113	3112	-	-	-
15	19 , 25 , 32 , 33 , 34	10	103	-	98	94	-	-	-
16	8 , 9 , 28 , 31 , 33	23	2809	-	2806	3443	644	431	-
17	6 , 12 , 21 , 27 , 32	6	1722	-	1822	306	2124	-	-
18	19 , 26 , 32 , 33 , 34	4	3137	-	3135	-	3134	696	-
19	9 , 13 , 15 , 26 , 33	6	1723	-	1719	370	2084	-	-
20	14 , 19 , 26 , 31 , 35	4	3029	311	3324	-	3323	-	-
21	8 , 9 , 15 , 18 , 25	6	1871	-	1868	-	1866	410	477
22	14 , 19 , 26 , 30 , 35	4	2997	-	3188	536	3723	-	-
23	21 , 33 , 34 , 36 , 37	9	76	-	72	-	68	57	-
24	19 , 26 , 32 , 33 , 34	26	1830	-	1827	-	1824	1820	-
25	21 , 33 , 34 , 36 , 37	9	76	-	72	-	68	57	-
26	14 , 19 , 25 , 34 , 35	26	1744	-	1910	-	1907	1903	-
27	21 , 33 , 34 , 36 , 37	9	76	-	72	-	68	57	-
28	14 , 19 , 25 , 33 , 34	26	1638	-	1739	291	2028	2023	-
29	21 , 33 , 34 , 36 , 37	9	76	-	72	-	68	57	-
30	7 , 14 , 24 , 32 , 33	26	1720	-	1716	-	1899	2321	443
31	7 , 9 , 23 , 32 , 33	19	314	-	309	-	334	-	323
32	7 , 14 , 25 , 31 , 33	7	1650	-	1646	-	1644	-	1639
33	7 , 9 , 23 , 32 , 33	19	314	-	309	-	334	-	323
34	11 , 12 , 15 , 20 , 37	7	1573	-	1722	-	1719	-	1714
35	6 , 13 , 26 , 33 , 34	19	314	-	309	-	333	-	323
36	11 , 12 , 15 , 20 , 27	7	1470	-	1560	261	1818	-	1813
37	7 , 9 , 23 , 32 , 33	19	314	-	309	-	334	-	323
38	11 , 14 , 17 , 20 , 28	7	1558	-	1554	-	1551	638	2178
I_{Lmax}			215	100	208	140	174	117	102

Table 6.7: Optimum values of TDSs of the recloser and constants of all fuses in the presence of multiple DGs in the IEEE 33-bus system

Recloser settings			Fuse settings						
Modes	PCS (A)	TDS	Constants	F1	F2	F3	F4	F5	F6
Fast	275	0.5000	a	-1.9483	-1.9483	-1.9483	-1.9483	-1.9483	-1.9483
Slow	275	3.7889	b	15.5010	15.5010	15.0626	15.3010	14.7143	15.1010

configurations in the presence of multiple DGs in this distribution system.

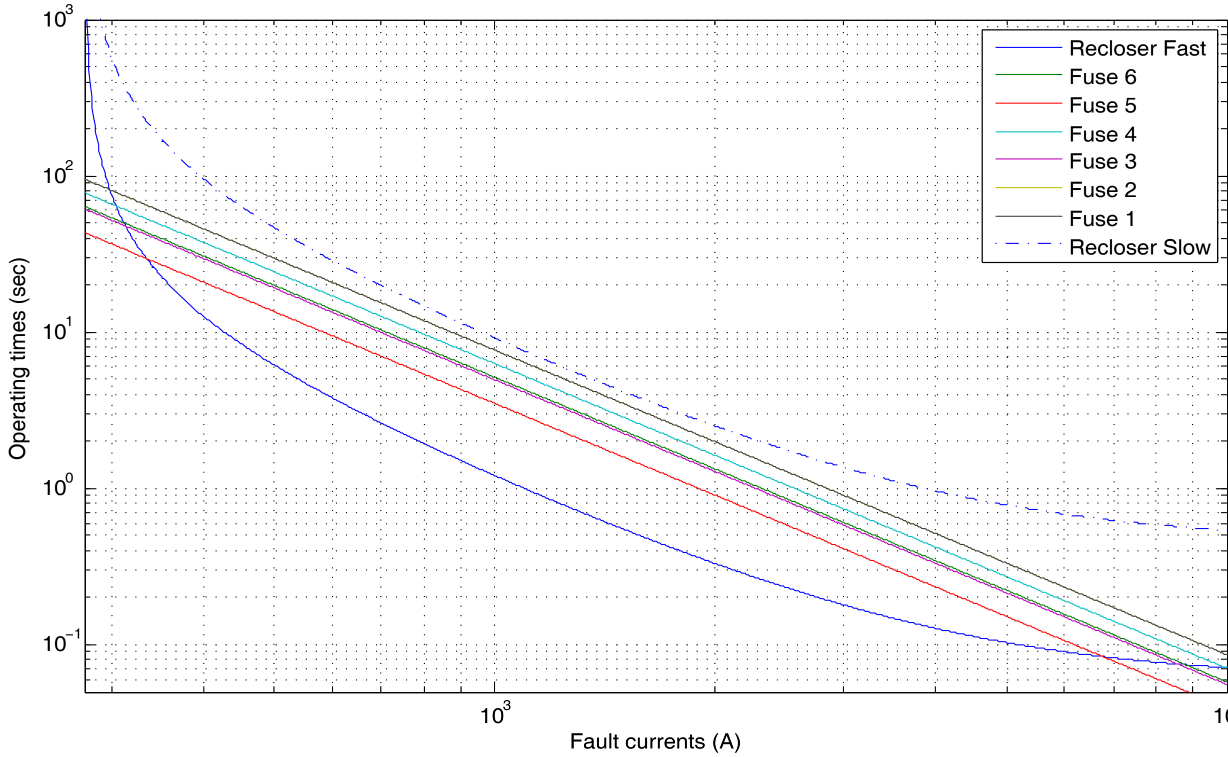

Figure 6.8: Optimum TCC curves of the protective devices in the presence of multiple DGs in the IEEE 33-bus system.

6.6.2 Results on the IEEE 69-bus system

Figure 6.9 shows the IEEE 69-bus system having 68 branches and 5 tie-switches (a total of 73 line) and supplied by a substation having a short-circuit capacity of 100 MVA. The detailed information about the system is available in [151]. For providing complete robust protection using recloser and fuses, one recloser and 13 fuses are required which are shown in the figure.

With these 13 fuses and recloser fast and slow modes of operation there are a total of 14 correct operating sequences (Table 6.8) of the protecting devices for a fault anywhere in the system under any configuration. Similar to the case of the IEEE 33-bus system, only one of the sequences of the protective devices is responsible to operate for a fault anywhere in the network under any configuration. As an example, for fault at node 52 under the base case configuration (all switches are open), the correct operating sequence of the protective devices is given in serial no. 7 in Table 6.8 where recloser in its fast mode (R_{FM}) will operate first followed by fuse no. 4 (F4), fuse no. 9 (F9) and fuse no. 8 (F8). Further, if all these devices fail to clear the fault then finally the recloser

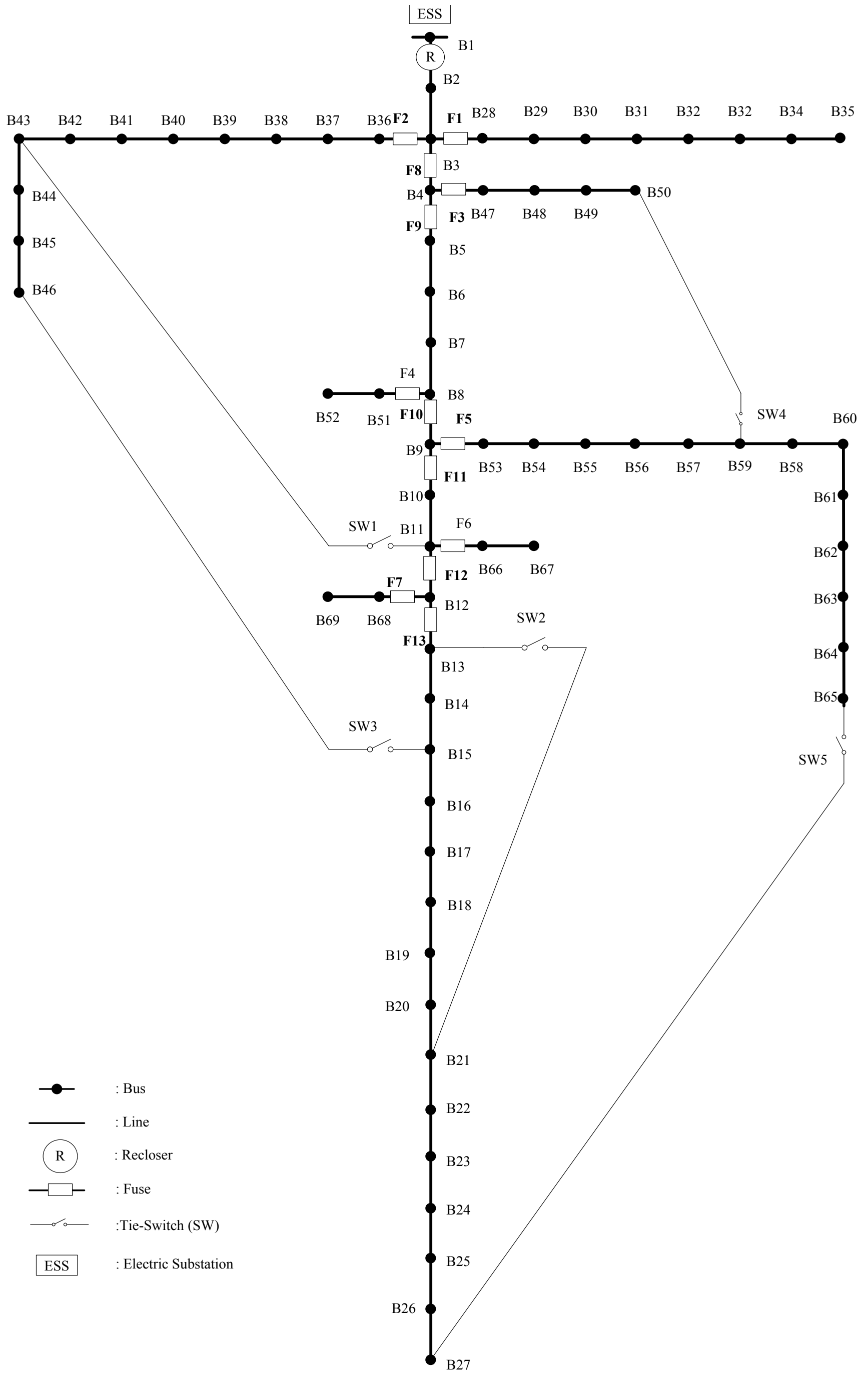

Figure 6.9: IEEE 69-bus system with tie-switches and protective devices.

in its slow mode of operation (R_{SM}) will operate to isolate the whole network. From Sl. no. 7 of Table 6.8, it is observed that F8 provides backup protection for F4 and F9 whereas F9 provides backup protection for F4. Also, it is observed that F8 provides backup protection for F3 and F9, F9 provides backup protection for F4 and F10, F10 provides backup protection for F5 and F11, F11 provides backup protection for F6 and F12, whereas F12 provides backup protection for F7 and F13, respectively. Further, it is also observed that fuses 1 to 7 (F1-F7) and fuse 13 (F13) work only as primary protection devices for any permanent fault in their respective protection zones. From Table 6.8, it is also observed that the sum of total number of operating devices in the fourteen protective devices (one recloser and thirteen fuses) is 57.

Table 6.8: Correct operating sequences of the various protective devices for fault at anywhere in the IEEE 69-bus system

Sl. No.	Correct operating sequences	No. of operating devices
1	$R_{FM} - R_{SM}$	1
2	$R_{FM} - F1 - R_{SM}$	2
3	$R_{FM} - F2 - R_{SM}$	2
4	$R_{FM} - F8 - R_{SM}$	2
5	$R_{FM} - F3 - F8 - R_{SM}$	3
6	$R_{FM} - F9 - F8 - R_{SM}$	3
7	$R_{FM} - F4 - F9 - F8 - R_{SM}$	4
8	$R_{FM} - F10 - F9 - F8 - R_{SM}$	4
9	$R_{FM} - F5 - F10 - F9 - F8 - R_{SM}$	5
10	$R_{FM} - F11 - F10 - F9 - F8 - R_{SM}$	5
11	$R_{FM} - F6 - F11 - F10 - F9 - F8 - R_{SM}$	6
12	$R_{FM} - F12 - F11 - F10 - F9 - F8 - R_{SM}$	6
13	$R_{FM} - F7 - F12 - F11 - F10 - F9 - F8 - R_{SM}$	7
14	$R_{FM} - F13 - F12 - F11 - F10 - F9 - F8 - R_{SM}$	7

6.6.2.1 Selection of feasible configurations in the IEEE 69-bus system

In the IEEE 69-bus system there are a total of 407924 possible radial network configurations (using the concepts discussed in Section 6.4). Out of these 407924 possible radial network configurations, feasible power flow solutions are obtained (i.e., the minimum and maximum values of voltage magnitude is more than 0.9 per unit and less than 1.1 p.u., respectively) for only 126169 radial network configurations. Further, to prevent reverse power flow through all the fuses placed in the network, branches 1 to 12 are kept connected so that power flow from substation to the junction points in the network is always maintained which results in a reduction of 75811 configurations. Thus, the total number of credible radial network configurations is 50358 only. Corresponding to fault on each branch of a feasible radial network, there are 68 cases of operation with different values of fault currents (using the fourteen original operating sequences of the protective devices given in Table 6.8).

Hence, there are a total of 50358×68 primary-backup cases of operation for coordination of recloser with downstream fuses.

6.6.2.2 Constraints reduction strategy in reconfigurable radial networks in the IEEE 69-bus system

In this system, the total number of operating devices present in all the fourteen operating sequences given in Table 6.8 is 57. Thus, the total number of critical values of fault currents in a given network configuration is 114 ($= 2 \times 57$). It is to be noted that the maximum possible number of the critical values is 114 as each protective device of a sequence has 2 critical values of fault currents. However, the minimum possible number of the critical values of fault currents is 28 ($= 2 \times 14$) as each sequence may have only 2 critical values (the maximum and minimum values of fault currents of one device may remain the same corresponding to the minimum and maximum values of fault currents for some other device of the sequence).

By utilizing these observations, all the primary-backup cases of operation in the fourteen operating sequences (which is equal to 50358$\times$68) can be reduced drastically to a number (depending on the network operating conditions) which lies between 28 to 114 as discussed above.

6.6.2.3 Results without DG in the IEEE 69-bus system

In this case, only substation is supplying all the loads through bus 1. The critical values of fault currents passing through the protective devices obtained in all feasible configurations are given in Table 6.9. From this table, it is observed that there are only 28 critical cases of operation in the original fourteen operating sequences under all feasible network configurations. Originally, there were a total of 114 primary-backup cases of operation in which many were repeated and hence have not been included in the table.

Table 6.9: Critical values of fault currents through various protective devices in all feasible radial network configurations without DG in the IEEE 69-bus system

	Configuration	Faulted	Fault currents passing through various protective devices (A)													
Sl. No.	(absent lines)	node	Recloser	Fuse 1	Fuse 2	Fuse 3	Fuse 4	Fuse 5	Fuse 6	Fuse 7	Fuse 8	Fuse 9	Fuse 10	Fuse 11	Fuse 12	Fuse 13
1	69,70,71,72,73	3	4553	-	-	-	-	-	-	-	-	-	-	-	-	-
2	69,70,71,72,73	2	4557	-	-	-	-	-	-	-	-	-	-	-	-	-
3	69,70,71,72,73	34	2636	2636	-	-	-	-	-	-	-	-	-	-	-	-
4	69,70,71,72,73	28	4523	4523	-	-	-	-	-	-	-	-	-	-	-	-
5	14,61,69,70,72	62	684	-	684	-	-	-	-	-	-	-	-	-	-	-
6	69,70,71,72,73	36	4523	-	4523	-	-	-	-	-	-	-	-	-	-	-
7	69,70,71,72,73	4	4543	-	-	-	-	-	-	-	4543	-	-	-	-	-
8	69,70,71,72,73	4	4543	-	-	-	-	-	-	-	4543	-	-	-	-	-

Continued on next page

Table 6.9 – continued from previous page

Sl. No.	Configuration (absent lines)	Faulted node	Fault currents passing through various protective devices (A)													
			Recloser	Fuse 1	Fuse 2	Fuse 3	Fuse 4	Fuse 5	Fuse 6	Fuse 7	Fuse 8	Fuse 9	Fuse 10	Fuse 11	Fuse 12	Fuse 13
9	14,45,53,69,70	46	618	-	-	618	-	-	-	-	618	-	-	-	-	-
10	69,70,71,72,73	47	4519	-	-	4519	-	-	-	-	4519	-	-	-	-	-
11	35,49,63,69,70	8	3177	-	-	-	-	-	-	-	3177	3177	-	-	-	-
12	20,53,69,70,71	5	4460	-	-	-	-	-	-	-	4460	4460	-	-	-	-
13	35,49,63,70,71	52	2769	-	-	-	2767	-	-	-	2769	2769	-	-	-	-
14	15,52,69,70,71	51	3135	-	-	-	3135	-	-	-	3135	3135	-	-	-	-
15	36,49,63,69,70	9	3114	-	-	-	-	-	-	-	3114	3114	3114	-	-	-
16	13,52,64,69,70	9	3187	-	-	-	-	-	-	-	3187	3187	3187	-	-	-
17	54,61,69,70,71	22	614	-	-	-	-	607	-	-	614	614	608	-	-	-
18	15,53,69,70,71	53	2986	-	-	-	-	2985	-	-	2986	2986	2985	-	-	-
19	14,35,49,61,70	62	627	-	-	-	-	-	-	-	627	627	621	620	-	-
20	13,52,69,70,73	10	2479	-	-	-	-	-	-	-	2479	2479	2477	2476	-	-
21	35,49,61,69,70	67	2152	-	-	-	-	-	2148	-	2152	2152	2149	2149	-	-
22	15,53,69,70,71	66	2222	-	-	-	-	-	2218	-	2222	2222	2219	2219	-	-
23	35,49,61,69,70	12	1873	-	-	-	-	-	-	-	1873	1873	1870	1869	1867	-
24	15,53,69,70,71	12	1941	-	-	-	-	-	-	-	1941	1941	1938	1937	1935	-
25	35,49,61,69,70	69	1577	-	-	-	-	-	-	1567	1577	1577	1573	1572	1568	-
26	13,53,69,70,73	68	1637	-	-	-	-	-	-	1627	1637	1637	1633	1632	1628	-
27	36,49,61,69,70	62	531	-	-	-	-	-	-	-	531	531	525	524	516	510
28	13,52,69,70,73	13	1541	-	-	-	-	-	-	-	1541	1541	1537	1536	1532	1530
I_{Lmax}			224	5	10	48	3	105	2	3	208	160	151	44	32	20

In this case, the optimum settings of TDSs for recloser and fuse constants for all the fuses for all feasible radial configurations are given in Table 6.10. The resulting TCC curves of recloser and fuses using their optimum coordination results are shown in Figure 6.10.

Table 6.10: Optimum values of TDSs of the recloser and constants of all fuses without DG in the IEEE 69-bus system

Recloser settings			Fuse settings													
Modes	PCS (A)	TDS	Constants	F1	F2	F3	F4	F5	F6	F7	F8	F9	F10	F11	F12	F13
Fast	300	0.5000	a	-1.4602	-1.4602	-1.4602	-1.4602	-1.4602	-1.4602	-1.4602	-1.4602	-1.4602	-1.4602	-1.4602	-1.4602	-1.4602
Slow	300	7.4544	b	11.9659	11.9659	11.8159	11.2291	10.9992	10.6007	10.3715	12.0159	11.8159	11.6159	11.4159	11.2159	11.0159

From Table 6.10, it is observed that the optimum values of TDSs for the fast and the slow modes of operation of the recloser for the network without DG are 0.5 and 7.4544, respectively. Further, the fuse constant a is -1.4602 for all the fuses and the fuse constant b for all the fuses are progressively higher than the corresponding primary one which confirms the correct coordination sequence 1-14 mentioned in Table 6.8. From Figure 6.10, it is observed that the optimum coordinated characteristic curves of the fuses lie well inside the operating times of recloser fast and slow modes of operation. Further, the operating sequences of the fuses are also maintained as

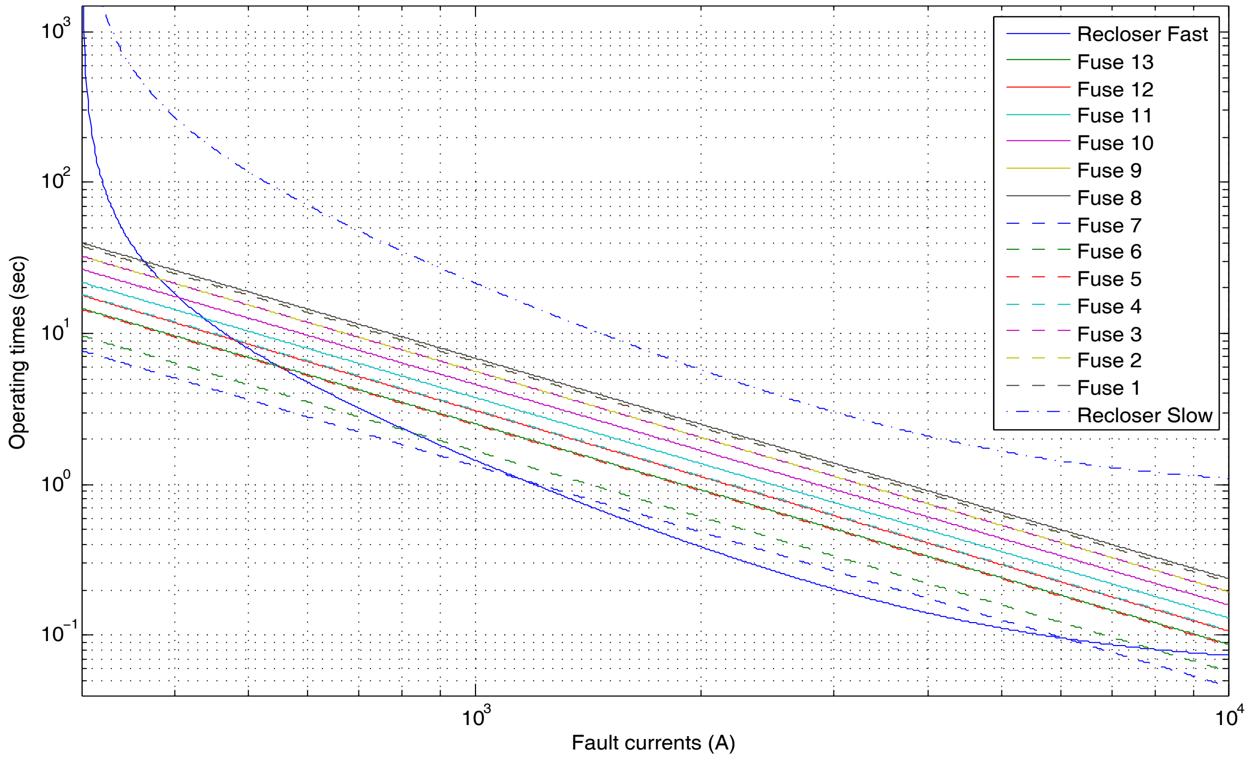

Figure 6.10: Optimum TCC curves of the protective devices without considering DG in the IEEE 69-bus system.

mentioned in Table 6.8 while maintaining MFCTI among the fuses. Therefore, the recloser-fuse settings obtained can provide protection of the system under all the credible configurations without considering DG in the IEEE 69-bus system.

6.6.2.4 Results in the presence of a single DG in the IEEE 69-bus system

In this case, one DG having a short circuit capacity of 20 MVA has been considered at bus 61 with 1.81 MW generation at unity power factor [147, 148].

The critical values of fault currents passing through the protective devices for this case are given in Table 6.11. From this table, it is observed that there are only 53 critical cases of operation in the original fourteen operating sequences under all the credible network configurations. As discussed in the previous case, in this case also originally there were a total of 114 primary-backup cases of operation in which many were duplicated. After ignoring the duplicate cases, the total number of critical cases of operation is reduced to 53 only.

Table 6.11: Critical values of fault currents through various protective devices in all feasible radial configurations in the presence of a single DG in the IEEE 69-bus system

Sl. No.	Configuration (absent lines)	Faulted node	Fault currents passing through various protective devices (A)													
			Recloser	Fuse 1	Fuse 2	Fuse 3	Fuse 4	Fuse 5	Fuse 6	Fuse 7	Fuse 8	Fuse 9	Fuse 10	Fuse 11	Fuse 12	Fuse 13
1	38,69,70,72,73	3	4553	-	-	-	-	-	-	-	-	-	-	-	-	-
2	35,44,49,61,70	2	4557	-	-	-	-	-	-	-	-	-	-	-	-	-
3	38,69,70,72,73	34	2404	2754	-	-	-	-	-	-	-	-	-	-	-	-
4	54,69,70,71,73	28	4518	5168	-	-	-	-	-	-	-	-	-	-	-	-
5	58,69,70,71,73	34	2413	2719	-	-	-	-	-	-	-	-	-	-	-	-
6	15,58,69,70,71	28	4518	5177	-	-	-	-	-	-	-	-	-	-	-	-
7	14,54,61,69,70	62	605	-	688	-	-	-	-	-	-	-	-	-	-	-
8	23,53,69,70,71	36	4518	-	5168	-	-	-	-	-	-	-	-	-	-	-
9	14,49,61,69,70	62	611	-	686	-	-	-	-	-	-	-	-	-	-	-
10	13,45,52,69,70	36	4518	-	5177	-	-	-	-	-	-	-	-	-	-	-
11	21,52,69,70,71	4	4543	-	-	-	-	-	-	-	4543	-	-	-	-	-
12	14,45,53,69,70	46	526	-	-	526	-	-	-	-	526	-	-	-	-	-
13	58,69,70,71,73	47	4519	-	-	4519	-	-	-	-	4519	-	-	-	-	-
14	36,49,63,69,70	47	4515	-	-	5092	-	-	-	-	4515	-	-	-	-	-
15	35,58,61,70,71	8	3041	-	-	-	-	-	-	-	3041	3472	-	-	-	-
16	14,20,23,69,72	5	4459	-	-	-	-	-	-	-	4459	4459	-	-	-	-
17	45,64,69,70,72	8	3213	-	-	-	-	-	-	-	3213	3213	-	-	-	-
18	64,69,70,71,72	5	4445	-	-	-	-	-	-	-	4445	5095	-	-	-	-
19	39,54,64,69,70	52	2604	-	-	-	2971	-	-	-	2604	2973	-	-	-	-
20	13,61,69,70,72	51	3109	-	-	-	3756	-	-	-	3109	3109	-	-	-	-
21	35,49,63,69,70	52	2716	-	-	-	3297	-	-	-	2716	2716	-	-	-	-
22	13,45,53,69,70	51	2936	-	-	-	3366	-	-	-	2936	3366	-	-	-	-
23	26,38,69,70,72	51	3088	-	-	-	3748	-	-	-	3088	3088	-	-	-	-
24	15,45,58,69,70	51	2933	-	-	-	3363	-	-	-	2933	3363	-	-	-	-
25	35,58,61,70,71	9	2975	-	-	-	-	-	-	-	2975	3397	3397	-	-	-
26	39,53,63,70,71	9	3184	-	-	-	-	-	-	-	3184	3184	3184	-	-	-
27	35,49,61,69,70	9	3150	-	-	-	-	-	-	-	3150	3150	3150	-	-	-
28	13,45,52,69,70	9	2991	-	-	-	-	-	-	-	2991	3429	3429	-	-	-
29	21,44,69,70,72	22	555	-	-	-	-	547	-	-	555	555	549	-	-	-
30	14,61,69,70,72	53	2983	-	-	-	-	2982	-	-	2983	2983	2982	-	-	-
31	13,53,69,70,71	53	2781	-	-	-	-	3186	-	-	2781	3187	3186	-	-	-
32	14,35,49,61,70	62	540	-	-	-	-	-	-	-	540	540	534	646	-	-
33	13,61,69,70,72	10	2353	-	-	-	-	-	-	-	2353	2353	2351	2851	-	-
34	45,63,69,70,72	10	2260	-	-	-	-	-	-	-	2260	2590	2588	2587	-	-
35	14,35,58,61,70	62	563	-	-	-	-	-	-	-	563	639	634	632	-	-
36	35,58,61,69,70	67	1983	-	-	-	-	-	2260	-	1983	2264	2261	2261	-	-
37	13,61,69,70,72	66	2072	-	-	-	-	-	2507	-	2072	2072	2069	2508	-	-
38	35,49,61,70,71	67	2027	-	-	-	-	-	2466	-	2027	2027	2024	2467	-	-
39	39,49,63,70,71	66	2009	-	-	-	-	-	2298	-	2009	2302	2299	2299	-	-
40	35,58,61,70,71	67	1984	-	-	-	-	-	2260	-	1984	2264	2261	2261	-	-
41	35,58,61,69,70	12	1712	-	-	-	-	-	-	-	1712	1954	1951	1950	1948	-
42	20,45,58,61,69	12	1775	-	-	-	-	-	-	-	1775	1775	1771	2146	2144	-
43	36,58,61,69,70	12	1729	-	-	-	-	-	-	-	1729	1729	1725	2102	2100	-
44	15,54,69,70,71	12	1741	-	-	-	-	-	-	-	1741	1994	1991	1990	1988	-
45	35,49,63,69,70	69	1427	-	-	-	-	-	-	1727	1427	1427	1422	1732	1729	-
46	14,61,69,70,72	68	1467	-	-	-	-	-	-	1766	1467	1467	1462	1771	1768	-
47	44,49,61,69,70	68	1457	-	-	-	-	-	-	1659	1457	1669	1665	1664	1660	-
48	20,35,58,61,69	69	1433	-	-	-	-	-	-	1624	1433	1634	1630	1629	1626	-
49	35,49,61,69,70	62	456	-	-	-	-	-	-	-	456	456	450	542	534	528
50	42,45,64,70,72	13	1373	-	-	-	-	-	-	-	1373	1567	1563	1562	1558	1556
51	14,35,49,63,70	13	1369	-	-	-	-	-	-	-	1369	1567	1563	1562	1558	1556
52	35,58,61,69,70	62	477	-	-	-	-	-	-	-	477	540	535	533	526	520
53	14,61,69,70,72	13	1372	-	-	-	-	-	-	-	1372	1372	1367	1656	1652	1650
I_{Lmax}			159	5	47	111	61	61	50	72	154	130	121	75	63	51

In this case, the optimum settings of TDSs for recloser and fuse constants for all the fuses are given in Table 6.12. The resulting TCC curves of recloser and fuses using their optimum coordination results are shown in Figure 6.11.

Table 6.12: Optimum values of TDSs of the recloser and constants of all fuses in the presence of single DG in the IEEE 69-bus system

Recloser settings			Fuse settings													
Modes	PCS (A)	TDS	Constants	F1	F2	F3	F4	F5	F6	F7	F8	F9	F10	F11	F12	F13
Fast	300	0.5000	a	-1.6146	-1.6146	-1.6146	-1.6146	-1.6146	-1.6146	-1.6146	-1.6146	-1.6146	-1.6146	-1.6146	-1.6146	-1.6146
Slow	300	7.4544	b	13.4838	13.4838	13.3084	12.7677	12.3831	12.0621	11.828	13.5126	13.3126	13.1126	12.9126	12.7126	12.5126

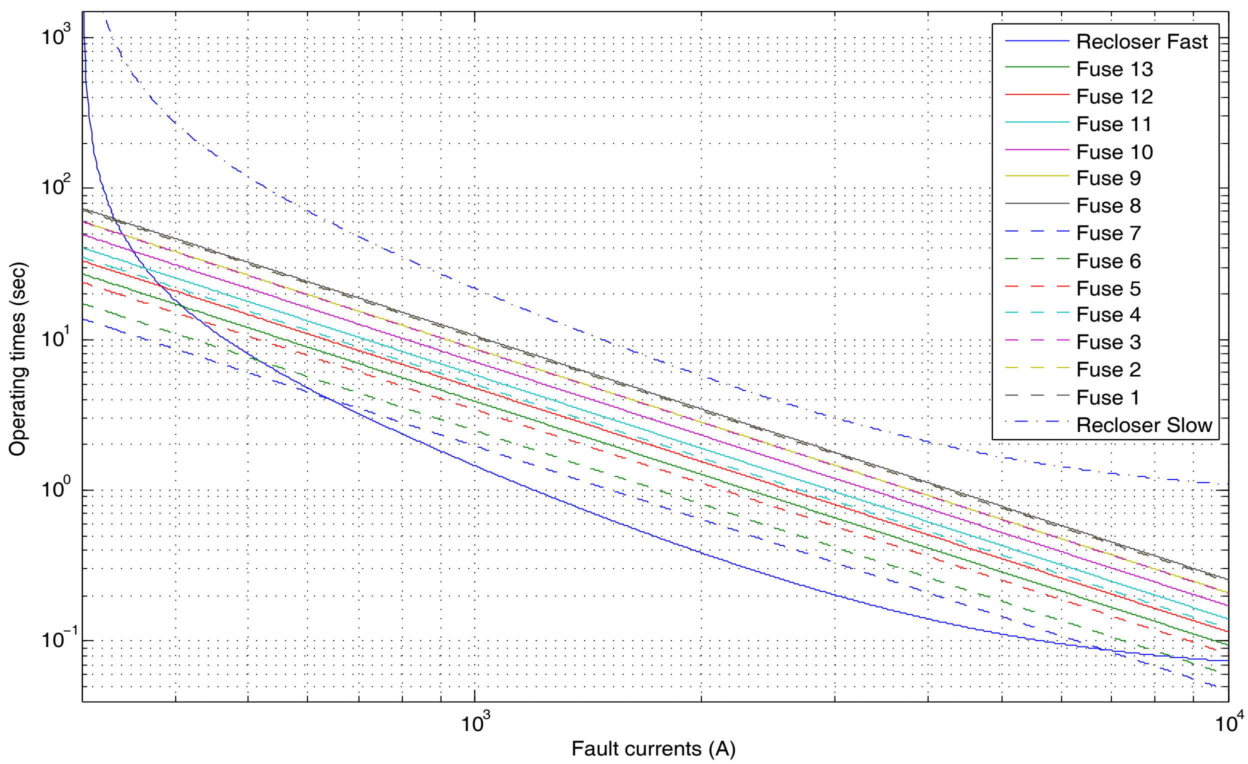

Figure 6.11: Optimum TCC curves of the protective devices in presence of single DG in the IEEE 69-bus system.

From Table 6.12, it is observed that the optimum values of TDSs for the fast and the slow modes of operation of the recloser are the same as that obtained without DG as given in Table 6.10. However, fuse constant a and b are different in the presence of single DG than those obtained without DG for all the fuses. In this case also, fuse constant b for all the fuses are progressively higher than the corresponding primary one which confirms the correct coordination sequence 1-14 mentioned in Table 6.8. Similar to the previous case, from Figure 6.11, it is observed that the optimum coordinated characteristic curves of fuses lie well inside the operating times of recloser fast and slow modes of operation. Thus, the obtained results can provide proper coordination among the protective devices for any fault in the system under all the feasible configurations in the presence of single DG.

6.6.2.5 Results in the presence of multiple DGs in the IEEE 69-bus system

In this case, multiple DGs are located at three different locations, i.e., bus 60, 61 and 62 with respective injections of 0.3525 MW, 1.0666 MW and 0.4527 MW, respectively, at unity power factor with a short-circuit level of 10 MVA each.

The critical values of fault currents for this case are given in Table 6.13. From this table, it is observed that there are only 81 critical cases of operation in the original fourteen operating sequences under all the credible network configurations. As discussed in two previous cases, in this case also, originally there were a total of 114 primary-backup operating sequences in which a few were repeated ones which have not been included in the table.

Table 6.13: Critical values of fault currents through various protective devices in all feasible radial configurations in the presence of multiple DGs in the IEEE 69-bus system

Sl. No.	Configuration (absent lines)	Faulted node	Fault currents passing through various protective devices (A)													
			Recloser	Fuse 1	Fuse 2	Fuse 3	Fuse 4	Fuse 5	Fuse 6	Fuse 7	Fuse 8	Fuse 9	Fuse 10	Fuse 11	Fuse 12	Fuse 13
1	36,70,71,72,73	3	4553	-	-	-	-	-	-	-	-	-	-	-	-	-
2	35,44,53,63,70	2	4557	-	-	-	-	-	-	-	-	-	-	-	-	-
3	38,58,63,69,70	34	2301	2805	-	-	-	-	-	-	-	-	-	-	-	-
4	23,39,70,71,72	28	4517	5205	-	-	-	-	-	-	-	-	-	-	-	-
5	49,63,69,70,71	34	2358	2717	-	-	-	-	-	-	-	-	-	-	-	-
6	20,36,53,61,69	28	4515	5504	-	-	-	-	-	-	-	-	-	-	-	-
7	14,58,62,69,70	63	594	-	700	-	-	-	-	-	-	-	-	-	-	-
8	14,49,61,69,70	36	4518	-	5121	-	-	-	-	-	-	-	-	-	-	-
9	14,49,62,69,70	63	607	-	696	-	-	-	-	-	-	-	-	-	-	-
10	39,54,70,71,73	36	4515	-	5504	-	-	-	-	-	-	-	-	-	-	-
11	20,42,61,69,72	4	4542	-	-	-	-	-	-	-	4848	-	-	-	-	-
12	23,53,69,70,71	4	4543	-	-	-	-	-	-	-	4543	-	-	-	-	-
13	14,45,53,69,70	46	481	-	-	481	-	-	-	-	481	-	-	-	-	-
14	58,69,70,71,73	47	4519	-	-	4519	-	-	-	-	4519	-	-	-	-	-
15	42,61,70,71,72	47	4516	-	-	4820	-	-	-	-	4820	-	-	-	-	-
16	14,49,61,69,70	47	4513	-	-	5427	-	-	-	-	4816	-	-	-	-	-
17	14,58,61,69,70	8	2970	-	-	-	-	-	-	-	3170	3614	-	-	-	-
18	14,17,36,61,72	5	4459	-	-	-	-	-	-	-	4459	4459	-	-	-	-
19	35,58,63,69,70	8	2980	-	-	-	-	-	-	-	2980	3530	-	-	-	-

Continued on next page

Table 6.13 – continued from previous page

Sl. No.	Configuration (absent lines)	Faulted node	Fault currents passing through various protective devices (A)													
			Recloser	Fuse 1	Fuse 2	Fuse 3	Fuse 4	Fuse 5	Fuse 6	Fuse 7	Fuse 8	Fuse 9	Fuse 10	Fuse 11	Fuse 12	Fuse 13
20	14,49,61,69,70	5	4451	-	-	-	-	-	-	-	4750	4750	-	-	-	-
21	35,49,63,70,71	8	3214	-	-	-	-	-	-	-	3214	3214	-	-	-	-
22	20,49,61,69,71	5	4437	-	-	-	-	-	-	-	4736	5400	-	-	-	-
23	44,53,61,69,70	52	2523	-	-	-	3068	-	-	-	2693	3070	-	-	-	-
24	14,63,69,70,72	51	3100	-	-	-	3941	-	-	-	3100	3100	-	-	-	-
25	39,45,49,61,70	52	2540	-	-	-	3007	-	-	-	2540	3009	-	-	-	-
26	13,61,69,70,72	51	3004	-	-	-	3883	-	-	-	3206	3206	-	-	-	-
27	20,35,49,61,71	52	2675	-	-	-	3567	-	-	-	2675	2675	-	-	-	-
28	39,49,61,70,71	51	2849	-	-	-	3468	-	-	-	3041	3468	-	-	-	-
29	44,69,70,72,73	51	3080	-	-	-	3932	-	-	-	3080	3080	-	-	-	-
30	20,35,58,61,69	51	2870	-	-	-	3412	-	-	-	2870	3412	-	-	-	-
31	13,58,61,69,70	9	2904	-	-	-	-	-	-	-	3100	3534	3534	-	-	-
32	14,63,69,70,72	9	3184	-	-	-	-	-	-	-	3184	3184	3184	-	-	-
33	38,44,49,61,70	9	2914	-	-	-	-	-	-	-	2914	3452	3452	-	-	-
34	38,63,70,71,72	9	3079	-	-	-	-	-	-	-	3286	3286	3286	-	-	-
35	45,54,69,70,73	9	3152	-	-	-	-	-	-	-	3152	3152	3152	-	-	-
36	25,53,69,70,71	9	2905	-	-	-	-	-	-	-	3100	3535	3535	-	-	-
37	21,36,69,70,72	22	510	-	-	-	-	502	-	-	510	510	504	-	-	-
38	14,63,69,70,72	53	2983	-	-	-	-	2982	-	-	2983	2983	2982	-	-	-
39	13,61,69,70,72	53	2872	-	-	-	-	3065	-	-	3066	3066	3065	-	-	-
40	14,53,61,69,70	53	2691	-	-	-	-	3274	-	-	2872	3275	3274	-	-	-
41	13,17,53,61,69	53	2757	-	-	-	-	3490	-	-	2757	3167	3166	-	-	-
42	14,35,49,62,70	63	525	-	-	-	-	-	-	-	525	525	519	660	-	-
43	36,53,64,69,70	10	2337	-	-	-	-	-	-	-	2337	2337	2335	2858	-	-
44	20,61,69,71,72	10	2241	-	-	-	-	-	-	-	2392	2392	2390	2906	-	-
45	61,69,70,71,72	10	2168	-	-	-	-	-	-	-	2314	2638	2636	2635	-	-
46	14,58,61,69,70	63	553	-	-	-	-	-	-	-	553	650	644	643	-	-
47	14,63,69,70,72	10	2306	-	-	-	-	-	-	-	2306	2306	2304	2946	-	-
48	49,63,69,70,71	67	1917	-	-	-	-	-	2328	-	2046	2332	2329	2329	-	-
49	13,20,61,69,72	66	2043	-	-	-	-	-	2814	-	2043	2043	2040	2496	-	-
50	20,35,61,71,72	67	1924	-	-	-	-	-	2275	-	1924	2279	2276	2276	-	-
51	42,61,70,71,72	66	1965	-	-	-	-	-	2544	-	2096	2096	2093	2545	-	-
52	35,49,63,69,70	67	1975	-	-	-	-	-	2533	-	1975	1975	1972	2534	-	-
53	39,63,70,71,72	66	1920	-	-	-	-	-	2332	-	2049	2336	2333	2333	-	-
54	45,58,64,69,70	67	1977	-	-	-	-	-	2587	-	1977	2269	2266	2265	-	-
55	14,63,69,70,72	66	2018	-	-	-	-	-	2575	-	2018	2018	2015	2576	-	-
56	35,58,63,70,71	67	1924	-	-	-	-	-	2274	-	1924	2278	2275	2275	-	-
57	58,61,69,70,71	12	1659	-	-	-	-	-	-	-	1659	1965	1962	1961	1959	-
58	14,20,61,69,72	12	1758	-	-	-	-	-	-	-	1758	1758	1754	2146	2144	-
59	14,20,42,61,72	12	1677	-	-	-	-	-	-	-	1789	1789	1785	2170	2168	-
60	45,54,61,69,70	12	1676	-	-	-	-	-	-	-	1676	1676	1672	2148	2146	-
61	20,42,61,71,72	12	1660	-	-	-	-	-	-	-	1771	2018	2014	2013	2011	-
62	58,63,69,70,71	12	1690	-	-	-	-	-	-	-	1690	1940	1936	1935	2198	-
63	20,40,61,69,72	12	1719	-	-	-	-	-	-	-	1719	1719	1715	2192	2190	-
64	64,69,70,71,72	12	1659	-	-	-	-	-	-	-	1659	1964	1961	1960	1958	-
65	45,58,69,70,73	12	1715	-	-	-	-	-	-	-	1715	1715	1711	2095	2354	-
66	49,63,69,70,71	69	1371	-	-	-	-	-	-	1773	1463	1463	1458	1778	1775	-
67	42,64,70,71,72	68	1421	-	-	-	-	-	-	1889	1421	1631	1626	1625	1622	-
68	35,49,63,69,70	69	1376	-	-	-	-	-	-	1755	1376	1376	1372	1760	1757	-
69	44,53,63,69,70	68	1384	-	-	-	-	-	-	1672	1477	1682	1678	1677	1673	-
70	14,35,54,61,70	69	1389	-	-	-	-	-	-	1800	1389	1593	1589	1587	1802	-
71	69,70,71,72,73	68	1414	-	-	-	-	-	-	1794	1414	1414	1409	1799	1796	-
72	35,53,61,69,70	69	1406	-	-	-	-	-	-	1867	1406	1613	1608	1607	1604	-
73	26,53,69,70,71	68	1392	-	-	-	-	-	-	1904	1392	1392	1388	1698	1906	-
74	35,53,63,69,70	69	1385	-	-	-	-	-	-	1629	1385	1639	1635	1634	1631	-
75	42,49,63,69,70	68	1420	-	-	-	-	-	-	1992	1420	1420	1416	1732	1728	-
76	35,49,62,69,70	63	442	-	-	-	-	-	-	-	442	442	436	553	545	539
77	23,39,69,70,72	13	1362	-	-	-	-	-	-	-	1362	1563	1559	1558	1554	1552

Continued on next page

Table 6.13 – continued from previous page

Sl. No.	Configuration (absent lines)	Faulted node	Fault currents passing through various protective devices (A)													
			Recloser	Fuse 1	Fuse 2	Fuse 3	Fuse 4	Fuse 5	Fuse 6	Fuse 7	Fuse 8	Fuse 9	Fuse 10	Fuse 11	Fuse 12	Fuse 13
78	52,64,69,70,71	13	1299	-	-	-	-	-	-	-	1386	1579	1575	1574	1570	1568
79	35,52,62,69,70	63	468	-	-	-	-	-	-	-	468	548	542	541	534	528
80	20,53,69,70,71	13	1321	-	-	-	-	-	-	-	1321	1321	1316	1680	1676	1674
81	45,53,64,69,70	13	1296	-	-	-	-	-	-	-	1296	1296	1291	1579	1771	1769
I_{Lmax}			157	5	45	109	63	63	48	71	153	128	119	72	60	49

In this case, the optimum settings of TDSs for recloser and fuse constants for all the fuses are given in Table 6.14. The resulting TCC curves of recloser and fuses are shown in Figure 6.12.

Table 6.14: Optimum values of TDSs of the recloser and constants of all fuses in the presence of multiple DGs in the IEEE 69-bus system

Recloser settings			Fuse settings													
Modes	PCS (A)	TDS	Constants	F1	F2	F3	F4	F5	F6	F7	F8	F9	F10	F11	F12	F13
Fast	300	0.5000	a	-1.6343	-1.6343	-1.6343	-1.6343	-1.6343	-1.6343	-1.6343	-1.6343	-1.6343	-1.6343	-1.6343	-1.6343	-1.6343
Slow	300	7.4544	b	13.753	13.753	13.5812	13.0102	12.697	12.421	12.2168	13.7812	13.5812	13.3812	13.1812	12.9812	12.7812

From Table 6.14, it is observed that for this case also, the optimum values of TDSs for the fast and the slow modes of operation of the recloser are same as obtained in the previous two cases. However, fuse constants a and b are different for all the fuses in the presence of multiple DGs than those obtained without DG and with single DG in this system. Similar to the previous two cases, fuse constant b for all the fuses are progressively higher than the corresponding primary one which confirms the correct coordination sequence 1-14 mentioned in Table 6.8. Further, from Figure 6.12, it is observed that the optimum coordinated characteristic curves of fuses lie well inside the operating times of recloser fast and slow modes of operation. Thus, the obtained results can provide proper coordination among the protective devices for any fault in the system under all the feasible configurations in the presence of multiple DGs.

6.7 Comparative assessment of recloser-fuse coordination results

In this section, to investigate the effectiveness of the recloser-fuse coordination results obtained in the two test systems (IEEE 33 and 69-bus) in three different network conditions (without DG, single DG and multiple DGs), the number of miscoordination has been calculated when the recloser and fuse settings obtained in any particular network condition are applied to all the three network

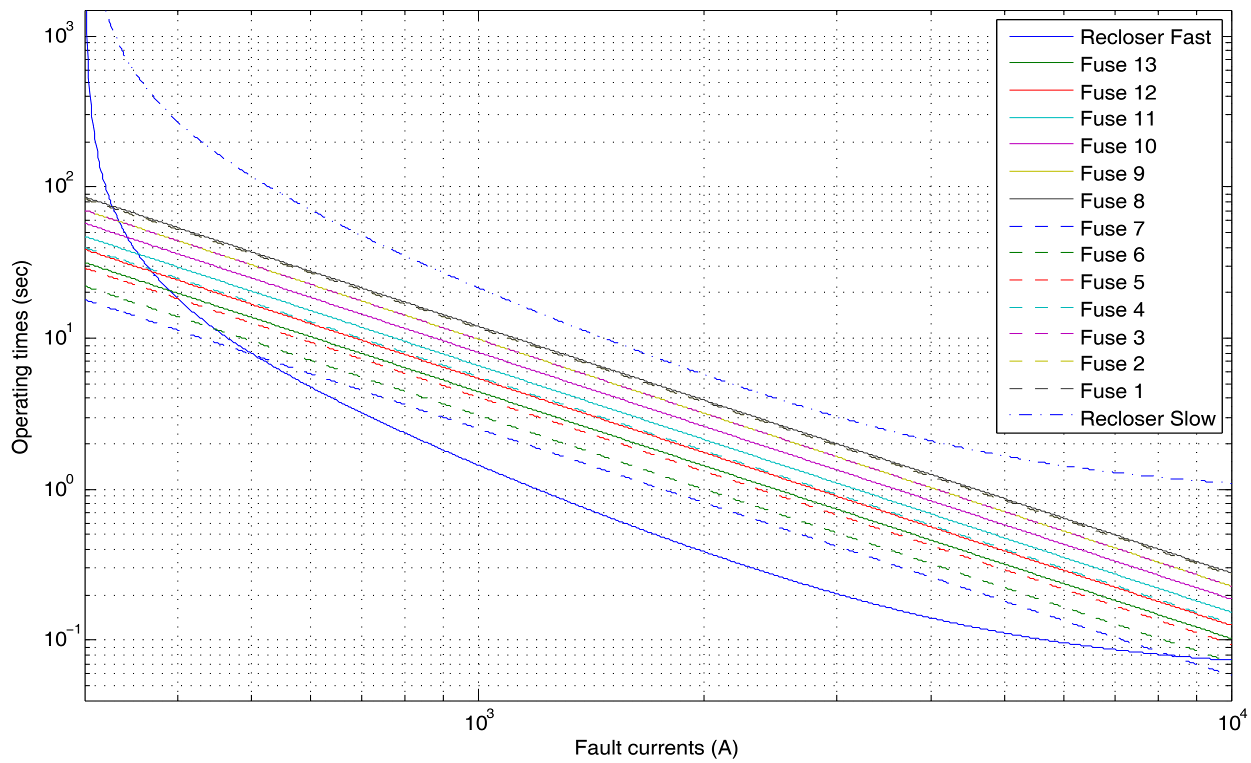

Figure 6.12: Optimum TCC curves of the protective devices in the presence of multiple DGs in the IEEE 69-bus system.

conditions. Table 6.15 gives the results of this investigation for the IEEE 33 and 69-bus radial distribution systems.

Table 6.15: Performance of various results of recloser-fuses coordination for fault currents in different situations

System	Settings obtained	Constraint violations with network condition		
		Without DG	Single DG	Multiple DGs
IEEE 33-bus	Without DG	0	78620	12203
	Single DG	0	0	91
	Multiple DGs	0	0	101
IEEE 69-bus	Without DG	0	115073	147456
	Single DG	0	0	9400
	Multiple DGs	0	0	0

From Table 6.15, it is observed that in the IEEE 33-bus system, there are 78620 and 12203 cases of constraint violations when the recloser-fuse coordination results obtained without considering DG are applied to the network in the presence of single and multiple DGs, respectively, in the IEEE 33-bus system. Also, there are 91 and 101 cases of constraint violations, respectively, when the recloser-fuse coordination results obtained in the presence of single DG and multiple DGs are applied to the network in the presence of multiple DGs. It is to be noted that these 91 and 101 cases of constraint violations occur because of the maximum load current being higher than the corresponding fault current passing through the recloser in these cases. However, in the IEEE 69-bus system, there are 115073 and 147456 cases of constraint violations when the recloser-fuse coordination results obtained without considering DG is applied to the network in the presence of single and multiple DGs, respectively. Also, there are 9400 cases of constraint violations when the recloser-fuse coordination results obtained in the presence of single DG is applied to the network in the presence of multiple DGs. In the other cases, there is no constraint violation. Thus, it is observed from this table that the recloser-fuse settings obtained in the presence of multiple DGs is robust as there is no constraint violation with the fault current calculation under any conditions in the IEEE 69-bus system.

6.8 Conclusion

This chapter proposes optimum recloser-fuse coordination for reconfigurable radial distribution system in the presence of distributed generators (DGs). On the basis of various case studies on the IEEE 33 and 69-bus systems, the following conclusions can be drawn;

(i) Recloser-fuse coordination problem can be formulated as an optimization problem.

(ii) Optimum recloser-fuse settings obtained considering all possible network configurations without DG cannot coordinate properly when DGs are present in the system.

(iii) Optimum recloser-fuse settings obtained considering presence of only one DG cannot coordinate properly in the presence of multiple DGs.

In the next chapter, final conclusion of the thesis is presented.

Chapter 7

Conclusion

This chapter highlights the major findings of this thesis and suggests some possible future works in the area of protection coordination of distribution systems.

7.1 Conclusions

Based on the work reported in this thesis, the following conclusions are drawn:

1. Differential evolution (DE) is the most suited optimization algorithm for solving directional overcurrent relays (DOCRs) coordination among metaheuristic algorithms.

2. Proposed IPM-IPM and IPM-BBM algorithms give better results than DE for solving the coordination problem of DOCRs. Further, IPM-IPM algorithm performs better than IPM-BBM algorithm.

3. Proposed new objective function (NOF) gives lower operating times of primary and backup relays along with least coordination time interval (CTI) between the operating times of primary and the corresponding backup relays.

4. Robust settings are suitable for coordinating DOCRs properly under all allowable (N-1) contingencies. A single protection coordination settings of DOCRs obtained under allowable (N-1) contingency can provide complete protection of the system successfully.

5. Optimum recloser-fuse settings give much improved coordination than the conventional methods in the presence of distributed generators (DGs).

6. Optimum recloser-fuse settings obtained considering network reconfiguration and multiple DG locations are robust.

7. IPM based algorithm is best suited for solving recloser-fuse coordination problems.

7.2 Scope of further works

- DOCRs coordination with distance relays can be studied to improve protection coordination in power systems.
- Optimum recloser-fuse coordination can be extended for protection of microgrids. Also, the optimum recloser-fuse protection coordination study in the presence of various kinds of renewable generation can be performed.
- Techno-economic analysis of various protection schemes in microgrids and smart grids can be performed.
- Effects of variable generation and energy storage on existing protection coordination scheme can be analyzed.

Publications from the Research Work

1. M. N. Alam, B. Das, and V. Pant, ”A comparative study of metaheuristic optimization approaches fordirectional overcurrent relays coordination,” Electric Power System Research, vol. 128, no. 1, pp. 39 - 52, Nov. 2015.

2. M. N. Alam, B. Das, and V. Pant, ”An interior point method based protection coordination scheme for directional overcurrent relays in meshed networks”, International Journal of Electrical Power & Energy Systems, vol. 81, no. 1, pp. 153 - 164, Oct. 2016.

Bibliography

[1] P. M. Anderson, *Power System Protection*. IEEE-Press, 1999.

[2] S. H. Horowitz and A. G. Phadke, *Power System Relaying*, 3rd ed. John Wiley & Sons, Ltd., 2008.

[3] *IEEE Recommended Practice for Protection and Coordination of Industrial and Commercial Power Systems*, IEEE Std 242-2001 Std., 2001.

[4] *Network Protection & Automation Guide*, 1st ed. Areva T&D, July 2002.

[5] C. S. Mardegan and R. Rifaat, "Considerations in applying IEEE recommended practice for protection coordination in industrial and commercial power systems - part I," *IEEE Transactions on Industry Applications*, vol. 52, no. 5, pp. 3705–3713, September 2016.

[6] E. Purwar, D. N. Vishwakarma, and S. P. Singh, "A novel constraints reduction based optimal relay coordination method considering variable operational status of distribution system with DGs," *IEEE Transactions on Smart Grid*, pp. 1–10, September 2017, (Early Access Articles).

[7] D. L. A. Negro and J. C. M. Vieira, "The local fit method for coordinating directional overcurrent relays," *IEEE Transactions on Power Delivery*, vol. 31, no. 4, pp. 1464–1472, August 2016.

[8] P. Jena and A. K. Pradhan, "An integrated approach for directional relaying of the double-circuit line," *IEEE Transactions on Power Delivery*, vol. 26, no. 3, pp. 1783–1792, July 2011.

[9] T. D. Le and M. Petit, "Directional relays without voltage sensors for distribution networks," *IET Generation, Transmission & Distribution*, vol. 8, no. 12, pp. 2074–2082, December 2014.

[10] P. Jena and A. K. Pradhan, "Directional relaying in the presence of a thyristor-controlled series capacitor," *IEEE Transactions on Power Delivery*, vol. 28, no. 2, pp. 628–636, April 2013.

[11] H. H. Zeineldin, Y. A. R. I. Mohamed, V. Khadkikar, and V. R. Pandi, "A protection coordination index for evaluating distributed generation impacts on protection for meshed distribution systems," *IEEE Transactions on Smart Grid*, vol. 4, no. 3, pp. 1523–1532, September 2013.

[12] Y. Damchi, J. Sadeh, and H. R. Mashhadi, "Optimal coordination of distance and overcurrent relays considering a non-standard tripping characteristic for distance relays," *IET Generation, Transmission & Distribution*, vol. 10, no. 6, pp. 1448–1457, May 2016.

[13] S. S. R. C. Dugan, M. F. McGranaghan and H. W. Beaty, *Electric Power Systems Quality*. McGraw-Hill, 2004.

[14] T. A. Short, *Electric Power Distribution Handbook*. CRC Press, 2004.

[15] S. Santoso and T. A. Short, "Identification of fuse and recloser operations in a radial distribution system," *IEEE Transactions on Power Delivery*, vol. 22, no. 4, pp. 2370–2377, October 2007.

[16] A. Elmitwally, E. Gouda, and S. Eladawy, "Restoring recloser-fuse coordination by optimal fault current limiters planning in DG-integrated distribution systems," *International Journal of Electrical Power & Energy Systems*, vol. 77, pp. 9–18, May 2016.

[17] S. Jamali and H. Borhani-Bahabadi, "Recloser time-current-voltage characteristic for fuse saving in distribution networks with DG," *IET Generation, Transmission & Distribution*, vol. 11, no. 1, pp. 272–279, January 2017.

[18] C. L. Wadhwa, *Electrical Power Systems*, 5th ed. New Age International Publishers, New Delhi, 2009.

[19] Y. Lu and J.-L. Chung, "Detecting and solving the coordination curve intersection problem of overcurrent relays in subtransmission systems with a new method," *Electric Power Systems Research*, vol. 95, no. 0, pp. 19–27, February 2013.

[20] M. J. Damborg, R. Ramaswami, S. S. Venkata, and J. M. Postforoosh, "Computer aided transmission protection system design part I: Algorithm," *IEEE Transactions on Power Apparatus and Systems*, vol. PAS-103, no. 1, pp. 51–59, January 1984.

[21] M. Ezzeddine and R. Kaczmarek, “A novel method for optimal coordination of directional overcurrent relays considering their available discrete settings and several operation characteristics,” *Electric Power Systems Research*, vol. 81, no. 7, pp. 1475–1481, July 2011.

[22] R. K. Gajbhiye, A. De, and S. A. Soman, “Computation of optimal break point set of relays - an integer linear programming approach,” *IEEE Transactions on Power Delivery*, vol. 22, no. 4, pp. 2087–2098, October 2007.

[23] H. A. Abyaneh, F. Razavi, M. Al-Dabbagh, H. Sedeghi, and H. Kazemikargar, “A comprehensive method for break points finding based on expert system for protection coordination in power systems,” *Electric Power Systems Research*, vol. 77, no. 5, pp. 660–672, April 2007.

[24] M. Ezzeddine, R. Kaczmarek, and M. U. Iftikhar, “Coordination of directional overcurrent relays using a novel method to select their settings,” *IET Generation, Transmission & Distribution*, vol. 5, no. 7, pp. 743–750, July 2011.

[25] H. Sharifian, H. Askarian Abyaneh, S. K. Salman, R. Mohammadi, and F. Razavi, “Determination of the minimum break point set using expert system and genetic algorithm,” *IEEE Transactions on Power Delivery*, vol. 25, no. 3, pp. 1284–1295, July 2010.

[26] L. G. Perez and A. J. Urdaneta, “Optimal coordination of directional overcurrent relays considering definite time backup relaying,” *IEEE Transactions on Power Delivery*, vol. 14, no. 4, pp. 1276–1284, October 1999.

[27] L. Huchel and H. H. Zeineldin, “Planning the coordination of directional overcurrent relays for distribution systems considering DG,” *IEEE Transactions on Smart Grid*, vol. 7, no. 3, pp. 1642–1649, May 2016.

[28] B. Chattopadhyay, M. S. Sachdev, and T. S. Sidhu, “An on-line relay coordination algorithm for adaptive protection using linear programming technique,” *IEEE Transactions on Power Delivery*, vol. 11, no. 1, pp. 165–173, January 1996.

[29] A. J. Urdaneta, H. Restrepo, S. Marquez, and J. Sanchez, “Coordination of directional overcurrent relay timing using linear programming,” *IEEE Transactions on Power Delivery*, vol. 11, no. 1, pp. 122–129, January 1996.

[30] D. Birla, R. P. Maheshwari, and H. O. Gupta, “A new nonlinear directional overcurrent relay coordination technique, and banes and boons of near-end faults based approach,” *IEEE Transactions on Power Delivery*, vol. 21, no. 3, pp. 1176–1182, July 2006.

[31] P. P. Bedekar and S. R. Bhide, “Optimum coordination of directional overcurrent relays using the hybrid GA-NLP approach,” *IEEE Transactions on Power Delivery*, vol. 26, no. 1, pp. 109–119, January 2011.

[32] J. Radosavljevic and M. Jevtic, “Hybrid GSA-SQP algorithm for optimal coordination of directional overcurrent relays,” *IET Generation, Transmission & Distribution*, vol. 10, no. 8, pp. 1928–1937, May 2016.

[33] V. A. Papaspiliotopoulos, G. N. Korres, and N. G. Maratos, “A novel quadratically constrained quadratic programming method for optimal coordination of directional overcurrent relays,” *IEEE Transactions on Power Delivery*, vol. 32, no. 1, pp. 3–10, February 2017.

[34] A. J. Urdaneta, R. Nadira, and L. G. Perez Jimenez, “Optimal coordination of directional overcurrent relays in interconnected power systems,” *IEEE Transactions on Power Delivery*, vol. 3, no. 3, pp. 903–911, July 1988.

[35] C. W. So and K. K. Li, “Time coordination method for power system protection by evolutionary algorithm,” in *Proc. IEEE Industry Applications Conference*, vol. 4, 1999, pp. 2348–2354.

[36] M. Barzegari, S. M. T. Bathaee, and M. Alizadeh, “Optimal coordination of directional overcurrent relays using harmony search algorithm,” in *9th International Conference on Environment and Electrical Engineering (EEEIC)*, May 2010, pp. 321–324.

[37] C. W. So and K. K. Li, “Overcurrent relay coordination by evolutionary programming,” *Electric Power Systems Research*, vol. 53, no. 2, pp. 83–90, February 2000.

[38] ——, “Time coordination method for power system protection by evolutionary algorithm,” *IEEE Transactions on Industry Applications*, vol. 36, no. 5, pp. 1235–1240, September 2000.

[39] M. M. Mansour, S. F. Mekhamer, and N. E.-S. El-Kharbawe, “A modified particle swarm optimizer for the coordination of directional overcurrent relays,” *IEEE Transactions on Power Delivery*, vol. 22, no. 3, pp. 1400–1410, July 2007.

[40] T. Amraee, "Coordination of directional overcurrent relays using seeker algorithm," *IEEE Transactions on Power Delivery*, vol. 27, no. 3, pp. 1415–1422, July 2012.

[41] H. Zayandehroodi, A. Mohamed, H. Shareef, and M. Farhoodnea, "A novel neural network and backtracking based protection coordination scheme for distribution system with distributed generation," *International Journal of Electrical Power & Energy Systems*, vol. 43, no. 1, pp. 868–879, December 2012.

[42] J. A. Sueiro, E. Diaz-Dorado, E. Miguez, and J. Cidras, "Coordination of directional overcurrent relay using evolutionary algorithm and linear programming," *International Journal of Electrical Power & Energy Systems*, vol. 42, no. 1, pp. 299–305, November 2012.

[43] M. Singh, B. K. Panigrahi, and A. R. Abhyankar, "Optimal coordination of directional overcurrent relays using teaching learning-based optimization (TLBO) algorithm," *International Journal of Electrical Power & Energy Systems*, vol. 50, pp. 33–41, September 2013.

[44] M. Alipour, S. Teimourzadeh, and H. Seyedi, "Improved group search optimization algorithm for coordination of directional overcurrent relays," *Swarm and Evolutionary Computation*, vol. 23, pp. 40–49, August 2015.

[45] F. A. Albasri, A. R. Alroomi, and J. H. Talaq, "Optimal coordination of directional overcurrent relays using biogeography-based optimization algorithms," *IEEE Transactions on Power Delivery*, vol. 30, no. 4, pp. 1810–1820, August 2015.

[46] S. S. Gokhale and V. S. Kale, "An application of a tent map initiated chaotic firefly algorithm for optimal overcurrent relay coordination," *International Journal of Electrical Power & Energy Systems*, vol. 78, pp. 336–342, June 2016.

[47] A. Srivastava, J. M. Tripathi, S. R. Mohanty, and B. Panda, "Optimal over-current relay coordination with distributed generation using hybrid particle swarm optimization-gravitational search algorithm," *Electric Power Components and Systems*, vol. 44, no. 5, pp. 506–517, February 2016.

[48] S. A. Ahmadi, H. Karami, M. J. Sanjari, H. Tarimoradi, and G. B. Gharehpetian, "Application of hyper-spherical search algorithm for optimal coordination of overcurrent relays considering different relay characteristics," *International Journal of Electrical Power & Energy Systems*, vol. 83, pp. 443–449, December 2016.

[49] E. Dehghanpour, H. Karegar, R. Kheirollahi, and T. Soleymani, "Optimal coordination of directional overcurrent relays in microgrids by using cuckoo-linear optimization algorithm and fault current limiter," *IEEE Transactions on Smart Grid*, vol. PP, no. 99, pp. 1–1, 2016, (Early Access Article).

[50] D. Saha, A. Datta, and P. Das, "Optimal coordination of directional overcurrent relays in power systems using symbiotic organism search optimisation technique," *IET Generation, Transmission & Distribution*, vol. 10, no. 11, pp. 2681–2688, August 2016.

[51] H. R. E. H. Bouchekara, M. Zellagui, and M. A. Abido, "Optimal coordination of directional overcurrent relays using a modified electromagnetic field optimization algorithm," *Applied Soft Computing*, vol. 54, pp. 267–283, May 2017.

[52] M. H. Costa, R. R. Saldanha, M. G. Ravetti, and E. G. Carrano, "Robust coordination of directional overcurrent relays using a matheuristic algorithm," *IET Generation, Transmission & Distribution*, vol. 11, no. 2, pp. 464–474, January 2017.

[53] F. Razavi, H. A. Abyaneh, M. Al-Dabbagh, R. Mohammadi, and H. Torkaman, "A new comprehensive genetic algorithm method for optimal overcurrent relays coordination," *Electric Power Systems Research*, vol. 78, no. 4, pp. 713–720, April 2008.

[54] R. Mohammadi, H. A. Abyaneh, F. Razavi, M. Al-Dabbagh, and S. H. H. Sadeghi, "Optimal relays coordination efficient method in interconnected power systems," *Journal of ELECTRICAL ENGINEERING*, vol. 61, no. 2, pp. 75–83, March 2010.

[55] R. Mohammadi, H. A. Abyaneh, H. M. Rudsari, S. H. Fathi, and H. Rastegar, "Overcurrent relays coordination considering the priority of constraints," *IEEE Transactions on Power Delivery*, vol. 26, no. 3, pp. 1927–1938, July 2011.

[56] X. Yang, D. Shi, and X. Duan, "Setting calculation of the directional relays considering dynamic changes in the network topology," in *Proc. IEEE Power System Technology*, Oct 2006, pp. 1–6.

[57] A. S. Noghabi, J. Sadeh, and H. R. Mashhadi, "Considering different network topologies in optimal overcurrent relay coordination using a hybrid GA," *IEEE Transactions on Power Delivery*, vol. 24, no. 4, pp. 185–1863, October 2009.

[58] A. S. Noghabi, H. R. Mashhadi, and J. Sadeh, "Optimal coordination of directional overcurrent relays considering different network topologies using interval linear programming," *IEEE Transactions on Power Delivery*, vol. 25, no. 3, pp. 1348–1354, July 2010.

[59] H. V. Padullaparti, P. Chirapongsananurak, M. E. Hernandez, and S. Santoso, "Analytical approach to estimate feeder accommodation limits based on protection criteria," *IEEE Access*, vol. 4, pp. 4066–4081, July 2016.

[60] J. Gers and E. Holmes, *Protection of Electricity Distribution Networks, 3rd Edition*, ser. IET power and energy series. Institution of Engineering and Technology, 2011.

[61] L. Wright and L. Ayers, "Mitigation of undesired operation of recloser controls due to distribution line inrush," *IEEE Transactions on Industry Applications*, vol. 53, no. 1, pp. 80–87, January 2017.

[62] H. B. Funmilayo, J. A. Silva, and K. L. Butler-Purry, "Overcurrent protection for the IEEE 34-node radial test feeder," *IEEE Transactions on Power Delivery*, vol. 27, no. 2, pp. 459–468, April 2012.

[63] E. Sorrentino, "Nontraditional relay curves for the coordination of the ground overcurrent function with downstream fuses," *IEEE Transactions on Power Delivery*, vol. 29, no. 3, pp. 1284–1291, June 2014.

[64] S. M. Brahma and A. A. Girgis, "Development of adaptive protection scheme for distribution systems with high penetration of distributed generation," *IEEE Transactions on Power Delivery*, vol. 19, no. 1, pp. 56–63, January 2004.

[65] B. Hussain, S. M. Sharkh, S. Hussain, and M. A. Abusara, "An adaptive relaying scheme for fuse saving in distribution networks with distributed generation," *IEEE Transactions on Power Delivery*, vol. 28, no. 2, pp. 669–677, April 2013.

[66] S. Chaitusaney and A. Yokoyama, "Prevention of reliability degradation from recloser and fuse miscoordination due to distributed generation," *IEEE Transactions on Power Delivery*, vol. 23, no. 4, pp. 2545–2554, October 2008.

[67] A. F. Naiem, Y. Hegazy, A. Y. Abdelaziz, and M. A. Elsharkawy, "A classification technique for recloser-fuse coordination in distribution systems with distributed generation," *IEEE Transactions on Power Delivery*, vol. 27, no. 1, pp. 176–185, January 2012.

[68] H. Yazdanpanahi, Y. W. Li, and W. Xu, "A new control strategy to mitigate the impact of inverter-based DGs on protection system," *IEEE Transactions on Smart Grid*, vol. 3, no. 3, pp. 1427–1436, September 2012.

[69] E. C. Piesciorovsky and N. N. Schulz, "Fuse relay adaptive overcurrent protection scheme for microgrid with distributed generators," *IET Generation, Transmission & Distribution*, vol. 11, no. 2, pp. 540–549, January 2017.

[70] B. Amanulla, S. Chakrabarti, and S. N. Singh, "Reconfiguration of power distribution systems considering reliability and power loss," *IEEE Transactions on Power Delivery*, vol. 27, no. 2, pp. 918–926, April 2012.

[71] Y. Y. Hsu and J. H. Yi, "Planning of distribution feeder reconfiguration with protective device coordination," *IEEE Transactions on Power Delivery*, vol. 8, no. 3, pp. 1340–1347, July 1993.

[72] B. Khorshid-Ghazani, H. Seyedi, B. Mohammadi-ivatloo, K. Zare, and S. Shargh, "Reconfiguration of distribution networks considering coordination of the protective devices," *IET Generation, Transmission & Distribution*, vol. 11, no. 1, pp. 82–92, January 2017.

[73] I. Xyngi and M. Popov, "An intelligent algorithm for the protection of smart power systems," *IEEE Transactions on Smart Grid*, vol. 4, no. 3, pp. 1541–1548, September 2013.

[74] MATLAB, Mathworks Inc., Massachusetts, USA, version R2012a.

[75] AMPL (a modeling language for mathematical programming). [Online]. Available: www.ampl.com.

[76] H. H. Zeineldin, E. F. El-Saadany, and M. M. A. Salama, "Optimal coordination of overcurrent relays using a modified particle swarm optimization," *Electric Power Systems Research*, vol. 76, no. 11, pp. 988–995, July 2006.

[77] C. A. C. Salazar, A. C. Enriquez, and S. E. Schaeffer, "Directional overcurrent relay coordination considering non-standardized time curves," *Electric Power Systems Research*, vol. 122, pp. 42–49, May 2015.

[78] Z. Moravej, F. Adelnia, and F. Abbasi, "Optimal coordination of directional overcurrent relays using NSGA-II," *Electric Power Systems Research*, vol. 119, pp. 228–236, February 2015.

[79] P. P. Bedekar and S. R. Bhide, "Optimum coordination of overcurrent relay timing using continuous genetic algorithm," *Expert Systems with Applications*, vol. 38, no. 9, pp. 11 286–11 292, September 2011.

[80] M. Thakur and A. Kumar, "Optimal coordination of directional over current relays using a modified real coded genetic algorithm: A comparative study," *International Journal of Electrical Power & Energy Systems*, vol. 82, pp. 484–495, November 2016.

[81] F. B. Bottura, W. M. Bernardes, M. Oleskovicz, and E. N. Asada, "Setting directional overcurrent protection parameters using hybrid GA optimizer," *Electric Power Systems Research*, vol. 143, pp. 400–408, February 2017.

[82] D. S. Alkaran, M. R. Vatani, M. J. Sanjari, G. B. Gharehpetian, and M. S. Naderi, "Optimal overcurrent relay coordination in interconnected networks by using fuzzy-based GA method," *IEEE Transactions on Smart Grid*, vol. PP, no. 99, pp. 1–1, 2016, (Early Access Article).

[83] J. Moirangthem, K. R. Krishnanand, S. S. Dash, and R. Ramaswami, "Adaptive differential evolution algorithm for solving non-linear coordination problem of directional overcurrent relays," *IET Generation, Transmission & Distribution*, vol. 7, no. 4, pp. 329–336, April 2013.

[84] M. Singh, B. K. Panigrahi, A. R. Abhyankar, and S. Das, "Optimal coordination of directional over-current relays using informative differential evolution algorithm," *Journal of Computational Science*, vol. 5, no. 2, pp. 269–276, March 2014.

[85] R. Thangaraj, M. Pant, and K. Deep, "Optimal coordination of over-current relays using modified differential evolution algorithms," *Engineering Applications of Artificial Intelligence*, vol. 23, no. 5, pp. 820–829, August 2010.

[86] M. Y. Shih, A. C. Enrquez, T.-Y. Hsiao, and L. M. T. Trevio, "Enhanced differential evolution algorithm for coordination of directional overcurrent relays," *Electric Power Systems Research*, vol. 143, pp. 365–375, February 2017.

[87] T. R. Chelliah, R. Thangaraj, S. Allamsetty, and M. Pant, "Coordination of directional overcurrent relays using opposition based chaotic differential evolution algorithm," *International Journal of Electrical Power & Energy Systems*, vol. 55, pp. 341–350, February 2014.

[88] A. Y. Abdelaziz, H. E. A. Talaat, A. I. Nosseir, and A. A. Hajjar, "An adaptive protection scheme for optimal coordination of overcurrent relays," *Electric Power Systems Research*, vol. 61, no. 1, pp. 1–9, February 2002.

[89] H. M. Sharaf, H. H. Zeineldin, D. K. Ibrahim, and E. E.-D. A. EL-Zahab, "A proposed coordination strategy for meshed distribution systems with DG considering user-defined characteristics of directional inverse time overcurrent relays," *International Journal of Electrical Power & Energy Systems*, vol. 65, pp. 49–58, February 2015.

[90] R. C. Eberhart and Y. Shi, "Comparing inertia weights and constriction factors in particle swarm optimization," in *Proc. IEEE Congress on Evolutionary Computation*, vol. 1, 2000, pp. 84–88 vol.1.

[91] S. Das and P. N. Suganthan, "Differential evolution: A survey of the state-of-the-art," *IEEE Transactions on Evolutionary Computation*, vol. 15, no. 1, pp. 4–31, February 2011.

[92] S. Das, A. Mukhopadhyay, A. Roy, A. Abraham, and B. K. Panigrahi, "Exploratory power of the harmony search algorithm: Analysis and improvements for global numerical optimization," *IEEE Transactions on Systems, Man, and Cybernetics, Part B (Cybernetics)*, vol. 41, no. 1, pp. 89–106, February 2011.

[93] C. Dai, W. Chen, Y. Zhu, and X. Zhang, "Seeker optimization algorithm for optimal reactive power dispatch," *IEEE Transactions on Power Systems*, vol. 24, no. 3, pp. 1218–1231, August 2009.

[94] R. Christie, Power system test cases, Aug. 1993. [Online]. Available: www.ee.washington.edu/research/pstca.

[95] H. Zhan, C. Wang, Y. Wang, X. Yang, X. Zhang, C. Wu, and Y. Chen, "Relay protection coordination integrated optimal placement and sizing of distributed generation sources in distribution networks," *IEEE Transactions on Smart Grid*, vol. 7, no. 1, pp. 55–65, January 2016.

[96] N. Duvvuru and K. S. Swarup, "A hybrid interior point assisted differential evolution algorithm for economic dispatch," *IEEE Transactions on Power Systems*, vol. 26, no. 2, pp. 541–549, May 2011.

[97] *IEEE Standard Inverse-Time Characteristic Equations for Overcurrent Relays*, IEEE Std C37.112-1996 Std., 1996.

[98] M. Ojaghi and R. Ghahremani, "Piece-wise linear characteristic for coordinating numerical overcurrent relays," *IEEE Transactions on Power Delivery*, vol. 32, no. 1, pp. 145–151, February 2017.

[99] A. Mahari and H. Seyedi, "An analytic approach for optimal coordination of overcurrent relays," *IET Generation, Transmission & Distribution*, vol. 7, no. 7, pp. 674–680, July 2013.

[100] D. S. Alkaran, M. R. Vatani, M. J. Sanjari, G. B. Gharehpetian, and A. H. Yatim, "Overcurrent relays coordination in interconnected networks using accurate analytical method and based on determination of fault critical point," *IEEE Transactions on Power Delivery*, vol. 30, no. 2, pp. 870–877, April 2015.

[101] S. A. Soman. Lecture on power system protection (web) module 4 and 5. Available [Online]: www.nptel.ac.in/courses/108101039/.

[102] R. J. Vanderbei and D. F. Shanno, "An interior-point algorithm for nonconvex nonlinear programming," Princeton University, Statistics and Operations Research (SOR-97-21), 1997.

[103] M. E. Dyer, W. O. Riha, and J. Walker, "A hybrid dynamic programming/branch-and-bound algorithm for the multiple-choice knapsack problem," *Journal of Computational and Applied Mathematics*, vol. 58, no. 1, pp. 43–54, March 1995.

[104] A. Mathur, V. Pant, and B. Das, "Unsymmetrical short-circuit analysis for distribution system considering loads," *International Journal of Electrical Power & Energy Systems*, vol. 70, pp. 27–38, September 2015.

[105] N. Daratha, B. Das, and J. Sharma, "Coordination between OLTC and SVC for voltage regulation in unbalanced distribution system distributed generation," *IEEE Transactions on Power Systems*, vol. 29, no. 1, pp. 289–299, January 2014.

[106] M. N. Alam, B. Das, and V. Pant, "A comparative study of metaheuristic optimization approaches for directional overcurrent relays coordination," *Electric Power Systems Research*, vol. 128, pp. 39–52, November 2015.

[107] A. J. Urdaneta, L. G. Perez, and H. Restrepo, "Optimal coordination of directional overcurrent relays considering dynamic changes in the network topology," *IEEE Transactions on Power Delivery*, vol. 12, no. 4, pp. 1458–1464, October 1997.

[108] M. Meskin, A. Domijan, and I. Grinberg, "Optimal co-ordination of overcurrent relays in the interconnected power systems using break points," *Electric Power Systems Research*, vol. 127, pp. 53–63, October 2015.

[109] M. Y. Shih, A. C. Enriquez, and L. M. T. Trevino, "On-line coordination of directional overcurrent relays: Performance evaluation among optimization algorithms," *Electric Power Systems Research*, vol. 110, pp. 122–132, May 2014.

[110] R. Correa, G. Cardoso, O. C. B. de Arajo, and L. Mariotto, "Online coordination of directional overcurrent relays using binary integer programming," *Electric Power Systems Research*, vol. 127, pp. 118–125, October 2015.

[111] M. Y. Shih, C. A. C. Salazar, and A. C. Enriquez, "Adaptive directional overcurrent relay coordination using ant colony optimisation," *IET Generation, Transmission & Distribution*, vol. 9, no. 14, pp. 2040–2049, October 2015.

[112] M. Tasdighi and M. Kezunovic, "Automated review of distance relay settings adequacy after the network topology changes," *IEEE Transactions on Power Delivery*, vol. 31, no. 4, pp. 1873–1881, August 2016.

[113] M. Singh, T. Vishnuvardhan, and S. G. Srivani, "Adaptive protection coordination scheme for power networks under penetration of distributed energy resources," *IET Generation, Transmission & Distribution*, vol. 10, no. 15, pp. 3919–3929, November 2016.

[114] P. Mahat, Z. Chen, B. Bak-Jensen, and C. L. Bak, "A simple adaptive overcurrent protection of distribution systems with distributed generation," *IEEE Transactions on Smart Grid*, vol. 2, no. 3, pp. 428–437, September 2011.

[115] F. Coffele, C. Booth, and A. Dysko, "An adaptive overcurrent protection scheme for distribution networks," *IEEE Transactions on Power Delivery*, vol. 30, no. 2, pp. 561–568, April 2015.

[116] A. M. Ibrahim, W. El-Khattam, M. ElMesallamy, and H. A. Talaat, "Adaptive protection coordination scheme for distribution network with distributed generation using ABC," *Journal*

of Electrical Systems and Information Technology, vol. 3, no. 2, pp. 320–332, September 2016.

[117] J. Srivani and K. S. Swarup, "Power system static security assessment and evaluation using external system equivalents," *International Journal of Electrical Power & Energy Systems*, vol. 30, no. 2, pp. 83–92, February 2008.

[118] R. Sunitha, S. K. Kumar, and A. T. Mathew, "Online static security assessment module using artificial neural networks," *IEEE Transactions on Power Systems*, vol. 28, no. 4, pp. 4328–4335, November 2013.

[119] R. Sunitha, K. R. Sreerama, and T. M. Abraham, "Development of a composite security index for static security evaluation," in *Proc. IEEE TENCON*, Jan. 2009, pp. 1–6.

[120] T. Jain, L. Srivastava, and S. N. Singh, "Fast voltage contingency screening using radial basis function neural network," *IEEE Transactions on Power Systems*, vol. 18, no. 4, pp. 1359–1366, November 2003.

[121] N. M. Peterson and W. S. Meyer, "Automatic adjustment of transformer and phase-shifter taps in the newton power flow," *IEEE Transactions on Power Apparatus and Systems*, vol. PAS-90, no. 1, pp. 103–108, January 1971.

[122] W. Wu, Z. Tian, and B. Zhang, "An exact linearization method for OLTC of transformer in branch flow model," *IEEE Transactions on Power Systems*, vol. 32, no. 3, pp. 2475–2476, May 2017.

[123] J. Grainger and W. Stevenson, *Power System Analysis*, ser. McGraw-Hill series in electrical and computer engineering: Power and energy. McGraw-Hill, 1994.

[124] D. F. Shanno and R. J. Vanderbei, "Interior-point methods for nonconvex nonlinear programming: Orderings and higher-order methods," Statistics and Operation Research, Princeton University, Technical Report SOR-99-5, 1999.

[125] L. S. Toth and A. Hannah, "Enhanced sectionalizing through proper testing of recloser time current curves," in *Proc. IEEE Rural Electric Power Conference*, Apr 1994, pp. B5/1–B5/7.

[126] J. F. Witte, S. R. Mendis, M. T. Bishop, and J. A. Kischefsky, "Computer-aided recloser applications for distribution systems," *IEEE Computer Applications in Power*, vol. 5, no. 3, pp. 27–32, July 1992.

[127] S. Conti, “Analysis of distribution network protection issues in presence of dispersed generation,” *Electric Power Systems Research*, vol. 79, no. 1, pp. 49–56, January 2009.

[128] S. M. Sharkh, M. A. Abu-Sara, G. I. Orfanoudakis, and B. Hussain, *An Adaptive Relaying Scheme for Fuse Saving*. Wiley-IEEE Press, 2014, pp. 352–375.

[129] A. Zamani, T. Sidhu, and A. Yazdani, “A strategy for protection coordination in radial distribution networks with distributed generators,” in *IEEE PES General Meeting*, July 2010, pp. 1–8.

[130] Y. Pan, W. Ren, S. Ray, R. Walling, and M. Reichard, “Impact of inverter interfaced distributed generation on overcurrent protection in distribution systems,” in *Proc. IEEE Power Engineering and Automation Conference*, vol. 2, Sept 2011, pp. 371–376.

[131] J. C. Gomez and M. M. Morcos, “Overcurrent coordination in systems with distributed generation,” *Electric Power Components and Systems*, vol. 39, no. 6, pp. 576–589, April 2011.

[132] A. Kamel, M. A. Alaam, A. M. Azmy, and A. Y. Abdelaziz, “Protection coordination for distribution systems in presence of distributed generators,” *Electric Power Components and Systems*, vol. 41, no. 15, pp. 1555–1566, October 2013.

[133] H. A. Abdel-Ghany, A. M. Azmy, N. I. Elkalashy, and E. M. Rashad, “Optimizing DG penetration in distribution networks concerning protection schemes and technical impact,” *Electric Power Systems Research*, vol. 128, pp. 113–122, November 2015.

[134] V. C. Nikolaidis, E. Papanikolaou, and A. S. Safigianni, “A communication-assisted overcurrent protection scheme for radial distribution systems with distributed generation,” *IEEE Transactions on Smart Grid*, vol. 7, no. 1, pp. 114–123, January 2016.

[135] P. H. Shah and B. R. Bhalja, “New adaptive digital relaying scheme to tackle recloser-fuse miscoordination during distributed generation interconnections,” *IET Generation, Transmission & Distribution*, vol. 8, no. 4, pp. 682–688, April 2014.

[136] A. F. Naiem, A. Y. Abdelaziz, Y. Hegazy, and M. A. Elsharkawy, “Recloser-fuse coordination assessment by classification technique for distribution systems with distributed generation,” *Electric Power Components and Systems*, vol. 39, no. 11, pp. 1077–1096, August 2011.

[137] L.-H. Chen, “Overcurrent protection for distribution feeders with renewable generation,” *International Journal of Electrical Power & Energy Systems*, vol. 84, pp. 202–213, January 2017.

[138] J. M. Gers, *Distribution System Analysis and Automation*, ser. Energy Engineering. Institution of Engineering and Technology, 2013.

[139] H. Haghighat and B. Zeng, “Distribution system reconfiguration under uncertain load and renewable generation,” *IEEE Transactions on Power Systems*, vol. 31, no. 4, pp. 2666–2675, July 2016.

[140] G. W. Chang, S. Y. Chu, and H. L. Wang, “An improved backward/forward sweep load flow algorithm for radial distribution systems,” *IEEE Transactions on Power Systems*, vol. 22, no. 2, pp. 882–884, May 2007.

[141] K. Narayanan, S. A. Siddiqui, and M. Fozdar, “Hybrid islanding detection method and priority-based load shedding for distribution networks in the presence of DG units,” *IET Generation, Transmission & Distribution*, vol. 11, no. 3, pp. 586–595, February 2017.

[142] M. E. Baran and F. F. Wu, “Optimal capacitor placement on radial distribution systems,” *IEEE Transactions on Power Delivery*, vol. 4, no. 1, pp. 725–734, January 1989.

[143] A. Kavousi-Fard, T. Niknam, and M. Fotuhi-Firuzabad, “A novel stochastic framework based on cloud theory and $theta$ -modified bat algorithm to solve the distribution feeder reconfiguration,” *IEEE Transactions on Smart Grid*, vol. 7, no. 2, pp. 740–750, March 2016.

[144] W. Sheng, K. Y. Liu, Y. Liu, X. Meng, and Y. Li, “Optimal placement and sizing of distributed generation via an improved nondominated sorting genetic algorithm II,” *IEEE Transactions on Power Delivery*, vol. 30, no. 2, pp. 569–578, April 2015.

[145] P. Kritavorn, T. Lantharthong, and N. Rugthaicharoencheep, “The combined loss reduction approach to apply in distribution system with distribution generation,” in *Proc. IEEE TENCON*, Oct 2014, pp. 1–5.

[146] M. E. Baran and F. F. Wu, “Network reconfiguration in distribution systems for loss reduction and load balancing,” *IEEE Transactions on Power Delivery*, vol. 4, no. 2, pp. 1401–1407, April 1989.

[147] N. Acharya, P. Mahat, and N. Mithulananthan, “An analytical approach for DG allocation in primary distribution network,” *International Journal of Electrical Power & Energy Systems*, vol. 28, no. 10, pp. 669–678, December 2006.

[148] S. N. Gopiya Naik, D. K. Khatod, and M. P. Sharma, “Analytical approach for optimal siting and sizing of distributed generation in radial distribution networks,” *IET Generation, Transmission & Distribution*, vol. 9, no. 3, pp. 209–220, February 2015.

[149] T. N. Shukla, S. P. Singh, V. Srinivasarao, and K. B. Naik, “Optimal sizing of distributed generation placed on radial distribution systems,” *Electric Power Components and Systems*, vol. 38, no. 3, pp. 260–274, January 2010.

[150] R. S. Rao, K. Ravindra, K. Satish, and S. V. L. Narasimham, “Power loss minimization in distribution system using network reconfiguration in the presence of distributed generation,” *IEEE Transactions on Power Systems*, vol. 28, no. 1, pp. 317–325, February 2013.

[151] J. S. Savier and D. Das, “Impact of network reconfiguration on loss allocation of radial distribution systems,” *IEEE Transactions on Power Delivery*, vol. 22, no. 4, pp. 2473–2480, October 2007.

[152] S. P. Singh, G. S. Raju, G. K. Rao, and M. Afsari, “A heuristic method for feeder reconfiguration and service restoration in distribution networks,” *International Journal of Electrical Power & Energy Systems*, vol. 31, no. 7, pp. 309–314, September 2009.

[153] A. Chakrabarti, *Circuit Theory (Analysis and Synthesis)*. Dhanpat Ray & Co., 2008.

[154] L. Liu and L. Fu, “Minimum breakpoint set determination for directional overcurrent relay coordination in large-scale power networks via matrix computations,” *IEEE Transactions on Power Delivery*, vol. 32, no. 4, pp. 1784–1789, August 2017.

[155] N. G. Paterakis, A. Mazza, S. F. Santos, O. Erdinc, G. Chicco, A. G. Bakirtzis, and J. P. S. Catalo, “Multi-objective reconfiguration of radial distribution systems using reliability indices,” *IEEE Transactions on Power Systems*, vol. 31, no. 2, pp. 1048–1062, March 2016.

[156] B. Venkatesh, R. Ranjan, and H. B. Gooi, “Optimal reconfiguration of radial distribution systems to maximize loadability,” *IEEE Transactions on Power Systems*, vol. 19, no. 1, pp. 260–266, February 2004.

[157] Y. C. Huang, “Enhanced genetic algorithm-based fuzzy multi-objective approach to distribution network reconfiguration,” *IEE Proceedings - Generation, Transmission and Distribution*, vol. 149, no. 5, pp. 615–620, September 2002.

[158] C. Lee, C. Liu, S. Mehrotra, and Z. Bie, “Robust distribution network reconfiguration,” *IEEE Transactions on Smart Grid*, vol. 6, no. 2, pp. 836–842, March 2015.

[159] P. M. de Quevedo, J. Contreras, M. J. Rider, and J. Allahdadian, “Contingency assessment and network reconfiguration in distribution grids including wind power and energy storage,” *IEEE Transactions on Sustainable Energy*, vol. 6, no. 4, pp. 1524–1533, October 2015.

[160] S. R. Tuladhar, J. G. Singh, and W. Ongsakul, “Multi-objective approach for distribution network reconfiguration with optimal DG power factor using NSPSO,” *IET Generation, Transmission & Distribution*, vol. 10, no. 12, pp. 2842–2851, August 2016.

[161] A. M. Eldurssi and R. M. O’Connell, “A fast nondominated sorting guided genetic algorithm for multi-objective power distribution system reconfiguration problem,” *IEEE Transactions on Power Systems*, vol. 30, no. 2, pp. 593–601, March 2015.

[162] M. R. Andervazh, J. Olamaei, and M. R. Haghifam, “Adaptive multi-objective distribution network reconfiguration using multi-objective discrete particles swarm optimisation algorithm and graph theory,” *IET Generation, Transmission & Distribution*, vol. 7, no. 12, pp. 1367–1382, December 2013.

[163] R. S. Rao, S. V. L. Narasimham, M. R. Raju, and A. S. Rao, “Optimal network reconfiguration of large-scale distribution system using harmony search algorithm,” *IEEE Transactions on Power Systems*, vol. 26, no. 3, pp. 1080–1088, August 2011.

[164] Y. K. Wu, C. Y. Lee, L. C. Liu, and S. H. Tsai, “Study of reconfiguration for the distribution system with distributed generators,” *IEEE Transactions on Power Delivery*, vol. 25, no. 3, pp. 1678–1685, July 2010.

[165] J. F. Franco, M. J. Rider, M. Lavorato, and R. Romero, “A mixed-integer LP model for the reconfiguration of radial electric distribution systems considering distributed generation,” *Electric Power Systems Research*, vol. 97, pp. 51–60, April 2013.

Appendix A

Various Systems Data

Table A.1: Maximum load current and minimum and maximum fault current for the IEEE 14-bus system

Sl. No.	I_{Lmax} (A)	I_{fmin} (A)	I_{fmax} (A)	Sl. No.	I_{Lmax} (A)	I_{fmin} (A)	I_{fmax} (A)	Sl. No.	I_{Lmax} (A)	I_{fmin} (A)	I_{fmax} (A)
1	1246	4178	9737	15	282	2597	3947	29	624	3616	5276
2	0	3184	7420	16	0	2250	3419	30	0	2855	4165
3	598	2910	5009	17	138	1480	2051	31	111	4328	6132
4	0	1942	3343	18	0	2132	2956	32	0	1449	2052
5	588	3073	5162	19	370	2457	3638	33	167	3386	4583
6	0	1558	2616	20	0	2419	3582	34	0	1297	1756
7	449	3015	5228	21	134	3714	5165	35	0	2793	3814
8	0	1949	3379	22	0	1610	2239	36	69	2083	2846
9	333	3022	5271	23	134	3551	4796	37	30	1549	2050
10	0	1984	3460	24	0	1080	1459	38	0	2661	3521
11	0	1815	2930	25	313	4193	5881	39	98	2427	3211
12	198	2458	3966	26	0	1374	1928	40	0	1677	2219
13	0	2542	4568	27	373	4288	6027	-	-	-	-
14	519	2773	4983	28	0	1155	1623	-	-	-	-

Table A.2: CTR of the relays for the IEEE 14-bus system

CTR	Relay No.	CTR	Relay No.
8000/5	1	1200/5	13,23,30,33
3500/5	29	1000/5	8,10,12,16,20,35,38,39
3000/5	2,3,5,14	800/5	6,11,17,18,36
2500/5	7	600/5	22,32,37,40
2000/5	2,9,19,27	500/5	26,28,34
1600/5	15,21,25,31	400/5	24

Table A.3: Primary/backup relay pairs along with the maximum fault current for the IEEE 14-bus system

Faulty Line	Serial No.	Primary Relay	Backup Relay	$I_{fprimary}$ (A)	$I_{fbackup}$ (A)	Faulty Line	Serial No.	Primary Relay	Backup Relay	$I_{fprimary}$ (A)	$I_{fbackup}$ (A)
L1	1	1	4	9737	201	L9	48	17	28	2051	658
	2	2	6	7420	773		49	17	30	2051	1640
	3	2	8	7420	587		50	18	15	2956	382
	4	2	10	7420	535		51	18	28	2956	658
L2	5	3	2	5009	322		52	18	32	2956	796
	6	4	9	3343	1156		53	18	34	2956	535
	7	4	13	3343	1715	L10	54	19	3	3638	1189
	8	4	20	3343	408		55	19	9	3638	1213
L3	9	5	1	5162	2378		56	19	13	3638	1274
	10	5	8	5162	155		57	20	22	3582	916
	11	5	10	5162	75		58	20	24	3582	189
	12	6	12	2616	1292		59	20	26	3582	598

Continued on next page

Table A.3 – continued from previous page

Faulty Line	Serial No.	Primary Relay	Backup Relay	$I_{fprimary}$ (A)	$I_{fbackup}$ (A)	Faulty Line	Serial No.	Primary Relay	Backup Relay	$I_{fprimary}$ (A)	$I_{fbackup}$ (A)
L4	13	7	1	5228	2513	L11	60	21	19	5165	1150
	14	7	6	5228	132		61	21	24	5165	154
	15	7	10	5228	503		62	21	26	5165	471
	16	8	11	3379	870		63	22	35	2239	2201
	17	8	14	3379	1862	L12	64	23	19	4796	1110
	18	8	18	3379	261		65	23	22	4796	933
	19	8	28	3379	787		66	23	26	4796	481
	20	8	30	3379	280		67	24	38	1459	1396
L5	21	9	1	5271	2395	L13	68	25	19	5881	1349
	22	9	6	5271	160		69	25	22	5881	1073
	23	9	8	5271	539		70	25	24	5881	491
	24	10	3	3460	1369		71	26	37	1928	530
	25	10	13	3460	1579		72	26	40	1928	1239
	26	10	20	3460	438	L15	73	30	17	4165	693
L6	27	11	5	2930	1632		74	30	32	4165	1486
	28	12	7	3966	1277		75	30	34	4165	989
	29	12	14	3966	2079	L16	76	31	15	6132	1119
	30	12	18	3966	251		77	31	17	6132	733
	31	12	28	3966	708		78	31	28	6132	931
	32	12	30	3966	271		79	31	34	6132	883
L7	33	13	7	4568	2174		80	32	36	2052	1923
	34	13	11	4568	1571	L17	81	33	15	4583	794
	35	13	18	4568	294		82	33	17	4583	522
	36	13	28	4568	1132		83	33	28	4583	684
	37	13	30	4568	363		84	33	32	4583	808
	38	14	3	4983	2204		85	34	39	1756	1611
	39	14	9	4983	2151	L18	86	35	31	3814	3719
	40	14	20	4983	443		87	36	21	2846	2810
L8	41	15	7	3947	1369	L19	88	37	23	2050	2010
	42	15	11	3947	960		89	38	25	3521	2376
	43	15	14	3947	1850		90	38	40	3521	1043
	44	15	18	3947	646	20	91	39	25	3211	2481
L9	45	17	7	2051	862		92	39	37	3211	646
	46	17	11	2051	606		93	40	33	2219	2100
	47	17	14	2051	1071		-	-	-	-	-

Table A.4: Maximum load current and minimum and maximum fault current for the IEEE 30-bus system

Sl. No.	I_{Lmax} (A)	I_{fmin} (A)	I_{fmax} (A)	Sl. No.	I_{Lmax} (A)	I_{fmin} (A)	I_{fmax} (A)	Sl. No.	I_{Lmax} (A)	I_{fmin} (A)	I_{fmax} (A)
1	724	2391	5925	29	0	1098	1703	57	72	2101	2897
2	0	1681	4165	30	4	900	1397	58	0	2991	4124
3	363	1895	3480	31	1481	11040	16438	59	49	2032	2692
4	0	964	1771	32	0	3270	4869	60	0	2124	2814
5	186	1611	2885	33	829	12961	18246	61	0	1679	2239
6	0	1140	2041	34	0	3453	4862	62	124	2645	3528
7	345	1659	2821	35	110	4778	6883	63	0	3217	4570
8	0	830	1411	36	0	1406	2025	64	20	2670	3792
9	253	1594	2853	37	163	4014	5539	65	161	3322	4539
10	0	1158	2074	38	0	1158	1597	66	0	1666	2277
11	352	940	1735	39	345	4611	6646	67	66	1827	2418
12	0	1954	3605	40	0	1628	2347	68	0	2318	3068
13	316	1456	2779	41	169	3602	5090	69	0	2536	3284
14	0	1599	3053	42	0	2144	3030	70	119	1021	1323
15	192	1327	1992	43	195	4593	6540	71	76	2104	2596
16	0	2510	3768	44	0	3593	5116	72	0	63	78

Continued on next page

Table A.4 – continued from previous page

Sl. No.	I_{Lmax} (A)	I_{fmin} (A)	I_{fmax} (A)	Sl. No.	I_{Lmax} (A)	I_{fmin} (A)	I_{fmax} (A)	Sl. No.	I_{Lmax} (A)	I_{fmin} (A)	I_{fmax} (A)
17	0	1132	1828	45	141	3644	4957	73	0	1631	2076
18	83	1107	1787	46	0	1202	1635	74	93	1382	1759
19	165	1923	3339	47	335	4093	5835	75	0	1049	1364
20	0	690	1198	48	0	1888	2692	76	78	630	819
21	128	2175	3948	49	138	3828	5364	77	115	1417	1725
22	0	641	1164	50	0	1676	2348	78	0	295	360
23	143	1453	2260	51	34	1571	2100	79	131	1139	1377
24	0	7099	11045	52	0	2945	3936	80	0	373	451
25	71	805	1128	53	106	3193	4303	81	69	656	785
26	0	2266	3176	54	0	1401	1888	82	0	562	673
27	76	2224	3856	55	125	3294	4445	-	-	-	-
28	0	369	641	56	0	1346	1816	-	-	-	-

Table A.5: CTR of the relays for the IEEE 30-bus system

CTR	Relay No.	CTR	Relay No.
8000/5	31	800/5	14, 23, 26, 42, 48, 57, 59, 60, 67, 68, 71, 79
5000/5	33	600/5	6, 10, 36, 40, 50, 51, 61, 66, 70, 73, 77
4000/5	1	500/5	4, 17, 18, 29, 46, 54, 56, 74
3000/5	24	400/5	8, 25, 30, 38, 75, 76, 81
2000/5	3, 7, 11, 35, 39, 43, 47	300/5	20, 22, 28, 82
1600/5	9, 13, 32, 34, 37, 41, 44, 45, 49	150/5	80
1200/5	2,53,55,63,65	100/5	78
1000/5	5, 12, 15, 16, 19, 21, 27, 52, 62, 64, 69	50/5	72

Table A.6: Primary/backup relay pairs along with the maximum fault current for the IEEE 30-bus system

Faulty Line	Serial No.	Primary Relay	Backup Relay	$I_{fprimary}$ (A)	$I_{fbackup}$ (A)	Faulty Line	Serial No.	Primary Relay	Backup Relay	$I_{fprimary}$ (A)	$I_{fbackup}$ (A)
L1	1	1	4	5925	123	L16	99	32	38	4869	834
	2	2	6	4165	396		100	32	40	4869	801
	3	2	8	4165	468		101	32	42	4869	482
	4	2	10	4165	459	L18	102	35	23	6883	601
L2	5	3	2	3480	335		103	35	25	6883	389
	6	4	12	1771	1769		104	35	34	6883	2658
L3	7	5	1	2885	1356		105	35	38	6883	738
	8	5	8	2885	119		106	35	40	6883	758
	9	5	10	2885	185		107	35	42	6883	455
	10	6	11	2041	753		108	36	57	2025	1898
	11	6	14	2041	1035	L19	109	37	23	5539	465
	12	6	16	2041	406		110	37	25	5539	301
L4	13	7	1	2821	1315		111	37	34	5539	2081
	14	7	6	2821	103		112	37	36	5539	886
	15	7	10	2821	44		113	37	40	5539	516
	16	8	18	1411	730		114	37	42	5539	305
L5	17	9	1	2853	1424		115	38	61	1597	1574
	18	9	6	2853	195	L20	116	39	23	6646	624
	19	9	8	2853	65		117	39	25	6646	404
	20	10	13	2074	875		118	39	34	6646	2728
	21	10	20	2074	386		119	39	36	6646	1387
	22	10	22	2074	444		120	39	38	6646	808
	23	10	26	2074	225		121	39	42	6646	764
	24	10	28	2074	101		122	40	64	2347	2083
	25	10	32	2074	259	L21	123	41	23	5090	561

Continued on next page

Table A.6 – continued from previous page

Faulty Line	Serial No.	Primary Relay	Backup Relay	$I_{fprimary}$ (A)	$I_{fbackup}$ (A)	Faulty Line	Serial No.	Primary Relay	Backup Relay	$I_{fprimary}$ (A)	$I_{fbackup}$ (A)
	26	10	34	2074	2102		124	41	25	5090	363
L6	27	11	3	1735	1734		125	41	34	5090	2460
	28	12	5	3605	1195		126	41	36	5090	1236
	29	12	14	3605	2011		127	41	38	5090	713
	30	12	16	3605	682		128	41	40	5090	1552
L7	31	13	5	2779	1168		129	42	63	3030	1739
	32	13	11	2779	1304		130	42	66	3030	1319
	33	13	16	2779	408	L22	131	43	15	6540	726
	34	14	9	3053	1119		132	43	46	6540	326
	35	14	20	3053	775		133	43	48	6540	1138
	36	14	22	3053	671		134	43	50	6540	1188
	37	14	26	3053	265	L23	135	45	15	4957	586
	38	14	28	3053	145		136	45	44	4957	2920
	39	14	32	3053	393		137	45	48	4957	151
	40	14	34	3053	3271		138	45	50	4957	891
L8	41	15	5	1992	609		139	46	52	1635	1570
	42	15	11	1992	651	L24	140	47	15	5835	726
	43	15	14	1992	764		141	47	44	5835	3672
	44	16	44	3768	3507		142	47	46	5835	395
	45	16	46	3768	270		143	47	50	5835	1008
	46	16	48	3768	916		144	48	51	2692	429
	47	16	50	3768	931		145	48	54	2692	1085
L9	48	17	7	1828	1088		146	48	56	2692	1099
	49	18	19	1787	1736	L25	147	49	15	5364	620
L10	50	19	9	3339	900		148	49	44	5364	3211
	51	19	13	3339	1437		149	49	46	5364	223
	52	19	22	3339	532		150	49	48	5364	741
	53	19	26	3339	295		151	50	58	2348	2312
	54	19	28	3339	124	L26	152	51	45	2100	2058
	55	19	32	3339	336		153	52	47	3936	2088
	56	19	34	3339	2496		154	52	54	3936	902
	57	20	17	1198	1133		155	52	56	3936	906
L11	58	21	9	3948	1153	L27	156	53	47	4303	2738
	59	21	13	3948	1784		157	53	51	4303	713
	60	21	20	3948	768		158	53	56	4303	817
	61	21	26	3948	349		159	54	60	1888	1859
	62	21	28	3948	169	L28	160	55	47	4445	2824
	63	21	32	3948	398		161	55	51	4445	735
	64	21	34	3948	2988		162	55	54	4445	847
	65	22	30	1164	237		163	56	68	1816	1775
L12	66	23	9	2260	669	L29	164	57	49	2897	2859
	67	23	13	2260	903		165	58	35	4124	4026
	68	23	20	2260	448	L30	166	59	53	2692	2663
	69	23	22	2260	363		167	60	62	2814	2719
	70	23	26	2260	677	L31	168	61	59	2239	2129
	71	23	28	2260	39		169	62	37	3528	3508
L13	72	25	9	1128	409	L32	170	63	39	4570	4327
	73	25	13	1128	499		171	64	41	3792	2208
	74	25	20	1128	275		172	64	66	3792	1612
	75	25	22	1128	219	L33	173	65	41	4539	1742
	76	25	28	1128	5		174	65	63	4539	2797
	77	25	32	1128	1615		175	66	67	2277	1324
	78	25	34	1128	1797		176	66	70	2277	872
	79	26	23	3176	210	L34	177	67	55	2418	2383
	80	26	34	3176	1797		178	68	65	3068	2236
	81	26	36	3176	713		179	68	70	3068	764
	82	26	38	3176	433	L35	180	69	65	3284	2101
	83	26	40	3176	414		181	69	67	3284	1122
	84	26	42	3176	245		182	70	74	1323	1274
L14	85	27	9	3856	1042	L36	183	71	69	2596	1585
	86	27	13	3856	1601		184	71	74	2596	1033

Continued on next page

Table A.6 – continued from previous page

Faulty Line	Serial No.	Primary Relay	Backup Relay	$I_{fprimary}$ (A)	$I_{fbackup}$ (A)	Faulty Line	Serial No.	Primary Relay	Backup Relay	$I_{fprimary}$ (A)	$I_{fbackup}$ (A)
	87	27	20	3856	694	L37	185	73	69	2076	2017
	88	27	22	3856	191		186	74	76	1759	374
	89	27	26	3856	279	L38	187	75	73	1364	1187
	90	27	32	3856	333		188	76	27	819	650
	91	27	34	3856	2737		189	76	29	819	188
	92	28	29	641	510	L39	190	77	73	1725	973
	93	28	75	641	419		191	77	76	1725	233
L15	94	29	21	1703	1123	L40	192	79	73	1377	841
	95	30	27	1397	1302		193	79	76	1377	201
	96	30	75	1397	310	L42	194	81	77	785	759
L16	97	32	25	4869	371		195	82	79	673	569
	98	32	36	4869	1383		-	-	-	-	-

Table A.7: Maximum load current and minimum and maximum fault current for the IEEE 118-bus system

Sl. No.	I_{Lmax} (A)	I_{fmin} (A)	I_{fmax} (A)	Sl. No.	I_{Lmax} (A)	I_{fmin} (A)	I_{fmax} (A)	Sl. No.	I_{Lmax} (A)	I_{fmin} (A)	I_{fmax} (A)
1	0	1572	3013	125	0	698	1886	249	0	1435	3432
2	78	1363	2612	126	317	996	2690	250	228	2376	5683
3	0	1598	3321	127	133	1072	2142	251	0	1400	2732
4	188	1668	3466	128	0	2041	4079	252	150	1634	3189
5	0	721	1620	129	69	2334	4616	253	204	2544	5772
6	167	2852	6403	130	0	735	1453	254	0	1084	2459
7	0	1214	2592	131	0	1357	2425	255	0	1261	2589
8	304	2150	4588	132	52	1260	2252	256	283	1980	4068
9	0	1219	2354	133	0	1141	2051	257	0	1711	3572
10	66	1752	3383	134	95	1506	2707	258	51	1594	3328
11	0	1250	3832	135	0	1021	1723	259	199	3971	13144
12	475	3285	10072	136	276	1311	2211	260	0	801	2652
13	272	1995	4876	137	0	1021	1723	261	0	2085	6769
14	0	1874	4580	138	276	1311	2211	262	402	2639	8567
15	374	2478	6356	139	0	843	1258	263	0	1881	4738
16	0	1532	3929	140	68	851	1269	264	190	2098	5284
17	0	2142	6816	141	0	508	823	265	94	2423	5844
18	572	994	3163	142	138	1646	2665	266	0	1446	3489
19	324	2127	5294	143	0	1011	1794	267	0	2939	7975
20	0	1802	4484	144	153	1595	2830	268	116	1278	3467
21	154	2085	5211	145	0	867	1577	269	0	1372	3642
22	0	1848	4618	146	209	1876	3414	270	283	2763	7335
23	76	1273	3388	147	0	1404	2696	271	266	2997	11040
24	0	2864	7621	148	128	1547	2969	272	0	824	3037
25	0	1182	3463	149	0	1303	2310	273	113	1789	3657
26	728	610	1786	150	63	1296	2299	274	0	1405	2872
27	133	869	2662	151	0	935	2342	275	144	2743	6317
28	0	952	2915	152	57	3029	7583	276	0	906	2087
29	0	707	1997	153	0	1116	1975	277	120	2673	5766
30	718	1045	2951	154	236	1476	2612	278	0	738	1593
31	227	1676	4895	155	0	450	1123	279	85	1750	3388
32	0	2747	8023	156	143	3510	8757	280	0	1215	2353
33	156	2668	5533	157	226	3055	6875	281	0	2443	5402
34	0	614	1274	158	0	556	1251	282	226	1108	2450
35	77	2799	6079	159	286	2210	4407	283	0	1697	4041
36	0	657	1427	160	0	930	1854	284	44	2120	5048
37	47	2616	5556	161	168	1343	2400	285	0	1546	2738
38	0	743	1577	162	0	1275	2278	286	124	1086	1924

Continued on next page

Table A.7 – continued from previous page

Sl. No.	I_{Lmax} (A)	I_{fmin} (A)	I_{fmax} (A)	Sl. No.	I_{Lmax} (A)	I_{fmin} (A)	I_{fmax} (A)	Sl. No.	I_{Lmax} (A)	I_{fmin} (A)	I_{fmax} (A)
39	90	2409	4151	163	165	1332	2363	287	0	1320	2496
40	0	54	93	164	0	1266	2244	288	190	1562	2954
41	5	987	1705	165	0	2066	5676	289	0	688	1351
42	0	1486	2567	166	537	2161	5936	290	160	2385	4687
43	29	1070	1954	167	0	2066	5676	291	77	2058	3651
44	0	1667	3046	168	537	2161	5936	292	0	518	919
45	0	1970	5719	169	0	1250	2190	293	0	1803	3675
46	445	2439	7079	170	197	1294	2266	294	217	1372	2796
47	49	2344	6442	171	156	1376	2398	295	0	1334	2733
48	0	1903	5230	172	0	1160	2022	296	302	1852	3796
49	27	2172	4225	173	127	1873	3247	297	0	972	1503
50	0	843	1640	174	0	636	1103	298	49	766	1185
51	0	1029	1936	175	83	1419	2567	299	0	793	1935
52	77	1820	3423	176	0	1294	2340	300	419	3053	7446
53	344	2625	7061	177	48	1041	1671	301	242	1736	3411
54	0	1543	4149	178	0	1058	1698	302	0	1303	2560
55	0	2287	7359	179	0	520	986	303	461	2386	5655
56	421	951	3059	180	59	2370	4495	304	0	1369	3245
57	78	1845	3756	181	33	2077	5103	305	842	2715	8458
58	0	1351	2750	182	0	1808	4443	306	0	1872	5833
59	92	3210	9056	183	83	2222	7184	307	266	1801	3879
60	0	1105	3117	184	0	2478	8013	308	0	1602	3450
61	89	1820	4622	185	0	1429	2722	309	24	1886	3979
62	0	2168	5504	186	135	1468	2796	310	0	1436	3030
63	0	2312	4320	187	0	1474	4464	311	0	1277	2670
64	57	505	944	188	97	3057	9259	312	51	2020	4224
65	0	1350	2450	189	0	1417	2726	313	246	2462	5436
66	29	1354	2458	190	154	1525	2935	314	0	1057	2334
67	0	1310	2099	191	0	2550	5184	315	225	1703	3505
68	125	758	1214	192	106	666	1353	316	0	1547	3183
69	0	928	1456	193	0	2497	5103	317	143	1267	2260
70	182	1028	1612	194	31	742	1517	318	0	1327	2367
71	0	582	1006	195	0	1361	2491	319	190	3097	7169
72	225	1865	3224	196	123	1389	2541	320	0	574	1328
73	37	2099	4761	197	0	1393	2583	321	202	1112	2418
74	0	1495	3392	198	129	1423	2639	322	0	2357	5125
75	0	1512	3683	199	0	1789	3897	323	180	2620	6163
76	673	2328	5668	200	181	1656	3607	324	0	1145	2692
77	387	1621	3469	201	0	1718	3774	325	89	1881	4254
78	0	1772	3792	202	217	1755	3855	326	0	1740	3936
79	0	976	1563	203	0	2594	7985	327	0	1631	4585
80	29	1058	1694	204	286	792	2436	328	199	2697	7581
81	25	1433	2532	205	0	1107	3637	329	0	1361	3079
82	0	1114	1969	206	470	3621	11897	330	82	2263	5119
83	0	2166	6907	207	0	2100	5483	331	0	2131	4483
84	133	981	3128	208	49	1969	5139	332	83	1188	2499
85	584	1779	3632	209	121	2752	8144	333	0	990	1891
86	0	1413	2885	210	0	1688	4996	334	25	1920	3668
87	381	847	2301	211	0	2318	8226	335	0	1131	2736
88	0	849	2307	212	135	1029	3652	336	96	2686	6497
89	138	2170	4222	213	0	1407	2751	337	0	2382	4805
90	0	822	1600	214	167	1601	3130	338	117	757	1527
91	50	1609	3581	215	0	2101	4287	339	501	2742	7942
92	0	1927	4288	216	115	1085	2214	340	0	1656	4798
93	89	2087	4229	217	0	615	2090	341	236	1651	3208
94	0	1070	2169	218	258	1306	4440	342	0	1329	2582
95	68	1142	2072	219	0	726	3018	343	252	1602	2923
96	0	1547	2807	220	307	1377	5723	344	0	1113	2031
97	0	688	1429	221	0	1177	4922	345	0	1096	1985

Continued on next page

Table A.7 – continued from previous page

Sl. No.	I_{Lmax} (A)	I_{fmin} (A)	I_{fmax} (A)	Sl. No.	I_{Lmax} (A)	I_{fmin} (A)	I_{fmax} (A)	Sl. No.	I_{Lmax} (A)	I_{fmin} (A)	I_{fmax} (A)
98	54	2584	5370	222	437	2273	9505	346	170	1574	2852
99	109	982	2886	223	19	1319	6935	347	139	1637	3267
100	0	793	2332	224	0	953	5010	348	0	1469	2931
101	0	1495	3193	225	227	2639	5844	349	183	1594	3184
102	131	1886	4029	226	0	866	1919	350	0	1526	3048
103	56	1447	2725	227	0	1015	4275	351	253	1594	3119
104	0	1419	2673	228	547	2748	11572	352	0	1412	2762
105	48	2486	5277	229	0	1432	5975	353	212	1701	4245
106	0	861	1828	230	328	682	2844	354	0	2228	5561
107	0	911	1726	231	380	2031	9693	355	54	2542	5621
108	76	1986	3764	232	0	426	2034	356	0	968	2140
109	130	2671	6808	233	451	2187	5133	357	116	1616	2909
110	0	1329	3388	234	0	1542	3619	358	0	1033	1861
111	0	1843	5272	235	462	2224	5187	359	108	2422	5124
112	447	2507	7173	236	0	1516	3537	360	0	935	1979
113	17	1982	3414	237	267	2255	6036	361	104	1338	2315
114	0	461	793	238	0	1931	5169	362	0	1124	1946
115	68	1235	2976	239	89	2693	6490	363	100	1587	3072
116	0	2572	6198	240	0	1115	2688	364	0	1410	2730
117	0	1340	3189	241	93	1743	3556	365	71	1052	2140
118	152	2422	5766	242	0	1460	2978	366	0	2143	4360
119	0	2109	6061	243	50	1642	3380	367	0	2108	4361
120	468	905	2600	244	0	1604	3302	368	154	1127	2332
121	237	2169	4395	245	47	1495	2683	369	321	2295	4718
122	0	1003	2032	246	0	1124	2017	370	0	931	1915
123	192	1647	3156	247	50	2292	4721	371	16	1690	3331
124	0	1300	2491	248	0	926	1908	372	0	1354	2669

Table A.8: CTR of the relays for the IEEE 118-bus system

CTR	Relay No.
5000/5	305
4000/5	26, 30
3500/5	76,259
3000/5	12, 18, 85, 116, 168, 206, 228, 271, 339
2500/5	32, 46, 56, 59, 112, 120, 156, 184, 188, 209, 211, 222, 231, 233, 235, 262, 300, 303
2000/5	6, 15, 17, 19, 24, 47, 53, 55, 77, 83, 87, 109, 152, 157, 183, 203, 223, 230, 239, 261, 267, 270, 319, 328, 336, 369
1600/5	8, 13, 21, 31, 33, 35, 37, 45, 48, 62, 98, 105, 111, 116, 118, 119, 126, 136, 138, 159, 165, 167, 181, 191, 193, 204, 207, 208, 210, 218, 220, 221, 224, 225, 229, 237, 238, 250, 253, 256, 264, 265, 275, 277, 281, 284, 296, 301
1200/5	14, 20, 22, 39, 49, 54, 61, 63, 72, 73, 89, 92, 93, 102, 121, 128, 129, 146, 154, 180, 182, 187, 202, 215, 227, 247, 263, 282, 283, 290, 294, 312, 315, 321, 325, 327, 331, 340, 341, 353, 366, 367
1000/5	3,4,10,11,16,23,25,52,57,70,74,75,78,91,108,110,113,123,161,163,170,173,199,200, 201, 205,212, 214,234,236,241,243,244,249,257,258,266,268,269,273,279,288,291,293,304,308,309,326,334,346,347, 349, 371
800/5	1,2,7,27,28,42,44,58,60,65,66,68,81,84,86,96,99,101,103,104,115,117,124,127,131, 134,142,144,147,148,171,175, 185,186,189,190,195,196,197,198,213,219, 240,242,245,251,252,254, 255,260, 272,274,285,286,287,295,302,310,311,316,317,324,329,332,335,342,348,350,352, 357, 363,364,368,372
600/5	9,67,88,94,95,100,122,132,133,149,150,151,162,164,169,172,176,192,216,217,232,246,276,280,314, 318,338,344,356,361, 365
500/5	5,29,41,43,50,51,80,82,90,106,107,125,135,137,143,153,160,177,178,226,248,299,333,345,358,360,362, 370
400/5	34,36,38,69,79,97,130,139,140,145,158,194,278,289,297, 320
300/5	64,71,155,174, 298
250/5	141,179, 292
200/5	114
50/5	40

Table A.9: Primary/backup relay pairs along with the maximum fault current for the IEEE 118-bus system

Faulty Line	Serial No.	Primary Relay	Backup Relay	$I_{fprimary}$ (A)	$I_{fbackup}$ (A)
L1	1	1	4	3013	1505
	2	2	6	2612	2574
L2	3	3	2	3321	1331
	4	4	8	3466	2095
	5	4	10	3466	1313
L3	6	5	1	1620	1571
	7	6	9	6403	165
	8	6	23	6403	1181
	9	6	31	6403	1848
	10	6	36	6403	573
	11	6	38	6403	618
	12	6	40	6403	46
L4	13	7	3	2592	1641
	14	7	10	2592	902
	15	8	11	4588	1112
	16	8	16	4588	704
	17	8	18	4588	999
	18	8	20	4588	450
L5	19	9	3	2354	1186
	20	9	8	2354	1133
	21	10	5	3383	189
	22	10	23	3383	624
	23	10	31	3383	907
	24	10	36	3383	361
	25	10	38	3383	388
	26	10	40	3383	29
L6	27	11	14	3832	1784
	28	12	7	10072	1193
	29	12	16	10072	2088
	30	12	18	10072	2302
	31	12	20	10072	1446
L7	32	13	12	4876	3619
	33	14	19	4580	576
	34	14	32	4580	3321
	35	14	34	4580	614
L8	36	15	7	6356	620
	37	15	11	6356	1647
	38	15	18	6356	1472
	39	15	20	6356	675
	40	16	22	3929	2278
L9	41	17	7	6816	1057
	42	17	11	6816	2645
	43	17	16	6816	1854
	44	17	20	6816	1398
	45	18	26	3163	1095
	46	18	28	3163	1418
L10	47	19	7	5294	518
	48	19	11	5294	683
	49	19	16	5294	853
	50	19	18	5294	1392
	51	20	13	4484	495
	52	20	32	4484	3298
	53	20	34	4484	623
L11	54	21	15	5211	3272
	55	22	24	4618	4597
L12	56	23	21	3388	3372
	57	24	5	7621	650
L95	593	190	202	2935	367
	594	190	204	2935	409
L96	595	191	183	5184	2064
	596	191	187	5184	1180
	597	191	194	5184	285
	598	191	196	5184	383
	599	191	198	5184	402
	600	192	171	1353	1333
L97	601	193	183	5103	1885
	602	193	187	5103	1187
	603	193	192	5103	329
	604	193	196	5103	393
	605	193	198	5103	412
	606	194	175	1517	1495
L98	607	195	183	2491	1060
	608	195	187	2491	502
	609	195	192	2491	208
	610	195	194	2491	187
	611	195	198	2491	27
	612	196	185	2541	18
	613	196	189	2541	9
	614	196	197	2541	29
	615	196	200	2541	319
	616	196	202	2541	324
	617	196	204	2541	361
L99	618	197	183	2583	1100
	619	197	187	2583	521
	620	197	192	2583	216
	621	197	194	2583	194
	622	197	196	2583	26
	623	198	185	2639	19
	624	198	189	2639	9
	625	198	195	2639	29
	626	198	200	2639	331
	627	198	202	2639	337
	628	198	204	2639	375
	629	199	185	3897	350
L100	630	199	189	3897	360
	631	199	195	3897	303
	632	199	197	3897	318
	633	199	202	3897	106
	634	199	204	3897	358
	635	200	206	3607	2726
	636	200	208	3607	864
L101	637	201	185	3774	349
	638	201	189	3774	358
	639	201	195	3774	302
	640	201	197	3774	316
	641	201	200	3774	76
	642	201	204	3774	325
	643	202	205	3855	357
	644	202	210	3855	709
	645	202	212	3855	548
L102	646	203	185	7985	727
	647	203	189	7985	746
	648	203	195	7985	629
	649	203	197	7985	659

Continued on next page

Table A.9 – continued from previous page

Faulty Line	Serial No.	Primary Relay	Backup Relay	$I_{fprimary}$ (A)	$I_{fbackup}$ (A)	Faulty Line	Serial No.	Primary Relay	Backup Relay	$I_{fprimary}$ (A)	$I_{fbackup}$ (A)
	58	24	9	7621	527		650	203	200	7985	782
	59	24	31	7621	2166		651	203	202	7985	777
	60	24	36	7621	760		652	204	218	2436	2274
	61	24	38	7621	819		653	205	199	3637	1618
	62	24	40	7621	61		654	205	208	3637	1945
	63	25	17	3463	3678	L103	655	206	201	11897	1198
L13	64	25	28	3463	1333		656	206	210	11897	1432
	65	26	30	1786	1870		657	206	212	11897	2141
	66	27	17	2662	3033		658	207	199	5483	1111
	67	27	26	2662	875		659	207	206	5483	4351
L14	68	28	55	2915	2573	L104	660	208	209	5139	1812
	69	28	87	2915	778		661	208	214	5139	961
	70	28	100	2915	900		662	208	216	5139	966
L15	71	29	25	1997	2078		663	209	201	8144	965
	72	31	13	4895	1898		664	209	205	8144	332
	73	31	19	4895	1998	L105	665	209	212	8144	1661
	74	31	34	4895	877		666	210	207	4996	1046
	75	32	5	8023	757		667	210	214	4996	1137
L16	76	32	9	8023	606		668	210	216	4996	1143
	77	32	23	8023	1639		669	211	201	8226	921
	78	32	36	8023	871		670	211	205	8226	1695
	79	32	38	8023	953	L106	671	211	210	8226	1850
	80	32	40	8023	72		672	212	217	3652	1012
	81	33	13	5533	1167		673	212	220	3652	2578
L17	82	33	19	5533	1239		674	213	207	2751	728
	83	33	32	5533	3054		675	213	209	2751	1254
	84	34	42	1274	1178		676	213	216	2751	191
	85	35	5	6079	471	L107	677	214	165	3130	441
	86	35	9	6079	403		678	214	167	3130	441
	87	35	23	6079	1119		679	214	221	3130	475
L18	88	35	31	6079	1721		680	214	226	3130	187
	89	35	38	6079	519		681	215	207	4287	1097
	90	35	40	6079	42	L108	682	215	209	4287	1891
	91	36	44	1427	1414		683	215	214	4287	459
	92	37	5	5556	434		684	216	225	2214	2183
	93	37	9	5556	370		685	217	203	2090	4250
	94	37	23	5556	1026	L109	686	218	211	4440	3965
L19	95	37	31	5556	1593		687	218	220	4440	2707
	96	37	36	5556	431		688	219	211	3018	4116
	97	37	40	5556	39		689	219	217	3018	1225
	98	38	52	1577	1525	L110	690	220	125	5723	557
	99	39	5	4151	292		691	220	222	5723	2415
	100	39	9	4151	251		692	220	224	5723	1917
L20	101	39	23	4151	699		693	221	125	4922	519
	102	39	31	4151	1111		694	221	219	4922	859
	103	39	36	4151	324		695	221	224	4922	1792
	104	39	38	4151	350	L111	696	222	165	9505	1546
	105	41	33	1705	1656		697	222	167	9505	1546
	106	42	43	2567	122		698	222	213	9505	582
L21	107	42	46	2567	898		699	222	226	9505	592
	108	42	48	2567	788		700	223	125	6935	773
	109	42	50	2567	246		701	223	219	6935	1488
	110	43	35	1954	1947	L112	702	223	222	6935	3758
	111	44	41	3046	128		703	224	228	5010	5094
L22	112	44	46	3046	1072		704	224	230	5010	1770
	113	44	48	3046	940		705	224	232	5010	1505
	114	44	50	3046	295	L113	706	225	165	5844	752
L23	115	45	41	5719	601		707	225	167	5844	752
	116	45	43	5719	719		708	225	213	5844	103
	117	45	48	5719	2029		709	225	221	5844	876
	118	45	50	5719	748		710	226	215	1919	1884

Continued on next page

Table A.9 – continued from previous page

Faulty Line	Serial No.	Primary Relay	Backup Relay	$I_{fprimary}$ (A)	$I_{fbackup}$ (A)	Faulty Line	Serial No.	Primary Relay	Backup Relay	$I_{fprimary}$ (A)	$I_{fbackup}$ (A)
	119	46	51	7079	629	L114	711	227	223	4275	2696
	120	46	54	7079	1079		712	227	230	4275	1140
	121	46	56	7079	1355		713	227	232	4275	1045
	122	46	58	7079	991		714	228	153	11572	489
	123	46	60	7079	1663		715	228	169	11572	476
L24	124	47	41	6442	638		716	228	234	11572	951
	125	47	43	6442	766		717	228	236	11572	854
	126	47	46	6442	2686		718	228	238	11572	1146
	127	47	50	6442	740	L115	719	229	223	5975	3293
	128	48	61	5230	2040		720	229	228	5975	4189
	129	48	64	5230	584		721	229	232	5975	1264
	130	48	66	5230	879		722	230	271	2844	5413
L25	131	49	41	4225	322	L115	723	231	223	9693	4553
	132	49	43	4225	387		724	231	228	9693	5961
	133	49	46	4225	1507		725	231	230	9693	2057
	134	49	48	4225	1197	L117	726	233	153	5133	216
	135	50	108	1640	1596		727	233	169	5133	213
L26	136	51	37	1936	1901		728	233	227	5133	609
	137	52	45	3423	756		729	233	236	5133	63
	138	52	54	3423	632		730	233	238	5133	482
	139	52	56	3423	503		731	234	79	3619	354
	140	52	58	3423	389		732	234	240	3619	1038
	141	52	60	3423	651		733	234	242	3619	636
L27	142	53	45	7061	1469		734	234	244	3619	627
	143	53	51	7061	629	L118	735	235	153	5187	223
	144	53	56	7061	1268		736	235	169	5187	220
	145	53	58	7061	904		737	235	227	5187	615
	146	53	60	7061	1516		738	235	234	5187	33
	147	54	62	4149	2391		739	235	238	5187	362
L28	148	55	45	7359	2307		740	236	243	3537	717
	149	55	51	7359	691		741	236	249	3537	1195
	150	55	54	7359	1768		742	236	252	3537	681
	151	55	58	7359	1058		743	236	254	3537	913
	152	55	60	7359	1783	L119	744	237	153	6036	259
	153	56	27	3059	1115		745	237	169	6036	254
	154	56	87	3059	883		746	237	227	6036	626
	155	56	100	3059	997		747	237	234	6036	402
L29	156	57	45	3756	984		748	237	236	6036	220
	157	57	51	3756	308		749	238	251	5169	347
	158	57	54	3756	727		750	238	255	5169	464
	159	57	56	3756	605		751	238	260	5169	734
	160	57	60	3756	525		752	238	262	5169	1443
	161	58	97	2750	552		753	238	264	5169	680
	162	58	102	2750	1041		754	238	266	5169	761
L30	163	59	45	9056	2444	L120	755	239	79	6490	554
	164	59	51	9056	760		756	239	233	6490	1961
	165	59	54	9056	1811		757	239	242	6490	1176
	166	59	56	9056	1515		758	239	244	6490	1220
	167	59	58	9056	996		759	240	246	2688	1176
	168	60	103	3117	1271		760	240	248	2688	1525
L31	169	61	53	4622	2914	L121	761	241	79	3556	337
	170	62	47	5504	2614		762	241	233	3556	1072
	171	62	64	5504	523		763	241	240	3556	987
	172	62	66	5504	820		764	241	244	3556	248
L32	173	63	47	4320	1719		765	242	250	2978	1782
	174	63	61	4320	1234	L122	766	243	79	3380	331
	175	63	66	4320	482		767	243	233	3380	1014
	176	64	68	944	918		768	243	240	3380	969
L33	177	65	47	2450	948		769	243	242	3380	168
	178	65	61	2450	740		770	244	235	3302	1071
	179	65	64	2450	193		771	244	249	3302	674

Continued on next page

Table A.9 – continued from previous page

Faulty Line	Serial No.	Primary Relay	Backup Relay	$I_{fprimary}$ (A)	$I_{fbackup}$ (A)	Faulty Line	Serial No.	Primary Relay	Backup Relay	$I_{fprimary}$ (A)	$I_{fbackup}$ (A)
	180	66	110	2458	472		772	244	252	3302	671
	181	66	112	2458	1289		773	244	254	3302	863
	182	66	114	2458	161	L123	774	245	239	2683	1994
L34	183	67	63	2099	2078		775	245	248	2683	701
	184	68	70	1214	1174		776	246	81	2017	825
L35	185	69	67	1456	1417	L124	777	247	239	4721	3725
	186	70	72	1612	1592		778	247	246	4721	1001
L36	187	71	69	1006	985	L125	779	249	241	3432	1478
	188	72	74	3224	1049		780	250	235	5683	1932
	189	72	76	3224	1322		781	250	243	5683	1064
	190	72	78	3224	860		782	250	252	5683	1156
L37	191	73	71	4761	578		783	250	254	5683	1477
	192	73	76	4761	2531	L126	784	251	235	2732	804
	193	73	78	4761	1666		785	251	243	2732	546
	194	74	80	3392	697		786	251	249	2732	864
	195	74	82	3392	1031		787	251	254	2732	495
L38	196	75	71	3683	512		788	252	237	3189	529
	197	75	74	3683	1801		789	252	255	3189	25
	198	75	78	3683	1384		790	252	260	3189	448
	199	76	84	5668	1082		791	252	262	3189	884
	200	76	86	5668	552		792	252	264	3189	417
L39	201	77	71	3469	391		793	252	266	3189	452
	202	77	74	3469	1421	L127	794	253	235	5772	1779
	203	77	76	3469	1666		795	253	243	5772	1146
	204	78	91	3792	777		796	253	249	5772	1791
	205	78	101	3792	872		797	253	252	5772	1008
	206	78	104	3792	657		798	254	257	2459	2371
	207	78	106	3792	422	L128	799	255	258	2589	1273
L40	208	79	73	1563	858		800	256	237	4068	739
	209	79	82	1563	224		801	256	251	4068	95
	210	80	233	1694	463		802	256	260	4068	551
	211	80	240	1694	294		803	256	262	4068	1088
	212	80	242	1694	278		804	256	264	4068	513
	213	80	244	1694	288		805	256	266	4068	551
L41	214	81	73	2532	1438	L129	806	257	256	3572	1659
	215	81	80	2532	288		807	258	253	3328	3244
	216	82	245	1969	838	L130	808	259	237	13144	2549
L42	217	83	75	6907	1718		809	259	251	13144	1076
	218	83	86	6907	1099		810	259	255	13144	1221
	219	84	88	3128	879		811	259	262	13144	3301
L43	220	85	75	3632	456		812	259	264	13144	1556
	221	85	84	3632	669		813	259	266	13144	1742
	222	86	90	2885	478		814	260	268	2652	2488
	223	86	92	2885	933	L131	815	261	237	6769	1820
	224	86	94	2885	502		816	261	251	6769	781
L44	225	87	83	2301	1906		817	261	255	6769	892
	226	88	27	2307	734		818	261	260	6769	518
	227	88	55	2307	1919		819	261	264	6769	430
	228	88	100	2307	654		820	261	266	6769	1097
L45	229	89	85	4222	1107		821	262	263	8567	432
	230	89	92	4222	1201		822	262	269	8567	419
	231	89	94	4222	647		823	262	272	8567	1122
	232	90	96	1600	1562		824	262	274	8567	400
L46	233	91	85	3581	1270		825	262	276	8567	410
	234	91	90	3581	594		826	262	278	8567	547
	235	91	94	3581	212		827	262	280	8567	628
	236	92	77	4288	1243	L132	828	263	237	4738	1190
	237	92	101	4288	963		829	263	251	4738	511
	238	92	104	4288	868		830	263	255	4738	583
	239	92	106	4288	171		831	263	260	4738	339
L47	240	93	85	4229	1209		832	263	262	4738	596

Continued on next page

Table A.9 – continued from previous page

Faulty Line	Serial No.	Primary Relay	Backup Relay	$I_{fprimary}$ (A)	$I_{fbackup}$ (A)	Faulty Line	Serial No.	Primary Relay	Backup Relay	$I_{fprimary}$ (A)	$I_{fbackup}$ (A)
	241	93	90	4229	645		833	263	266	4738	717
	242	93	92	4229	976		834	264	261	5284	600
	243	94	371	2169	2129		835	264	269	5284	274
L48	244	95	89	2072	2040		836	264	272	5284	734
	245	96	98	2807	2780		837	264	274	5284	262
L49	246	97	95	1429	1391		838	264	276	5284	268
	247	98	57	5370	1619		839	264	278	5284	357
	248	98	102	5370	1817		840	264	280	5284	411
L50	249	99	27	2886	961	L133	841	265	237	5844	1181
	250	99	55	2886	2465		842	265	251	5844	499
	251	99	87	2886	740		843	265	255	5844	567
	252	100	119	2332	2452		844	265	260	5844	725
	253	100	126	2332	912		845	265	262	5844	1414
L51	254	101	57	3193	1203		846	265	264	5844	666
	255	101	97	3193	476		847	266	282	3489	1357
	256	102	77	4029	1086		848	266	284	3489	2083
	257	102	91	4029	709	L134	849	267	259	7975	7839
	258	102	104	4029	673		850	268	270	3467	3400
	259	102	106	4029	388	L135	851	269	267	3642	3585
L52	260	103	77	2725	651		852	270	261	7335	166
	261	103	91	2725	558		853	270	263	7335	78
	262	103	101	2725	492		854	270	272	7335	876
	263	103	106	2725	303		855	270	274	7335	345
	264	104	59	2673	2000		856	270	276	7335	352
L53	265	105	77	5277	1300		857	270	278	7335	424
	266	105	91	5277	581		858	270	280	7335	486
	267	105	101	5277	1106	L136	859	271	261	11040	1447
	268	105	104	5277	889		860	271	263	11040	682
	269	106	372	1828	1812		861	271	269	11040	695
L54	270	107	49	1726	1683		862	271	274	11040	556
	271	108	111	3764	1427		863	271	276	11040	566
	272	108	117	3764	361		864	271	278	11040	600
	273	108	120	3764	697		865	271	280	11040	685
	274	108	122	3764	400		866	272	229	3037	2824
	275	108	124	3764	385	L137	867	273	261	3657	377
L55	276	109	65	6808	968		868	273	263	3657	178
	277	109	112	6808	3629		869	273	269	3657	185
	278	109	114	6808	510		870	273	272	3657	458
	279	110	115	3388	1409		871	273	276	3657	396
L56	280	111	65	5272	1163		872	273	278	3657	163
	281	111	110	5272	1424		873	273	280	3657	207
	282	111	114	5272	619		874	274	283	2872	953
	283	112	107	7173	1079		875	274	325	2872	780
	284	112	117	7173	508		876	274	329	2872	712
	285	112	120	7173	1991		877	274	332	2872	402
	286	112	122	7173	1088	L138	878	275	261	6317	718
	287	112	124	7173	1047		879	275	263	6317	338
L57	288	113	65	3414	371		880	275	269	6317	347
	289	113	110	3414	594		881	275	272	6317	682
	290	113	112	3414	1799		882	275	274	6317	112
	291	114	140	793	757		883	275	278	6317	290
L58	292	115	118	2976	2916		884	275	280	6317	345
	293	116	109	6198	4152		885	276	331	2087	2053
L59	294	117	116	3189	3140	L139	886	277	261	5766	701
	295	118	107	5766	768		887	277	263	5766	330
	296	118	111	5766	1035		888	277	269	5766	336
	297	118	120	5766	1412		889	277	272	5766	580
	298	118	122	5766	771		890	277	274	5766	221
	299	118	124	5766	742		891	277	276	5766	225
L60	300	119	107	6061	823		892	277	280	5766	246
	301	119	111	6061	3247		893	278	334	1593	1549

Continued on next page

Table A.9 – continued from previous page

Faulty Line	Serial No.	Primary Relay	Backup Relay	$I_{fprimary}$ (A)	$I_{fbackup}$ (A)	Faulty Line	Serial No.	Primary Relay	Backup Relay	$I_{fprimary}$ (A)	$I_{fbackup}$ (A)
	302	119	117	6061	802	L140	894	279	261	3388	422
	303	119	122	6061	870		895	279	263	3388	199
	304	119	124	6061	838		896	279	269	3388	203
	305	120	99	2600	1319		897	279	272	3388	355
	306	120	126	2600	1036		898	279	274	3388	113
L61	307	121	107	4395	500		899	279	276	3388	116
	308	121	111	4395	1878		900	279	278	3388	65
	309	121	117	4395	461		901	280	336	2353	1530
	310	121	120	4395	914	L141	902	281	265	5402	2595
	311	121	124	4395	34		903	281	284	5402	2746
	312	122	128	2032	1981		904	282	286	2450	1019
L62	313	123	107	3156	395		905	282	288	2450	1426
	314	123	111	3156	1479	L142	906	283	265	4041	2406
	315	123	117	3156	364		907	283	282	4041	1573
	316	123	120	3156	721		908	284	273	5048	1113
	317	123	122	3156	333		909	284	325	5048	1447
	318	124	127	2491	359		910	284	329	5048	1320
	319	124	130	2491	539		911	284	332	5048	1122
	320	124	132	2491	516	L143	912	285	281	2738	2255
L63	321	125	99	1886	844		913	285	288	2738	486
	322	125	119	1886	1819		914	286	290	1924	1897
	323	126	219	2690	454	L144	915	287	281	2496	2312
	324	126	222	2690	1129		916	287	286	2496	181
	325	126	224	2690	812		917	288	289	2954	174
L64	326	127	121	2142	2080		918	288	292	2954	368
	327	128	123	4079	948		919	288	294	2954	872
	328	128	130	4079	794		920	288	296	2954	874
	329	128	132	4079	761	L145	921	289	285	1351	1314
L65	330	129	123	4616	1165		922	290	287	4687	502
	331	129	127	4616	1217		923	290	292	4687	492
	332	129	132	4616	595		924	290	294	4687	1179
	333	130	134	1453	1378		925	290	296	4687	1182
L66	334	131	123	2425	720	L146	926	291	287	3651	572
	335	131	127	2425	752		927	291	289	3651	417
	336	131	130	2425	71		928	291	294	3651	855
	337	132	133	2252	101		929	291	296	3651	857
	338	132	136	2252	538		930	292	298	919	754
	339	132	138	2252	538	L147	931	293	287	3675	691
L67	340	133	129	2051	2001		932	293	289	3675	504
	341	134	131	2707	290		933	293	292	3675	436
	342	134	136	2707	604		934	293	296	3675	878
	343	134	138	2707	604		935	294	300	2796	2748
L68	344	135	131	1723	387	L148	936	295	287	2733	537
	345	135	133	1723	389		937	295	289	2733	392
	346	135	138	1723	242		938	295	292	2733	345
	347	136	137	2211	246		939	295	294	2733	535
	348	136	145	2211	79		940	296	299	3796	522
	349	136	151	2211	187		941	296	302	3796	157
	350	136	155	2211	82		942	296	304	3796	298
	351	136	158	2211	113		943	296	306	3796	637
	352	136	160	2211	138		944	296	308	3796	201
	353	136	162	2211	117	L149	945	297	291	1503	1467
	354	136	164	2211	115	L150	946	299	293	1935	1866
	355	136	166	2211	367		947	300	295	7446	70
	356	136	168	2211	367		948	300	302	7446	271
	357	136	170	2211	139		949	300	304	7446	515
L69	358	137	131	1723	387		950	300	306	7446	1155
	359	137	133	1723	389	L151	951	300	308	7446	364
	360	137	136	1723	242		952	301	295	3411	247
	361	138	135	2211	246		953	301	299	3411	254
	362	138	145	2211	79		954	301	304	3411	813

Continued on next page

Table A.9 – continued from previous page

Faulty Line	Serial No.	Primary Relay	Backup Relay	$I_{fprimary}$ (A)	$I_{fbackup}$ (A)	Faulty Line	Serial No.	Primary Relay	Backup Relay	$I_{fprimary}$ (A)	$I_{fbackup}$ (A)
	363	138	151	2211	187		955	301	306	3411	529
	364	138	155	2211	82		956	301	308	3411	167
	365	138	158	2211	113		957	302	303	2560	806
	366	138	160	2211	138		958	302	310	2560	807
	367	138	162	2211	117	L152	959	303	295	5655	369
	368	138	164	2211	115		960	303	299	5655	378
	369	138	166	2211	367		961	303	302	5655	636
	370	138	168	2211	367		962	303	306	5655	789
	371	138	170	2211	139		963	303	308	5655	248
L70	372	139	113	1258	1234		964	304	301	3245	631
	373	140	142	1269	1265		965	304	310	3245	1202
L71	374	141	139	823	819	L153	966	305	295	8458	541
	375	142	144	2665	1310		967	305	299	8458	557
	376	142	146	2665	1280		968	305	302	8458	264
L72	377	143	141	1794	520		969	305	304	8458	502
	378	143	146	1794	1191		970	305	308	8458	424
	379	144	148	2830	922		971	306	307	5833	419
	380	144	150	2830	643		972	306	311	5833	862
L73	381	145	141	1577	464		973	306	314	5833	912
	382	145	144	1577	1049		974	306	316	5833	904
	383	146	135	3414	146		975	306	318	5833	680
	384	146	137	3414	146		976	306	320	5833	697
	385	146	151	3414	35	L154	977	307	295	3879	278
	386	146	155	3414	138		978	307	299	3879	286
	387	146	158	3414	174		979	307	302	3879	136
	388	146	160	3414	212		980	307	304	3879	258
	389	146	162	3414	181		981	307	306	3879	687
	390	146	164	3414	178		982	308	305	3450	683
	391	146	166	3414	568		983	308	311	3450	443
	392	146	168	3414	568		984	308	314	3450	468
	393	146	170	3414	212		985	308	316	3450	464
L74	394	147	143	2696	659		986	308	318	3450	349
	395	147	150	2696	654		987	308	320	3450	358
	396	148	152	2969	2247	L155	988	309	301	3979	898
	397	148	154	2969	709		989	309	303	3979	1708
L75	398	149	143	2310	500		990	310	312	3030	1565
	399	149	148	2310	716	L156	991	311	309	2670	1429
	400	150	156	2299	2299		992	312	305	4224	1415
L76	401	151	147	2342	1241		993	312	307	4224	446
	402	151	154	2342	1083		994	312	314	4224	478
	403	152	135	7583	324		995	312	316	4224	474
	404	152	137	7583	324		996	312	318	4224	352
	405	152	145	7583	104		997	312	320	4224	361
	406	152	155	7583	39	L157	998	313	305	5436	2119
	407	152	158	7583	368		999	313	307	5436	669
	408	152	160	7583	449		1000	313	311	5436	699
	409	152	162	7583	383		1001	313	316	5436	242
	410	152	164	7583	376		1002	313	318	5436	396
	411	152	166	7583	1199		1003	313	320	5436	408
	412	152	168	7583	1199		1004	314	322	2334	2304
	413	152	170	7583	425	L158	1005	315	305	3505	1525
L77	414	153	147	1975	542		1006	315	307	3505	481
	415	153	152	1975	1426		1007	315	311	3505	507
	416	154	169	2612	10		1008	315	314	3505	165
	417	154	227	2612	270		1009	315	318	3505	237
	418	154	234	2612	189		1010	315	320	3505	246
	419	154	236	2612	175		1011	316	321	3183	170
	420	154	238	2612	262		1012	316	324	3183	659
L78	421	155	149	1123	1125		1013	316	326	3183	710
	422	156	135	8757	351		1014	316	328	3183	1619
	423	156	137	8757	351	L159	1015	317	305	2260	918

Continued on next page

Table A.9 – continued from previous page

Faulty Line	Serial No.	Primary Relay	Backup Relay	$I_{fprimary}$ (A)	$I_{fbackup}$ (A)	Faulty Line	Serial No.	Primary Relay	Backup Relay	$I_{fprimary}$ (A)	$I_{fbackup}$ (A)
	424	156	145	8757	176		1016	317	307	2260	290
	425	156	151	8757	422		1017	317	311	2260	303
	426	156	158	8757	398		1018	317	314	2260	150
	427	156	160	8757	485		1019	317	316	2260	147
	428	156	162	8757	414		1020	317	320	2260	59
	429	156	164	8757	407		1021	318	327	2367	139
	430	156	166	8757	1303		1022	318	333	2367	168
	431	156	168	8757	1303		1023	318	335	2367	294
	432	156	170	8757	488		1024	318	338	2367	49
	433	157	135	6875	277		1025	318	340	2367	479
	434	157	137	6875	277		1026	318	342	2367	166
	435	157	145	6875	248		1027	318	344	2367	140
	436	157	151	6875	525		1028	319	305	7169	2554
	437	157	155	6875	234		1029	319	307	7169	806
L79	438	157	160	6875	295		1030	319	311	7169	839
	439	157	162	6875	256	L160	1031	319	314	7169	700
	440	157	164	6875	251		1032	319	316	7169	694
	441	157	166	6875	1017		1033	319	318	7169	494
	442	157	168	6875	1017		1034	320	345	1328	1317
	443	157	170	6875	385		1035	321	313	2418	2389
	444	158	172	1251	1220		1036	322	315	5125	655
	445	159	135	4407	189	L161	1037	322	324	5125	958
	446	159	137	4407	189		1038	322	326	5125	1032
	447	159	145	4407	169		1039	322	328	5125	2439
	448	159	151	4407	358		1040	323	315	6163	1119
	449	159	155	4407	159		1041	323	321	6163	1128
	450	159	158	4407	94	L162	1042	323	326	6163	733
L80	451	159	162	4407	96		1043	323	328	6163	3128
	452	159	164	4407	94		1044	324	330	2692	2538
	453	159	166	4407	687		1045	325	315	4254	895
	454	159	168	4407	687		1046	325	321	4254	902
	455	159	170	4407	262		1047	325	324	4254	98
	456	160	174	1854	623	L163	1048	325	328	4254	2501
	457	160	176	1854	1196		1049	326	273	3936	998
	458	161	135	2400	116		1050	326	283	3936	1712
	459	161	137	2400	116		1051	326	329	3936	185
	460	161	145	2400	104		1052	326	332	3936	1006
	461	161	151	2400	219		1053	327	315	4585	1036
	462	161	155	2400	98		1054	327	321	4585	1045
	463	161	158	2400	24		1055	327	324	4585	1180
	464	161	160	2400	40		1056	327	326	4585	1270
L81	465	161	164	2400	61		1057	328	317	7581	267
	466	161	166	2400	413	L164	1058	328	333	7581	482
	467	161	168	2400	413		1059	328	335	7581	883
	468	161	170	2400	160		1060	328	338	7581	284
	469	162	163	2278	59		1061	328	340	7581	1492
	470	162	179	2278	48		1062	328	342	7581	517
	471	162	182	2278	215		1063	328	344	7581	436
	472	162	184	2278	1068		1064	329	323	3079	2938
	473	162	186	2278	222		1065	330	273	5119	1141
	474	163	135	2363	114	L165	1066	330	283	5119	1962
	475	163	137	2363	114		1067	330	325	5119	822
	476	163	145	2363	102		1068	330	332	5119	1150
	477	163	151	2363	216		1069	331	273	4483	788
	478	163	155	2363	96		1070	331	283	4483	1497
	479	163	158	2363	24	L166	1071	331	325	4483	1130
	480	163	160	2363	39		1072	331	329	4483	1030
L82	481	163	162	2363	61		1073	332	275	2499	2468
	482	163	166	2363	407	L167	1074	333	277	1891	1860
	483	163	168	2363	407		1075	334	317	3668	182
	484	163	170	2363	158		1076	334	327	3668	517

Continued on next page

Table A.9 – continued from previous page

Faulty Line	Serial No.	Primary Relay	Backup Relay	$I_{fprimary}$ (A)	$I_{fbackup}$ (A)	Faulty Line	Serial No.	Primary Relay	Backup Relay	$I_{fprimary}$ (A)	$I_{fbackup}$ (A)
	485	164	161	2244	59		1077	334	335	3668	335
	486	164	179	2244	47		1078	334	338	3668	188
	487	164	182	2244	211		1079	334	340	3668	646
	488	164	184	2244	1052		1080	334	342	3668	224
	489	164	186	2244	219		1081	334	344	3668	189
L83	490	165	135	5676	287	L168	1082	335	279	2736	1261
	491	165	137	5676	287		1083	336	317	6497	334
	492	165	145	5676	256		1084	336	327	6497	1041
	493	165	151	5676	538		1085	336	333	6497	374
	494	165	155	5676	244		1086	336	338	6497	345
	495	165	158	5676	316		1087	336	340	6497	1163
	496	165	160	5676	386		1088	336	342	6497	403
	497	165	162	5676	329		1089	336	344	6497	340
	498	165	164	5676	323	L169	1090	337	317	4805	135
	499	165	168	5676	170		1091	337	327	4805	619
	500	165	170	5676	388		1092	337	333	4805	307
	501	166	167	5936	171		1093	337	335	4805	529
	502	166	213	5936	399		1094	337	340	4805	849
	503	166	221	5936	1102		1095	337	342	4805	294
	504	166	226	5936	404		1096	337	344	4805	248
L84	505	167	135	5676	287		1097	338	346	1527	1469
	506	167	137	5676	287	L170	1098	339	317	7942	461
	507	167	145	5676	256		1099	339	327	7942	1494
	508	167	151	5676	538		1100	339	333	7942	583
	509	167	155	5676	244		1101	339	335	7942	994
	510	167	158	5676	316		1102	339	338	7942	476
	511	167	160	5676	386		1103	339	342	7942	257
	512	167	162	5676	329		1104	339	344	7942	275
	513	167	164	5676	323		1105	340	348	4798	849
	514	167	166	5676	170		1106	340	350	4798	890
	515	167	170	5676	388		1107	340	352	4798	1058
	516	168	165	5936	171	L171	1108	341	317	3208	191
	517	168	213	5936	399		1109	341	327	3208	619
	518	168	221	5936	1102		1110	341	333	3208	241
	519	168	226	5936	404		1111	341	335	3208	411
L85	520	169	135	2190	91		1112	341	338	3208	197
	521	169	137	2190	91		1113	341	340	3208	159
	522	169	145	2190	77		1114	341	344	3208	17
	523	169	151	2190	105		1115	342	347	2582	446
	524	169	155	2190	71		1116	342	354	2582	1328
	525	169	158	2190	102	L172	1117	343	317	2923	166
	526	169	160	2190	124		1118	343	327	2923	538
	527	169	162	2190	106		1119	343	333	2923	210
	528	169	164	2190	104		1120	343	335	2923	358
	529	169	166	2190	315		1121	343	338	2923	171
	530	169	168	2190	315		1122	343	340	2923	259
	531	170	153	2266	23		1123	343	342	2923	4
	532	170	227	2266	229		1124	344	355	2031	1520
	533	170	234	2266	167		1125	344	362	2031	470
	534	170	236	2266	155	L173	1126	345	337	1985	1930
	535	170	238	2266	231		1127	346	319	2852	2845
L86	536	171	157	2398	2379	L174	1128	347	339	3267	1583
	537	172	191	2022	2007		1129	347	350	3267	160
L87	538	173	159	3247	1840		1130	347	352	3267	489
	539	173	176	3247	1368		1131	348	341	2931	548
	540	174	178	1103	1068		1132	348	354	2931	1419
L88	541	175	159	2567	1842	L175	1133	349	339	3184	1594
	542	175	174	2567	686		1134	349	348	3184	132
	543	176	193	2340	2320		1135	349	352	3184	438
L89	544	177	173	1671	1642		1136	350	353	3048	862
	545	178	180	1698	1654		1137	350	356	3048	511

Continued on next page

Table A.9 – continued from previous page

Faulty Line	Serial No.	Primary Relay	Backup Relay	$I_{fprimary}$ (A)	$I_{fbackup}$ (A)	Faulty Line	Serial No.	Primary Relay	Backup Relay	$I_{fprimary}$ (A)	$I_{fbackup}$ (A)
L90	546	179	177	986	920		1138	350	358	3048	337
	547	180	161	4495	326		1139	350	360	3048	499
	548	180	163	4495	320	L176	1140	351	339	3119	1519
	549	180	182	4495	380		1141	351	348	3119	371
	550	180	184	4495	1903		1142	351	350	3119	335
	551	180	186	4495	400		1143	352	365	2762	486
L91	552	181	161	5103	585		1144	352	368	2762	745
	553	181	163	5103	574		1145	352	370	2762	642
	554	181	179	5103	267	L177	1146	353	341	4245	1221
	555	181	184	5103	1077		1147	353	347	4245	1201
	556	181	186	5103	633		1148	354	349	5561	1008
	557	182	188	4443	2187		1149	354	356	5561	1103
	558	182	190	4443	782		1150	354	358	5561	668
L92	559	183	161	7184	958		1151	354	360	5561	1149
	560	183	163	7184	940	L178	1152	355	349	5621	938
	561	183	179	7184	425		1153	355	353	5621	2028
	562	183	182	7184	566		1154	355	358	5621	303
	563	183	186	7184	1064		1155	355	360	5621	983
	564	184	187	8013	2349		1156	356	343	2140	1234
	565	184	192	8013	880		1157	356	362	2140	819
	566	184	194	8013	742	L179	1158	357	349	2909	522
	567	184	196	8013	929		1159	357	353	2909	1124
	568	184	198	8013	974		1160	357	356	2909	26
L93	569	185	161	2722	244		1161	357	360	2909	538
	570	185	163	2722	239		1162	358	361	1861	521
	571	185	179	2722	118	L180	1163	359	349	5124	799
	572	185	182	2722	203		1164	359	353	5124	1786
	573	185	184	2722	1083		1165	359	356	5124	839
	574	186	189	2796	27		1166	359	358	5124	494
	575	186	195	2796	11		1167	360	364	1979	1976
	576	186	197	2796	11	L181	1168	361	343	2315	703
	577	186	200	2796	345		1169	361	355	2315	1566
	578	186	202	2796	351		1170	362	357	1946	651
	579	186	204	2796	391	L182	1171	363	359	3072	3068
L94	580	187	181	4464	1076		1172	364	366	2730	2713
	581	187	190	4464	1174	L183	1173	365	363	2140	2124
	582	188	183	9259	4036		1174	366	351	4360	932
	583	188	192	9259	821		1175	366	368	4360	1119
	584	188	194	9259	734		1176	366	370	4360	965
	585	188	196	9259	837	L184	1177	367	351	4361	1030
	586	188	198	9259	877		1178	367	365	4361	1006
L95	587	189	181	2726	447		1179	367	370	4361	978
	588	189	188	2726	1605	L185	1180	369	351	4718	1076
	589	190	185	2935	39		1181	369	365	4718	1051
	590	190	195	2935	11		1182	369	368	4718	1185
	591	190	197	2935	11	L186	1183	371	105	3331	3313
	592	190	200	2935	361		1184	372	93	2669	2621

Table A.10: Primary/backup relay pairs for the standard IEEE 14-bus system

Faulty line	Serial No.	Primary relay	Backup relay	Faulty line No.	Serial	Primary relay	Backup relay	Faulty line No.	Serial	Primary relay	Backup relay
L1	1	1	4	L7	33	13	7	L12	65	23	19
	2	2	6		34	13	11		66	23	22
	3	2	8		35	13	18		67	23	26
	4	2	10		36	13	28		68	24	38

Continued on next page

Table A.10 – continued from previous page

Faulty line	Serial No.	Primary relay	Backup relay	Faulty line No.	Serial	Primary relay	Backup relay	Faulty line No.	Serial	Primary relay	Backup relay
L2	5	3	2		37	13	30	L13	69	25	19
	6	4	9		38	14	3		70	25	22
	7	4	13		39	14	9		71	25	24
	8	4	20		40	14	20		72	26	37
L3	9	5	1	L8	41	15	7		73	26	40
	10	5	8		42	15	11	L15	74	30	17
	11	5	10		43	15	14		75	30	32
	12	6	12		44	15	18		76	30	34
L4	13	7	1	L9	45	17	7	L16	77	31	15
	14	7	6		46	17	11		78	31	17
	15	7	10		47	17	14		79	31	28
	16	8	11		48	17	28		80	31	34
	17	8	14		49	17	30		81	32	36
	18	8	18		50	18	15	L17	82	33	15
	19	8	28		51	18	28		83	33	17
	20	8	30		52	18	32		84	33	28
L5	21	9	1		53	18	34		85	33	32
	22	9	6	L10	54	19	3		86	34	39
	23	9	8		55	19	9	L18	87	35	31
	24	10	3		56	19	13		88	36	21
	25	10	13		57	20	22	L19	89	37	23
	26	10	20		58	20	24		90	38	25
L6	27	11	5		59	20	26		91	38	40
	28	12	7	L11	60	21	19	L20	92	39	25
	29	12	14		61	21	24		93	39	37
	30	12	18		62	21	26		94	40	33
	31	12	28		63	22	35		95	-	-
	32	12	30		64	-	-		96	-	-

Table A.11: Primary/backup relay pairs for the standard IEEE 30-bus system

Faulty line	Serial No.	Primary relay	Backup relay	Faulty line No.	Serial	Primary relay	Backup relay	Faulty line No.	Serial	Primary relay	Backup relay
L1	1	1	4	L12	66	23	9	L22	131	43	15
	2	2	6		67	23	13		132	43	46
	3	2	8		68	23	20		133	43	48
	4	2	10		69	23	22		134	43	50
L2	5	3	2		70	23	26	L23	135	45	15
	6	4	12		71	23	28		136	45	44
L3	7	5	1	L13	72	25	9		137	45	48
	8	5	8		73	25	13		138	45	50
	9	5	10		74	25	20		139	46	52
	10	6	11		75	25	22	L24	140	47	15
	11	6	14		76	25	28		141	47	44
	12	6	16		77	25	32		142	47	46
L4	13	7	1		78	25	34		143	47	50
	14	7	6		79	26	23		144	48	51
	15	7	10		80	26	34		145	48	54
	16	8	18		81	26	36		146	48	56
L5	17	9	1		82	26	38	L25	147	49	15
	18	9	6		83	26	40		148	49	44
	19	9	8		84	26	42		149	49	46
	20	10	13	L14	85	27	9		150	49	48
	21	10	20		86	27	13		151	50	58
	22	10	22		87	27	20	L26	152	51	45
	23	10	26		88	27	22		153	52	47
	24	10	28		89	27	26		154	52	54

Continued on next page

Table A.11 – continued from previous page

Faulty line	Serial No.	Primary relay	Backup relay	Faulty line No.	Serial	Primary relay	Backup relay	Faulty line No.	Serial	Primary relay	Backup relay
	25	10	32		90	27	32		155	52	56
	26	10	34		91	27	34	L27	156	53	47
L6	27	11	3		92	28	29		157	53	51
	28	12	5		93	28	75		158	53	56
	29	12	14	L15	94	29	21		159	54	60
	30	12	16		95	30	27	L28	160	55	47
L7	31	13	5		96	30	75		161	55	51
	32	13	11	L16	97	32	25		162	55	54
	33	13	16		98	32	36		163	56	68
	34	14	9		99	32	38	L29	164	57	49
	35	14	20		100	32	40		165	58	35
	36	14	22		101	32	42	L30	166	59	53
	37	14	26	L18	102	35	23		167	60	62
	38	14	28		103	35	25	L31	168	61	59
	39	14	32		104	35	34		169	62	37
	40	14	34		105	35	38	L32	170	63	39
L8	41	15	5		106	35	40		171	64	41
	42	15	11		107	35	42		172	64	66
	43	15	14		108	36	57	L33	173	65	41
	44	16	44	L19	109	37	23		174	65	63
	45	16	46		110	37	25		175	66	67
	46	16	48		111	37	34		176	66	70
	47	16	50		112	37	36	L34	177	67	55
L9	48	17	7		113	37	40		178	68	65
	49	18	19		114	37	42		179	68	70
L10	50	19	9		115	38	61	L35	180	69	65
	51	19	13	L20	116	39	23		181	69	67
	52	19	22		117	39	25		182	70	74
	53	19	26		118	39	34	L36	183	71	69
	54	19	28		119	39	36		184	71	74
	55	19	32		120	39	38	L37	185	73	69
	56	19	34		121	39	42		186	74	76
	57	20	17		122	40	64	L38	187	75	73
L11	58	21	9	L21	123	41	23		188	76	27
	59	21	13		124	41	25		189	76	29
	60	21	20		125	41	34	L39	190	77	73
	61	21	26		126	41	36		191	77	76
	62	21	28		127	41	38	L40	192	79	73
	63	21	32		128	41	40		193	79	76
	64	21	34		129	42	63	L41	194	81	77
	65	22	30		130	42	66		195	82	79

Table A.12: Primary/backup relay pairs for the standard IEEE 118-bus system

Faulty line	Serial No.	Primary relay	Backup relay	Faulty line No.	Serial	Primary relay	Backup relay	Faulty line No.	Serial	Primary relay	Backup relay
L1	1	1	4	L74	396	148	152	L126	791	252	262
	2	2	6		397	148	154		792	252	264
L2	3	3	2	L75	398	149	143		793	252	266
	4	4	8		399	149	148	L127	794	253	235
	5	4	10		400	150	156		795	253	243
L3	6	5	1	L76	401	151	147		796	253	249
	7	6	9		402	151	154		797	253	252
	8	6	23		403	152	135		798	254	257
	9	6	31		404	152	137	L128	799	255	258
	10	6	36		405	152	145		800	256	237
	11	6	38		406	152	155		801	256	251

Continued on next page

Table A.12 – continued from previous page

Faulty line	Serial No.	Primary relay	Backup relay	Faulty line No.	Serial	Primary relay	Backup relay	Faulty line No.	Serial	Primary relay	Backup relay
	12	6	40		407	152	158		802	256	260
L4	13	7	3		408	152	160		803	256	262
	14	7	10		409	152	162		804	256	264
	15	8	11		410	152	164		805	256	266
	16	8	16		411	152	166	L129	806	257	256
	17	8	18		412	152	168		807	258	253
	18	8	20		413	152	170	L130	808	259	237
L5	19	9	3	L77	414	153	147		809	259	251
	20	9	8		415	153	152		810	259	255
	21	10	5		416	154	169		811	259	262
	22	10	23		417	154	227		812	259	264
	23	10	31		418	154	234		813	259	266
	24	10	36		419	154	236		814	260	268
	25	10	38		420	154	238	L131	815	261	237
	26	10	40	L78	421	155	149		816	261	251
L6	27	11	14		422	156	135		817	261	255
	28	12	7		423	156	137		818	261	260
	29	12	16		424	156	145		819	261	264
	30	12	18		425	156	151		820	261	266
	31	12	20		426	156	158		821	262	263
L7	32	13	12		427	156	160		822	262	269
	33	14	19		428	156	162		823	262	272
	34	14	32		429	156	164		824	262	274
	35	14	34		430	156	166		825	262	276
L8	36	15	7		431	156	168		826	262	278
	37	15	11		432	156	170		827	262	280
	38	15	18	L79	433	157	135	L132	828	263	237
	39	15	20		434	157	137		829	263	251
	40	16	22		435	157	145		830	263	255
L9	41	17	7		436	157	151		831	263	260
	42	17	11		437	157	155		832	263	262
	43	17	16		438	157	160		833	263	266
	44	17	20		439	157	162		834	264	261
	45	18	26		440	157	164		835	264	269
	46	18	28		441	157	166		836	264	272
L10	47	19	7		442	157	168		837	264	274
	48	19	11		443	157	170		838	264	276
	49	19	16		444	158	172		839	264	278
	50	19	18	L80	445	159	135		840	264	280
	51	20	13		446	159	137	L133	841	265	237
	52	20	32		447	159	145		842	265	251
	53	20	34		448	159	151		843	265	255
L11	54	21	15		449	159	155		844	265	260
	55	22	24		450	159	158		845	265	262
L12	56	23	21		451	159	162		846	265	264
	57	24	5		452	159	164		847	266	282
	58	24	9		453	159	166		848	266	284
	59	24	31		454	159	168	L134	849	267	259
	60	24	36		455	159	170		850	268	270
	61	24	38		456	160	174	L135	851	269	267
	62	24	40		457	160	176		852	270	261
L13	63	25	17	L81	458	161	135		853	270	263
	64	25	28		459	161	137		854	270	272
	65	26	30		460	161	145		855	270	274
L14	66	27	17		461	161	151		856	270	276
	67	27	26		462	161	155		857	270	278
	68	28	55		463	161	158		858	270	280
	69	28	87		464	161	160	L136	859	271	261
	70	28	100		465	161	164		860	271	263
L15	71	29	25		466	161	166		861	271	269
L16	72	31	13		467	161	168		862	271	274

Continued on next page

Table A.12 – continued from previous page

Faulty line	Serial No.	Primary relay	Backup relay	Faulty line No.	Serial	Primary relay	Backup relay	Faulty line No.	Serial	Primary relay	Backup relay
	73	31	19		468	161	170		863	271	276
	74	31	34		469	162	163		864	271	278
	75	32	5		470	162	179		865	271	280
	76	32	9		471	162	182		866	272	229
	77	32	23		472	162	184	L137	867	273	261
	78	32	36		473	162	186		868	273	263
	79	32	38	L82	474	163	135		869	273	269
	80	32	40		475	163	137		870	273	272
L17	81	33	13		476	163	145		871	273	276
	82	33	19		477	163	151		872	273	278
	83	33	32		478	163	155		873	273	280
	84	34	42		479	163	158		874	274	283
L18	85	35	5		480	163	160		875	274	325
	86	35	9		481	163	162		876	274	329
	87	35	23		482	163	166		877	274	332
	88	35	31		483	163	168	L138	878	275	261
	89	35	38		484	163	170		879	275	263
	90	35	40		485	164	161		880	275	269
	91	36	44		486	164	179		881	275	272
L19	92	37	5		487	164	182		882	275	274
	93	37	9		488	164	184		883	275	278
	94	37	23		489	164	186		884	275	280
	95	37	31	L83	490	165	135		885	276	331
	96	37	36		491	165	137	L139	886	277	261
	97	37	40		492	165	145		887	277	263
	98	38	52		493	165	151		888	277	269
L20	99	39	5		494	165	155		889	277	272
	100	39	9		495	165	158		890	277	274
	101	39	23		496	165	160		891	277	276
	102	39	31		497	165	162		892	277	280
	103	39	36		498	165	164		893	278	334
	104	39	38		499	165	168	L140	894	279	261
L21	105	41	33		500	165	170		895	279	263
	106	42	43		501	166	167		896	279	269
	107	42	46		502	166	213		897	279	272
	108	42	48		503	166	221		898	279	274
	109	42	50		504	166	226		899	279	276
L22	110	43	35	L84	505	167	135		900	279	278
	111	44	41		506	167	137		901	280	336
	112	44	46		507	167	145	L141	902	281	265
	113	44	48		508	167	151		903	281	284
	114	44	50		509	167	155		904	282	286
L23	115	45	41		510	167	158		905	282	288
	116	45	43		511	167	160	L142	906	283	265
	117	45	48		512	167	162		907	283	282
	118	45	50		513	167	164		908	284	273
	119	46	51		514	167	166		909	284	325
	120	46	54		515	167	170		910	284	329
	121	46	56		516	168	165		911	284	332
	122	46	58		517	168	213	L143	912	285	281
	123	46	60		518	168	221		913	285	288
L24	124	47	41		519	168	226		914	286	290
	125	47	43	L85	520	169	135	L144	915	287	281
	126	47	46		521	169	137		916	287	286
	127	47	50		522	169	145		917	288	289
	128	48	61		523	169	151		918	288	292
	129	48	64		524	169	155		919	288	294
	130	48	66		525	169	158		920	288	296
L25	131	49	41		526	169	160	L145	921	289	285
	132	49	43		527	169	162		922	290	287
	133	49	46		528	169	164		923	290	292

Continued on next page

Table A.12 – continued from previous page

Faulty line	Serial No.	Primary relay	Backup relay	Faulty line No.	Serial	Primary relay	Backup relay	Faulty line No.	Serial	Primary relay	Backup relay
	134	49	48		529	169	166		924	290	294
	135	50	108		530	169	168		925	290	296
L26	136	51	37		531	170	153	L146	926	291	287
	137	52	45		532	170	227		927	291	289
	138	52	54		533	170	234		928	291	294
	139	52	56		534	170	236		929	291	296
	140	52	58		535	170	238		930	292	298
	141	52	60	L86	536	171	157	L147	931	293	287
L27	142	53	45		537	172	191		932	293	289
	143	53	51	L87	538	173	159		933	293	292
	144	53	56		539	173	176		934	293	296
	145	53	58		540	174	178		935	294	300
	146	53	60	L88	541	175	159	L148	936	295	287
	147	54	62		542	175	174		937	295	289
L28	148	55	45		543	176	193		938	295	292
	149	55	51	L89	544	177	173		939	295	294
	150	55	54		545	178	180		940	296	299
	151	55	58	L90	546	179	177		941	296	302
	152	55	60		547	180	161		942	296	304
	153	56	27		548	180	163		943	296	306
	154	56	87		549	180	182		944	296	308
	155	56	100		550	180	184	L149	945	297	291
L29	156	57	45		551	180	186	L150	946	299	293
	157	57	51	L91	552	181	161		947	300	295
	158	57	54		553	181	163		948	300	302
	159	57	56		554	181	179		949	300	304
	160	57	60		555	181	184		950	300	306
	161	58	97		556	181	186		951	300	308
	162	58	102		557	182	188	L151	952	301	295
L30	163	59	45		558	182	190		953	301	299
	164	59	51	L92	559	183	161		954	301	304
	165	59	54		560	183	163		955	301	306
	166	59	56		561	183	179		956	301	308
	167	59	58		562	183	182		957	302	303
	168	60	103		563	183	186		958	302	310
L31	169	61	53		564	184	187	L152	959	303	295
	170	62	47		565	184	192		960	303	299
	171	62	64		566	184	194		961	303	302
	172	62	66		567	184	196		962	303	306
L32	173	63	47		568	184	198		963	303	308
	174	63	61	L93	569	185	161		964	304	301
	175	63	66		570	185	163		965	304	310
	176	64	68		571	185	179	L153	966	305	295
L33	177	65	47		572	185	182		967	305	299
	178	65	61		573	185	184		968	305	302
	179	65	64		574	186	189		969	305	304
	180	66	110		575	186	195		970	305	308
	181	66	112		576	186	197		971	306	307
	182	66	114		577	186	200		972	306	311
L34	183	67	63		578	186	202		973	306	314
	184	68	70		579	186	204		974	306	316
L35	185	69	67	L94	580	187	181		975	306	318
	186	70	72		581	187	190		976	306	320
L36	187	71	69		582	188	183	L154	977	307	295
	188	72	74		583	188	192		978	307	299
	189	72	76		584	188	194		979	307	302
	190	72	78		585	188	196		980	307	304
L37	191	73	71		586	188	198		981	307	306
	192	73	76	L95	587	189	181		982	308	305
	193	73	78		588	189	188		983	308	311
	194	74	80		589	190	185		984	308	314

Continued on next page

Table A.12 – continued from previous page

Faulty line	Serial No.	Primary relay	Backup relay	Faulty line No.	Serial	Primary relay	Backup relay	Faulty line No.	Serial	Primary relay	Backup relay
	195	74	82		590	190	195		985	308	316
L38	196	75	71		591	190	197		986	308	318
	197	75	74		592	190	200		987	308	320
	198	75	78		593	190	202	L155	988	309	301
	199	76	84		594	190	204		989	309	303
	200	76	86	L96	595	191	183		990	310	312
L39	201	77	71		596	191	187	L156	991	311	309
	202	77	74		597	191	194		992	312	305
	203	77	76		598	191	196		993	312	307
	204	78	91		599	191	198		994	312	314
	205	78	101		600	192	171		995	312	316
	206	78	104	L97	601	193	183		996	312	318
	207	78	106		602	193	187		997	312	320
L40	208	79	73		603	193	192	L157	998	313	305
	209	79	82		604	193	196		999	313	307
	210	80	233		605	193	198		1000	313	311
	211	80	240		606	194	175		1001	313	316
	212	80	242	L98	607	195	183		1002	313	318
	213	80	244		608	195	187		1003	313	320
L41	214	81	73		609	195	192		1004	314	322
	215	81	80		610	195	194	L158	1005	315	305
	216	82	245		611	195	198		1006	315	307
L42	217	83	75		612	196	185		1007	315	311
	218	83	86		613	196	189		1008	315	314
	219	84	88		614	196	197		1009	315	318
L43	220	85	75		615	196	200		1010	315	320
	221	85	84		616	196	202		1011	316	321
	222	86	90		617	196	204		1012	316	324
	223	86	92	L99	618	197	183		1013	316	326
	224	86	94		619	197	187		1014	316	328
L44	225	87	83		620	197	192	L159	1015	317	305
	226	88	27		621	197	194		1016	317	307
	227	88	55		622	197	196		1017	317	311
	228	88	100		623	198	185		1018	317	314
L45	229	89	85		624	198	189		1019	317	316
	230	89	92		625	198	195		1020	317	320
	231	89	94		626	198	200		1021	318	327
	232	90	96		627	198	202		1022	318	333
L46	233	91	85		628	198	204		1023	318	335
	234	91	90		629	199	185		1024	318	338
	235	91	94	L100	630	199	189		1025	318	340
	236	92	77		631	199	195		1026	318	342
	237	92	101		632	199	197		1027	318	344
	238	92	104		633	199	202	L160	1028	319	305
	239	92	106		634	199	204		1029	319	307
L47	240	93	85		635	200	206		1030	319	311
	241	93	90		636	200	208		1031	319	314
	242	93	92	L101	637	201	185		1032	319	316
	243	94	371		638	201	189		1033	319	318
L48	244	95	89		639	201	195		1034	320	345
	245	96	98		640	201	197	L161	1035	321	313
L49	246	97	95		641	201	200		1036	322	315
	247	98	57		642	201	204		1037	322	324
	248	98	102		643	202	205		1038	322	326
L50	249	99	27		644	202	210		1039	322	328
	250	99	55		645	202	212	L162	1040	323	315
	251	99	87	L102	646	203	185		1041	323	321
	252	100	119		647	203	189		1042	323	326
	253	100	126		648	203	195		1043	323	328
L51	254	101	57		649	203	197		1044	324	330
	255	101	97		650	203	200	L163	1045	325	315

Continued on next page

Table A.12 – continued from previous page

Faulty line	Serial No.	Primary relay	Backup relay	Faulty line No.	Serial	Primary relay	Backup relay	Faulty line No.	Serial	Primary relay	Backup relay
	256	102	77		651	203	202		1046	325	321
	257	102	91		652	204	218		1047	325	324
	258	102	104		653	205	199		1048	325	328
	259	102	106		654	205	208		1049	326	273
	260	103	77	L103	655	206	201		1050	326	283
	261	103	91		656	206	210		1051	326	329
L52	262	103	101		657	206	212		1052	326	332
	263	103	106		658	207	199		1053	327	315
	264	104	59		659	207	206		1054	327	321
	265	105	77	L104	660	208	209		1055	327	324
	266	105	91		661	208	214		1056	327	326
L53	267	105	101		662	208	216		1057	328	317
	268	105	104		663	209	201	L164	1058	328	333
	269	106	372		664	209	205		1059	328	335
	270	107	49	L105	665	209	212		1060	328	338
	271	108	111		666	210	207		1061	328	340
L54	272	108	117		667	210	214		1062	328	342
	273	108	120		668	210	216		1063	328	344
	274	108	122		669	211	201		1064	329	323
	275	108	124		670	211	205		1065	330	273
	276	109	65	L106	671	211	210	L165	1066	330	283
L55	277	109	112		672	212	217		1067	330	325
	278	109	114		673	212	220		1068	330	332
	279	110	115		674	213	207		1069	331	273
	280	111	65		675	213	209		1070	331	283
	281	111	110		676	213	216	L166	1071	331	325
	282	111	114	L107	677	214	165		1072	331	329
L56	283	112	107		678	214	167		1073	332	275
	284	112	117		679	214	221		1074	333	277
	285	112	120		680	214	226		1075	334	317
	286	112	122		681	215	207		1076	334	327
	287	112	124	L108	682	215	209	L167	1077	334	335
	288	113	65		683	215	214		1078	334	338
L57	289	113	110		684	216	225		1079	334	340
	290	113	112		685	217	203		1080	334	342
	291	114	140	L109	686	218	211		1081	334	344
L58	292	115	118		687	218	220		1082	335	279
	293	116	109		688	219	211		1083	336	317
	294	117	116		689	219	217		1084	336	327
	295	118	107	L110	690	220	125	L168	1085	336	333
L59	296	118	111		691	220	222		1086	336	338
	297	118	120		692	220	224		1087	336	340
	298	118	122		693	221	125		1088	336	342
	299	118	124		694	221	219		1089	336	344
	300	119	107		695	221	224		1090	337	317
	301	119	111	L111	696	222	165		1091	337	327
	302	119	117		697	222	167		1092	337	333
L60	303	119	122		698	222	213	L169	1093	337	335
	304	119	124		699	222	226		1094	337	340
	305	120	99		700	223	125		1095	337	342
	306	120	126		701	223	219		1096	337	344
	307	121	107	L112	702	223	222		1097	338	346
L61	308	121	111		703	224	228		1098	339	317
	309	121	117		704	224	230		1099	339	327
	310	121	120		705	224	232		1100	339	333
	311	121	124		706	225	165		1101	339	335
	312	122	128		707	225	167	L170	1102	339	338
	313	123	107	L113	708	225	213		1103	339	342
	314	123	111		709	225	221		1104	339	344
	315	123	117		710	226	215		1105	340	348
L62	316	123	120	L114	711	227	223		1106	340	350

Continued on next page

Table A.12 – continued from previous page

Faulty line	Serial No.	Primary relay	Backup relay	Faulty line No.	Serial	Primary relay	Backup relay	Faulty line No.	Serial	Primary relay	Backup relay
	317	123	122		712	227	230		1107	340	352
	318	124	127		713	227	232	L171	1108	341	317
	319	124	130		714	228	153		1109	341	327
	320	124	132		715	228	169		1110	341	333
L63	321	125	99		716	228	234		1111	341	335
	322	125	119		717	228	236		1112	341	338
	323	126	219		718	228	238		1113	341	340
	324	126	222	L115	719	229	223		1114	341	344
	325	126	224		720	229	228		1115	342	347
L64	326	127	121		721	229	232		1116	342	354
	327	128	123		722	230	271	L172	1117	343	317
	328	128	130	L115	723	231	223		1118	343	327
	329	128	132		724	231	228		1119	343	333
L65	330	129	123		725	231	230		1120	343	335
	331	129	127	L117	726	233	153		1121	343	338
	332	129	132		727	233	169		1122	343	340
	333	130	134		728	233	227		1123	343	342
L66	334	131	123		729	233	236		1124	344	355
	335	131	127		730	233	238		1125	344	362
	336	131	130		731	234	79	L173	1126	345	337
	337	132	133		732	234	240		1127	346	319
	338	132	136		733	234	242	L174	1128	347	339
	339	132	138		734	234	244		1129	347	350
L67	340	133	129	L118	735	235	153		1130	347	352
	341	134	131		736	235	169		1131	348	341
	342	134	136		737	235	227		1132	348	354
	343	134	138		738	235	234	L175	1133	349	339
L68	344	135	131		739	235	238		1134	349	348
	345	135	133		740	236	243		1135	349	352
	346	135	138		741	236	249		1136	350	353
	347	136	137		742	236	252		1137	350	356
	348	136	145		743	236	254		1138	350	358
	349	136	151	L119	744	237	153		1139	350	360
	350	136	155		745	237	169	L176	1140	351	339
	351	136	158		746	237	227		1141	351	348
	352	136	160		747	237	234		1142	351	350
	353	136	162		748	237	236		1143	352	365
	354	136	164		749	238	251		1144	352	368
	355	136	166		750	238	255		1145	352	370
	356	136	168		751	238	260	L177	1146	353	341
	357	136	170		752	238	262		1147	353	347
L69	358	137	131		753	238	264		1148	354	349
	359	137	133		754	238	266		1149	354	356
	360	137	136	L120	755	239	79		1150	354	358
	361	138	135		756	239	233		1151	354	360
	362	138	145		757	239	242	L178	1152	355	349
	363	138	151		758	239	244		1153	355	353
	364	138	155		759	240	246		1154	355	358
	365	138	158		760	240	248		1155	355	360
	366	138	160	L121	761	241	79		1156	356	343
	367	138	162		762	241	233		1157	356	362
	368	138	164		763	241	240	L179	1158	357	349
	369	138	166		764	241	244		1159	357	353
	370	138	168		765	242	250		1160	357	356
	371	138	170	L122	766	243	79		1161	357	360
L70	372	139	113		767	243	233		1162	358	361
	373	140	142		768	243	240	L180	1163	359	349
L71	374	141	139		769	243	242		1164	359	353
	375	142	144		770	244	235		1165	359	356
	376	142	146		771	244	249		1166	359	358
L72	377	143	141		772	244	252		1167	360	364

Continued on next page

Table A.12 – continued from previous page

Faulty line	Serial No.	Primary relay	Backup relay	Faulty line No.	Serial	Primary relay	Backup relay	Faulty line No.	Serial	Primary relay	Backup relay
	378	143	146		773	244	254	L181	1168	361	343
	379	144	148	L123	774	245	239		1169	361	355
	380	144	150		775	245	248		1170	362	357
L73	381	145	141		776	246	81	L182	1171	363	359
	382	145	144	L124	777	247	239		1172	364	366
	383	146	135		778	247	246	L183	1173	365	363
	384	146	137	L125	779	249	241		1174	366	351
	385	146	151		780	250	235		1175	366	368
	386	146	155		781	250	243		1176	366	370
	387	146	158		782	250	252	L184	1177	367	351
	388	146	160		783	250	254		1178	367	365
	389	146	162	L126	784	251	235		1179	367	370
	390	146	164		785	251	243	L185	1180	369	351
	391	146	166		786	251	249		1181	369	365
	392	146	168		787	251	254		1182	369	368
	393	146	170		788	252	237	L186	1183	371	105
L74	394	147	143		789	252	255		1184	372	93
	395	147	150		790	252	260		1185	-	-